

NASA Technical Library



3 1176 01422 2724

NATIONAL ADVISORY COMMITTEE FOR AERONAUTICS

TECHNICAL NOTE

No. 1291

COLLECTION AND ANALYSIS OF WIND-TUNNEL DATA ON THE
CHARACTERISTICS OF ISOLATED TAIL SURFACES
WITH AND WITHOUT END PLATES

By William R. Bates

Langley Memorial Aeronautical Laboratory
Langley Field, Va.



Washington

May 1947

NATIONAL ADVISORY COMMITTEE FOR AERONAUTICS

TECHNICAL NOTE No. 1291

COLLECTION AND ANALYSIS OF WIND-TUNNEL DATA ON THE
CHARACTERISTICS OF ISOLATED TAIL SURFACES
WITH AND WITHOUT END PLATES

By William R. Bates

SUMMARY

The aerodynamic characteristics of 19 isolated tail surfaces have been determined by wind-tunnel tests and tests have also been made of rectangular airfoils of various aspect ratios with and without double end plates of various shapes. The data from these tests have been collected and analyzed.

The analysis indicated that the slope of the lift curve could be predicted within 10 percent for all models by use of lifting-surface-theory equations. The increase in lift-curve slope provided by tip-located double end plates was shown to be dependent upon the square root of the area of the end plate divided by the airfoil span.

About three-fourths of the computed values of the elevator lift-effectiveness parameters $\frac{\Delta a}{\Delta S}$ agree within 10 percent of the measured values.

The hinge-moment parameters were computed by means of lifting-surface-theory procedures for comparison with measured values. The parameters of elevators with cut-outs could not be predicted accurately. For elevators with no cut-outs, about 55 percent of the calculated values for the rate of change of hinge-moment coefficient with angle of attack C_{h_a} and about 65 percent of the calculated values for the rate of change of hinge-moment coefficient with elevator deflection C_{h_S} are within ± 0.0010 of the measured values.

INTRODUCTION

In order to provide fundamental design data the National Advisory Committee for Aeronautics has undertaken the expedient of publishing collections of data obtained in specific investigations and, whenever possible, analysis of the data. The present paper contains a collection and analysis of data that includes 19 tail surfaces tested in the Langley 4- by 6-foot vertical tunnel. These tail surfaces are from complete airplane models that have been tested for stability and control characteristics in the Langley 7- by 10-foot tunnel. Some data from other tunnels (references 1 to 5) are presented for comparisons. In addition, some data are presented on tests of isolated tails cut to various spans and equipped with end plates of various shapes.

COEFFICIENTS AND SYMBOLS

C_L	lift coefficient $\left(\frac{L}{qS} \right)$
c_l	airfoil section lift coefficient $\left(\frac{l}{qc} \right)$
C_{h_e}	elevator hinge-moment coefficient $\left(\frac{H_e}{ab_e c_e^2} \right)$
L	force perpendicular to relative wind, positive when directed upward
l	airfoil section lift
H_e	elevator hinge moment, positive when it tends to deflect elevator down
q	dynamic pressure of free air stream $\left(\frac{\rho V^2}{2} \right)$
ρ	mass density of air at sea level
V	airspeed
S	horizontal tail area

- S_e elevator area
 S_b area of overhang (balancing surface)
 S_{ep} area of end plate
 c chord of airfoil section
 c_e chord of elevator behind hinge axis measured at any airfoil section
 c_e' root-mean-square chord of elevator behind hinge axis
 \bar{c} average chord of airfoil section
 \bar{c}_b average chord of overhang $\left(\frac{S_b}{b_b} \right)$
 \bar{c}_e average chord of elevator
 b span of airfoil
 b_e elevator span
 b_b span of overhang (balancing surface)
 h height of end plate
 t airfoil maximum thickness
 A aspect ratio $\left(\frac{b^2}{S} \right)$
 A' effective aspect ratio
 λ taper ratio; ratio of tip chord to root chord
 α angle of attack of finite-span airfoil
 α_0 angle of attack for infinite aspect ratio
 δ deflection of elevator with respect to airfoil chord line
 ϕ trailing-edge angle

- E_e effective edge-velocity factor taken from reference 6
- $\frac{\Delta\alpha}{\Delta\delta}$ elevator lift-effectiveness parameter; effective change in section angle of attack per unit change in elevator deflection

$$c_{L_\alpha} = \left(\frac{\partial c_L}{\partial \alpha} \right)_{\delta}$$

$$c_{L_{\alpha_{ep}}} = \left(\frac{\partial c_L}{\partial \alpha} \right)_{\delta} \quad (\text{for airfoil with end plates})$$

$$c_{l_\alpha} = \left(\frac{\partial c_l}{\partial \alpha} \right)_{\delta}$$

$$c_{l_{\alpha_0}} = \left(\frac{\partial c_l}{\partial \alpha_0} \right)_{\delta}$$

$$c_{L_\delta} = \left(\frac{\partial c_L}{\partial \delta} \right)_{\alpha}$$

$$\frac{\Delta\alpha}{\Delta\delta} = \left(\frac{\partial \alpha}{\partial \delta} \right)_{C_L}$$

$$c_{h_\alpha} = \left(\frac{\partial c_h}{\partial \alpha} \right)_{\delta}$$

$$c_{h_\delta} = \left(\frac{\partial c_h}{\partial \delta} \right)_{\alpha}$$

The subscripts outside the parenthesis indicate the factors held constant during measurement of the parameters.

Subscripts:

F front elevator

R rear elevator

APPARATUS AND MODELS

The tests were made in the Langley 4- by 6-foot vertical tunnel described in reference 7. The test section of this tunnel has been converted from the original open, circular, 5-foot-diameter jet to a closed, rectangular, 4- by 6-foot throat (reference 8).

The models were constructed of laminated mahogany. Various geometric characteristics of the models are given in tables I to IV. Detail drawings of all models are given in figures 1 to 19. Model 2 was tested with the slot open and filled (see fig. 2); model 8 was equipped with a double flap; models 18 and 19 were tested with and without circular and elliptical end plates. The spans of models 18 and 19 were varied, as shown in figures 18 and 19, in order to vary the aspect ratio.

Unnecessary holes in the surfaces of all the models were filled to form smooth surfaces. For some tests the gaps at the noses of the elevators were filled with modeling clay and faired to the airfoil contour. For tests in which hinge moments were read the gap was filled with grease. For elevator-free tests the elevator was statically balanced. The trailing-edge angles were measured from the models with a vernier protractor. Model 17 was tested as a complete tail assembly mounted on a dummy fuselage with No. 60 carborundum grains located at the 0.17c station over the entire stabilizer span. Except for models 10 and 11, which were equipped with sealed internal balances, the models had plain elevators or elevators with plain overhang balances.

Figure 20 shows the regular setup of the electrical strain-gage unit with which the hinge moments were read; figure 21 gives a sketch of the tare setup.

TESTS AND METHODS

Most of the tests were made at a dynamic pressure of 13 pounds per square foot, which corresponds to an air velocity of about 72 miles per

hour at standard sea-level conditions. Models 18 and 19 were tested at a dynamic pressure of 15 pounds per square foot, which corresponds to an air velocity of about 76 miles per hour at standard sea-level conditions. The Reynolds numbers for the tests of the various models varied from 144,000 to 292,000. The effective Reynolds numbers (for maximum lift coefficients) varied from 278,000 to 653,000 based on a turbulence factor of 1.93 for the Langley 4- by 6-foot vertical tunnel.

For each model, tests were made by varying the angle of attack with several fixed elevator settings.

The lift data have been corrected for tares caused by the model support strut and fork. In order to find the effect of the strut and fork, tests were run with and without a dummy strut and fork in place. For model 17 a dummy fuselage was mounted on the fork and tested. Jet-boundary corrections were applied to lift and angle of attack (table I). The corrections to hinge moment were very small and therefore were not applied.

The following elevator-gap conditions of the models were tested both for elevator cut-out open and filled: unsealed, sealed with grease, and sealed and faired to airfoil contour with modeling clay.

RESULTS AND DISCUSSION

Lift and hinge-moment characteristics of models 1 to 17 are presented in figures 22 to 38, respectively, as plots of lift coefficient and elevator hinge-moment coefficient against angle of attack for various elevator deflections. Lift characteristics of models 18 and 19 are presented in figures 39 and 40, respectively. The aerodynamic parameters of the models are given in table V.

Lift of Models without End Plates

An equation, based on lifting-surface theory (reference 9), for the lift-curve slope is

$$C_{L_a} = \frac{Ac_{l_a}}{AE_e + \frac{57.3}{\pi} c_{l_a}} \quad (1)$$

where E_e is an effective edge-velocity correction factor which is given in reference 6. For the theoretical section lift-curve slope, $c_{l\alpha} = \frac{2\pi}{57.3}$, the following equation is obtained:

$$C_{L\alpha} = 0.1095 \frac{A}{AE_e + 2} \quad (2)$$

Theoretical values were computed by equation (2) and compared with experimental data in figure 41. The data scatter considerably and are below the theoretical curve. A curve representing the average of the experimental values corresponds approximately to equation (2) with the constant changed to 0.090 or

$$C_{L\alpha} = 0.090 \frac{A}{AE_e + 2} \quad (3)$$

Because equation (3) does not account for any variation in the value of the lift-curve slope an attempt has been made to determine how much of the scatter on figure 41 can be eliminated by estimating the value of $c_{l\alpha}$ for each specific model. The effects of trailing-edge angle, airfoil-section thickness, gap size, and gap location were considered. The value of $c_{l\alpha}$ for a given section is expressed

empirically as follows

$$c_{l\alpha} = c_{l\alpha_0} \frac{(c_{l\alpha})_{gap\ open}}{(c_{l\alpha})_{gap\ sealed}} \frac{(c_{l\alpha})_{sealed}}{(c_{l\alpha})_{faired}}$$

where $c_{l\alpha_0}$ is read from figure 42, which shows the effect of airfoil thickness and trailing-edge angle on section lift-curve slope. In preparing figure 42 data was taken from references 10 to 14, and the slope $c_{l\alpha_0}$ was plotted against ϕ for various constant thickness ratios t/c . The average value of $\frac{\partial c_{l\alpha}}{\partial \phi}$ determined was 0.0006.

This value was used in correcting $c_{l\alpha_0}$ to zero trailing-edge angle. The curves at the other values of ϕ (fig. 42) were obtained by subtracting an increment equal to $\frac{\partial c_{l\alpha}}{\partial \phi} \phi$ from the curve for $\phi = 0^\circ$.

Data obtained from references 15 and 16 are presented in a plot of $\left(\frac{c_{l\alpha}}{c_{l\alpha}}\right)_{\text{gap open}}$ against break location for various gap sizes for the NACA 0009 and NACA 0015 airfoils in figure 43. These curves show that $\left(\frac{c_{l\alpha}}{c_{l\alpha}}\right)_{\text{gap open}}$ decreases as the gap is moved toward the leading edge of the airfoil until it reaches a position of about $0.50c$. The gap sizes range from $0.001c$ to $0.010c$ and the data indicate a

decrease in $\left(\frac{c_{l\alpha}}{c_{l\alpha}}\right)_{\text{gap open}}$ as the gap size increases.

Figure 44 presents a plot of $\left(\frac{c_{l\alpha}}{c_{l\alpha}}\right)_{\text{sealed}}$ against break location giving the effect of the break in the airfoil contour on $\left(\frac{c_{l\alpha}}{c_{l\alpha}}\right)_{\text{sealed}}$.

The nose shape of the balance had very little effect on the lift-curve slope.

Equation (1) may be rewritten as follows

$$\frac{C_L\alpha}{c_{l\alpha}} = \frac{1}{E_e + \frac{57.3}{\pi} \frac{c_{l\alpha}}{A}} \quad (4)$$

which may be represented by a single curve of $\frac{C_L\alpha}{c_{l\alpha}}$ plotted

against $\frac{A}{c_{l\alpha}}$ provided that the second-order effects of variations in $c_{l\alpha}$ on the values of E_e corresponding to a given value of $\frac{A}{c_{l\alpha}}$ are neglected. For determining values of E_e , a constant value of $c_{l\alpha} = 0.10$ was assumed. Varying $c_{l\alpha}$ produced such a small change in E_e that it was neglected.

A comparison of theoretical and experimental values of $\frac{c_{L\alpha}}{c_{l\alpha}}$ plotted against $\frac{A}{c_{l\alpha}}$ is given in figure 45. The scatter of points is somewhat less than that in figure 41. A curve representing the average of the test points is slightly below the theoretical curve. The data considered herein therefore indicate that the theoretical values of E_e are too small.

The lift-curve slopes for finite-aspect ratios were computed by use of equation (1) so that a comparison could be made between computed and measured values. This comparison is presented in figure 46 and shows that all values could be computed within 10 percent of the measured values.

Lift of Airfoils with End Plates

In determining the effects of tip-located double end plates on the airfoil lift-curve slope, data from the present tests, from references 17 to 20, and from unpublished sources were collected and analyzed.

Attempts were made to correlate the end plate effect, given as $\frac{A}{A'}$ or as $\frac{C_{L\alpha ep}}{C_{L\alpha}}$, with such ratios as $\frac{h}{b}$, $\frac{S_{ep}}{S}$, and $\frac{\sqrt{S_{ep}}}{b}$.

The best correlation was obtained when $\frac{A}{A'}$ was plotted against $\frac{\sqrt{S_{ep}}}{b}$.

The relation obtained and equation (4) were used to construct

figure 47. By use of the curves in figure 47, values of $\frac{C_{L\alpha ep}}{C_{L\alpha}}$ were calculated and plotted against measured values of $\frac{C_{L\alpha ep}}{C_{L\alpha}}$ in figure 48.

Elevator Effectiveness

The lift effectiveness $\frac{\Delta\alpha}{\Delta\delta}$ was estimated by use of data in references 21, 22, 23, and the present paper. The following empirical equation was used

$$\frac{\Delta\alpha}{\Delta\delta} = \begin{cases} \left(\frac{\Delta\alpha}{\Delta\delta}\right)_{\text{plain sealed}} & \text{with overhang} \\ \left(\frac{\Delta\alpha}{\Delta\delta}\right)_{\text{plain sealed}} & \text{without cut-out} \end{cases}$$

$$\frac{\left(\frac{\Delta\alpha}{\Delta\delta}\right)}{\left(\frac{\Delta\alpha}{\Delta\delta}\right)_{\text{plain sealed}}} \quad \frac{\left(\frac{\Delta\alpha}{\Delta\delta}\right)}{\left(\frac{\Delta\alpha}{\Delta\delta}\right)_{\text{without cut-out}}}$$

Figure 49, which presents the variation of $\frac{\Delta\alpha}{\Delta\delta}$ with $\frac{c_e}{c}$ for various trailing-edge angles, was derived from figures 16 and 17 of reference 22. The effect of the overhang was obtained from figure 26 of reference 22. The effect of the elevator cut-out was obtained from a correlation (fig. 50) of data from the present paper.

The measured values of $\frac{\Delta\alpha}{\Delta\delta}$ are plotted against the calculated values in figure 51. About three-fourths of the computed values agree within 10 percent of the measured values.

Elevator Hinge Moments

The hinge-moment parameters were calculated according to lifting-surface theory by the method developed in reference 9 for use on a wing of elliptical plan form. The section values for the plain flap used in the computations were obtained from reference 22. The balance effect also found in reference 22 was added to the plain-flap values which had been corrected for aspect ratio. The effect of the horn balance was obtained from reference 4. The measured values of hinge-moment parameters are plotted against the calculated values in figures 52 to 55.

No attempt was made in the calculations to account for the effects of cut-outs, because accurate estimates of the values of the section parameters in the regions of the cut-outs could not be made. With cut-outs open, the agreement between measured and calculated values was poor; the measured values generally are considerably less negative than the calculated values. Better

agreement was obtained when the elevator cut-outs were filled. For this condition about 55 percent of the calculated values of $C_{h\alpha}$ and about 65 percent of the calculated values of $C_{h\delta}$ are within ± 0.0010 of the measured values.

CONCLUSIONS

From an analysis of test data on 19 isolated tail surfaces the following conclusions may be drawn:

1. The slope of the lift curve was predicted within 10 percent for all the models by use of the lifting-surface-theory equations.
2. The increase in lift-curve slope provided by tip-located double end plates was shown to be dependent upon the square root of the area of the end plate divided by the airfoil span.
3. For computed values of the elevator lift-effectiveness parameters $\frac{\Delta\alpha}{\Delta\delta}$ about three-fourths of the points agree within 10 percent of the measured values.
4. The hinge-moment parameters of elevators with cut-outs could not be predicted accurately. For elevators with no cut-outs, about 55 percent of the calculated values of the rate of change of hinge-moment coefficient with angle of attack $C_{h\alpha}$ and about 65 percent of the calculated values of the rate of change of hinge-moment coefficient with flap deflection $C_{h\delta}$ are within ± 0.0010 of the measured values.

Langley Memorial Aeronautical Laboratory
National Advisory Committee for Aeronautics
Langley Field, Va., February 19, 1946

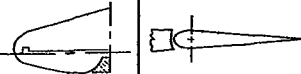
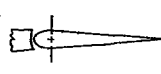
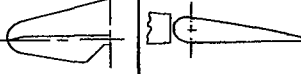
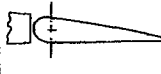
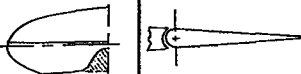
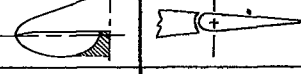
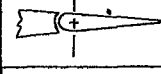
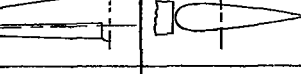
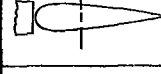
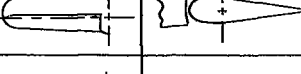
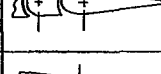
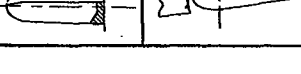
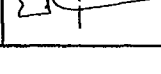
REFERENCES

1. Silverstoin, Abe, and Katzoff, S.: Aerodynamic Characteristics of Horizontal Tail Surfaces. NACA Rep. No. 688, 1940.
2. Garner, I. Elizabeth: Wind-Tunnel Investigation of Control-Surface Characteristics. XX - Plain and Balanced Flaps on an NACA 0009 Rectangular Semispan Tail Surface. NACA ARR No. L4111f, 1944.
3. Geett, Harry J., and Reeder, J. P.: Effects of Elevator Nose Shape, Gap, Balance, and Tabs on the Aerodynamic Characteristics of a Horizontal Tail Surface. NACA Rep. No. 675, 1939.
4. Lowry, John G., Maloney, James A., and Garner, I. Elizabeth: Wind-Tunnel Investigation of Shielded Horn Balances and Tabs on a 0.7-Scale Model of the XF6F Vertical Tail Surface. NACA ACR No. 4C11, 1944.
5. Sears, Richard I., and Hoggard, H. Page, Jr.: Characteristics of Plain and Balanced Elevators on a Typical Pursuit Fuselage at Attitudes Simulating Normal-Flight and Spin Conditions. NACA ARR, March 1942.
6. Swanson, Robert S., and Priddy, E. LaVerne: Lifting-Surface-Theory Values of the Damping in Roll and of the Parameter Used in Estimating Aileron Stick Forces. NACA ARP No. L5F23, 1945.
7. Wenzinger, Carl J., and Harris, Thomas A.: The Vertical Wind Tunnel of the National Advisory Committee for Aeronautics. NACA Rep. No. 387, 1931.
8. Ames, Milton B., Jr., and Sears, Richard I.: Pressure-Distribution Investigation of an N.A.C.A. 0009 Airfoil with a 30-Percent-Chord Plain Flap and Three Tabs. NACA TN No. 759, 1940.
9. Swanson, Robert S., and Crandall, Stewart M.: Lifting-Surface-Theory Aspect-Ratio Corrections to the Lift and Hinge-Moment Parameters for Full-Span Elevators on Horizontal Tail Surfaces. NACA TN No. 1175, 1947.
10. Pinkerton, Robert M., and Greenberg, Harry: Aerodynamic Characteristics of a Large Number of Airfoils Tested in the Variable-Density Wind Tunnel. NACA Rep. No. 628, 1938.

11. Jacobs, Eastman N., Ward, Kenneth E., and Pinkerton, Robert M.: The Characteristics of 78 Related Airfoil Sections from Tests in the Variable-Density Wind Tunnel. NACA Rep. No. 460, 1933.
12. Abbott, Ira H., von Doenhoff, Albert E., and Stivers, Louis S., Jr.: Summary of Airfoil Data. NACA ACR No. L5C05, 1945.
13. Purser, Paul E., and Riebe, John M.: Wind-Tunnel Investigation of Control-Surface Characteristics. XV - Various Contour Modifications of a 0.30-Airfoil-Chord Plain Flap on an NACA 66(215)-014 Airfoil. NACA ACR No. 3L20, 1943.
14. Underwood, William J., Braslow, Albert L., and Cahill, Jones F.: Two-Dimensional Wind-Tunnel Investigation of 0.20-Airfoil-Chord Plain Ailerons of Different Contour on an NACA 65₁-210 Airfoil Section. NACA ACR No. L5F27, 1945.
15. Sears, Richard I.: Wind-Tunnel Data on the Aerodynamic Characteristics of Airplane Control Surfaces. NACA ACR No. 3L08, 1943.
16. Riebe, John M., and Church, Oleta: Wind-Tunnel Investigation of Control-Surface Characteristics. XXI - Medium and Large Aerodynamic Balances of Two Nose Shapes and a Plain Overhang Used with a 0.40-Airfoil-Chord Flap on an NACA 0009 Airfoil. NACA ARR No. L5C01, 1945.
17. Mangler, W.: The Lift Distribution of Wings with End Plates. NACA TM No. 856, 1938.
18. von Kármán, Th., and Burgers, J. M.: General Aerodynamic Theory - Perfect Fluids. Airfoils and Airfoil Systems of Finite Span. Vol. II of Aerodynamic Theory, div. E, ch. IV, sec. 19, W. F. Durand, ed., Julius Springer (Berlin), 1935, pp. 211-212.
19. Betz, A., and Nagel, F.: Untersuchungen an Flügeln mit Endscheiben. Ergebni. Aerodyn. Versuchsanst. Göttingen, Lfg. III, 1927, pp. 95-99.
20. Reid, Elliott G.: The Effects of Shielding the Tips of Airfoils. NACA Rep. No. 201, 1924.

21. Swanson, Robert S., and Crandall, Stewart M.: Analysis of Available Data on the Effectiveness of Ailerons without Exposed Overhang Balance. NACA ACR No. L4E01, 1944.
22. Langley Research Department: Summary of Lateral-Control Research. (Compiled by Thomas A. Toll.) NACA TN No. 1245, 1947.
23. Purser, Paul E., and Toll, Thomas A.: Analysis of Available Data on Control Surfaces Having Plain-Overhang and Frise Balances. NACA ACR No. L4E13, 1944.

TABLE I.—INFORMATION REGARDING THREE-DIMENSIONAL-FLOW MODELS TESTED IN LANGLEY 4- BY 6-FOOT VERTICAL TUNNEL
[Turbulence factor, 1.93]

Model and figure	Data on figure	Plan form	Balance section	Airfoil section	Average gap	Test Reynolds number	λ	Aspect ratio		S _e /S		S _b /S _e		Corrections added to test data	
								Open (a)	Filled (a)	Open (a)	Filled (a)	Open (a)	Filled (a)	Open (a)	Filled (a)
1	22			NACA 0009	.0046	255,000	Elliptical	3.45	3.27	0.342	0.376	0.200	-----	$\Delta\alpha=1.384C_L$ $\Delta C_L=0.032C_L$	$\Delta\alpha=1.484C_L$ $\Delta C_L=0.030C_L$
2	23			Clark Y	.0036	259,000	0.438	3.41	-----	.336	-----	.203	-----	$\Delta\alpha=1.128C_L$ $\Delta C_L=0.040C_L$	-----
3	24			NACA 0009	.0036	280,000	Elliptical	3.65	3.42	.455	.489	Radius nose	-----	$\Delta\alpha=1.384C_L$ $\Delta C_L=0.032C_L$	$\Delta\alpha=1.482C_L$ $\Delta C_L=0.030C_L$
4	25			NACA 0009	.0016	292,000	Elliptical	3.50	3.39	.217	.244	Radius nose	-----	$\Delta\alpha=1.480C_L$ $\Delta C_L=0.031C_L$	$\Delta\alpha=1.718C_L$ $\Delta C_L=0.029C_L$
5	26			NACA 0009, sharp nose	.0046	233,000	.365	4.22	4.04	.308	.339	.202	0.185	$\Delta\alpha=0.894C_L$ $\Delta C_L=0.044C_L$	$\Delta\alpha=0.950C_L$ $\Delta C_L=0.041C_L$
6	27			NACA 0011-64	.0106	188,000	.377	5.55	-----	.299	-----	.329	-----	$\Delta\alpha=0.872C_L$ $\Delta C_L=0.046C_L$	-----
7	28			NACA 0012-64	.0026	186,000	.446	5.21	-----	.274	-----	.373	-----	$\Delta\alpha=0.891C_L$ $\Delta C_L=0.051C_L$	-----
8	29			NACA 0012-64	.0046	186,000	.446	5.20	-----	^b .445 _c .237	-----	^b Radius _c .351	-----	$\Delta\alpha=0.891C_L$ $\Delta C_L=0.051C_L$	-----
9	30			Root, NACA 0013.4-64 Tip, NACA 0010.5-64	.0056	259,000	.525	4.39	4.29	.331	.354	.324	-----	$\Delta\alpha=1.200C_L$ $\Delta C_L=0.031C_L$	$\Delta\alpha=1.240C_L$ $\Delta C_L=0.030C_L$

^aOpen and filled refer to rudder cut-out condition, see cross-hatched areas in plan forms.

^bRefers to forward elevator.

^cRefers to rear elevator.

TABLE I.- INFORMATION REGARDING THREE-DIMENSIONAL-FLOW MODELS TESTED IN LANGLEY 4- BY 6-FOOT VERTICAL TUNNEL - Concluded

Model and figure	Data on figure	Plan form	Balance section	Airfoil section	Average gap	Test Reynolds number	λ	Aspect ratio		S _e /S		S _D /S _e		Corrections added to test data	
								Open (a)	Filled (a)	Open (a)	Filled (a)	Open (a)	Filled (a)	Open (a)	Filled (a)
10	31			Root, NACA 65-2-015 Tip, NACA 65-2-012	Sealed	212,000	0.589	4.73	-----	0.272	-----	0.272	-----	$\Delta\alpha=1.145C_L$ $\Delta C_L=0.0420L$	-----
11	32			Root, NACA 65(25)-015.5 Tip, NACA 65-2-012	Sealed	223,000	.559	5.16	-----	.274	-----	.268	-----	$\Delta\alpha=1.470C_L$ $\Delta C_L=0.0366L$	-----
12	33			0.0166	228,000	.467	4.78	4.67	.360	0.373	.274	0.265	$\Delta\alpha=1.386C_L$ $\Delta C_L=0.0370L$	$\Delta\alpha=1.426C_L$ $\Delta C_L=0.0370L$	
13	34			Root, NACA 66-2-015 Tip, NACA 66-2-009	.0016	167,000	.587	4.26	-----	.281	-----	.132	-----	$\Delta\alpha=1.097C_L$ $\Delta C_L=0.0480L$	-----
14	35			NACA 0009	.0016	242,000	.500	3.40	3.26	.274	.302	.302	.262	$\Delta\alpha=0.932C_L$ $\Delta C_L=0.0400L$	$\Delta\alpha=0.976C_L$ $\Delta C_L=0.0380L$
15	36			Root, NACA 0015-63 Tip, NACA 0008-63	.0096	208,000	.646	4.53	-----	.337	-----	.350	-----	$\Delta\alpha=0.733C_L$ $\Delta C_L=0.0510L$	-----
16	37			NACA 0015	.0068	198,000	.653	4.21	-----	.291	-----	-----	-----	$\Delta\alpha=0.482C_L$ $\Delta C_L=0.0680L$	-----
17	38			NACA 66-009	.0046	194,000	.500	4.65	-----	.265	-----	.480	-----	$\Delta\alpha=0.911C_L$ $\Delta C_L=0.0520L$	-----
18	39			NACA 84	-----	146,000	1.000	1.5 to 6.03	-----	-----	-----	-----	-----	-----	-----
19	40			NACA 0009	-----	184,000	1.000	.586 to 6.02	-----	-----	-----	-----	-----	-----	-----

*Open and filled refer to rudder cut out condition, see cross-hatched areas in plan forms

NATIONAL ADVISORY
COMMITTEE FOR AERONAUTICS

TABLE II.- GEOMETRIC CHARACTERISTICS OF THE ISOLATED HORIZONTAL TAILS

[Filled in indicates that the elevator cut-out has been filled
and faired to airfoil contour]

Model	1	2	3	4	5	6	7	8 (\bar{a})	9	10	11	12	13	14	15	16	17
Total area, sq ft	1.884	1.920	2.400	2.500	1.684	1.452	1.498	1.500	2.163	1.825	2.15	2.062	1.80	1.672	1.315	0.988	1.47
Total area (filled in), sq ft	1.986	-----	2.560	2.590	1.758	-----	-----	-----	2.237	-----	2.115	-----	1.741	-----	-----	-----	-----
Elevator area behind hinge, sq ft	0.645	0.645	1.090	0.543	0.525	0.433	0.408	-----	0.716	0.496	0.590	0.741	0.507	0.457	0.444	0.287	0.39
Elevator area behind hinge (filled in), sq ft	0.747	-----	1.250	0.633	0.595	-----	-----	-----	0.790	-----	0.788	-----	0.526	-----	-----	-----	-----
Span of complete tail, ft	2.55	2.56	2.96	2.96	2.667	2.04	2.79	2.79	3.08	2.94	3.33	3.14	2.78	2.380	2.44	2.05	2.61
Span of elevators, ft	2.55	2.56	2.79	2.76	2.550	2.60	2.55	-----	3.08	2.64	3.07	2.99	2.64	1.990	2.284	1.84	2.60
Span of elevators (filled in), ft	2.55	-----	2.96	2.96	2.650	-----	-----	-----	3.08	-----	3.13	-----	1.990	-----	-----	-----	-----
Aspect ratio	3.45	3.41	3.65	3.50	4.22	5.55	5.21	5.20	4.39	4.73	5.16	4.78	4.26	3.40	4.53	4.21	4.65
Aspect ratio (filled in)	3.27	-----	3.42	3.39	4.04	-----	-----	-----	4.25	-----	4.67	-----	3.26	-----	-----	-----	-----
c_e^1 , ft	0.278	0.264	0.407	0.197	0.217	0.172	0.169	-----	0.247	0.197	0.198	0.249	0.191	0.241	0.199	-----	0.165
c_e^1 (filled in), ft	0.302	-----	0.439	0.220	0.231	-----	-----	-----	0.258	-----	0.252	-----	0.266	-----	-----	-----	-----
Stabilizer average chord, ft	0.436	0.437	-----	-----	0.395	0.308	0.335	-----	0.395	0.407	0.421	0.356	0.442	0.301	0.293	-----	0.342
Tail average chord, ft	0.739	0.751	0.812	0.847	0.633	0.511	0.537	0.540	0.702	0.621	0.645	0.656	0.648	0.702	0.562	0.481	0.563
Tail average chord (filled in), ft	0.778	-----	0.864	0.878	0.660	-----	-----	-----	0.724	-----	0.674	-----	0.732	-----	-----	-----	-----
c_e/\bar{c}	0.376	0.336	0.482	0.233	0.325	0.326	0.298	-----	0.438	0.299	0.298	0.480	0.296	0.326	0.345	0.324	0.267
c_e/\bar{c} (filled in)	0.388	-----	0.489	0.244	0.339	-----	-----	-----	0.458	-----	0.472	-----	0.360	-----	-----	-----	-----
Total elevator area, sq ft	0.774	0.776	-----	-----	0.631	0.576	0.560	-----	0.948	0.631	0.748	0.944	0.574	0.595	0.599	-----	0.577
Total elevator area (filled in), sq ft	0.876	-----	-----	-----	0.705	-----	-----	-----	1.022	-----	0.997	-----	0.664	-----	-----	-----	-----
Elevator average chord, ft	0.253	0.252	0.392	0.197	0.206	0.166	0.160	-----	0.307	0.186	0.192	0.315	0.192	0.229	0.194	0.156	0.150
Elevator average chord (filled in), ft	0.293	-----	0.422	0.214	0.224	-----	-----	-----	0.331	-----	0.318	-----	0.264	-----	-----	-----	-----
Stabilizer area, sq ft	1.110	1.114	-----	-----	1.053	0.877	0.938	-----	1.215	1.194	1.40	1.118	1.226	1.077	0.716	-----	0.893
Tip section chord (theoretical), ft	-----	0.500	-----	-----	0.349	0.283	0.335	0.335	0.515	0.471	0.471	0.437	0.480	0.507	0.431	0.383	0.349
Root section chord, ft	1.042	1.140	1.059	1.063	0.959	0.751	0.751	0.751	0.981	0.800	0.844	0.935	0.818	1.01	0.668	0.586	0.955
Area of balance, sq ft	0.129	0.131	-----	-----	0.106	0.143	0.152	-----	0.232	0.135	0.158	0.203	0.067	0.138	0.155	-----	0.187
Area of balance (filled in), sq ft	0.129	-----	-----	-----	0.110	-----	-----	-----	0.232	-----	0.209	-----	0.138	-----	-----	-----	-----
Average chord of balance, ft	0.0506	0.0512	-----	-----	0.0431	0.0608	0.0597	-----	0.0754	0.051	0.051	0.0679	0.026	0.0689	0.068	-----	0.072
Average chord of balance (filled in), ft	0.0506	-----	-----	-----	0.0428	-----	-----	-----	0.0754	-----	0.0665	-----	0.0689	-----	-----	-----	-----
\bar{c}_b/\bar{c}_e	0.182	0.203	-----	-----	0.209	0.365	0.373	-----	0.242	0.274	0.266	0.274	0.137	0.301	0.351	-----	0.48
\bar{c}_b/\bar{c}_e (filled in)	0.168	-----	-----	-----	0.191	-----	-----	-----	0.224	-----	0.263	-----	0.261	-----	-----	-----	-----
Area of horn balance, sq ft	0.017	-----	-----	-----	-----	-----	-----	-----	-----	-----	-----	-----	-----	-----	-----	-----	-----
Trailing-edge angle, deg	10	14	20	20	10.5	17.5	20	16	12	15	15.0	14.75	20.75	11.75	14.75	15.0	12.75

^aComplete data found in Table III.

TABLE III.- GEOMETRIC CHARACTERISTICS OF
HORIZONTAL TAIL 8

Area of tail, sq ft	1.50
Area of forward elevator, sq ft	0.667
Area of rear elevator, sq ft	0.356
Span of tail, ft	2.79
Span of forward elevator, ft	2.55
Span of rear elevator, ft	2.52
Aspect ratio of tail	5.2
Aspect ratio of forward elevator	6.5
Aspect ratio of rear elevator	17.9
Average chord of tail, ft	0.54
Average chord of forward elevator, ft . . .	0.262
Average chord of rear elevator, ft	0.141
Area of rear-elevator balance, sq ft . . .	0.125
Average chord of rear-elevator balance, ft.	0.0496
Average trailing-edge angle, deg	16
c_{eR} , ft	0.1465
c_{eF} , ft	0.270
$\bar{c}_{eF}/\bar{c}_{eR}$	1.86
$\bar{c}_{bR}/\bar{c}_{eR}$	0.352

NATIONAL ADVISORY
COMMITTEE FOR AERONAUTICS

TABLE IV.— GEOMETRIC CHARACTERISTICS OF AIRFOILS 18 AND 19

Model	End plate	Span	Area (sq in.)	Aspect ratio	Tip	Corrections added to test data	
						$\Delta\alpha$	ΔC_L
Airfoil 18							
a	None	30.11	150.38	6.03	Faired	0.5670 _L	0.0740 _L
b	None	29.00	145.00	5.80	Rectangular	.5370 _L	.0760 _L
c	○	29.00	145.00	5.80	---do---	.5370 _L	.0760 _L
d	○○	29.00	145.00	5.80	---do---	.5370 _L	.0760 _L
e	○	29.00	145.00	5.30	---do---	.5370 _L	.0760 _L
f	None	23.61	117.88	4.73	Faired	.3880 _L	.0810 _L
g	None	22.50	112.50	4.50	Rectangular	.3610 _L	.0850 _L
h	○	22.50	112.50	4.50	---do---	.3610 _L	.0850 _L
i	○○	22.50	112.50	4.50	---do---	.3610 _L	.0850 _L
j	○	22.50	112.50	4.50	---do---	.3610 _L	.0850 _L
k	None	16.11	80.38	3.23	Faired	.2190 _L	.1190 _L
m	None	15.00	75.00	3.00	Rectangular	.1990 _L	.1280 _L
n	○	15.00	75.00	3.00	---do---	.1990 _L	.1280 _L
p	○○	15.00	75.00	3.00	---do---	.1990 _L	.1280 _L
q	○	15.00	75.00	3.00	---do---	.1990 _L	.1280 _L
r	None	8.59	42.88	1.72	Faired	.0930 _L	.2240 _L
s	None	7.50	37.50	1.50	Rectangular	.0780 _L	.2560 _L
t	○	7.50	37.50	1.50	---do---	.0780 _L	.2560 _L
u	○○	7.50	37.50	1.50	---do---	.0780 _L	.2560 _L
v	○○	7.50	37.50	1.50	---do---	.0780 _L	.2560 _L
Airfoil 19							
a	None	36.00	215.42	6.00	Elliptical	0.9610 _L	0.0450 _L
b	None	26.57	155.52	5.86	---do---	.5560 _L	.0620 _L
c	○	26.57	155.52	5.86	---do---	.5560 _L	.0620 _L
d	○○	26.57	155.52	5.86	---do---	.5560 _L	.0620 _L
e	○	26.57	155.52	5.86	---do---	.5560 _L	.0620 _L
f	None	23.18	148.61	6.41	Rectangular	.4930 _L	.0650 _L
g	None	16.57	91.15	5.51	Elliptical	.2540 _L	.1660 _L
h	○	16.57	91.15	5.51	---do---	.2540 _L	.1660 _L
i	○○	16.57	91.15	5.51	---do---	.2540 _L	.1660 _L
j	○	16.57	91.15	5.51	---do---	.2540 _L	.1660 _L
k	None	13.75	88.27	6.41	Rectangular	.2800 _L	.1430 _L
m	None	3.75	24.05	6.41	---do---	.0440 _L	.3990 _L
n	○	3.75	24.05	6.41	---do---	.0440 _L	.3990 _L
p	○○	3.75	24.05	6.41	---do---	.0440 _L	.3990 _L
q	○	3.75	24.05	6.41	---do---	.0440 _L	.3990 _L
r	None	12.82	67.25	5.23	Elliptical	.2320 _L	.1090 _L

TABLE V.- PARAMETER VALUES OF ISOLATED HORIZONTAL TAIL SURFACES

Model	C_{L_a}						C_{L_b}					
	Elevator gap open		Elevator gap sealed				Elevator gap open		Elevator gap sealed			
	Cut-out filled	Cut-out open	Cut-out filled	Cut-out open	Cut-out open	Cut-out open	Cut-out filled	Cut-out open	Cut-out filled	Cut-out open	Cut-out open	Cut-out open
1	0.052	0.052	0.055	0.055	0.055	0.055	0.030	0.025	0.031	0.030	-----	-----
2	-----	.052	-----	.056	.055	-----	-----	.030	-----	.033	-----	-----
3	.054	.052	.057	.056	.056	.056	.039	.030	.037	.029	-----	-----
4	.056	.057	.057	.057	.060	.060	.026	.023	.028	.026	-----	-----
5	.058	.059	.059	-----	.061	.061	.038	.029	.031	-----	-----	-----
6	.056	-----	.061	-----	.063	.063	.030	-----	.028	-----	-----	-----
7	.052	-----	.064	-----	.065	.065	.023	-----	.040	-----	-----	-----
8	.052	-----	.061	-----	.061	.061	.019	-----	.027	-----	-----	-----
9	.053	.055	-----	-----	-----	-----	.028	.027	-----	-----	-----	-----
10	-----	-----	-----	.058	-----	-----	-----	-----	-----	.032	-----	-----
11	-----	-----	-----	.060	-----	-----	-----	-----	-----	.033	-----	-----
12	.054	.054	.062	.060	.063	.063	.032	.029	.034	.031	-----	-----
13	-----	.057	-----	-----	.057	.057	-----	.034	-----	-----	-----	-----
14	.054	.053	-----	-----	-----	-----	.031	.029	^b .031	^b .031	-----	-----
14	-----	^b .064	^b .066	^b .065	^b .066	^b .066	-----	.032	-----	.037	-----	-----
15	-----	.055	-----	.060	.062	.062	-----	.032	-----	-----	-----	-----
16	-----	.053	-----	-----	.065	.065	-----	.031	-----	-----	-----	-----
16	-----	^b .064	-----	-----	-----	-----	-----	-----	-----	-----	-----	-----
17	-----	.054	-----	-----	-----	-----	-----	-----	-----	-----	-----	-----

^a Internal balance.^b End plates on.

TABLE V. - PARAMETER VALUES OF ISOLATED HORIZONTAL TAIL SURFACES - Concluded

Model	$C_{h\alpha}$				$C_{h\delta}$				$\Delta\alpha/\Delta\delta$			
	Elevator gap open		Elevator gap sealed		Elevator gap open		Elevator gap sealed		Elevator gap open		Elevator gap sealed	
	Cut-out filled	Cut-out open	Cut-out filled	Cut-out open	Cut-out filled	Cut-out open	Cut-out filled	Cut-out open	Cut-out filled	Cut-out open	Cut-out filled	Cut-out open
1	-0.0020	-0.0022	-0.0012	-0.0020	-0.0074	-0.0053	-0.0052	-0.0045	-0.62	-0.48	-0.65	-0.60
2	-----	-0.0010	-----	-0.0008	-----	-0.0063	-----	-0.0042	-----	-0.55	-----	-0.60
3	-.0028	-.0005	-.0028	-.0007	-.0081	-.0048	-.0079	-.0066	-.73	-.54	-.72	-.58
4	.0002	.0007	-.0002	.0001	-.0057	-.0057	-.0062	-.0059	-.46	-.42	-.50	-.46
5	-.0027	-.0020	-----	-.0022	-.0075	-.0065	-----	-----	-.60	-.52	-----	-.52
6	.0015	-----	.0012	-----	-.0022	-----	-.0032	-----	-.56	-----	-.48	-----
7	.0024	-----	.0005	-----	-.0006	-----	-.0010	-----	-.45	-----	-.54	-----
8	.0016	-----	-.0054	-----	-.0041	-----	-----	-----	-.38	-----	-----	-----
9	-.0014	-.0009	-----	-----	-.0048	-.0038	-----	-----	-.59	-.53	-----	-----
10	-----	-----	-----	-.0008	-----	-----	-----	-.0058	-----	-----	-----	^a -.55
11	-----	-----	-----	-.0010	-----	-----	-----	-.0059	-----	-----	-----	^a -.55
12	-.0022	-.0020	-.0008	-.0011	-.0050	-.0050	-.0039	-.0034	-.60	-.61	-.56	-.54
13	.0006	-----	-----	-----	-.0057	-----	-----	-----	-.55	-----	-----	-.58
14	-.0022	-.0013	-.0016	-.0009	-.0065	-.0040	-.0061	-.0032	-.53	-.50	^b -.51	^b -.51
15	-.0004	-----	-.0006	-----	-.0024	-----	-----	-----	-.55	-----	-.60	-----
16	-----	-----	-----	-----	-----	-----	-----	-----	-.53	-----	-.61	-----
17	.0002	-----	-----	-----	-.0024	-----	-----	-----	-.54	-----	-----	-----

^aInternal balance.^bEnd plates on.

Fig. 1

NATIONAL ADVISORY
COMMITTEE FOR AERONAUTICS

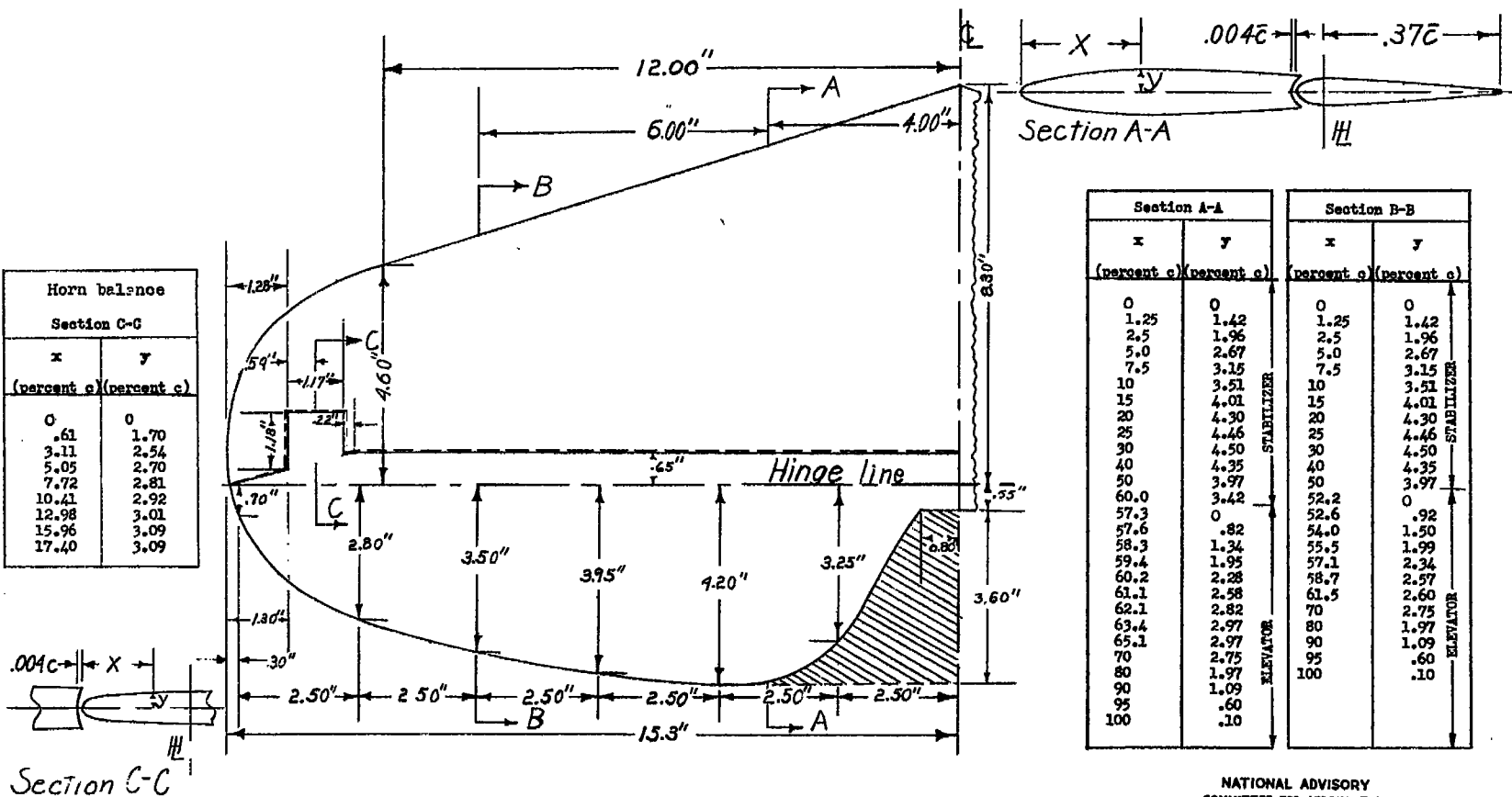


Figure 1.- Plan form of horizontal tail 1.

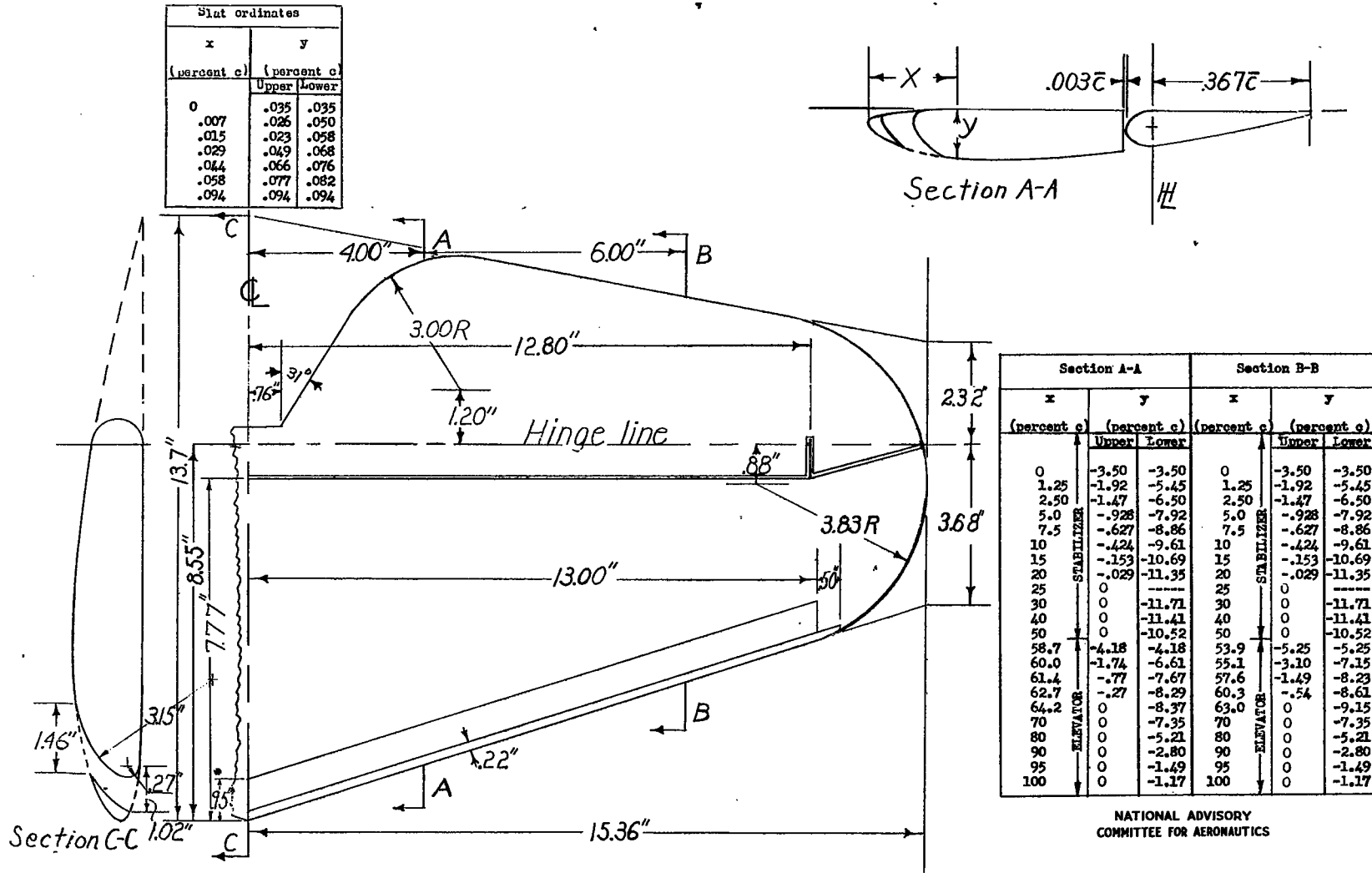


Figure 2.- Plan form of horizontal tail 2.

FIG. 3

NACA TN No. 1291

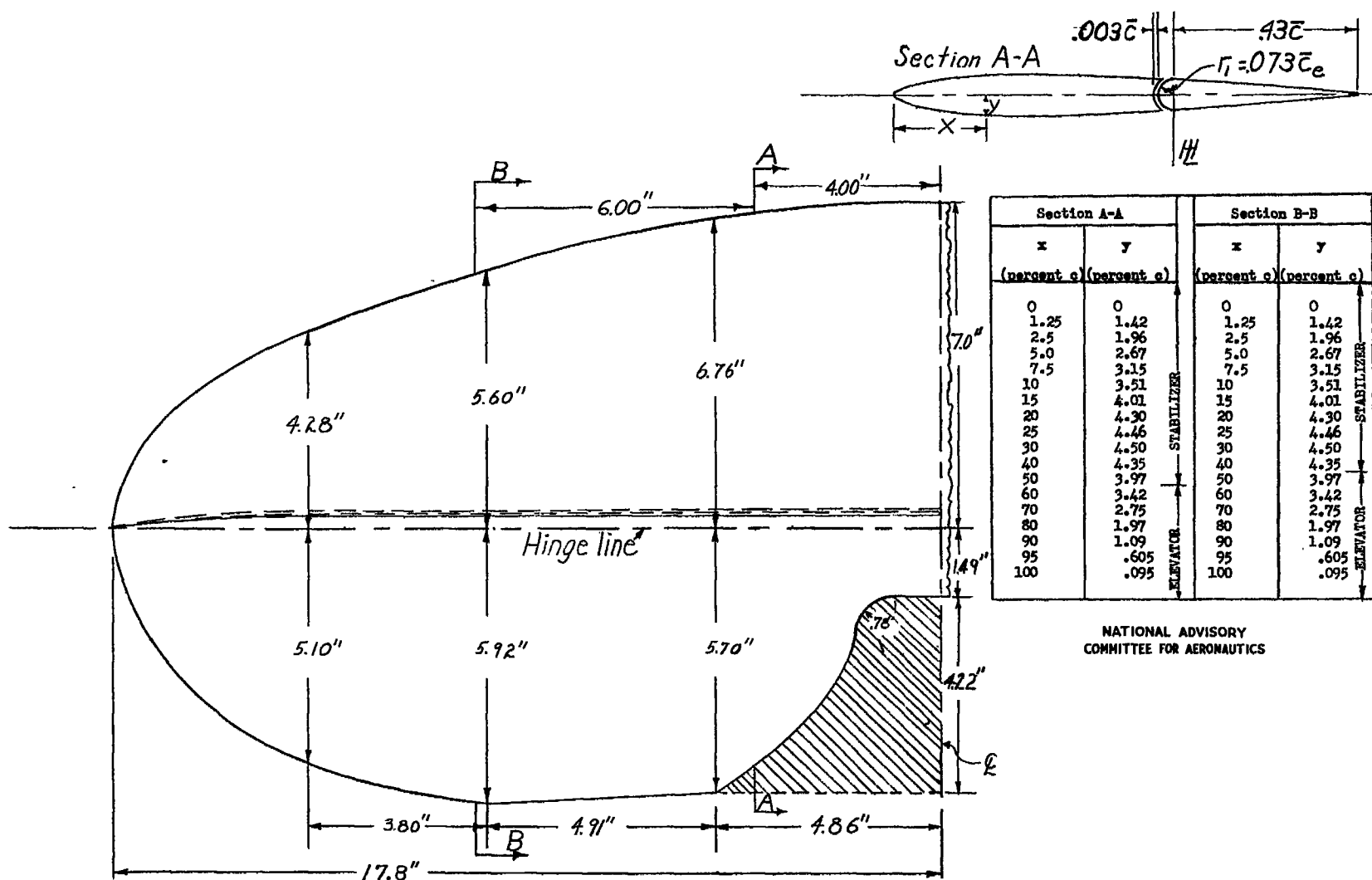


Figure 3.- Plan form of horizontal tail 3.

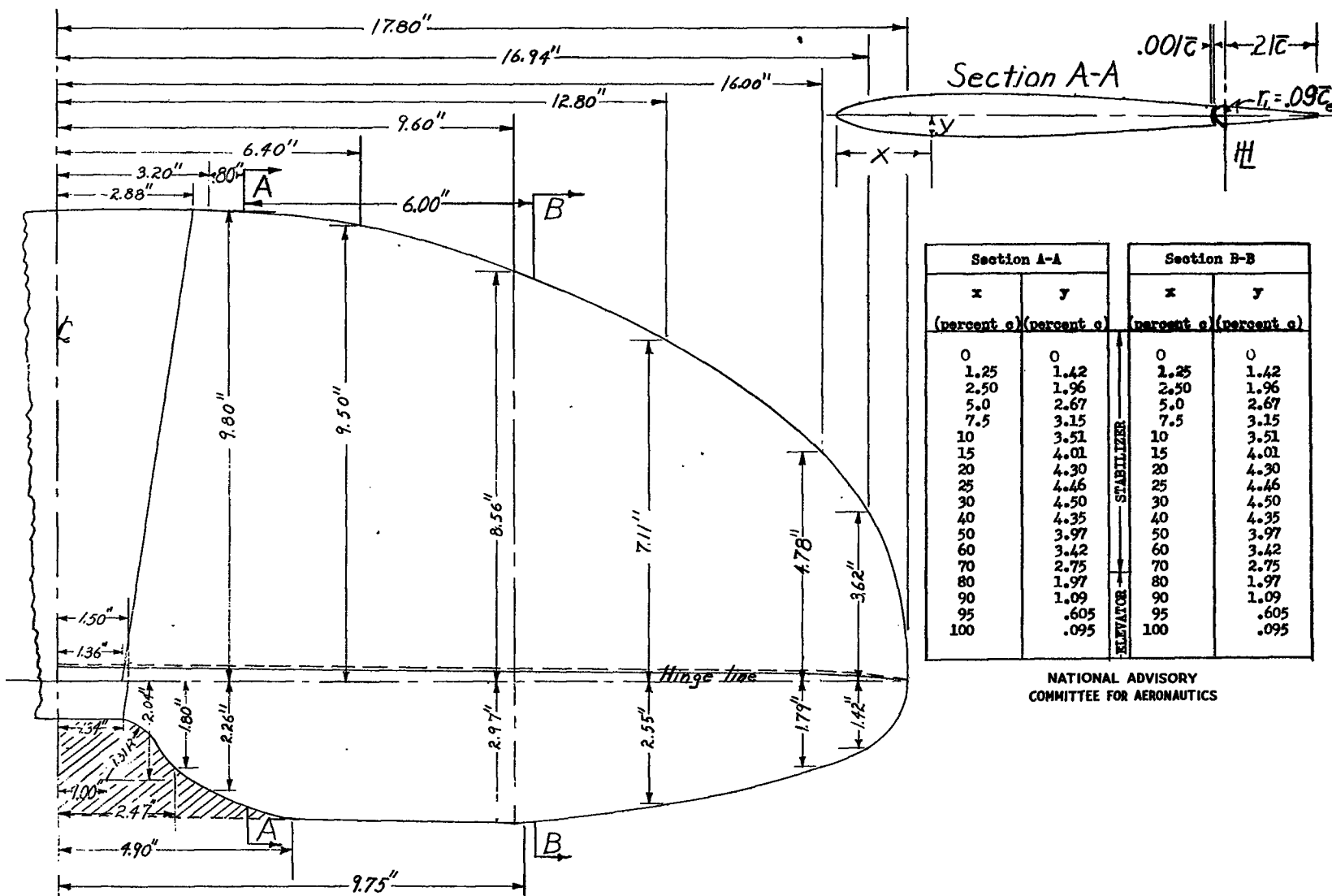


Figure 4.- Plan form of horizontal tail 4.

Fig. 5

NACA TN No. 1291

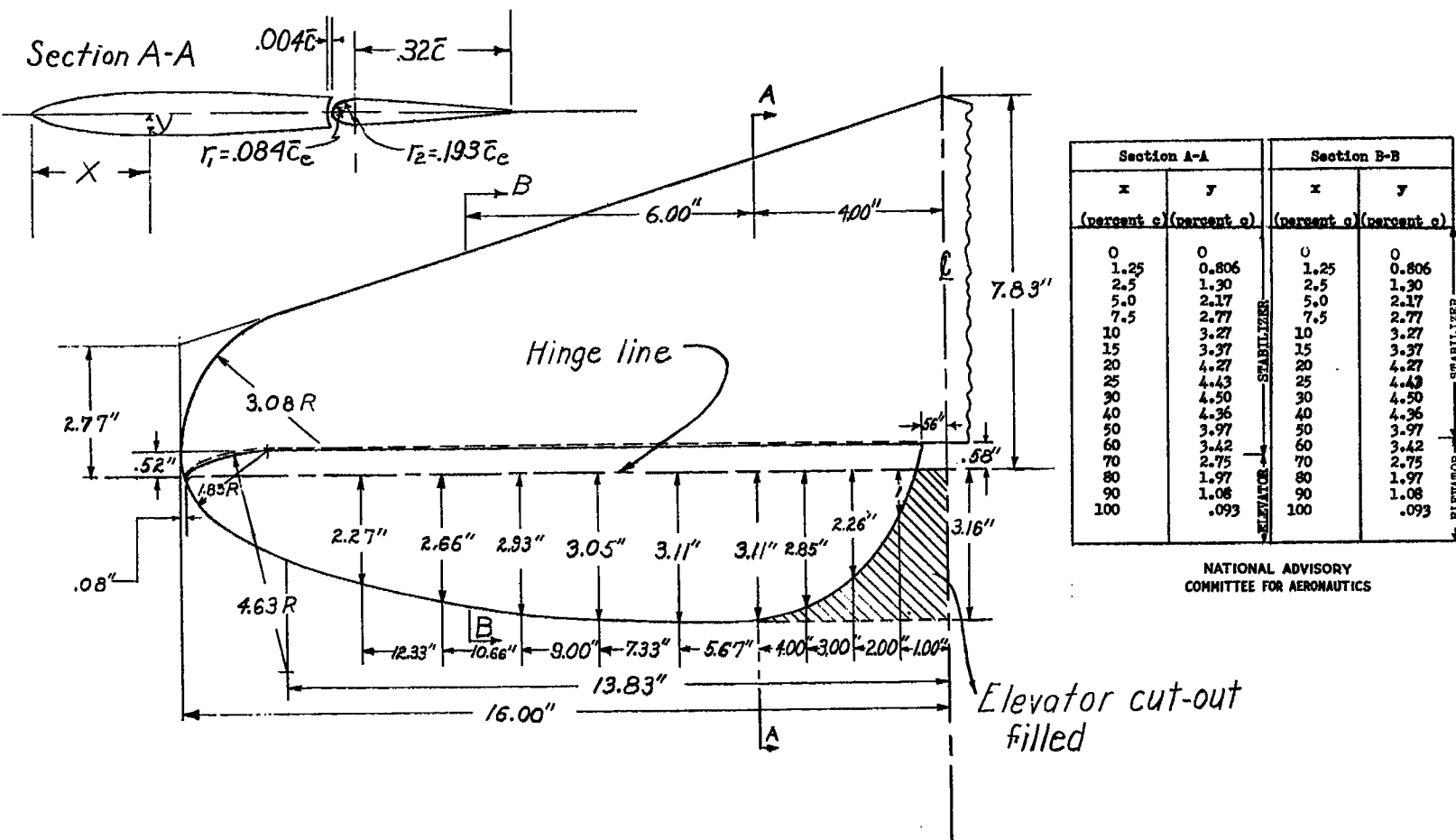


Figure 5.- Plan form of horizontal tail 5.

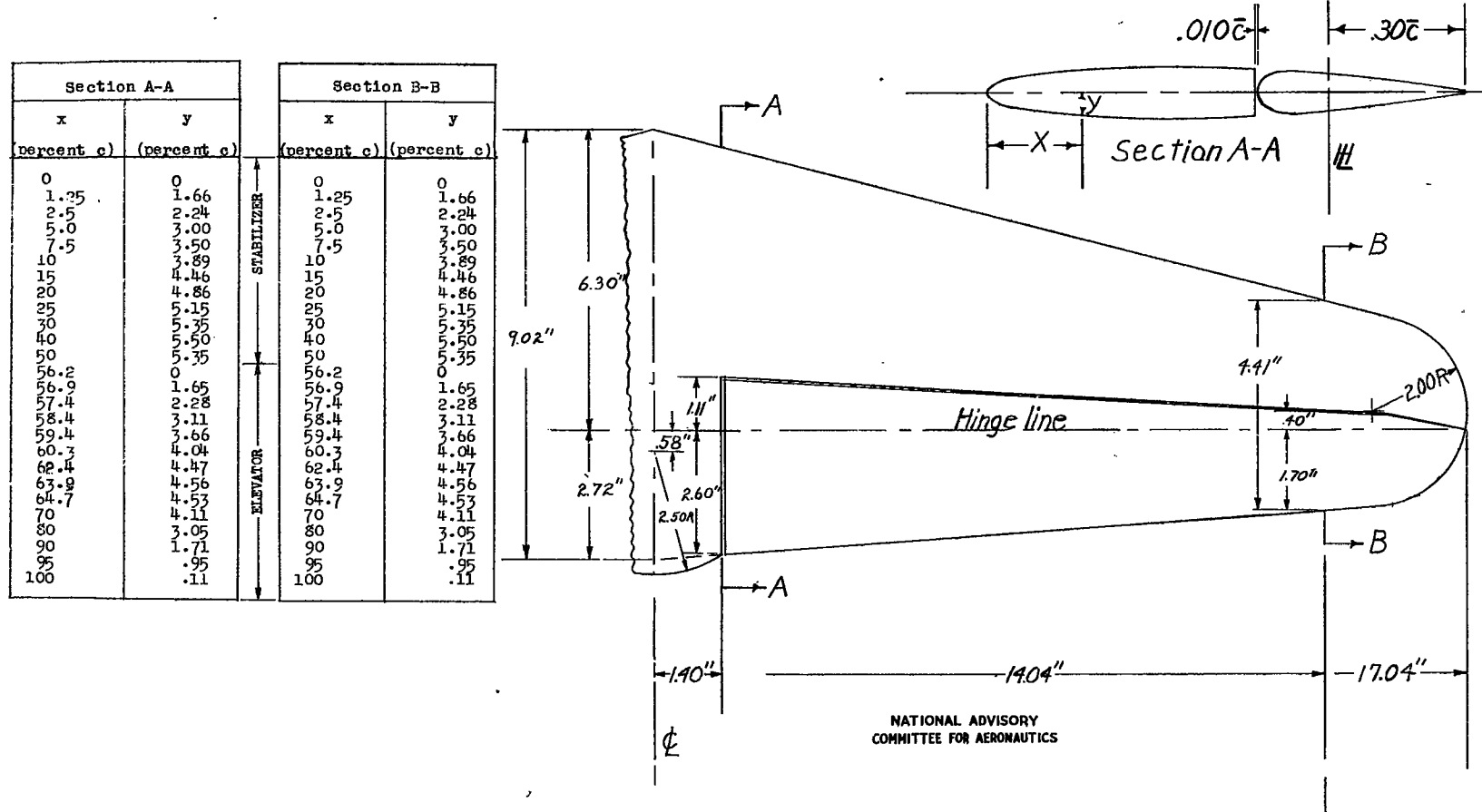


Figure 6.- Plan form of horizontal tail 6.

Fig. 7

NACA TN No. 1291

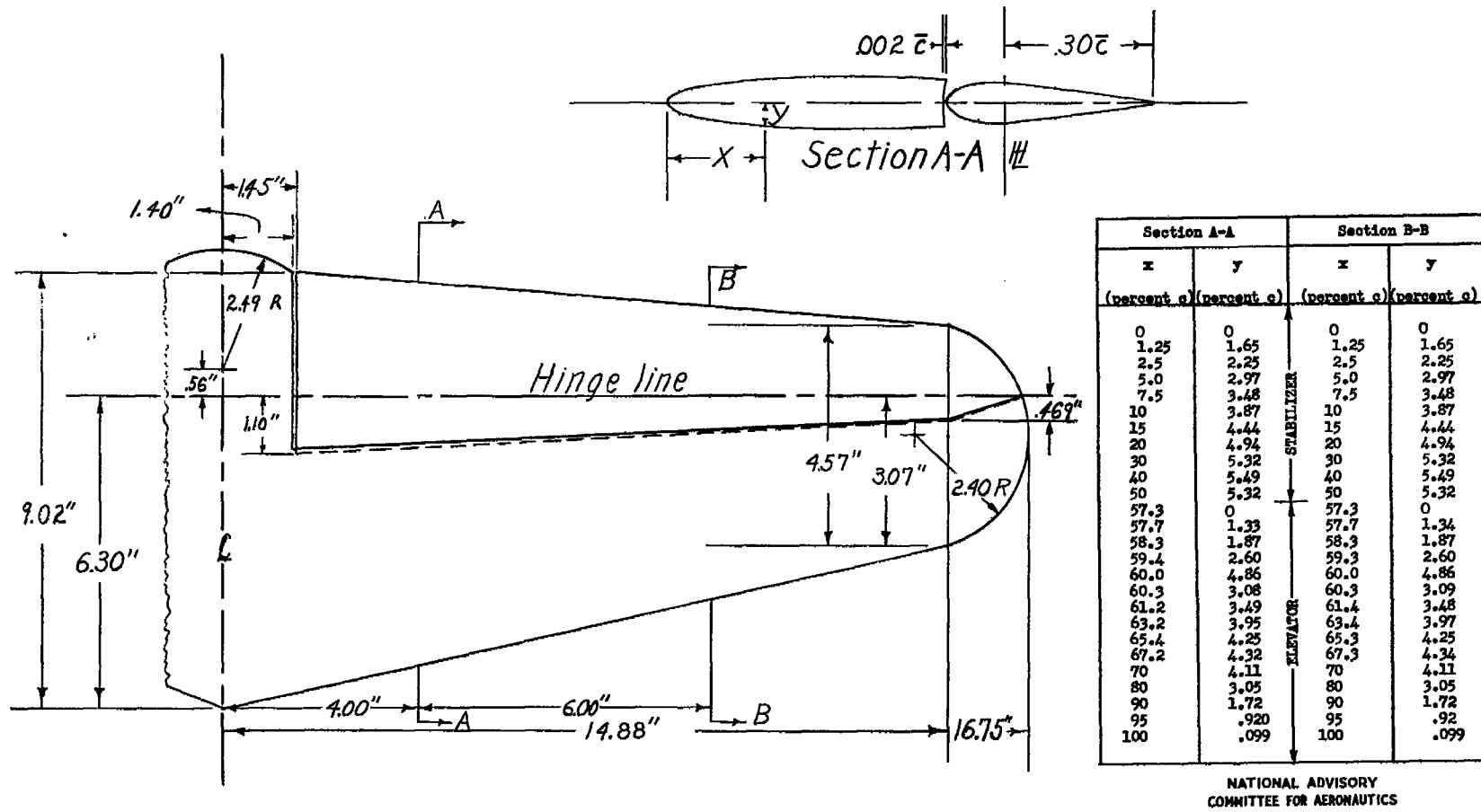


Figure 7.- Plan form of horizontal tail 7.

Section A-A		Section B-B	
x (percent c)	y (percent c)	x (percent c)	y (percent c)
0	0	0	0
1.25	1.65	1.25	1.65
2.5	2.25	2.5	2.25
5.0	2.97	5.0	2.97
7.5	3.48	7.5	3.48
10	3.87	10	3.87
15	4.44	15	4.44
20	4.94	20	4.94
30	5.32	30	5.32
40	5.49	40	5.49
50	5.32	50	5.32
60	4.86	60	4.86
63.7	0	63.7	0
62.9	.58	63.9	.532
63.1	1.16	64.1	1.06
63.7	1.74	64.3	1.59
64.3	2.32	65.0	2.13
65.3	2.90	65.7	2.68
66.7	3.48	67.0	3.19
69.4	3.94	70.4	3.83
70.9	4.06	71.7	3.90
72.4	3.94	73.2	3.83
80	3.05	80	3.05
90	1.72	90	1.72
95	.92	95	.92
100	.099	100	.099

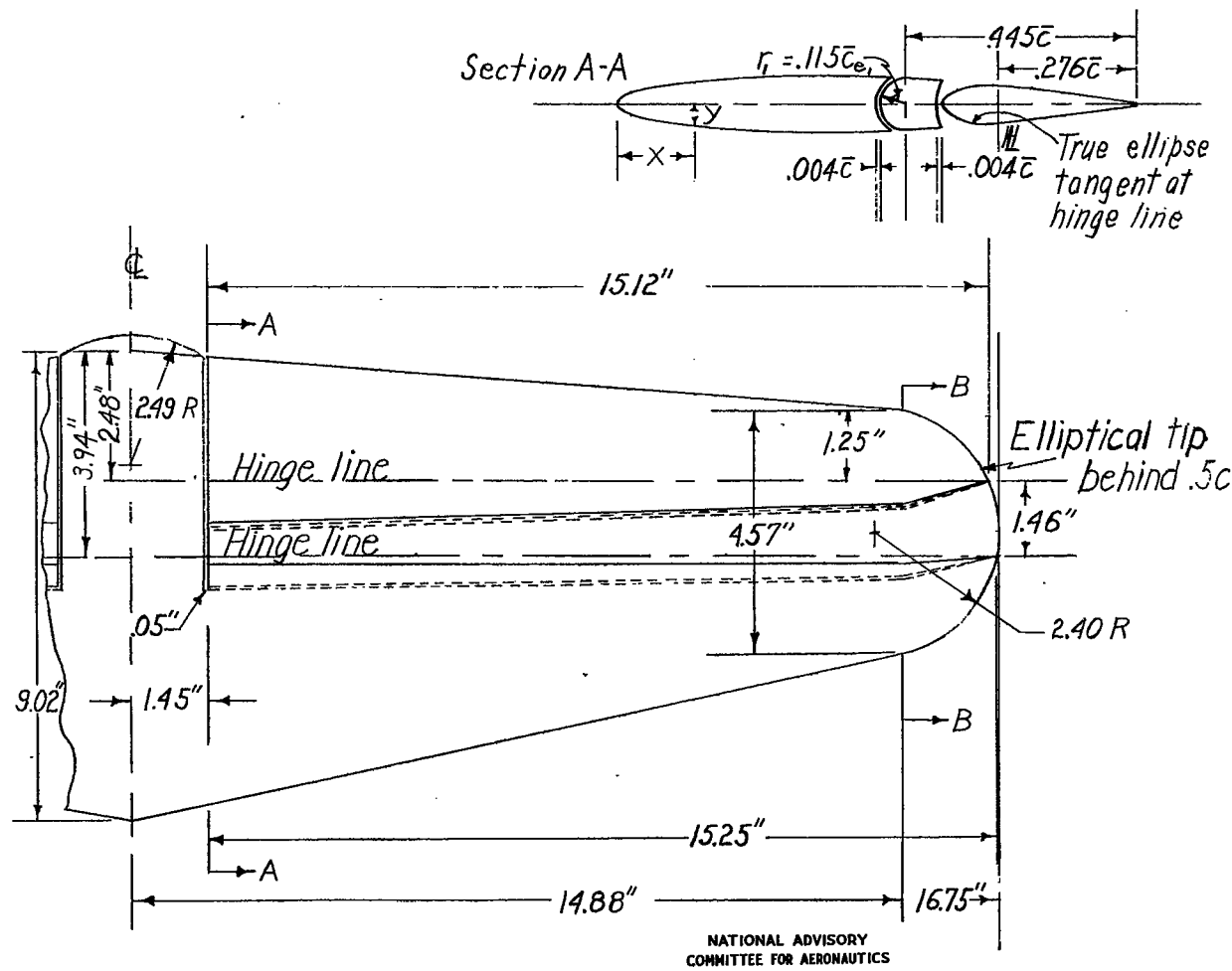
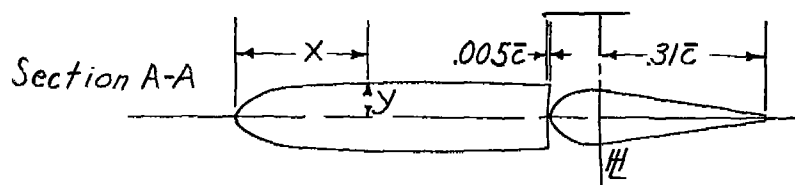


Figure 8.- Plan form of horizontal tail 8.

Fig. 9

NACA TN No. 1291



Section A-A	
x (percent c)	y (percent c)
0	0
1.25	2.02
2.5	2.74
5.0	3.65
7.5	4.27
10	5.74
15	5.44
20	5.92
25	6.27
30	6.51
40	6.70
50	6.51
59.8	0
50	5.95
50.1	1.63
60.9	2.59
62.1	3.54
64.3	4.51
66.2	4.86
70	5.00
80	3.72
90	2.09
95	1.15
100	.13

Section B-B	
x (percent c)	y (percent c)
0	0
1.25	1.58
2.5	2.14
5.0	2.86
7.5	3.24
10	3.72
15	4.25
20	4.63
25	4.91
30	5.11
40	5.25
50	5.11
50.5	0
50.6	.99
51.3	2.16
52.9	3.33
56.3	4.30
60	4.66
70	3.92
80	2.92
90	1.64
95	.901
100	.105

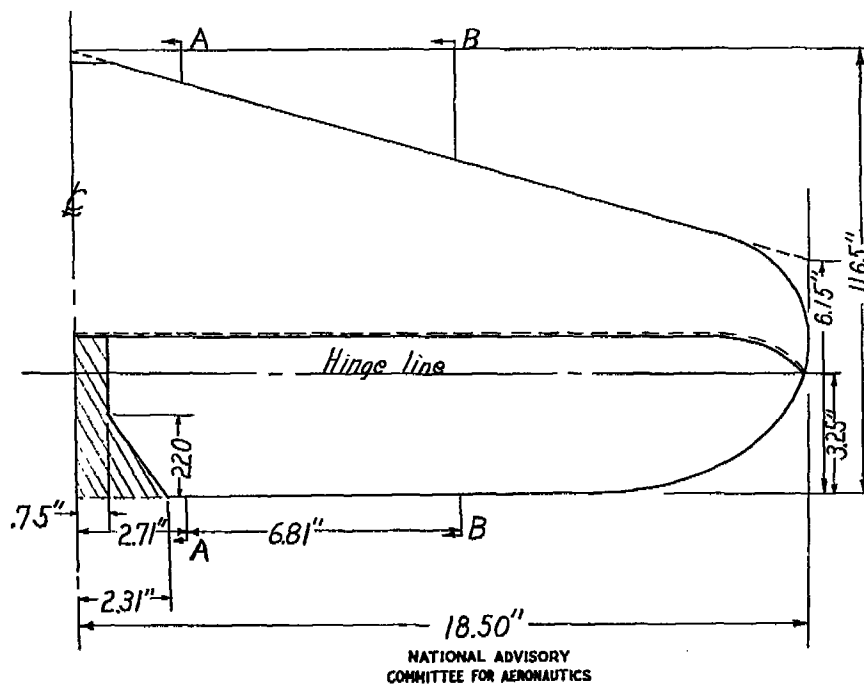


Figure 9.- Plan form of horizontal tail 9.

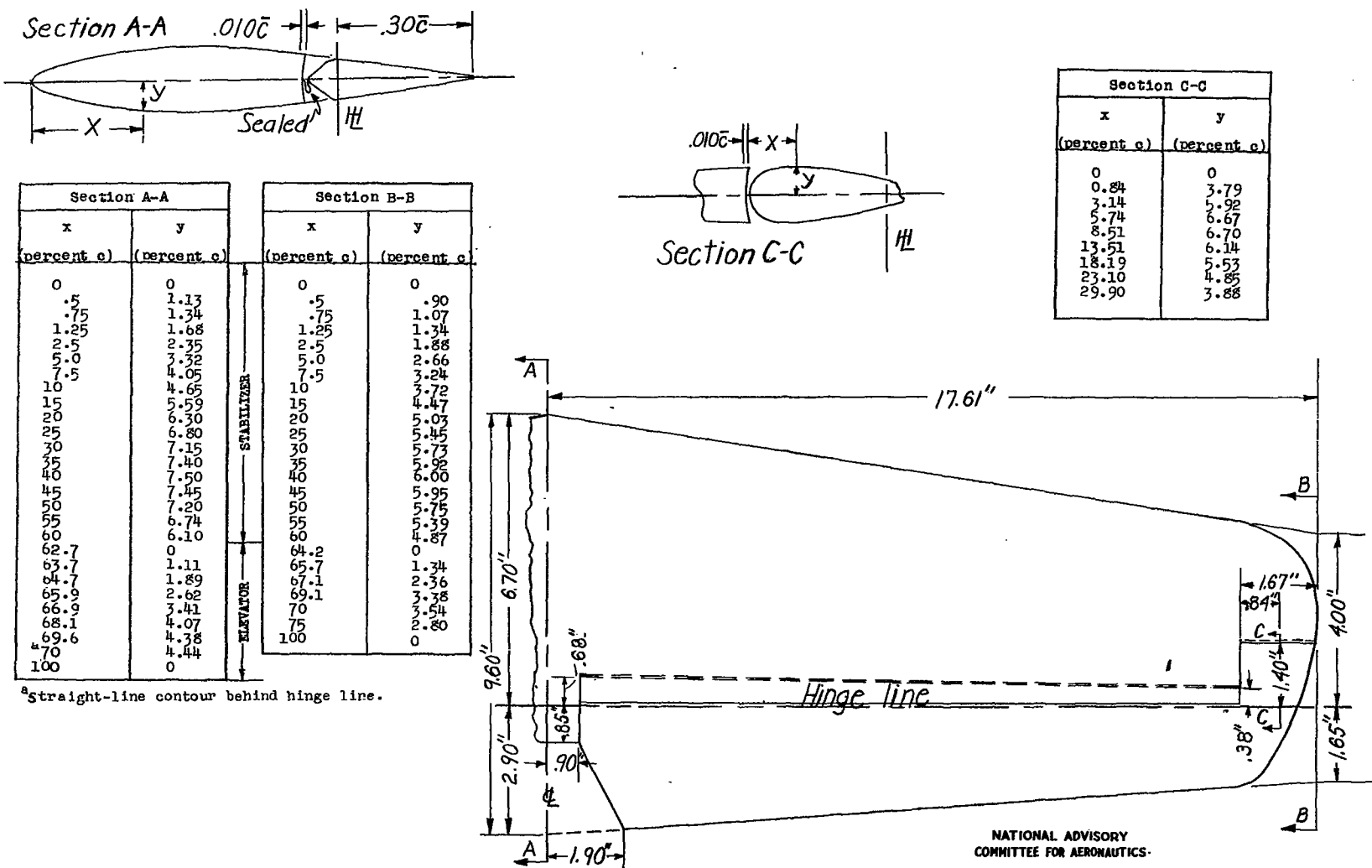


Figure 10.- Plan form of horizontal tail 10.

Fig. 11

NACA TN No. 1291

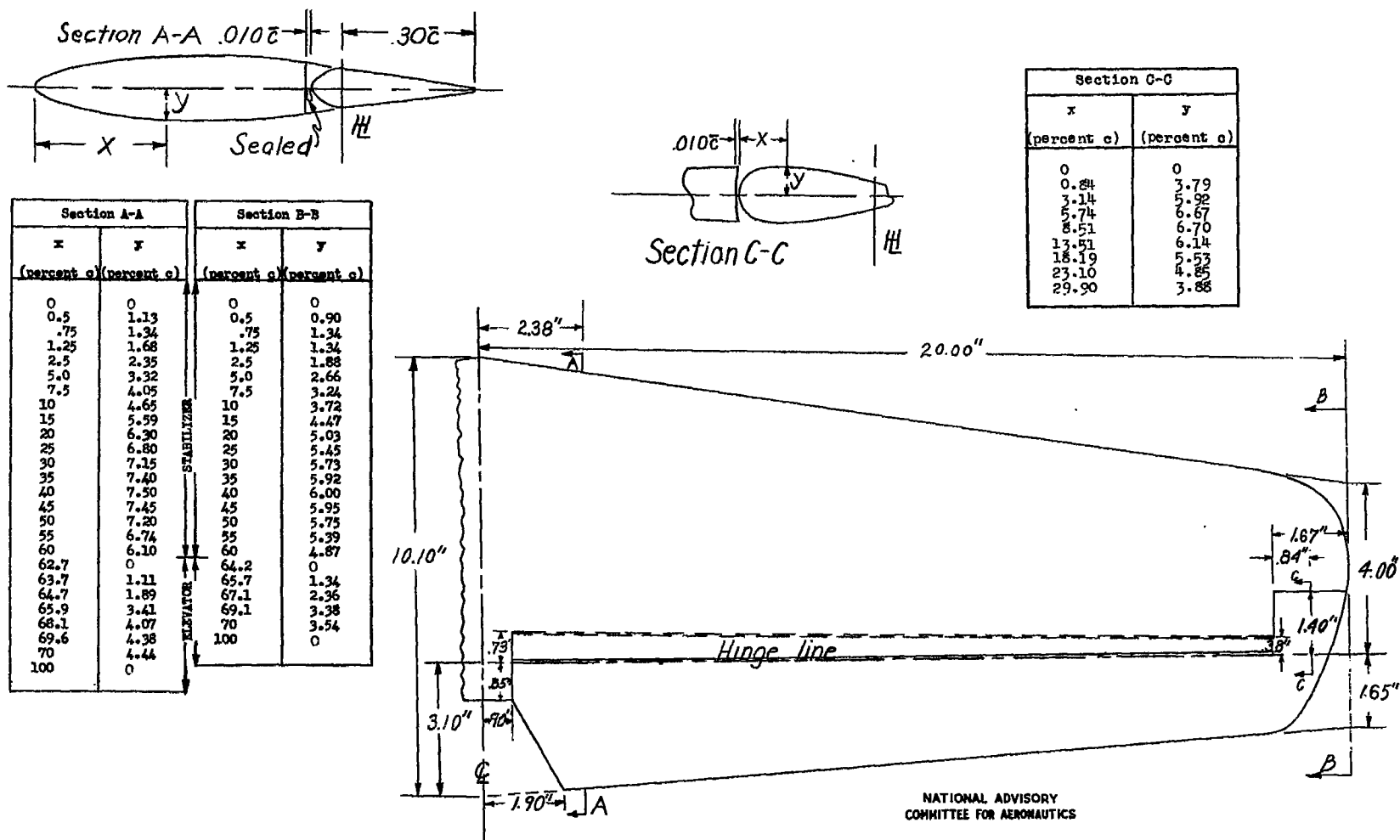


Figure 11.- Plan form of horizontal tail 11.

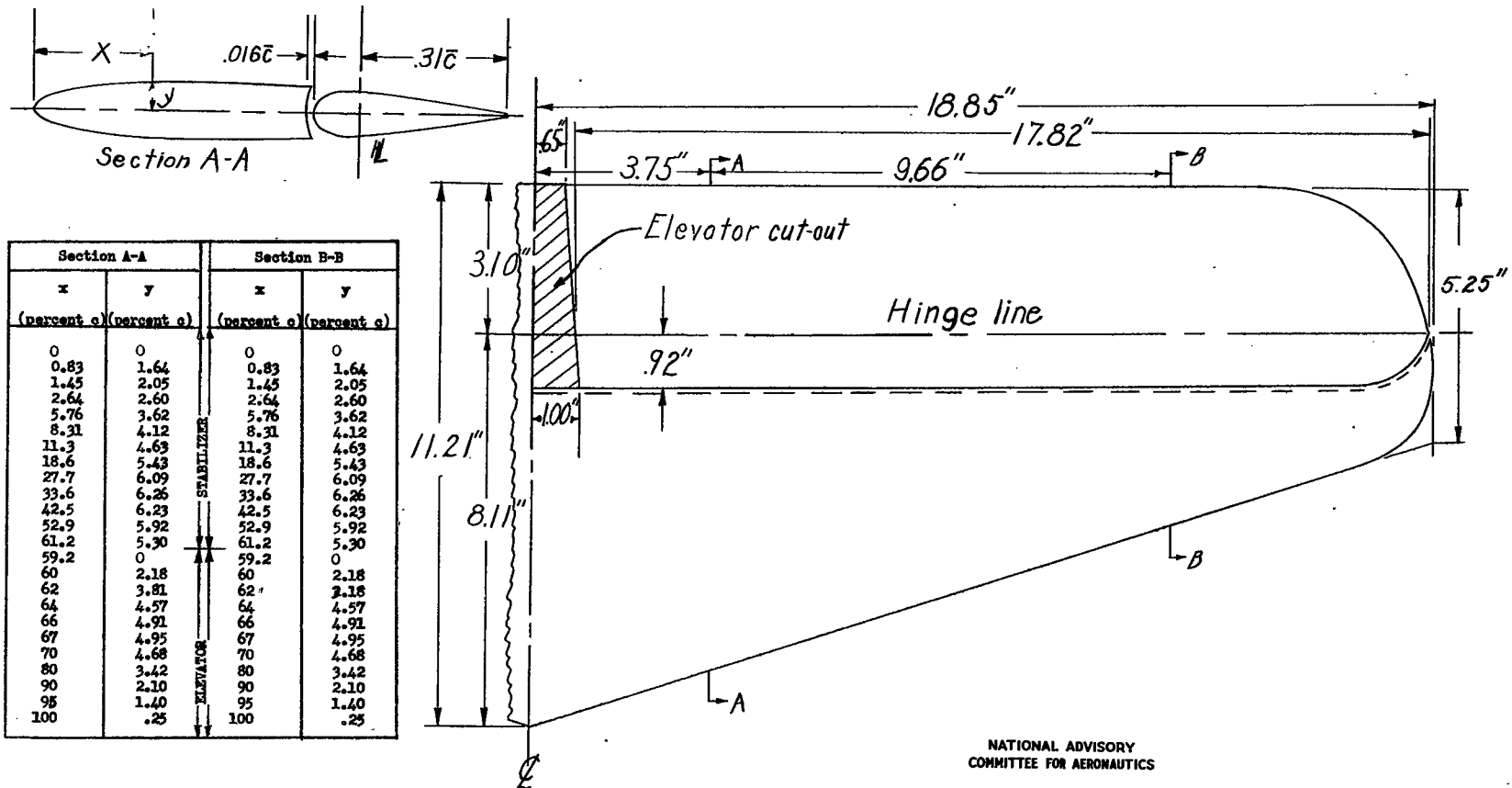


Figure 12.- Plan form of horizontal tail 12.

Fig. 13

NACA TN No. 1291

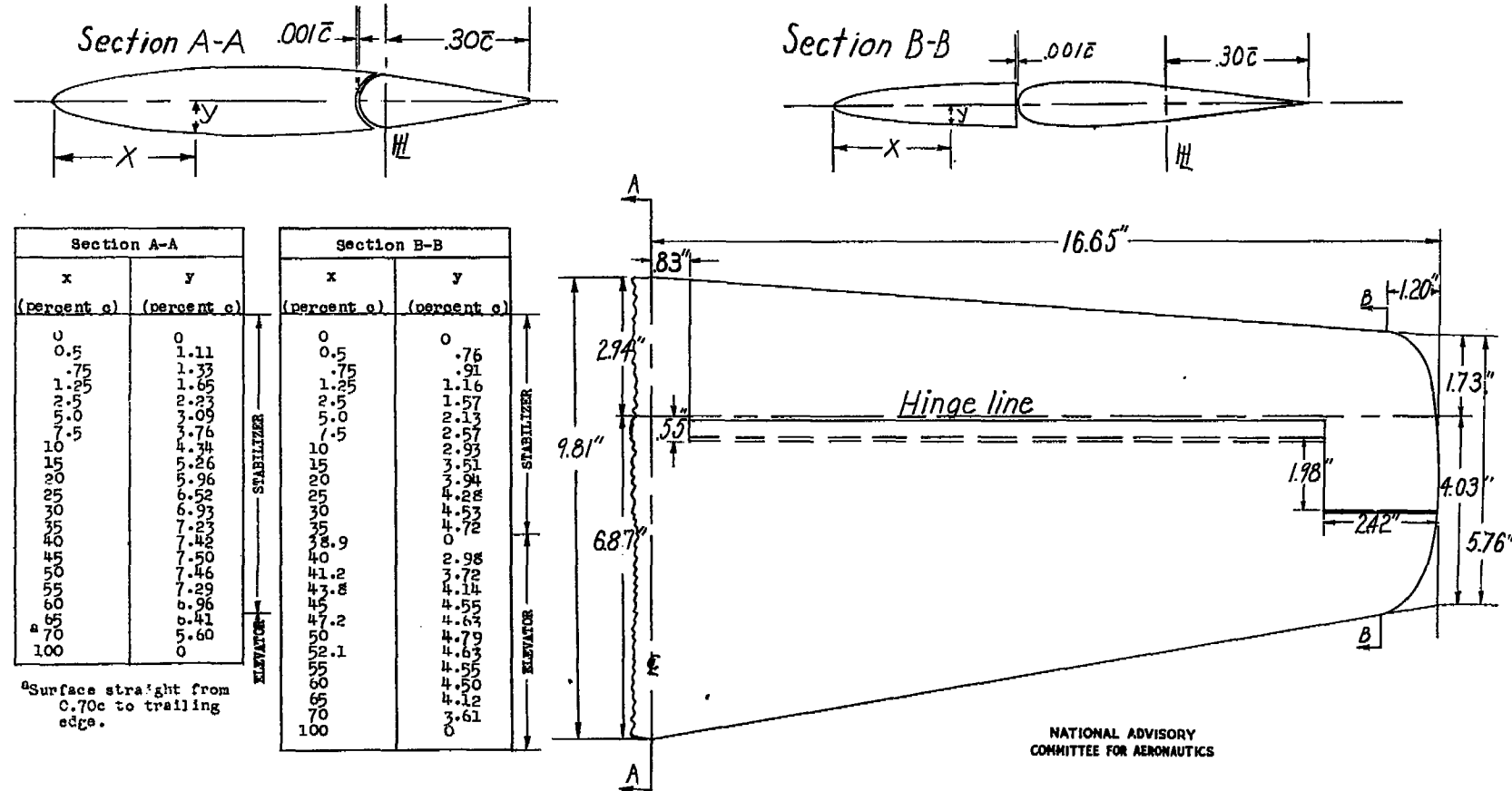


Figure 13.- Plan form of horizontal tail 13.

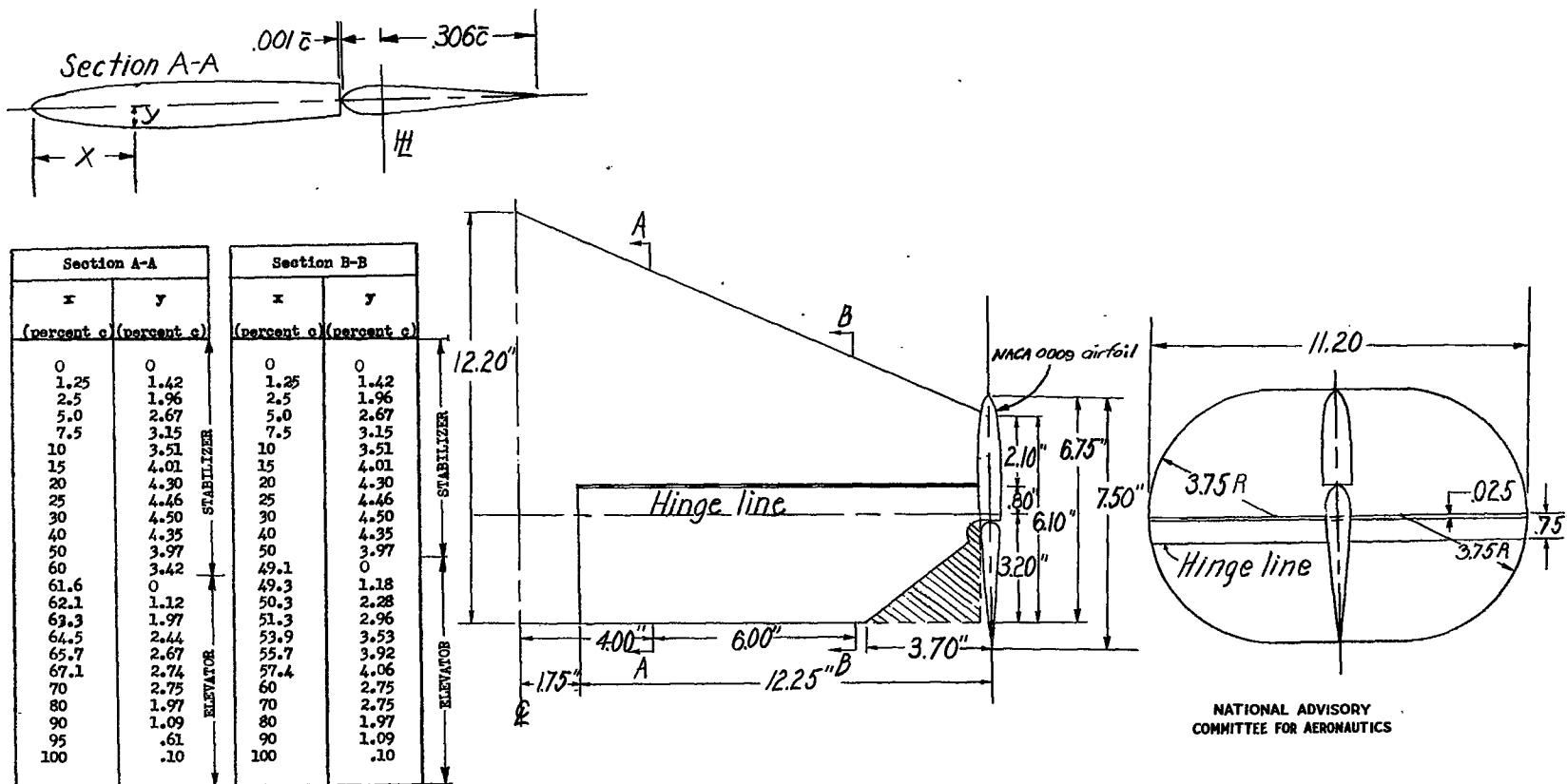
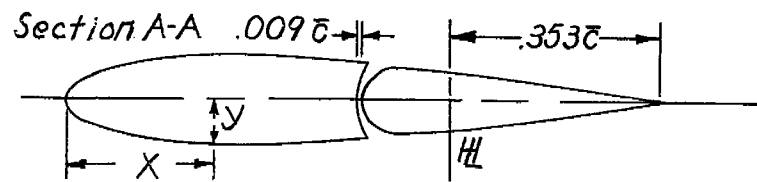


Figure 14.- Plan form of horizontal tail 14.

Fig. 15

NACA TN No. 1291



Section A-A		Section B-B	
x (percent c)	y (percent c)	x (percent c)	y (percent c)
0	0	0	0
1.25	2.39	1.25	1.27
2.5	3.32	2.5	1.77
5.0	4.53	5.0	2.42
7.5	5.36	7.5	2.86
10	5.36	10	3.18
15	6.77	15	3.61
20	7.25	20	3.86
25	7.45	25	3.97
30	7.51	30	4.00
40	7.32	40	3.90
50	6.77	50	3.61
50	0	49.2	0
50.3	2.05	50.1	1.54
51.3	3.69	51.4	2.41
53.3	5.07	53.2	2.93
55.2	5.77	55.3	3.25
57.3	6.18	57.3	3.39
60	5.90	60	3.15
70	4.77	70	2.54
80	3.40	80	1.81
90	1.85	90	.99
95	1.01	95	.54
100	.15	100	.08

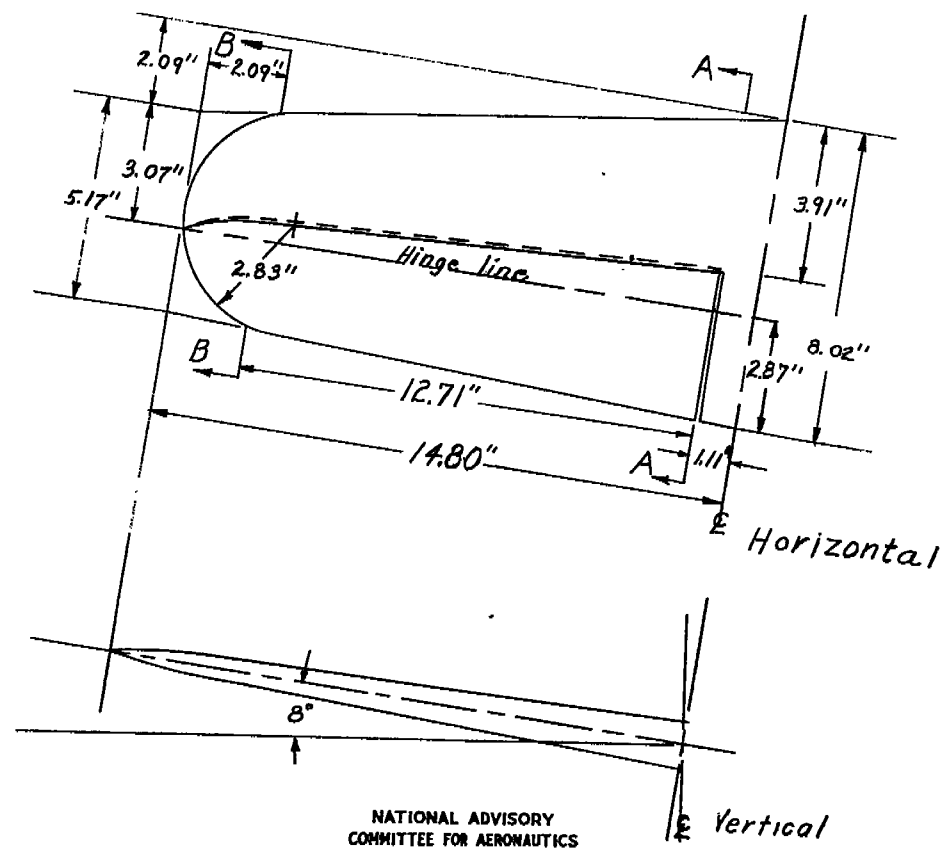


Figure 15.- Plan form of horizontal tail 15.

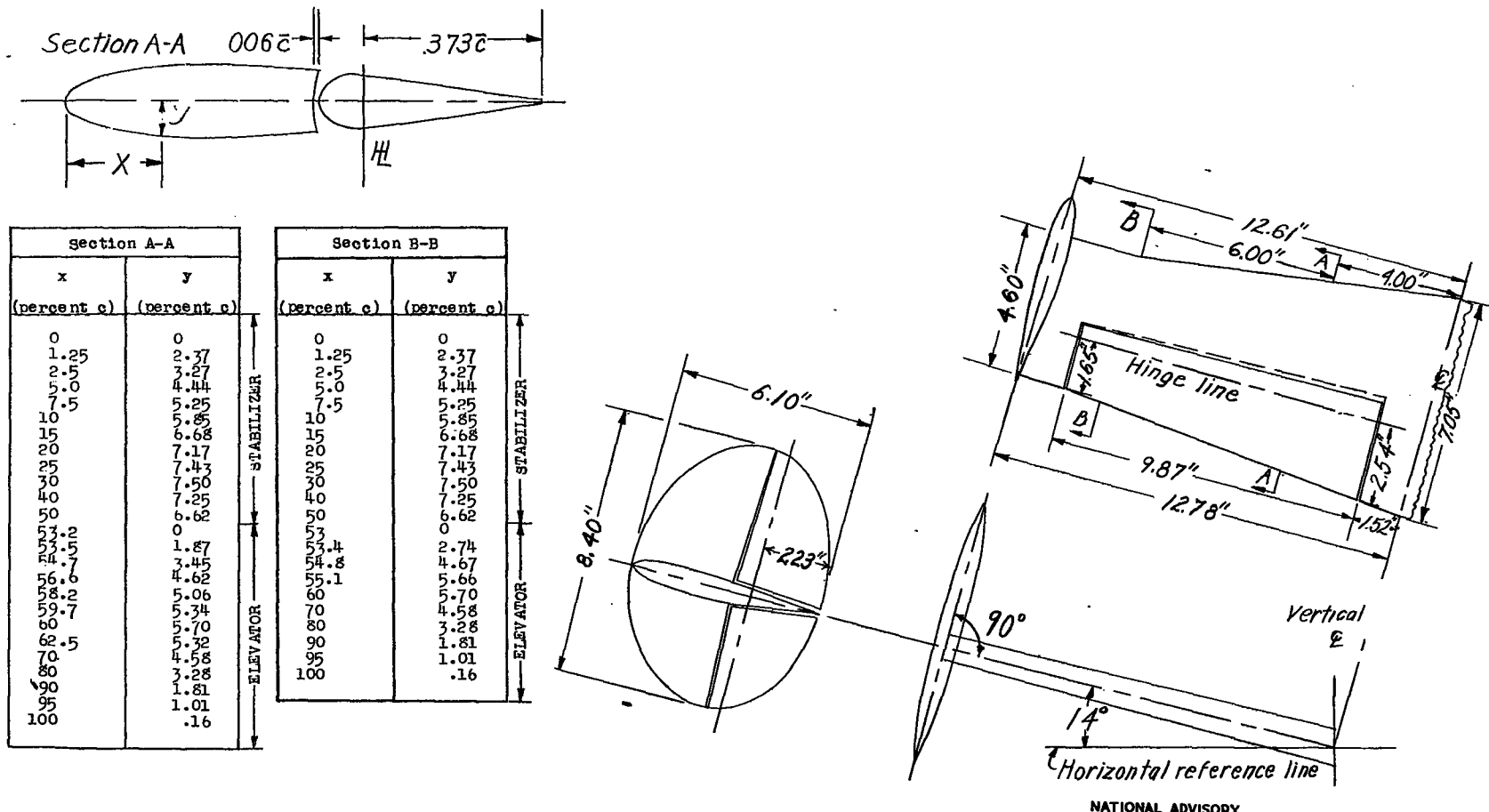


Figure 16.- Plan form of horizontal tail 16.

NATIONAL ADVISORY
COMMITTEE FOR AERONAUTICS

Fig. 17

NACA TN No. 1291

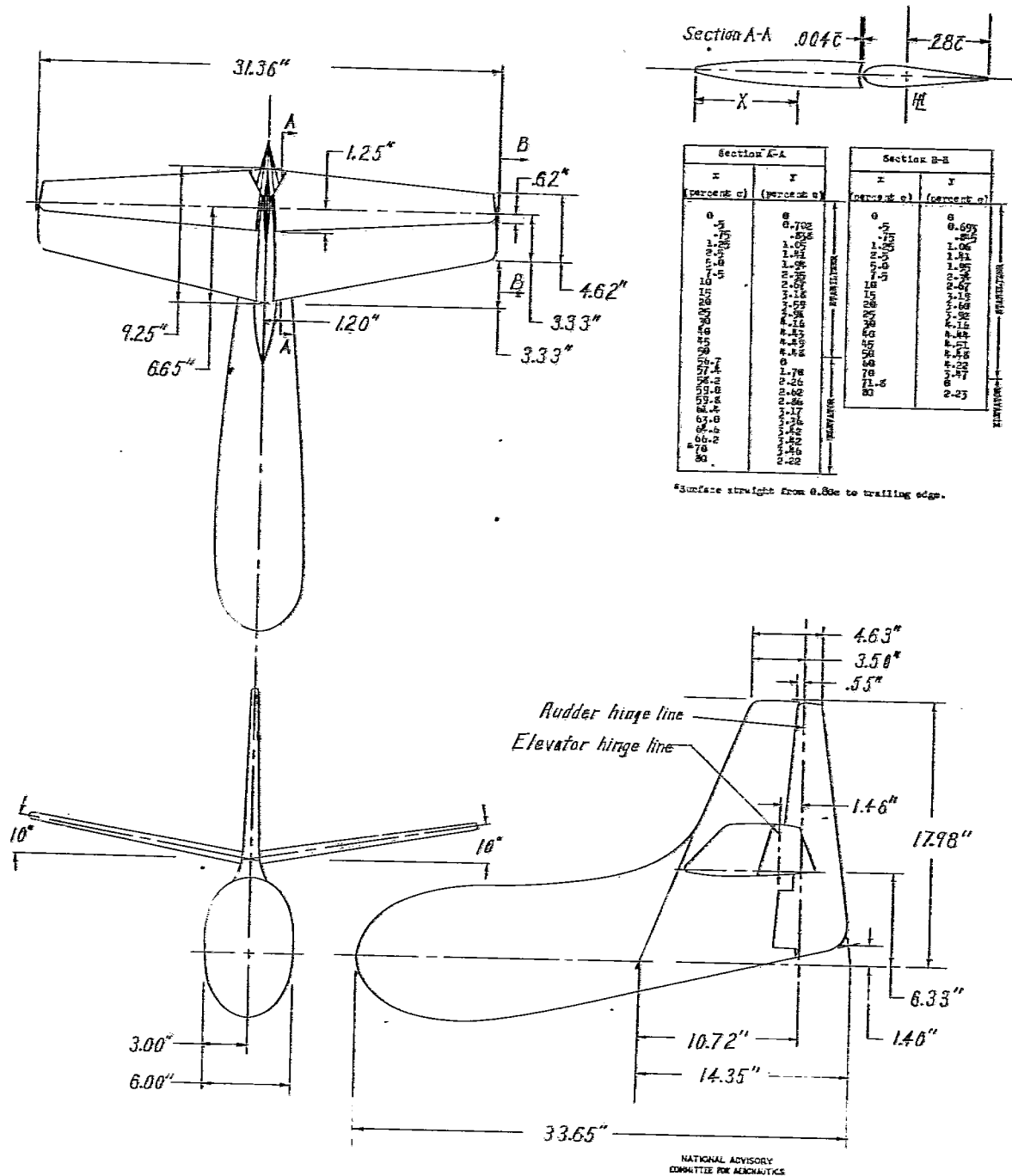


Figure 17.- Three-view drawing of horizontal tail 17.

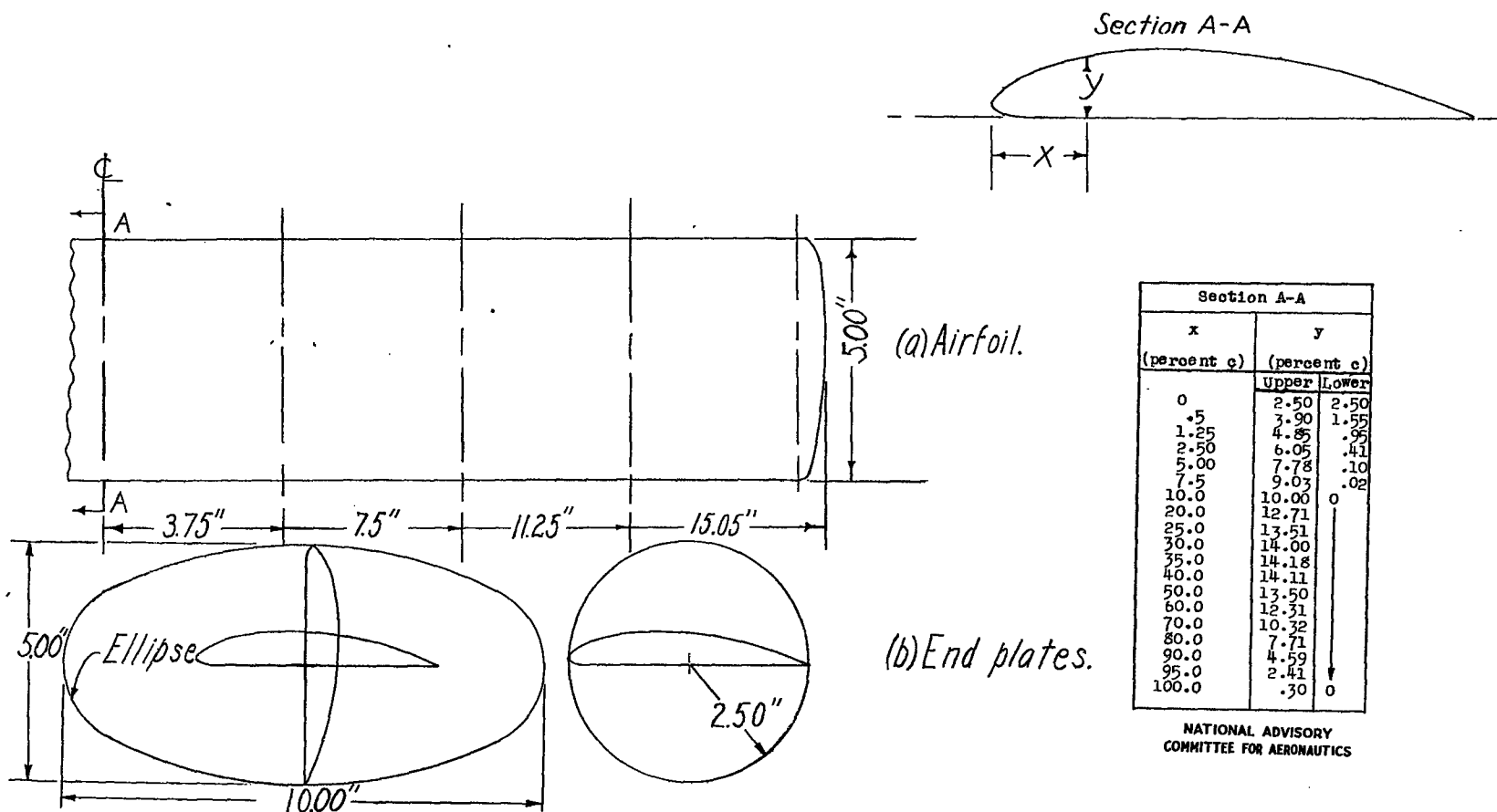


Figure 18.- Plan form of horizontal tail 18.

Fig. 19

NACA TN No. 1291

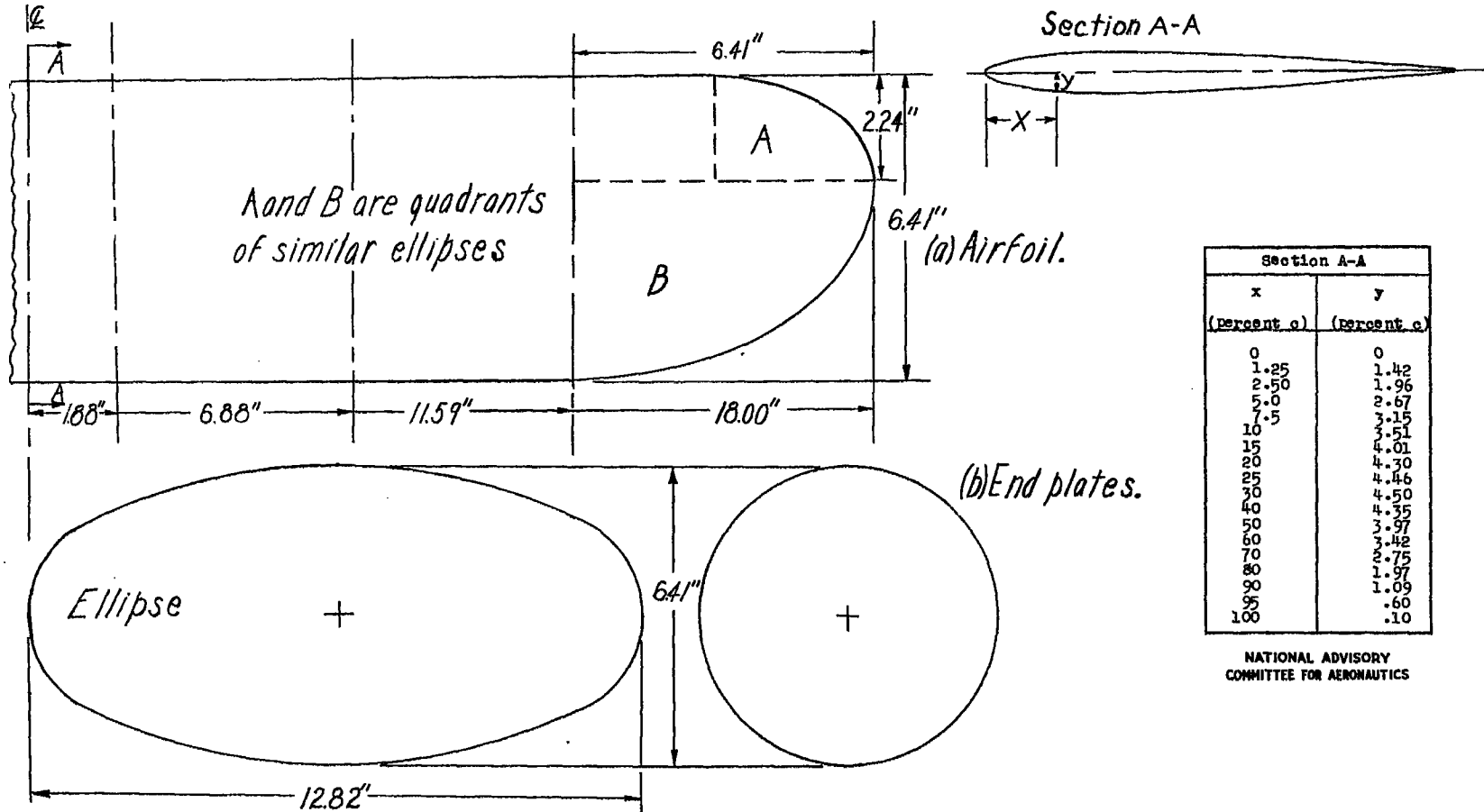


Figure 19.- Plan form of horizontal tail 19.

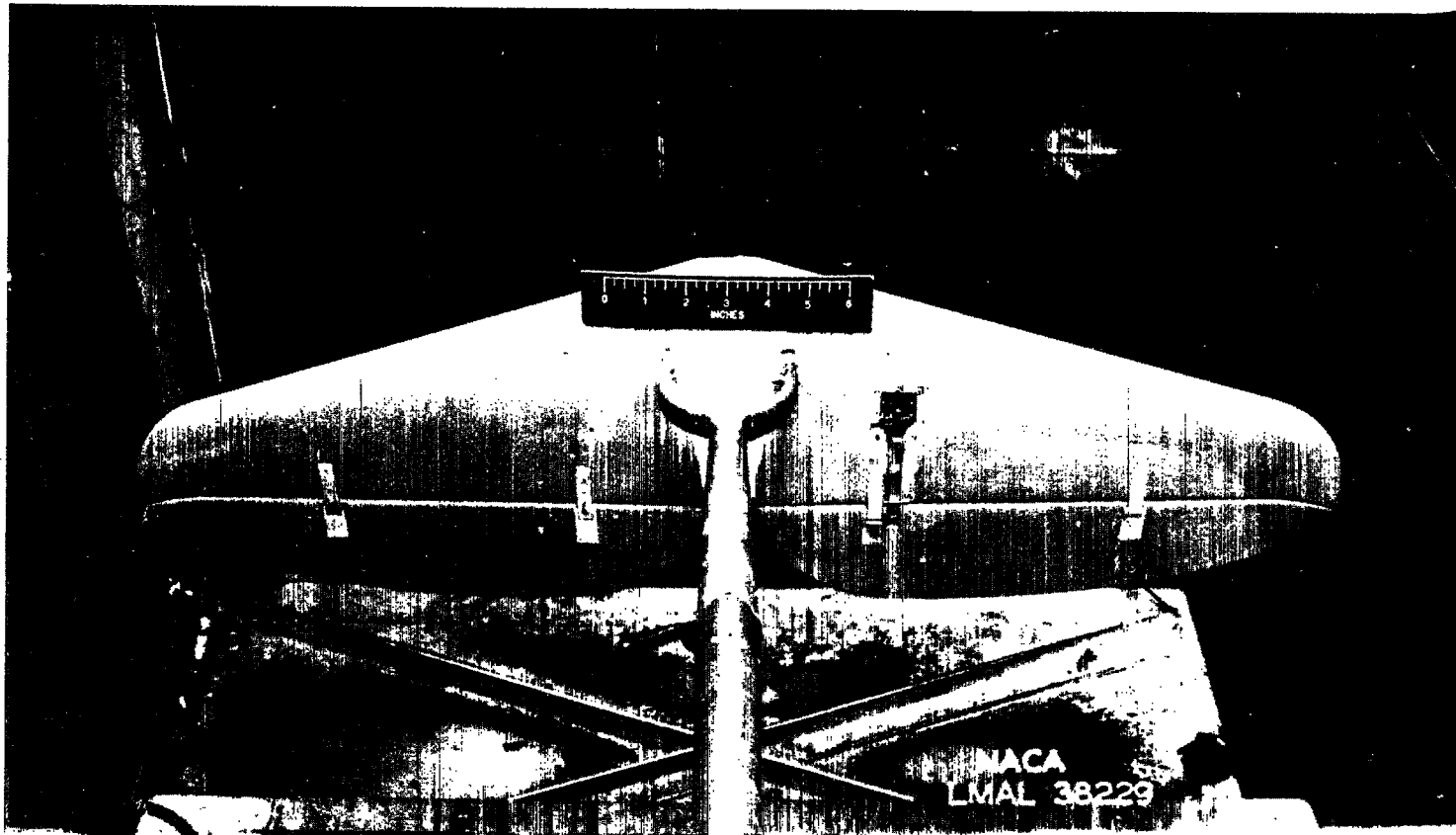
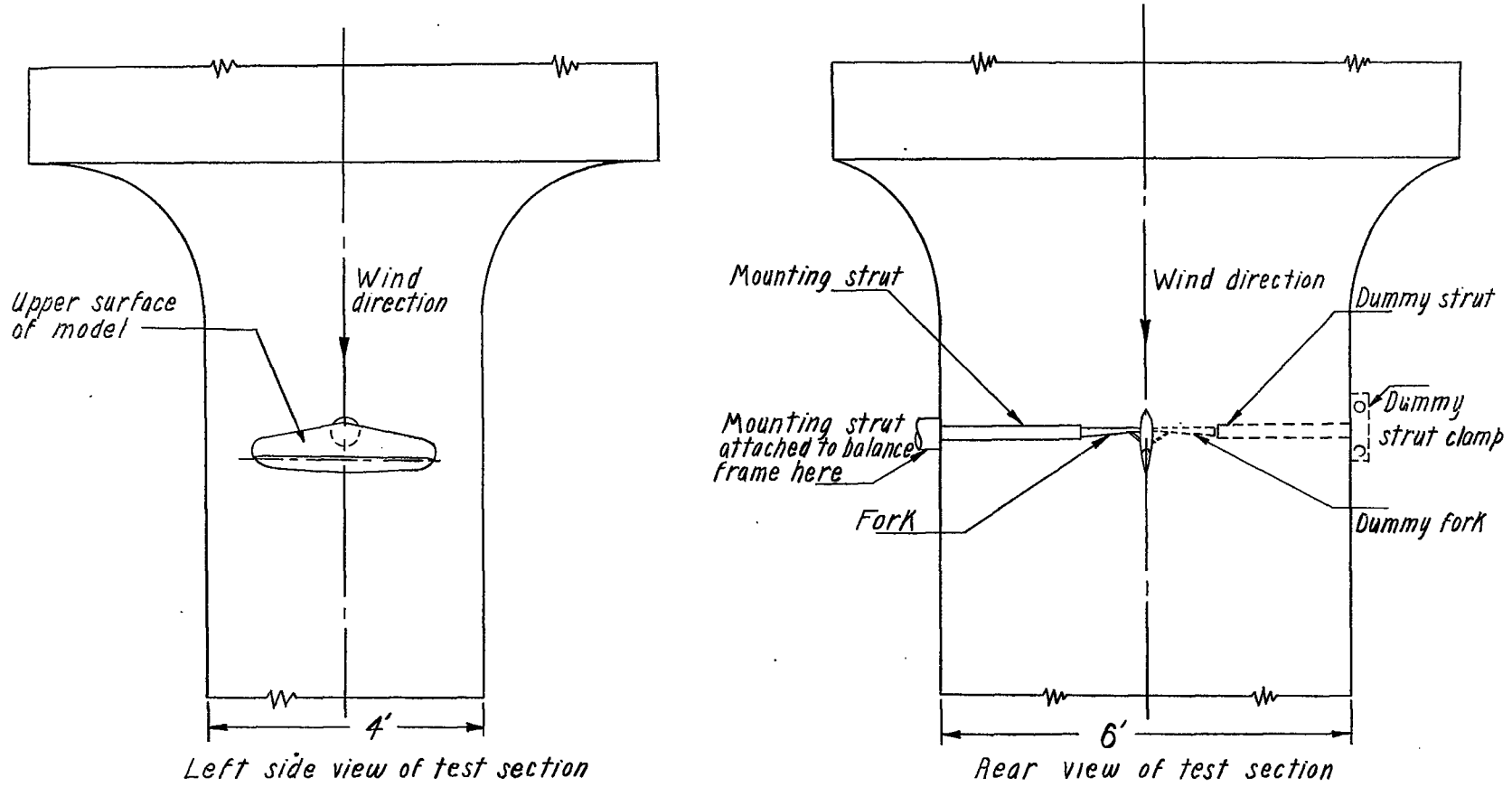
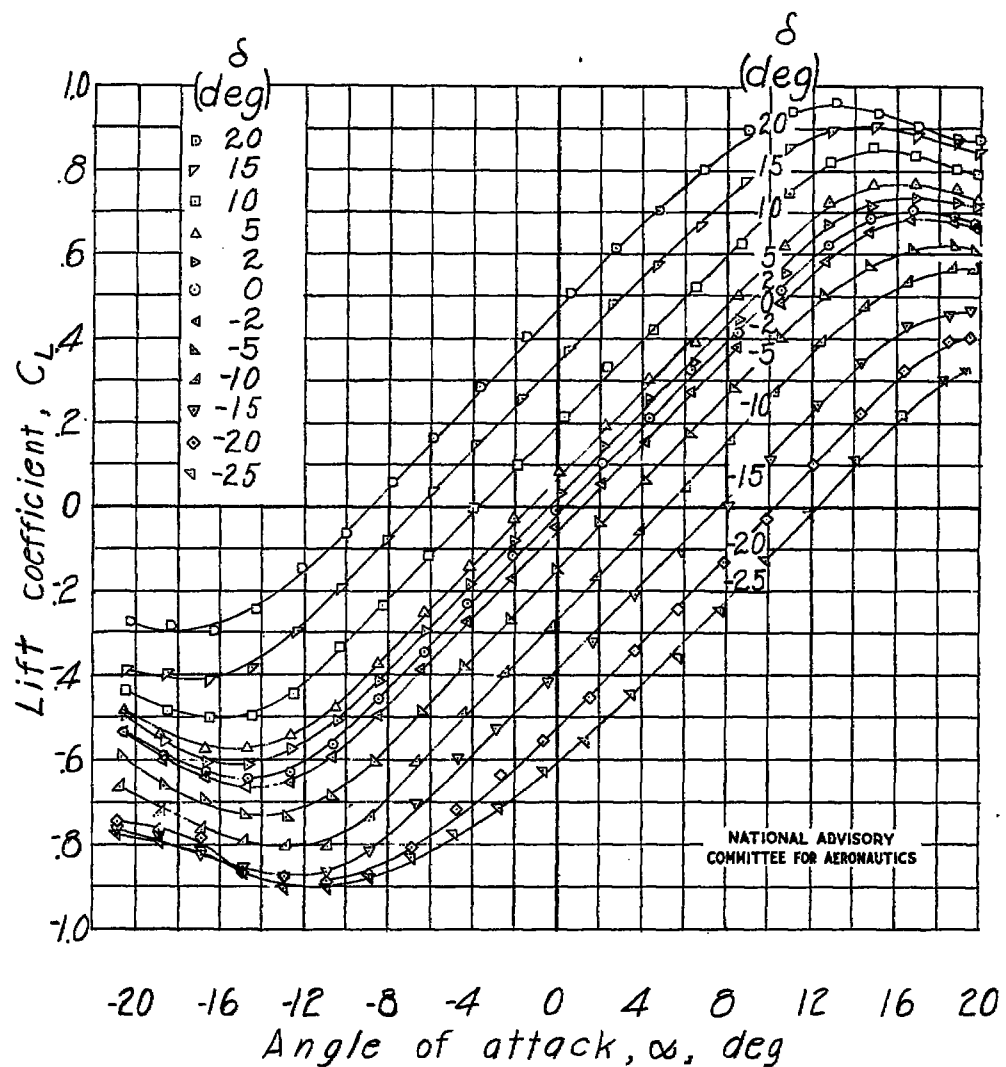


Figure 20.- Lower surface of model showing hinge-moment measuring device and position of mounting strut and fork. (Tail 5.)



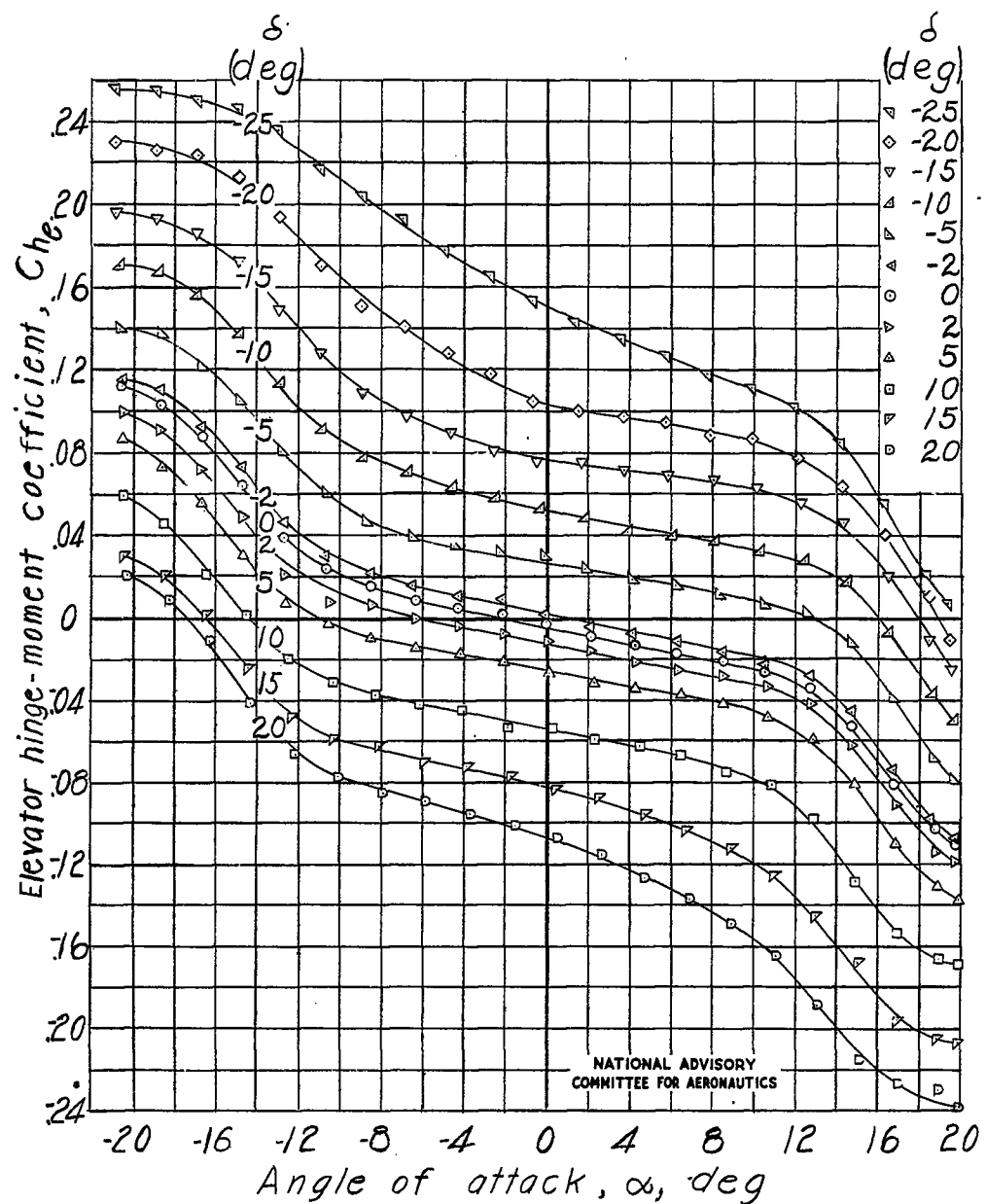
NATIONAL ADVISORY
COMMITTEE FOR AERONAUTICS

Figure 21.- Views of test section of Langley 4- by 6-foot vertical tunnel with isolated tail in place. Dummy fork and strut in place for tare tests.



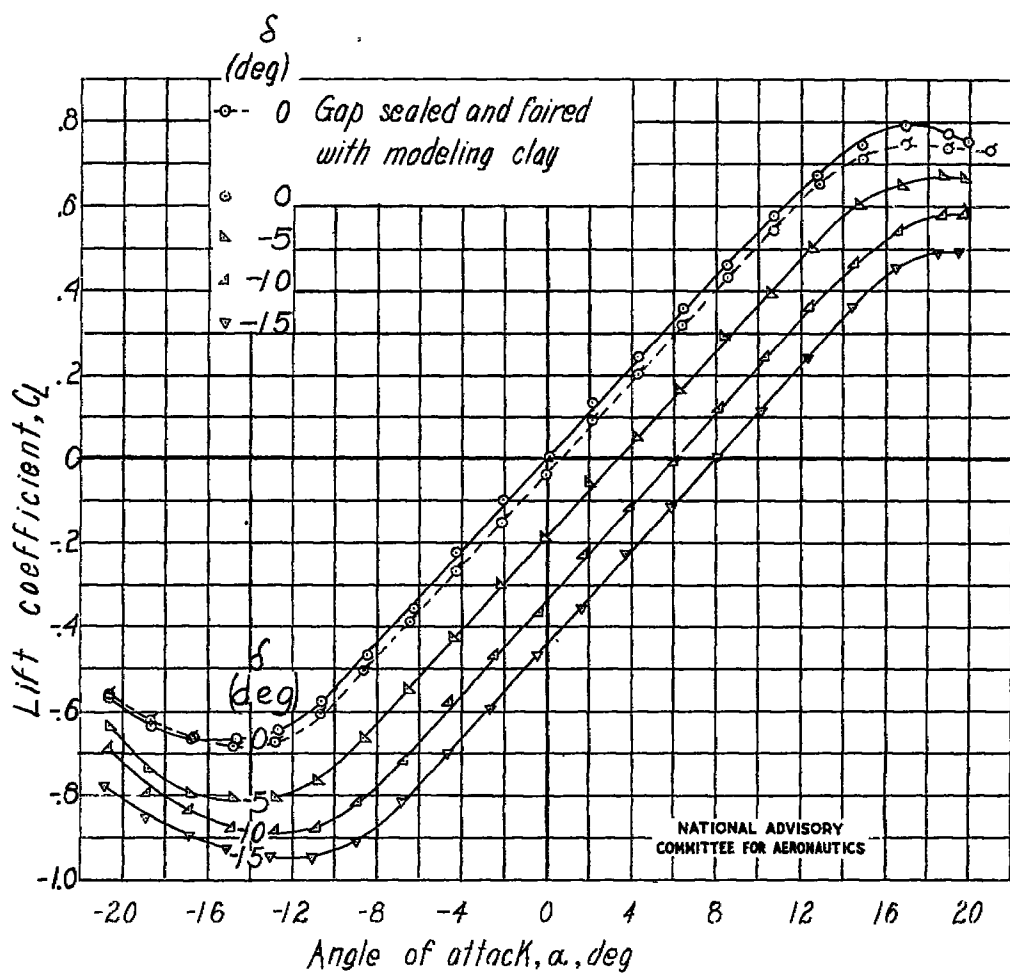
(a) Elevator gap open.

Figure 22.- Lift and hinge-moment characteristics of horizontal tail 1.



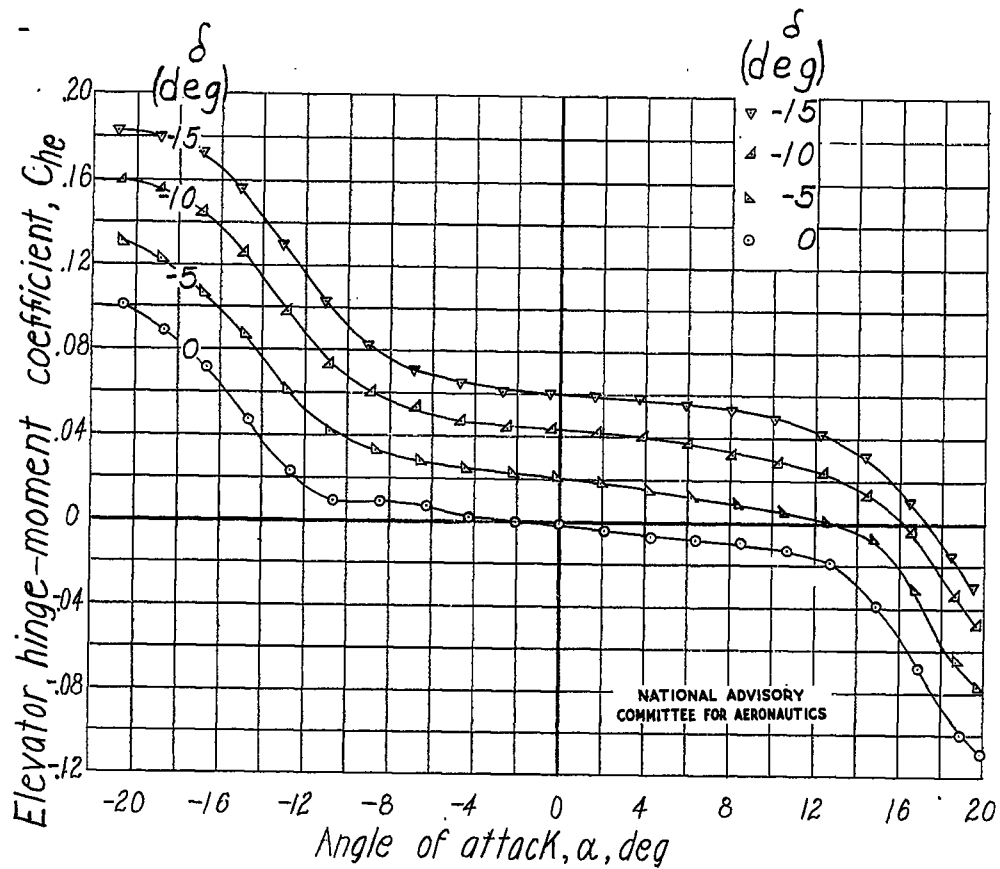
(a) Concluded.

Figure 22.- Continued. Tail 1.



(b) Elevator gap sealed with grease except where noted.

Figure 22.- Continued. Tail 1.

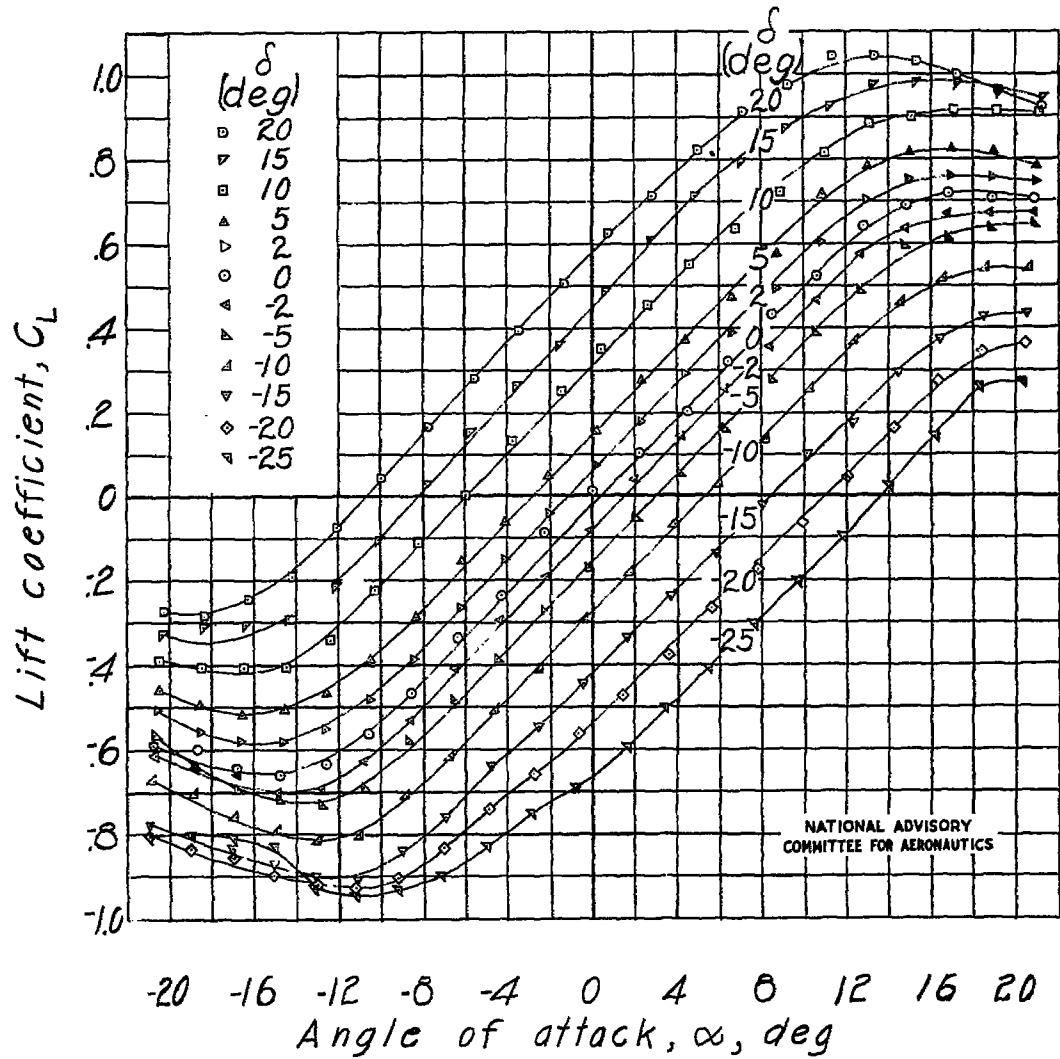


(b) Concluded.

Figure 22.- Continued. Tail 1.

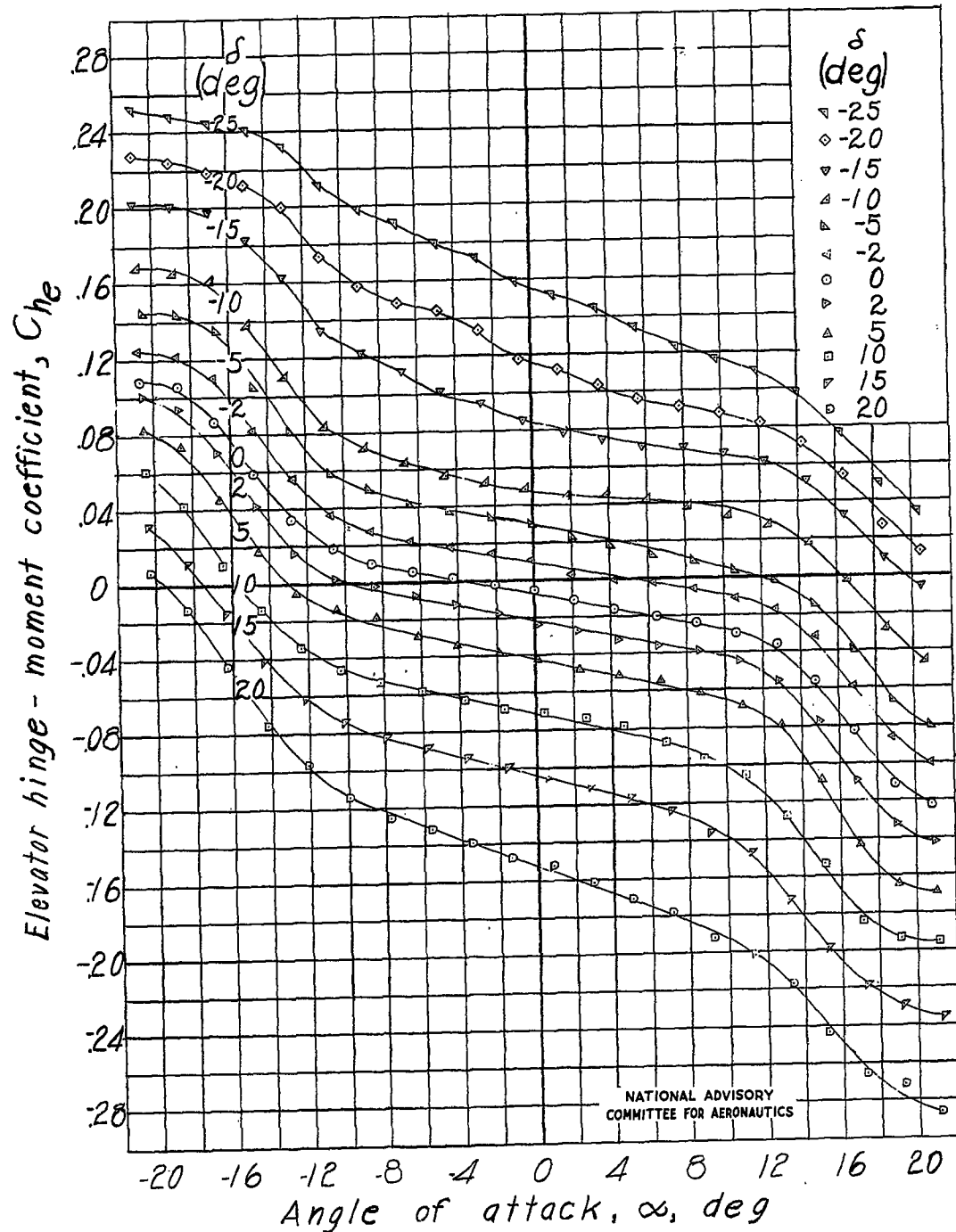
Fig. 22c

NACA TN No. 1291



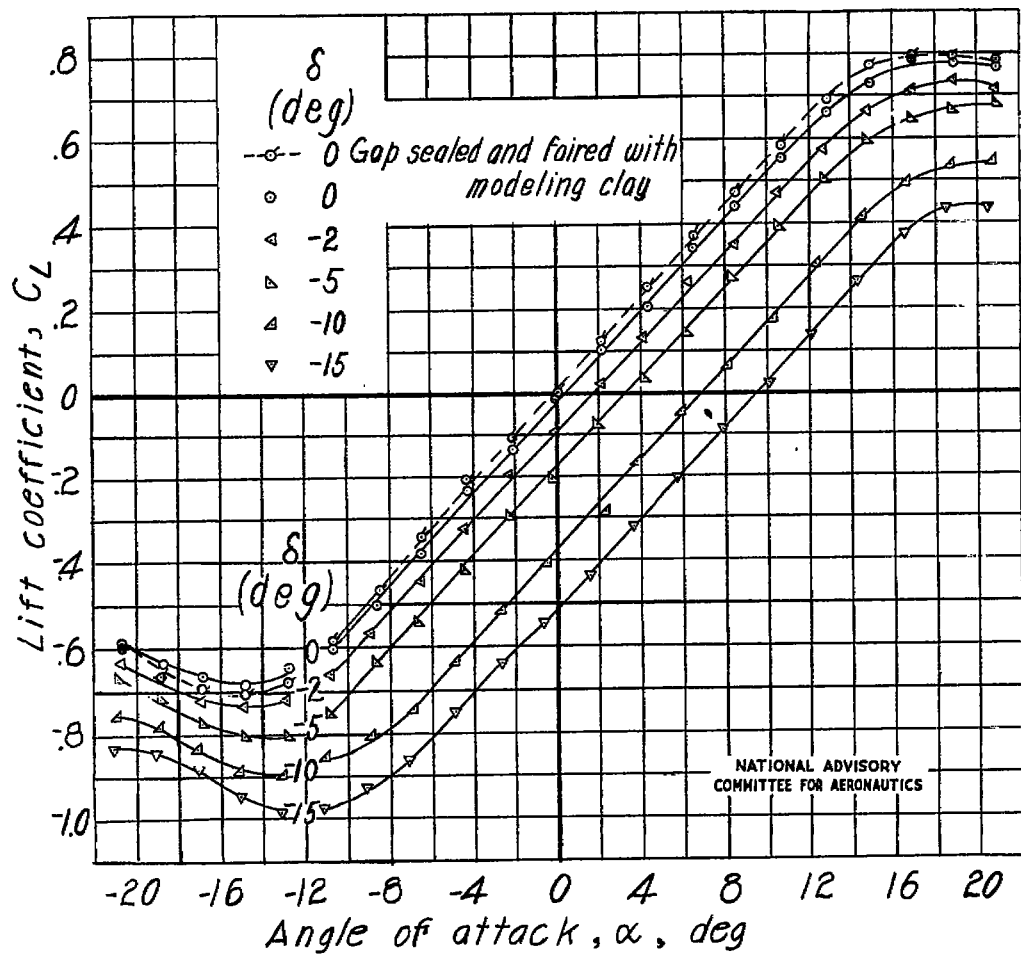
(c) Elevator cut-out filled and elevator gap open.

Figure 22.- Continued. Tail 1.



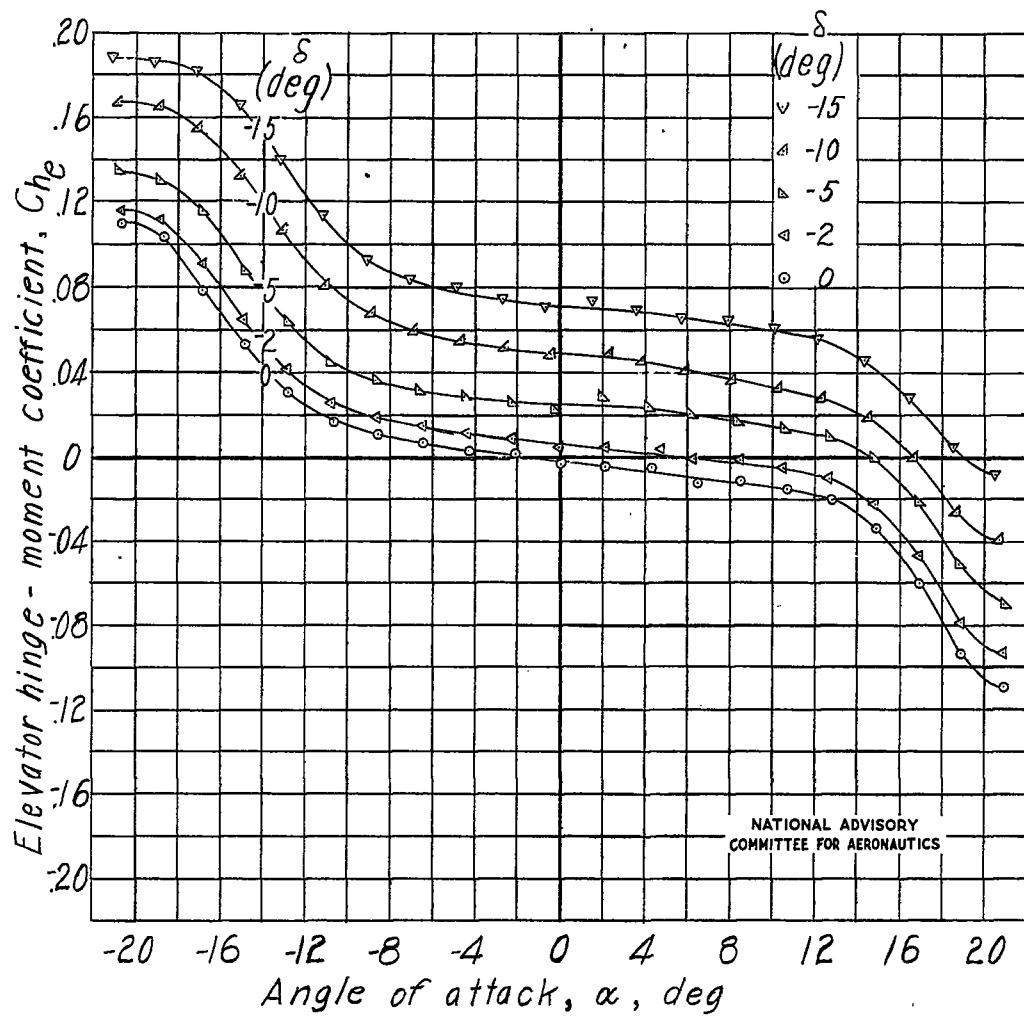
(c) Concluded.

Figure 22.- Continued. Tail 1.



(d) Elevator cut-out filled and elevator gap sealed with grease except where noted.

Figure 22.- Continued. Tail 1.

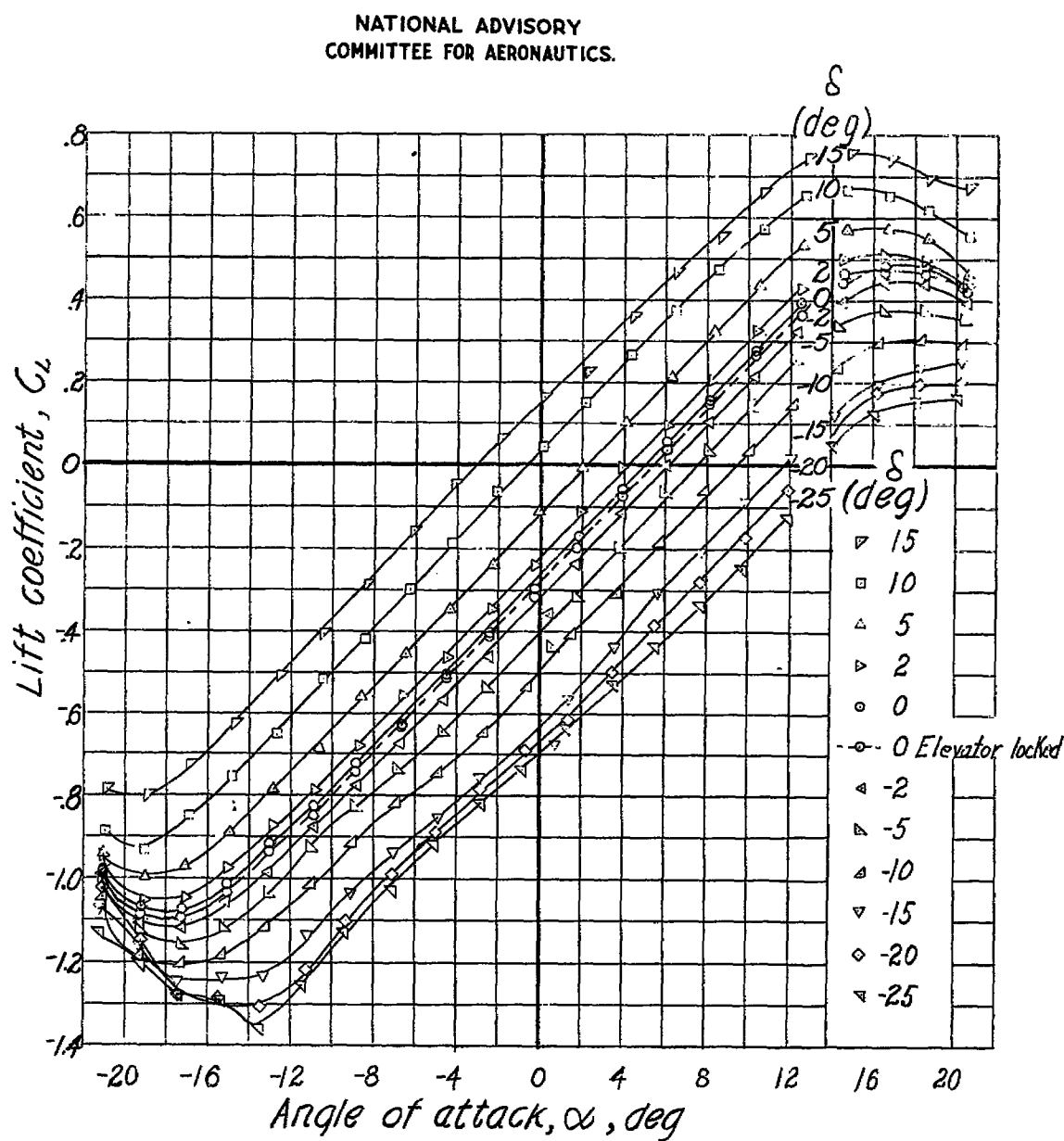


(d) Concluded.

Figure 22.- Concluded. Tail 1.

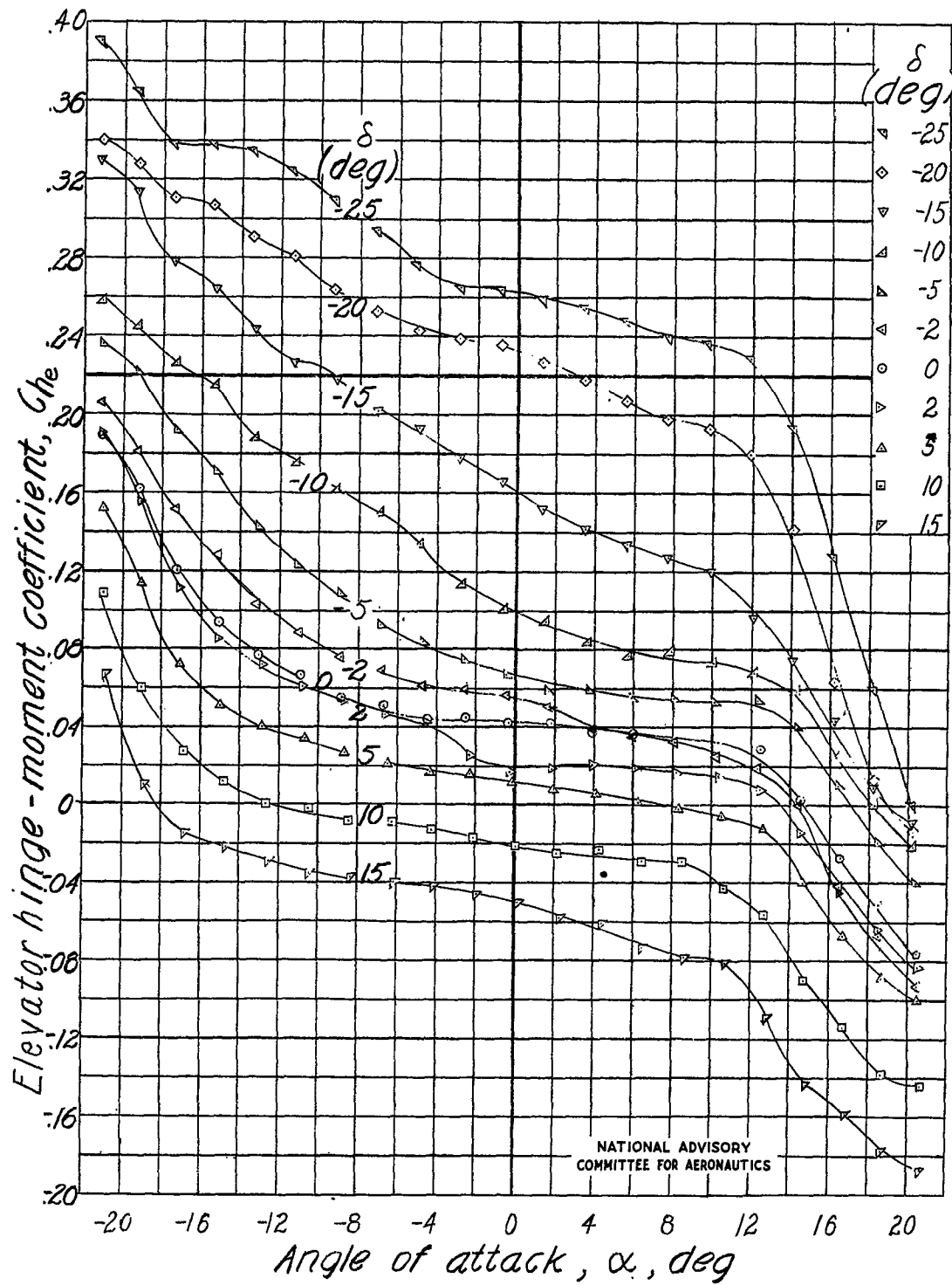
Fig. 23a

NACA TN No. 1291



(a) Elevator gap open and slot filled.

Figure 23.- Lift and hinge-moment characteristics of horizontal tail 2.

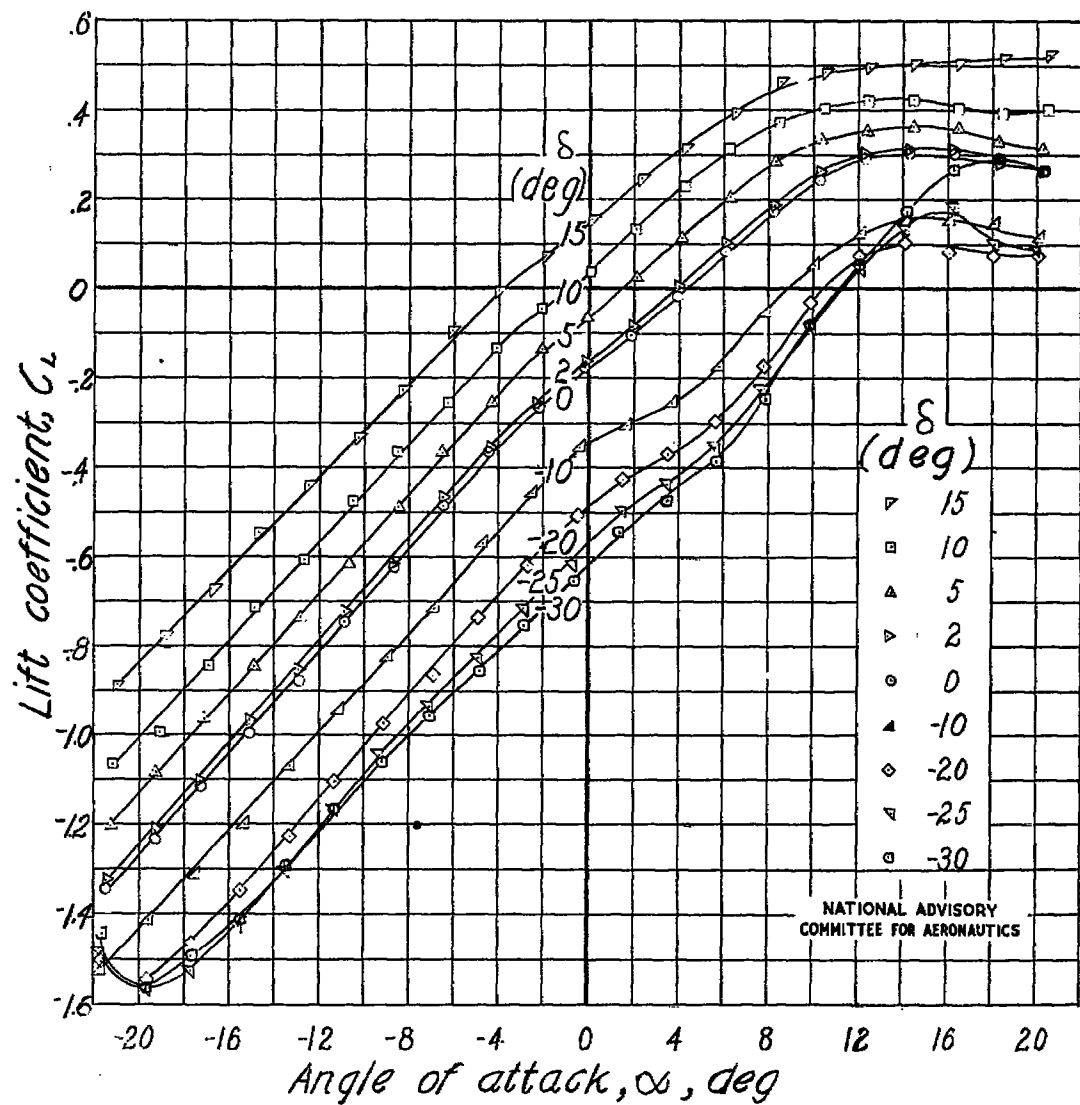


(a) Concluded.

Figure 23.- Continued. Tail 2.

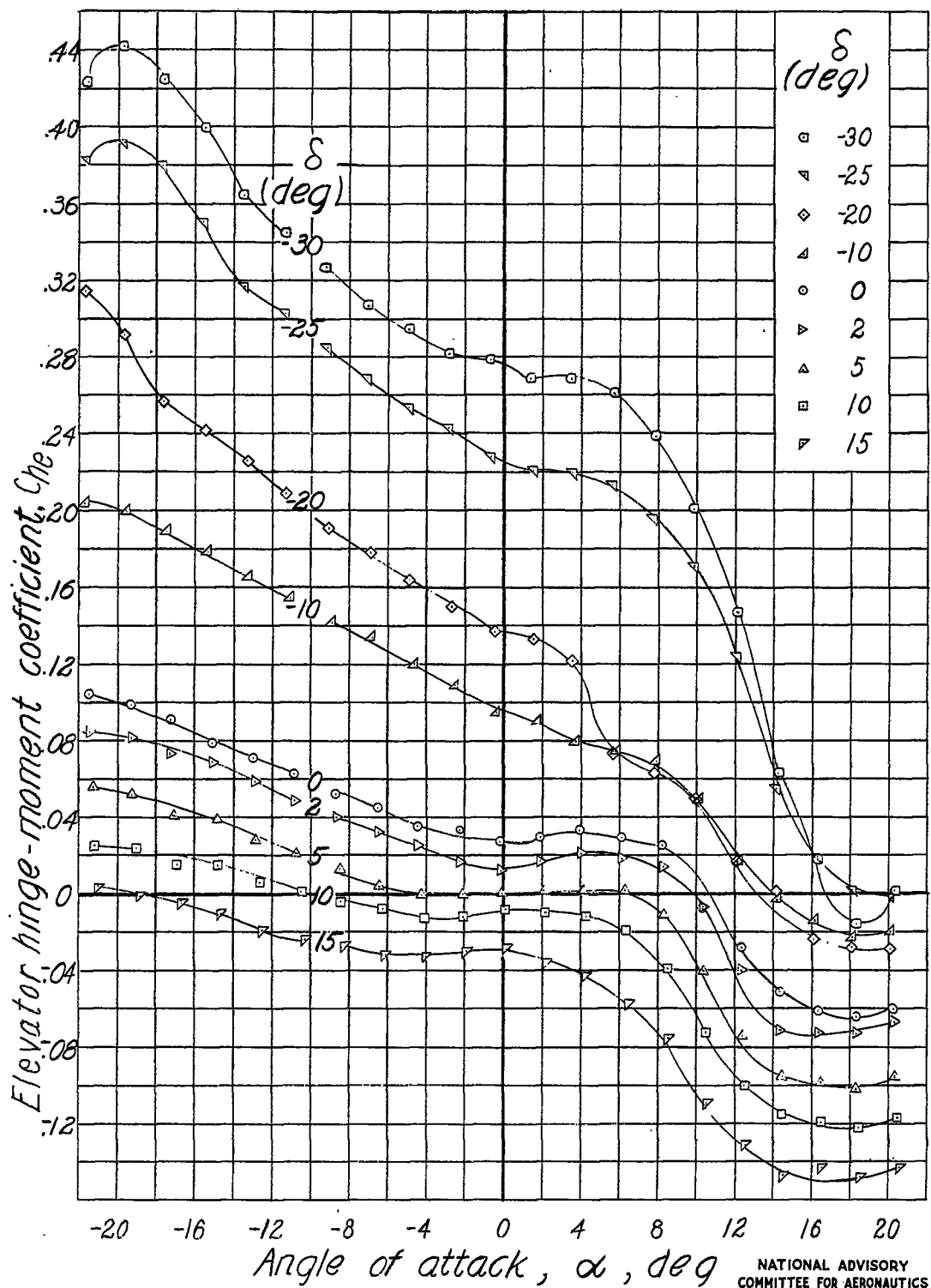
Fig. 23b

NACA TN No. 1291



(b) Elevator gap open and slot open.

Figure 23.- Continued. Tail 2.

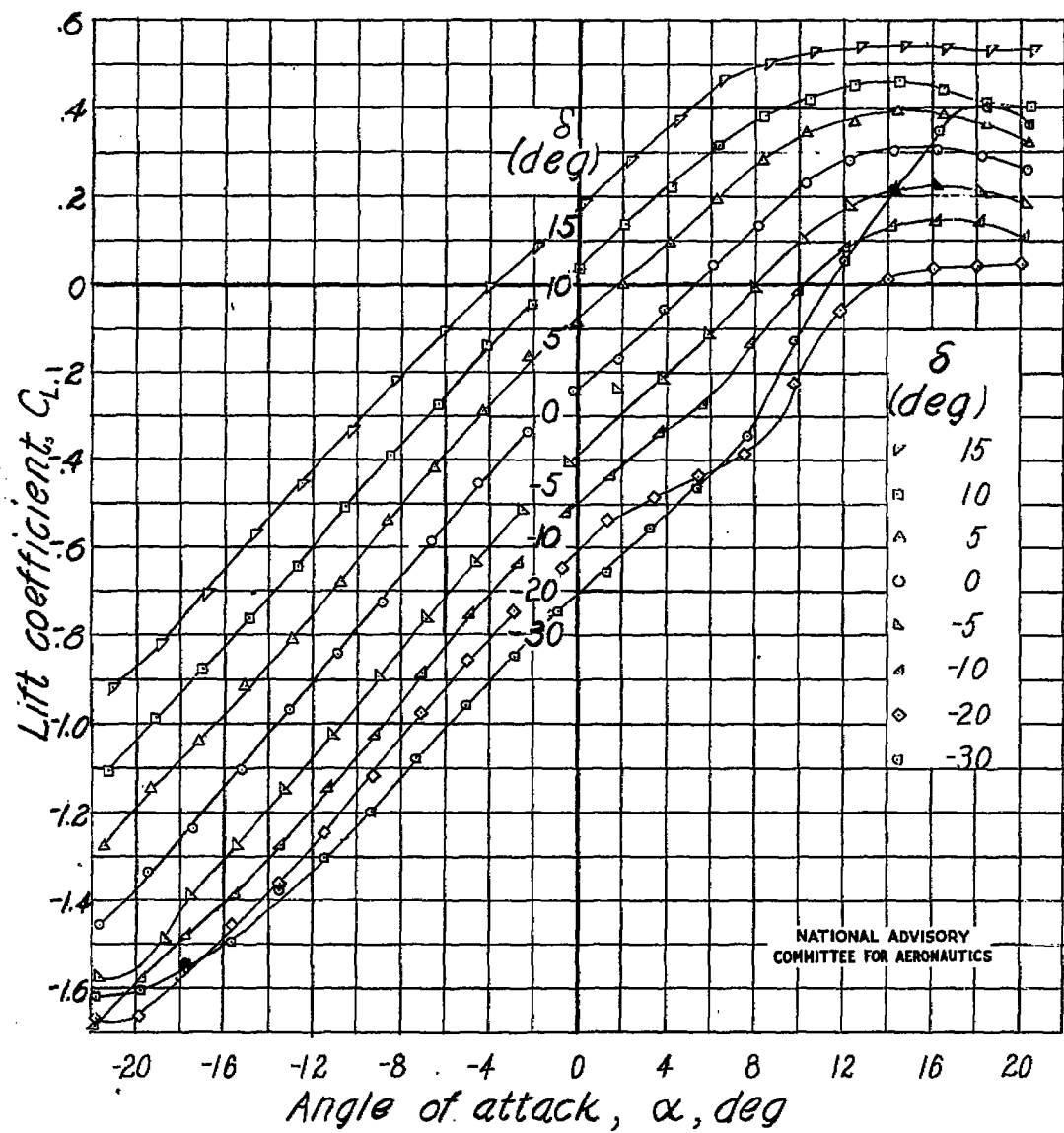


(b) Concluded.

Figure 23.- Continued. Tail 2.

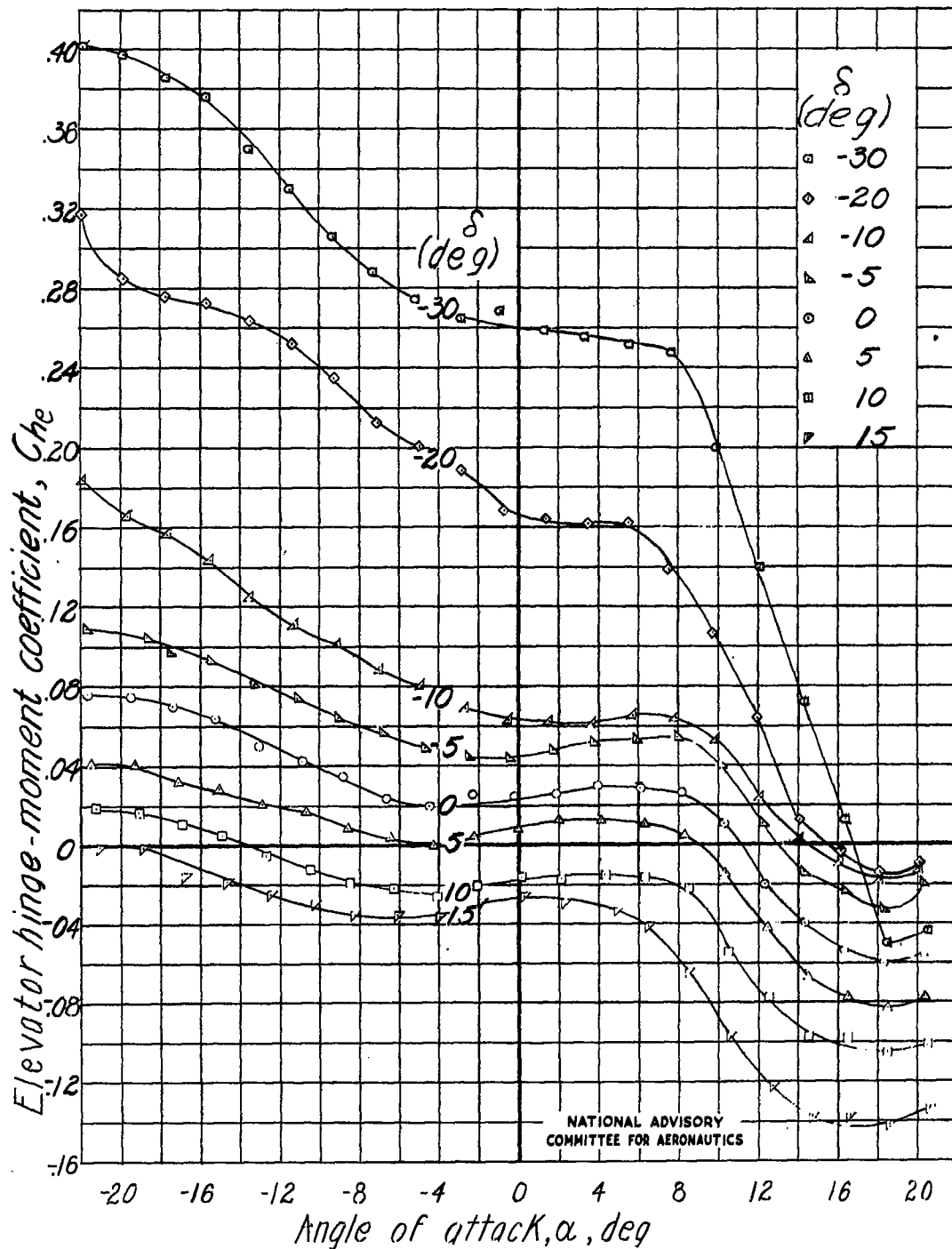
Fig. 23c

NACA TN No. 1291



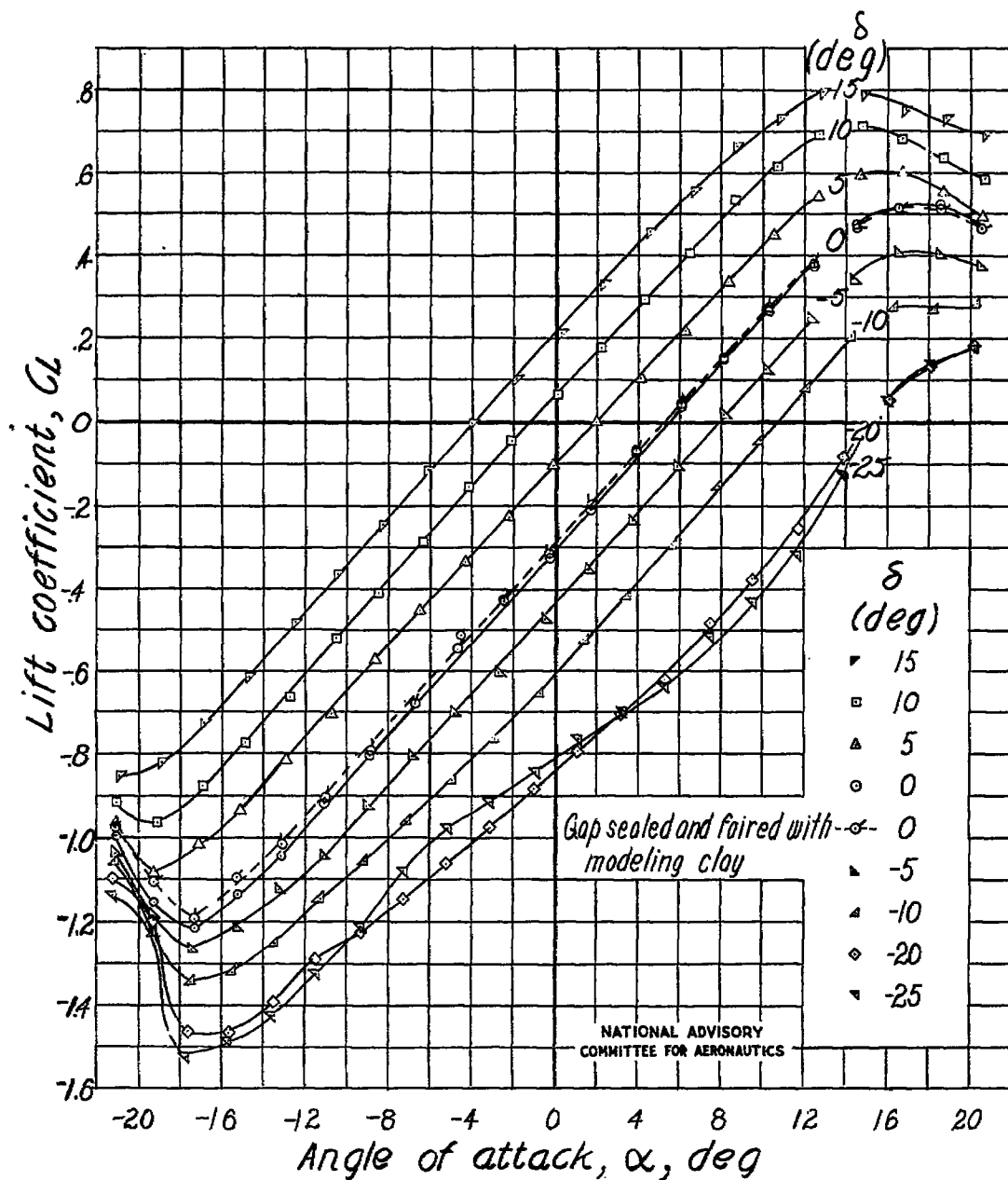
(c) Elevator gap sealed with grease and slot open.

Figure 23.- Continued. Tail 2.



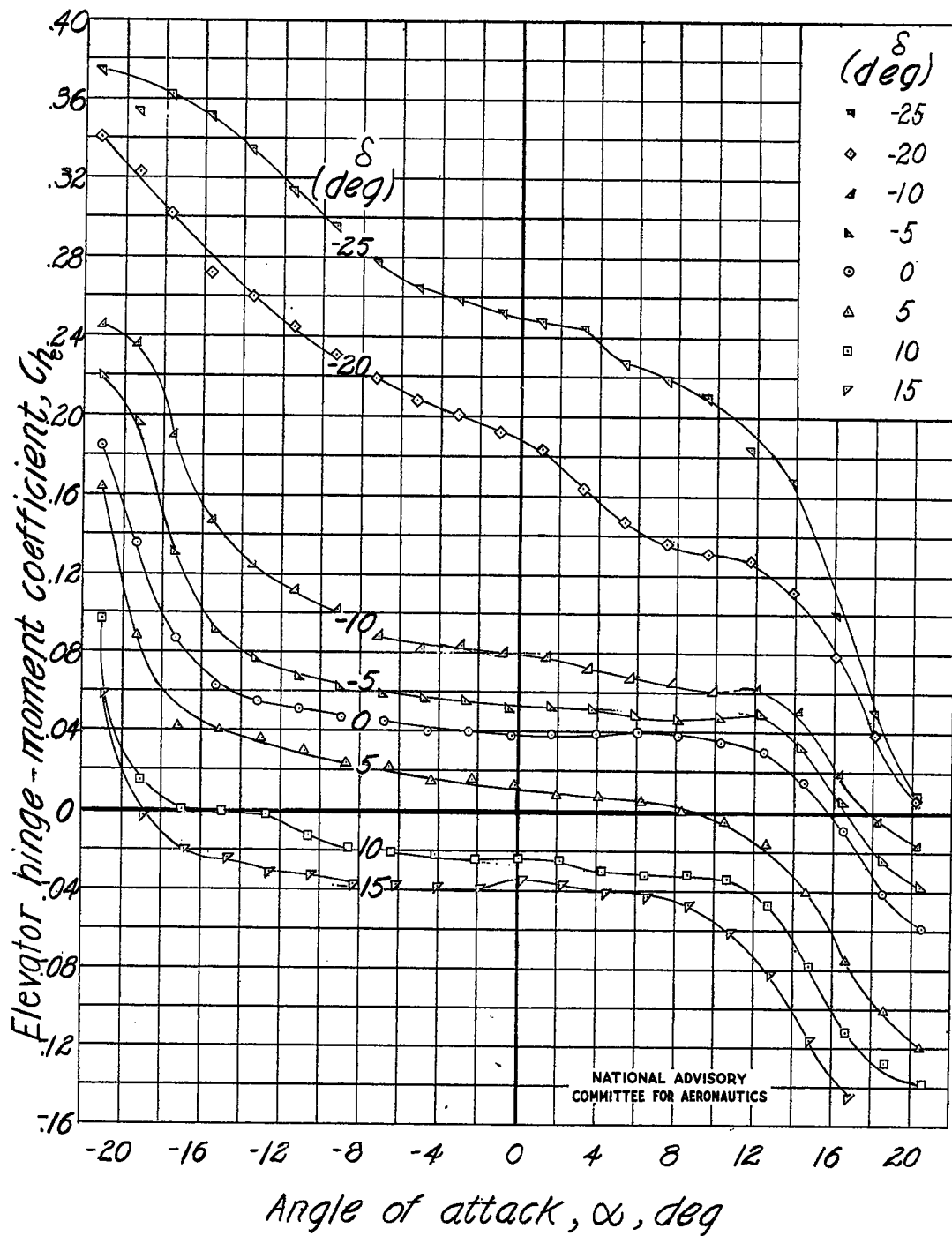
(c) Concluded.

Figure 23.- Continued. Tail 2.



(d) Elevator gap sealed with grease, except where noted, and slot filled.

Figure 23.- Continued. Tail 2.

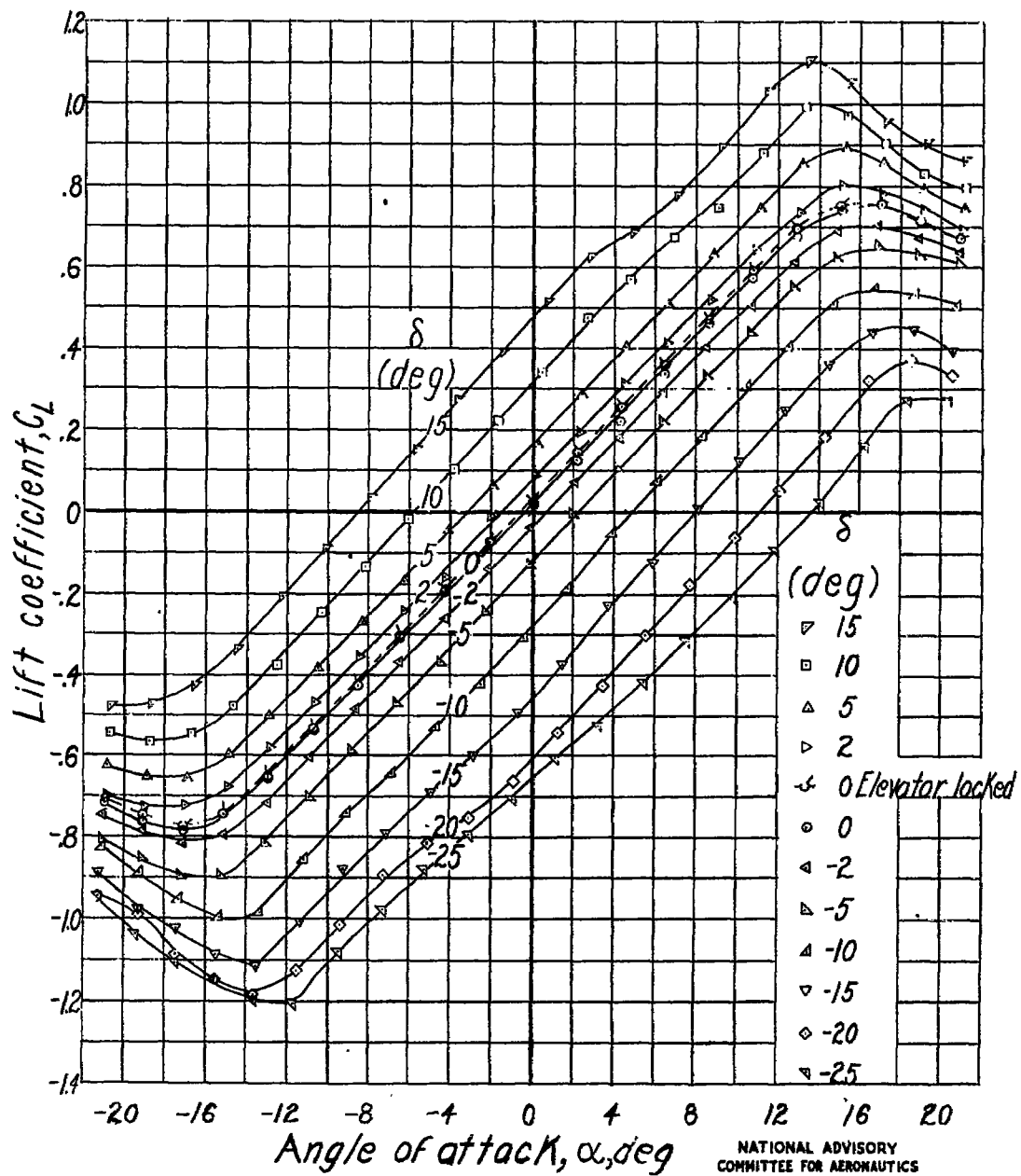


(d) Concluded.

Figure 23.- Concluded. Tail 2.

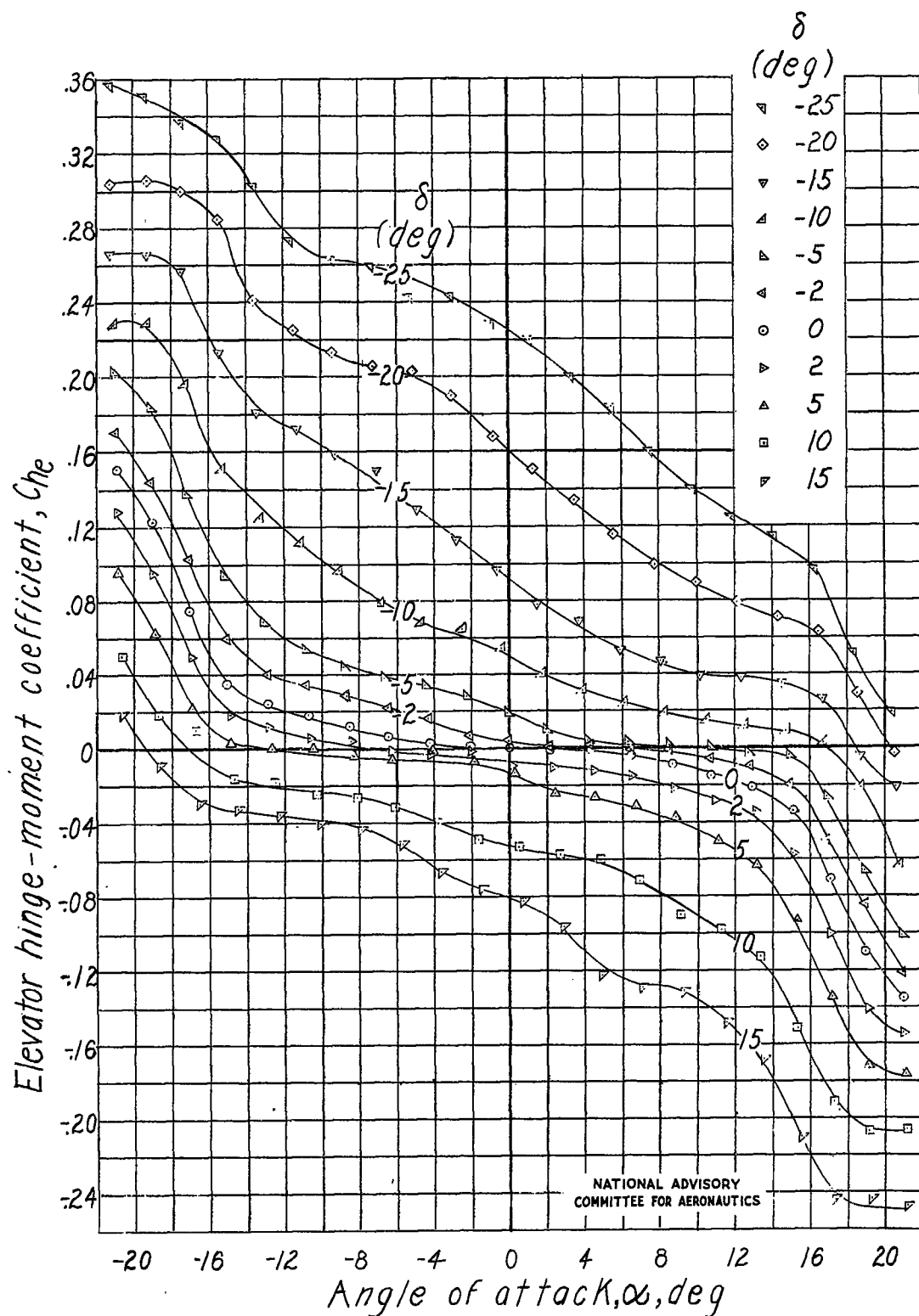
Fig. 24a

NACA TN No. 1291



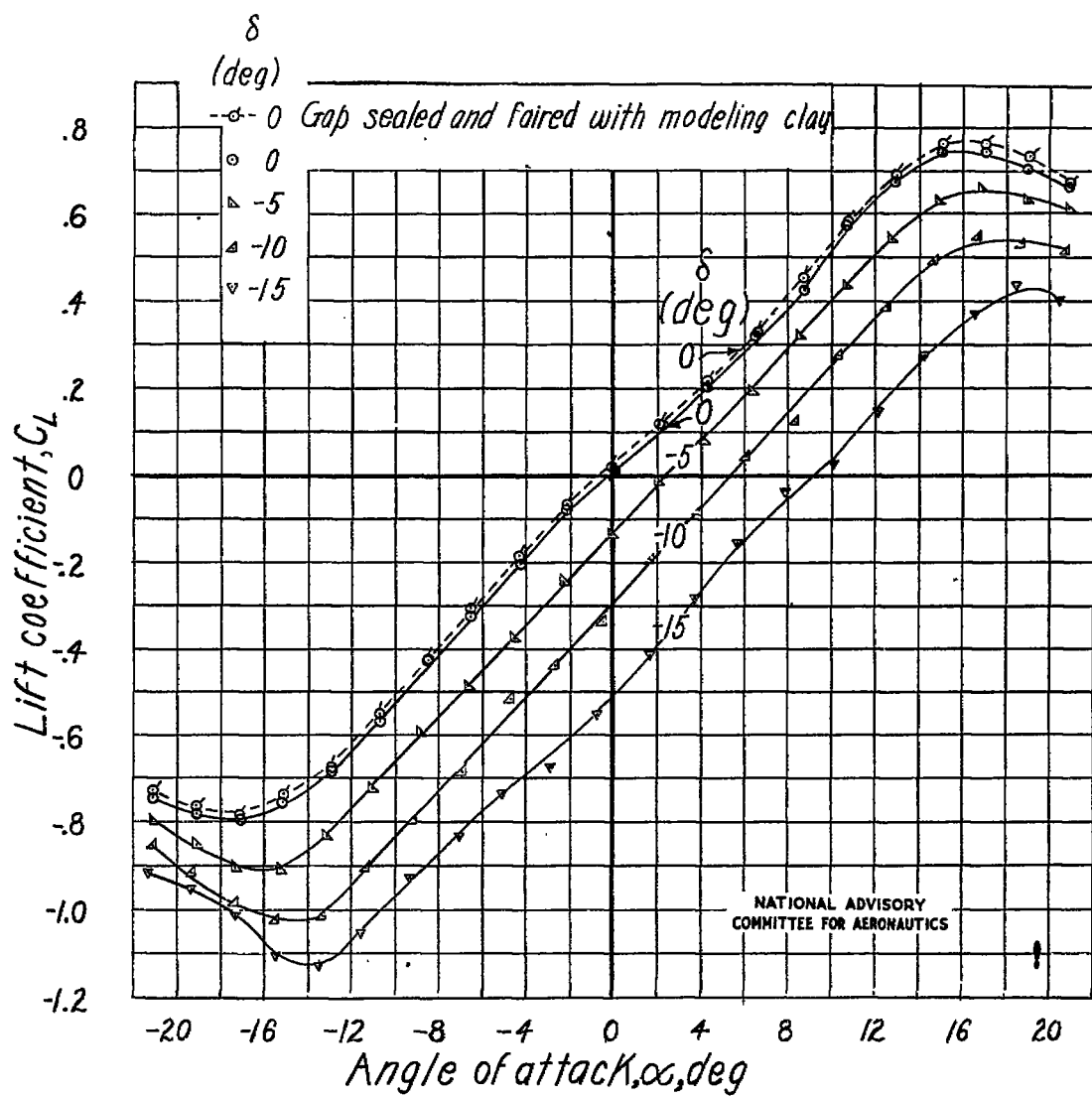
(a) Elevator gap open.

Figure 24.- Lift and hinge-moment characteristics of horizontal tail 3.



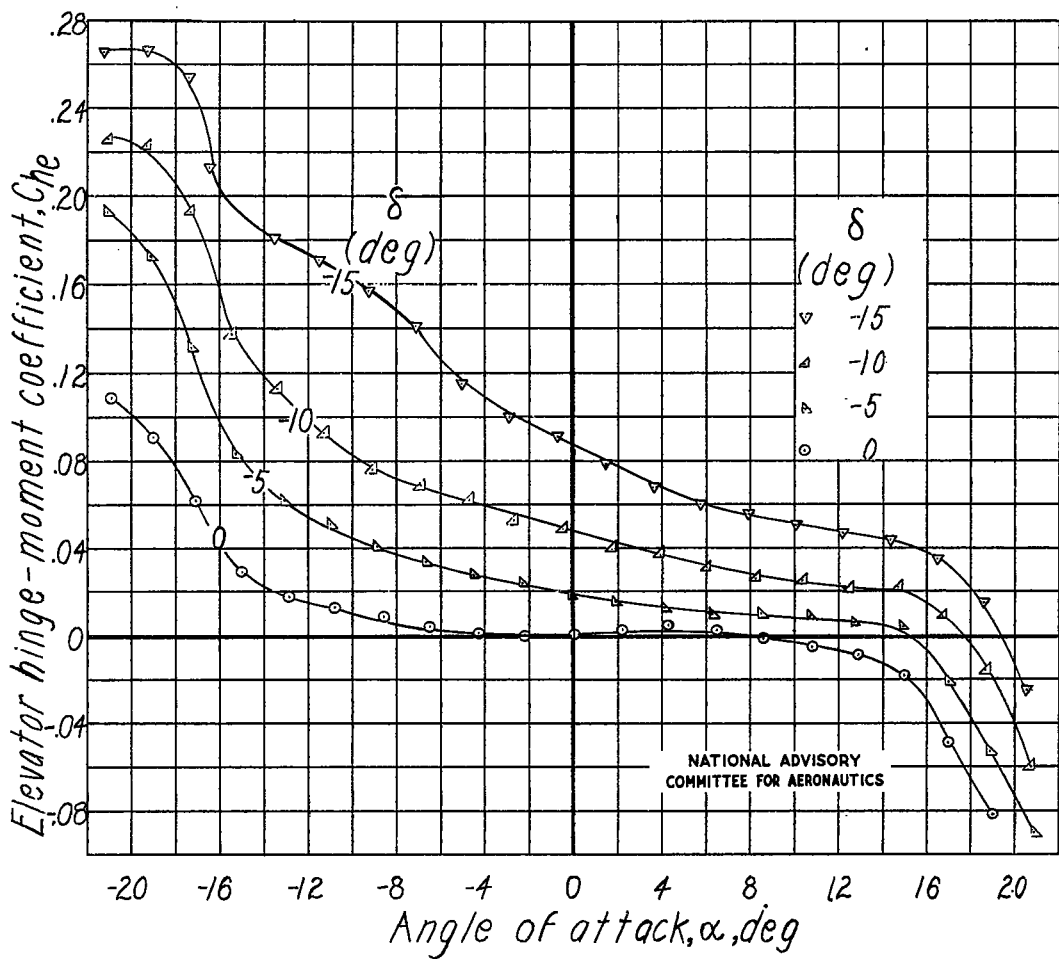
(a) Concluded.

Figure 24.- Continued. Tail 3.



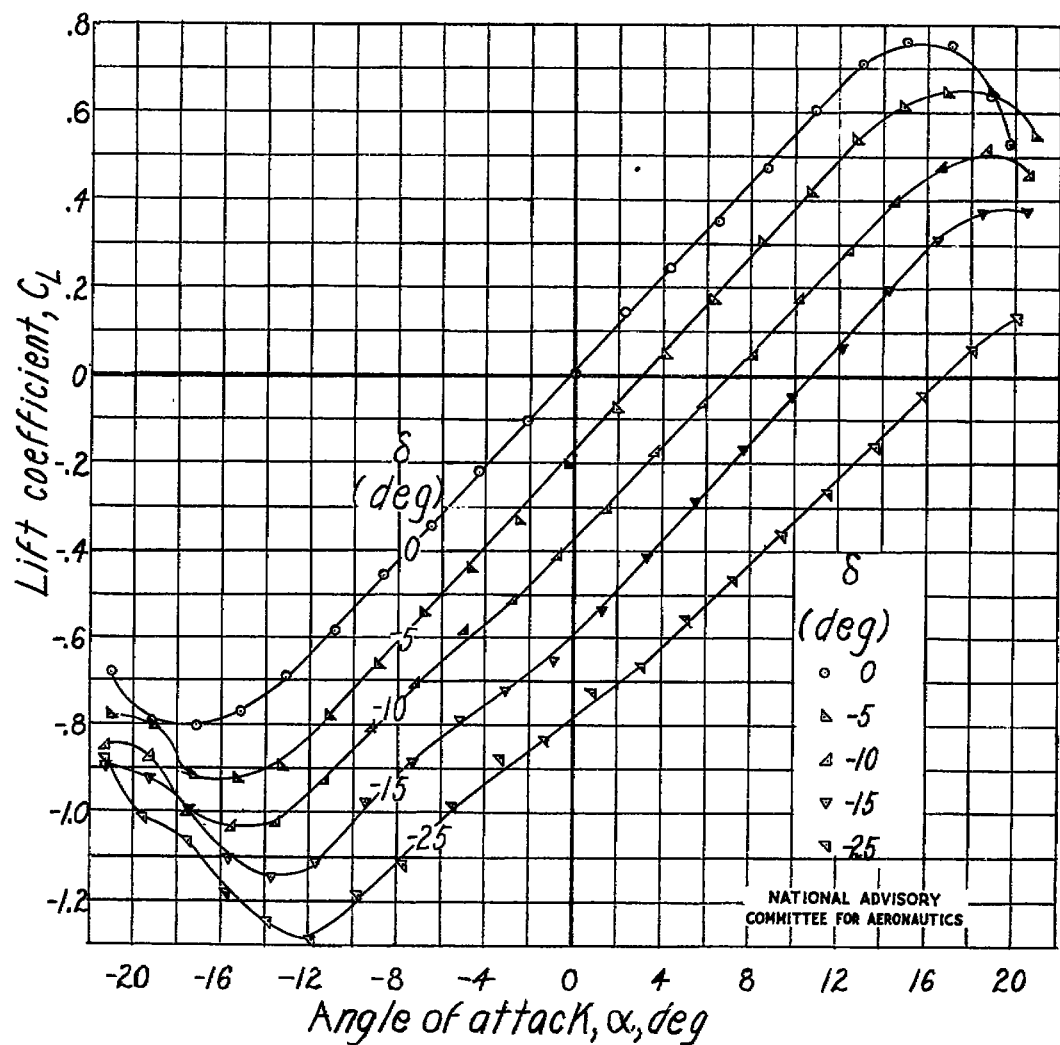
(b) Elevator gap sealed with grease except where noted.

Figure 24.- Continued. Tail 3.



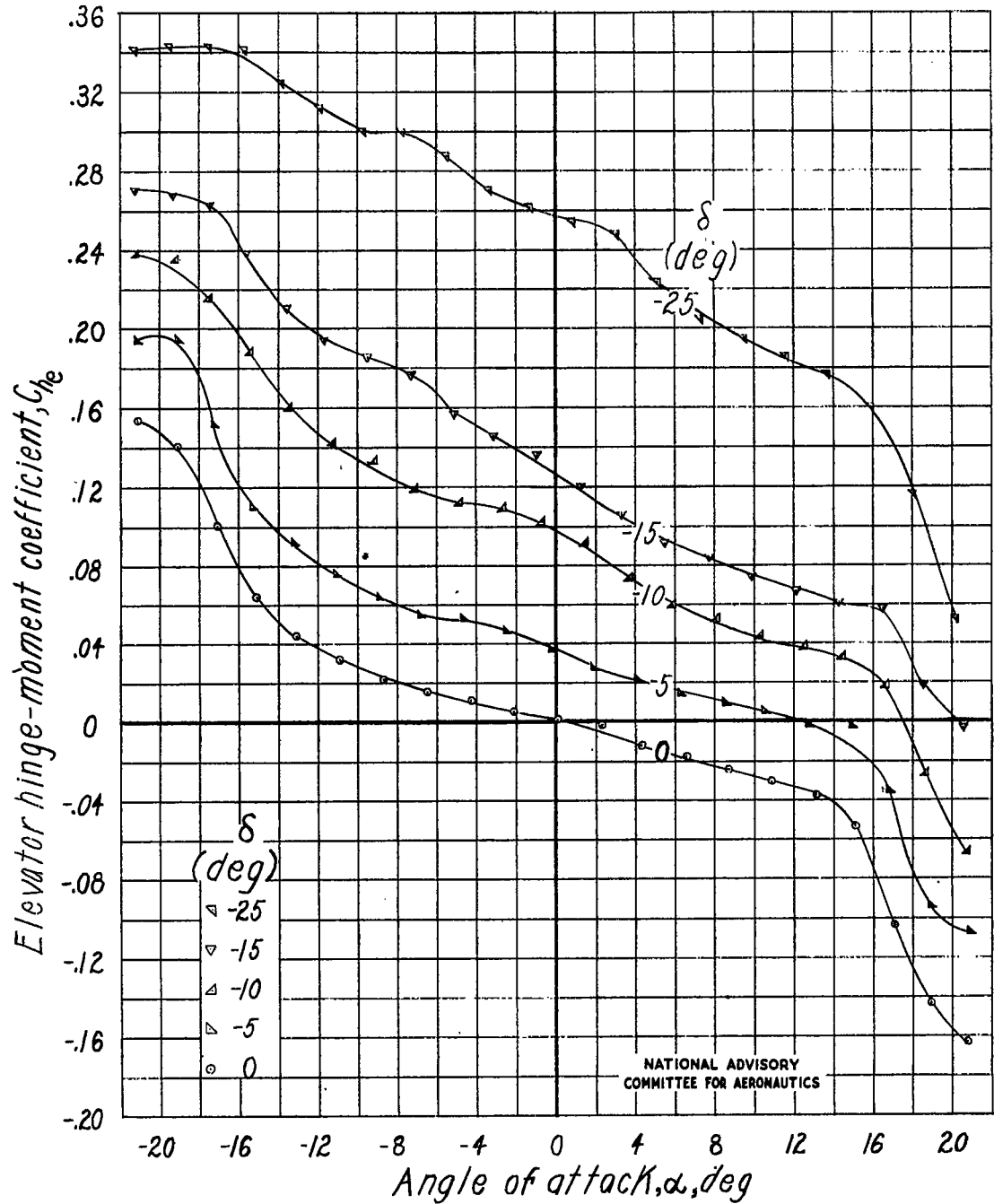
(b) Concluded.

Figure 24.- Continued. Tail 3.



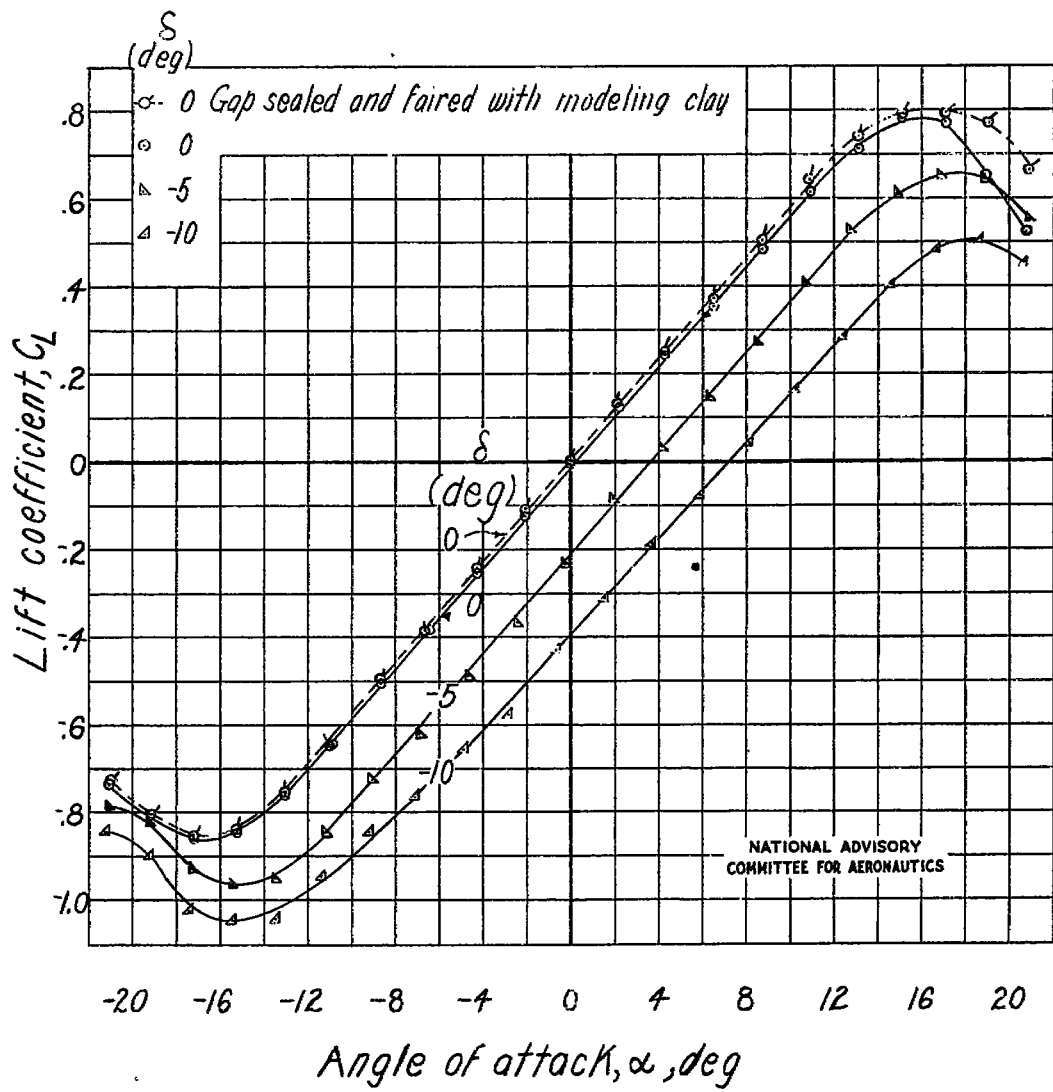
(c) Elevator cut-out filled and gap open.

Figure 24.- Continued. Tail 3.



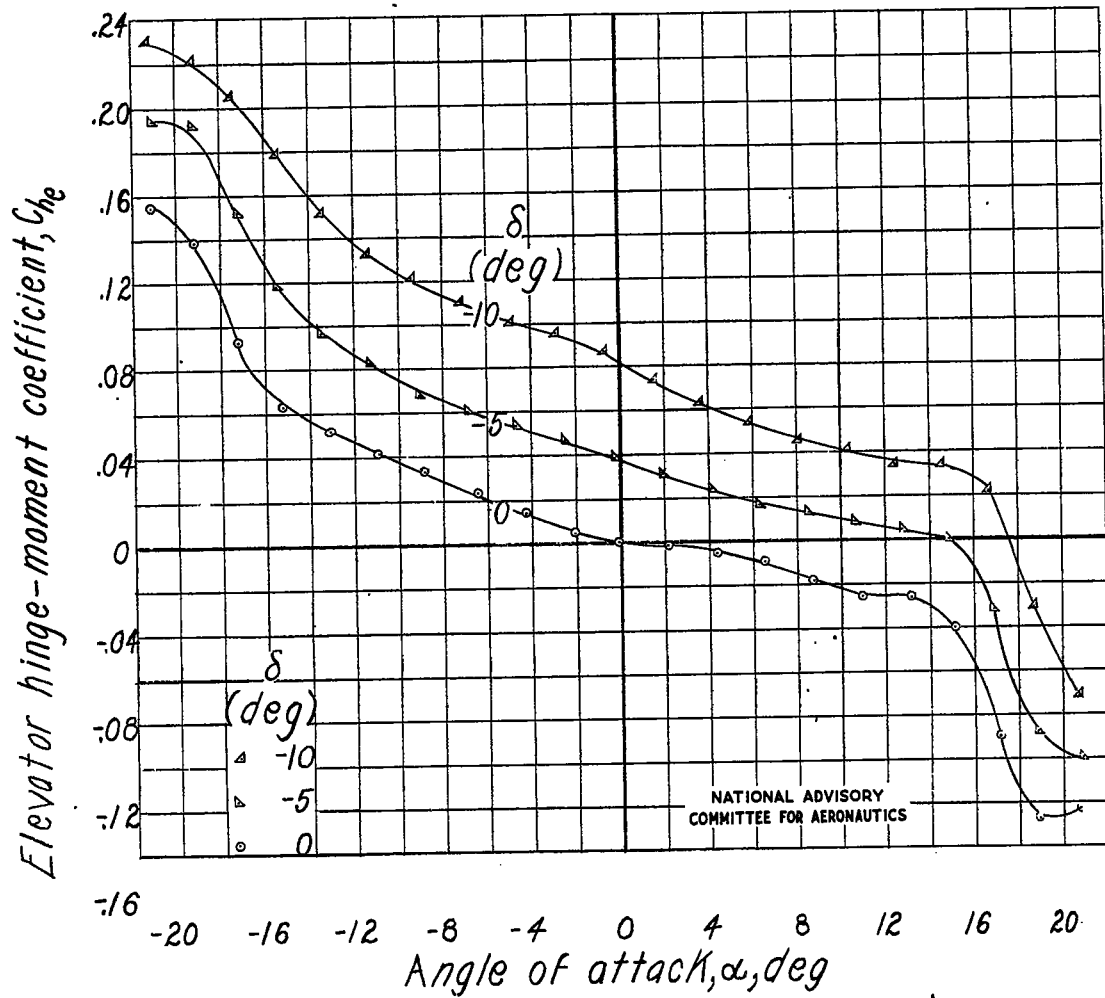
(c) Concluded.

Figure 24.- Continued. Tail 3.



- (d) Elevator cut-out filled and gap sealed with grease except where noted.

Figure 24.- Continued. Tail 3.

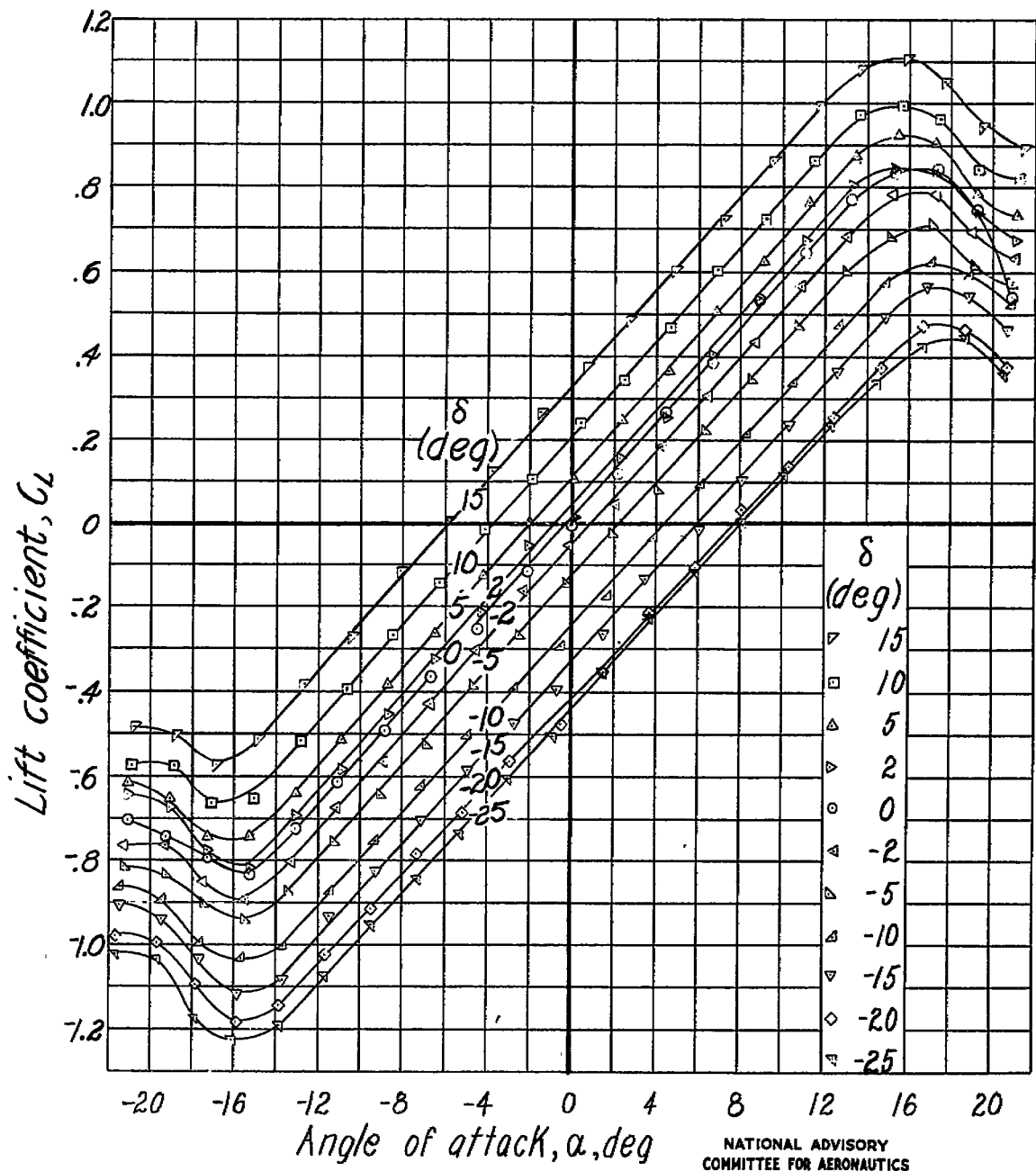


(d) Concluded.

Figure 24.- Concluded. Tail 3.

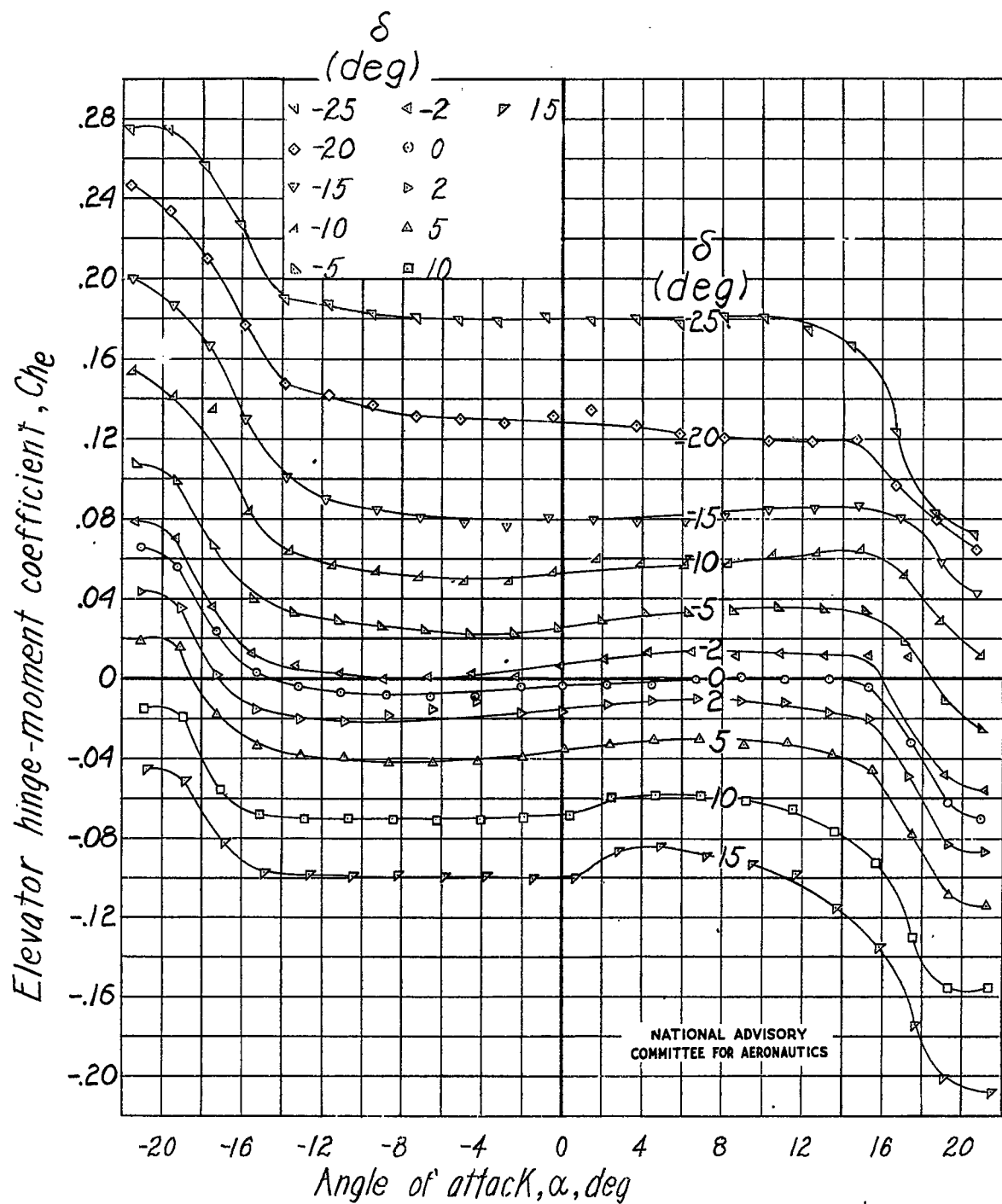
Fig. 25a

NACA TN No. 1291



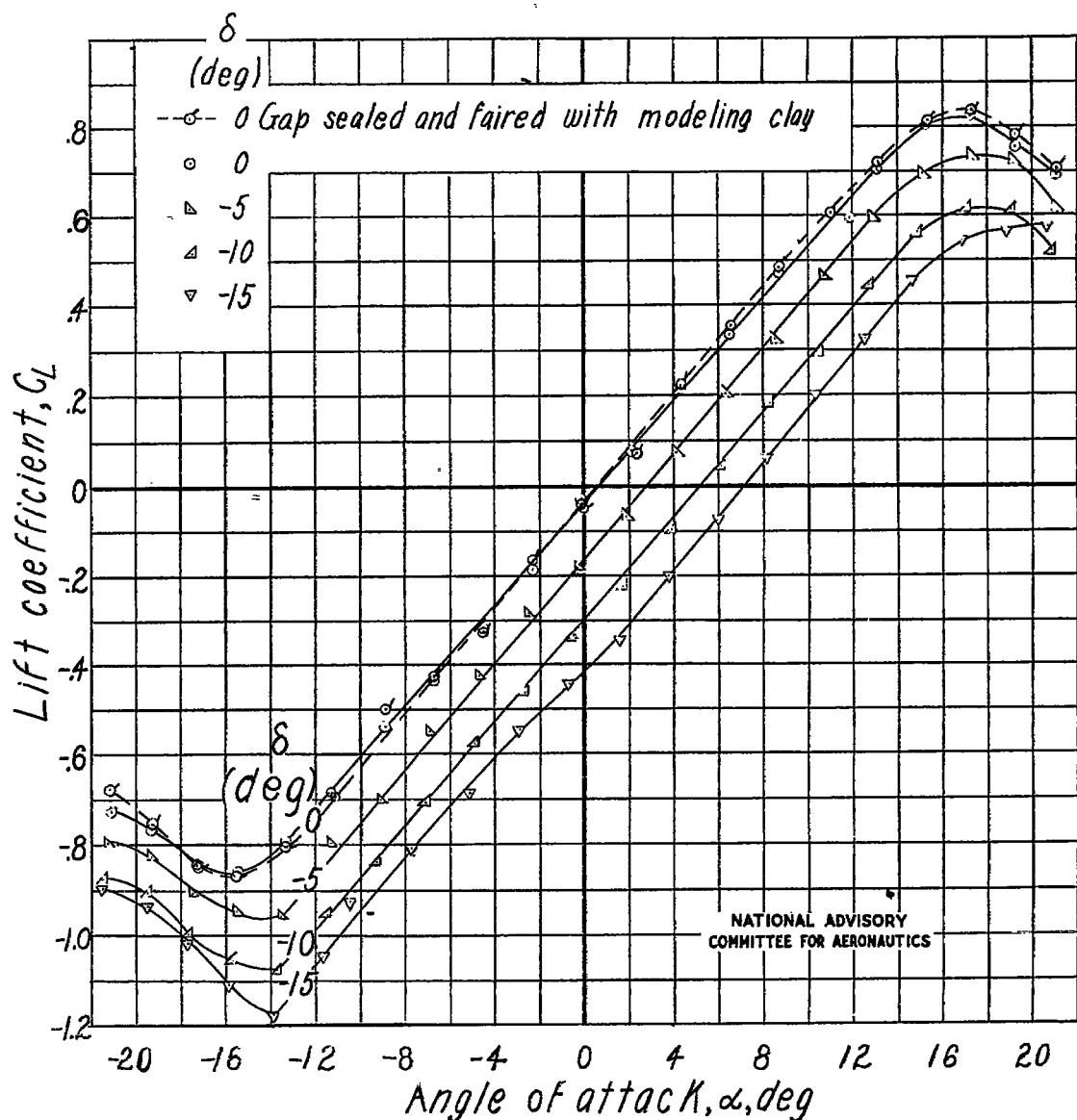
(a) Elevator gap open.

Figure 25.- Lift and hinge-moment characteristics of horizontal tail 4.



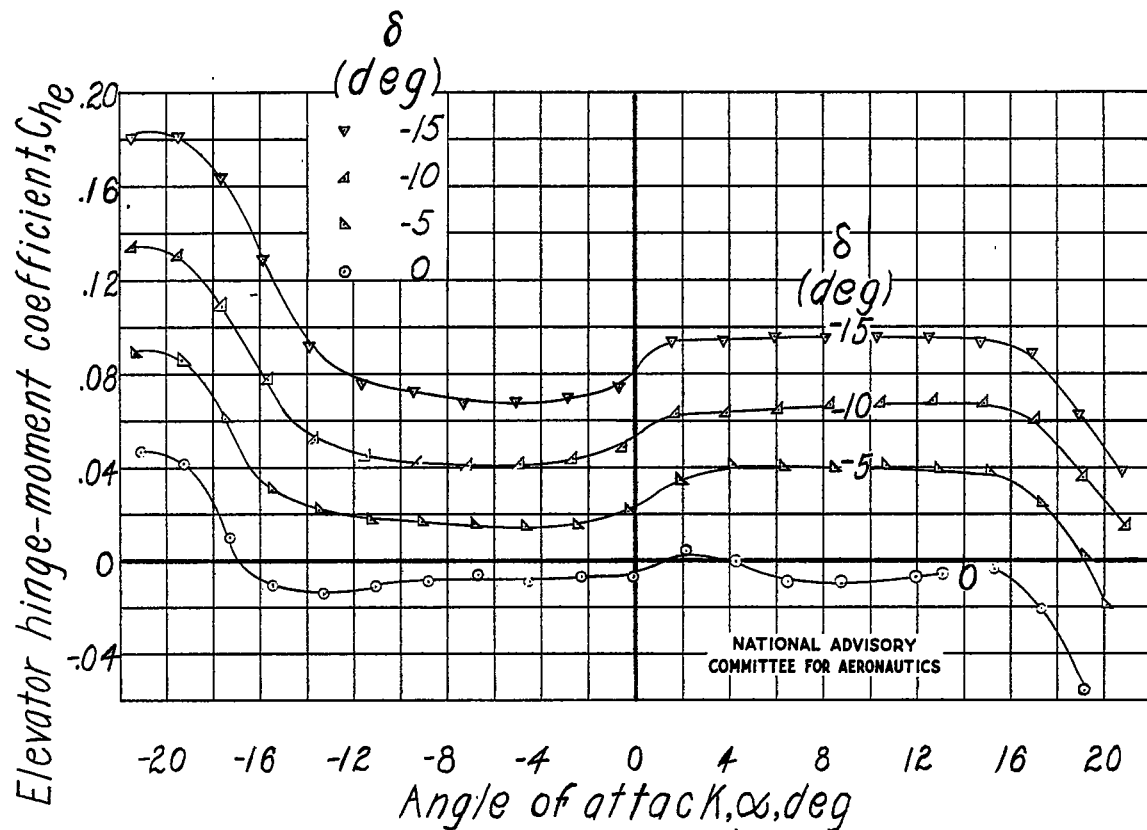
(a) Concluded.

Figure 25.- Continued. Tail 4.



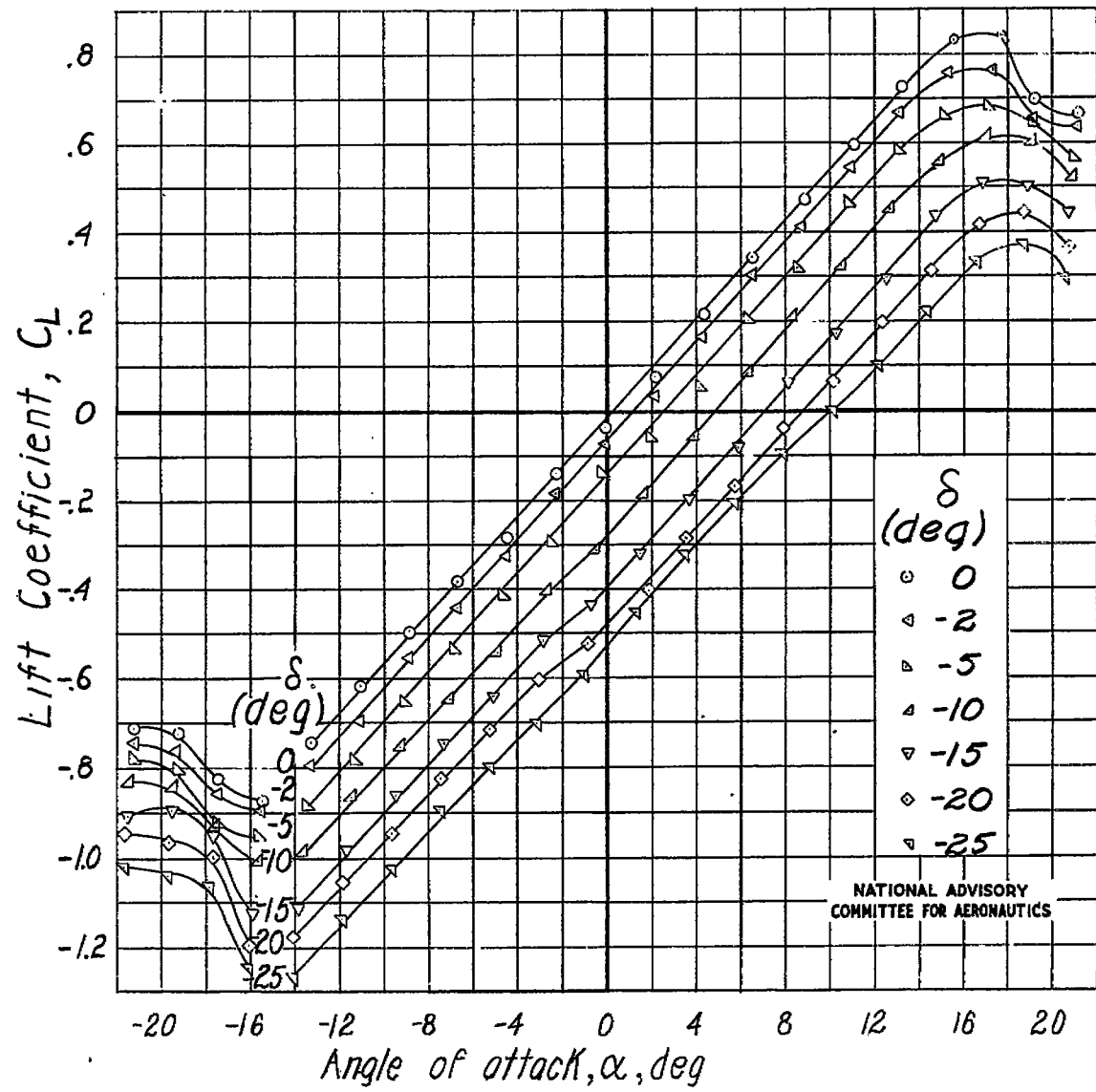
(b) Elevator gap sealed with grease except where noted.

Figure 25.- Continued. Tail 4.



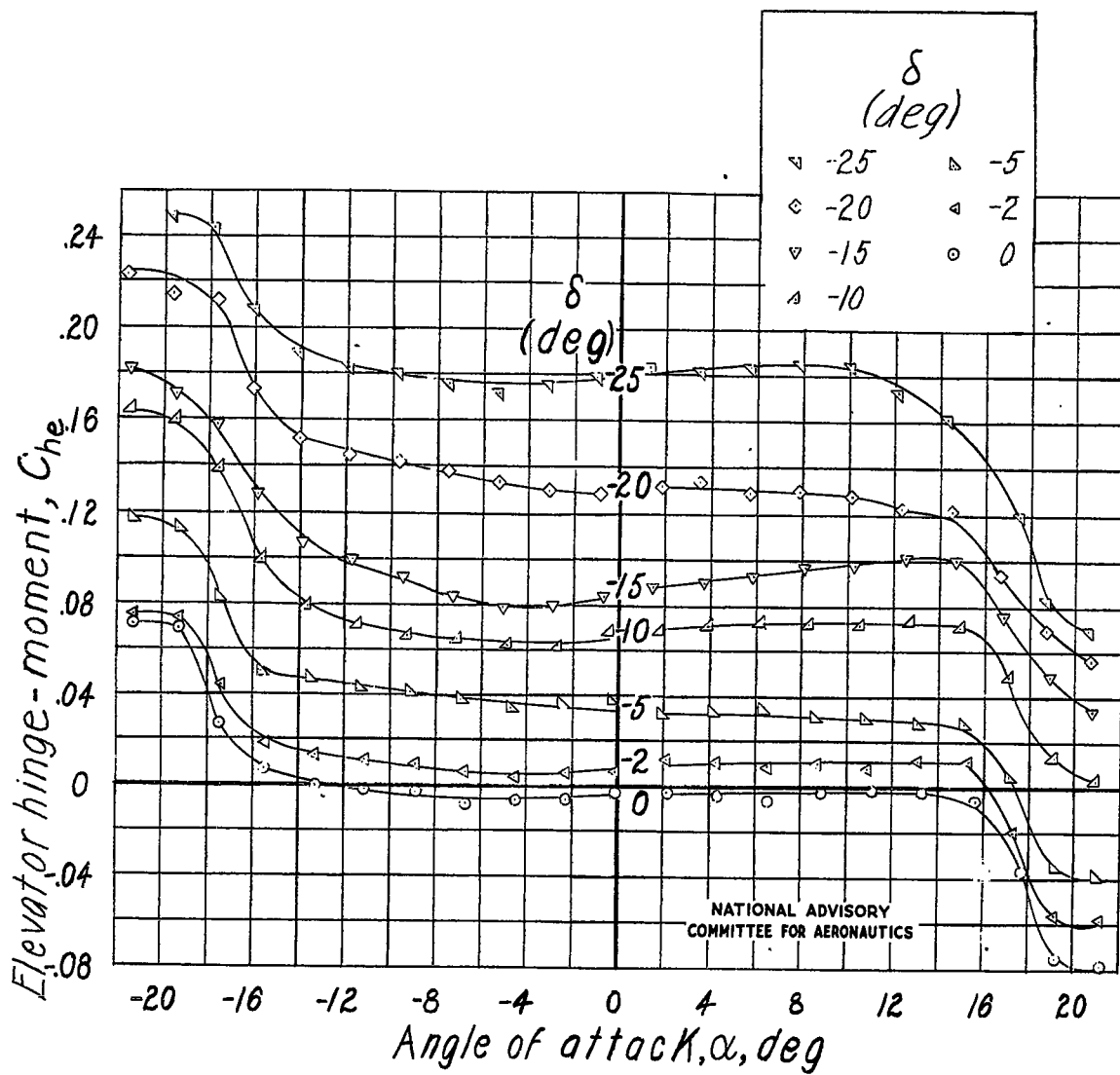
(b) Concluded.

Figure 25.- Continued. Tail 4.



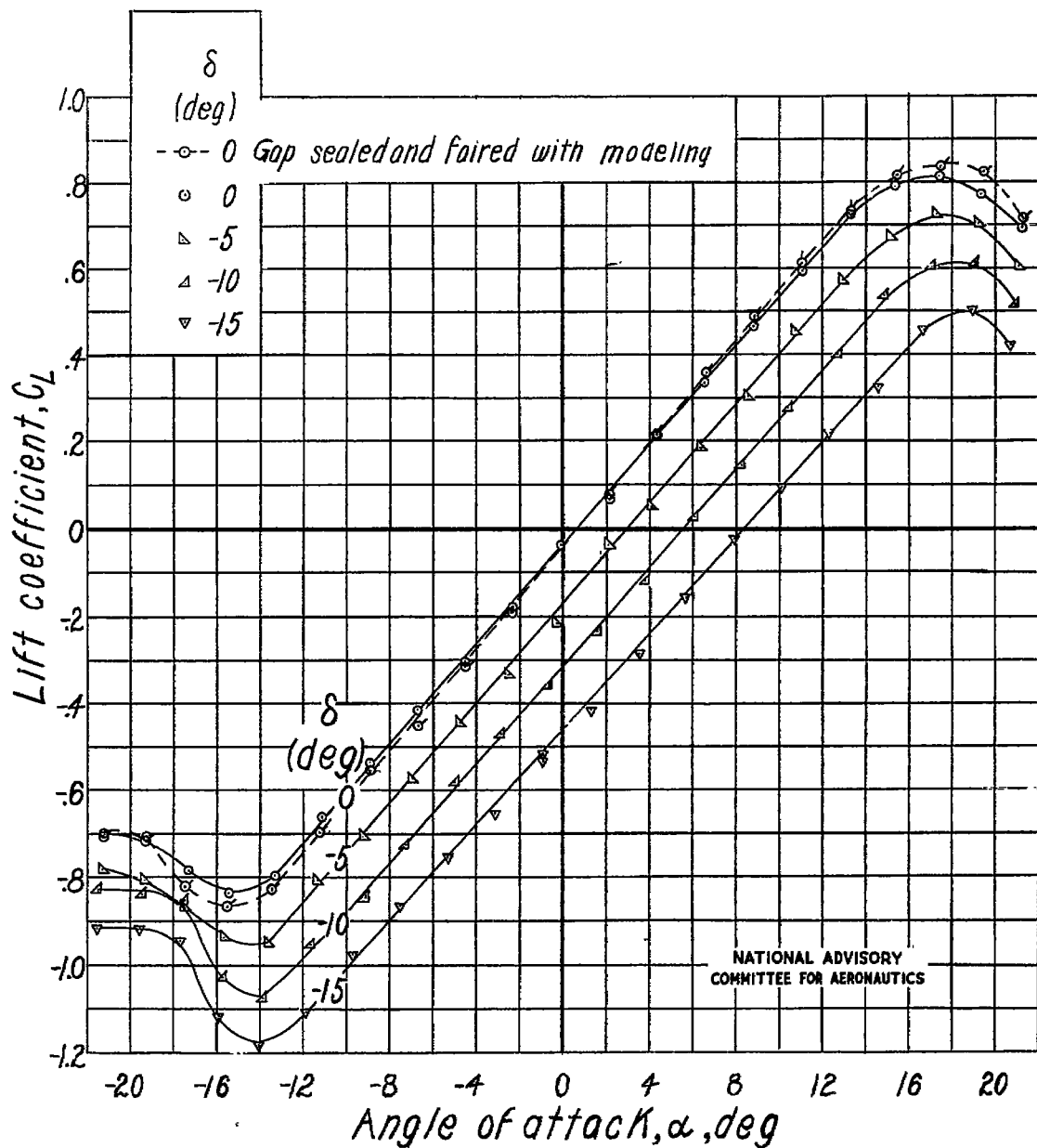
(c) Elevator cut-out filled and gap open.

Figure 25.- Continued. Tail 4.



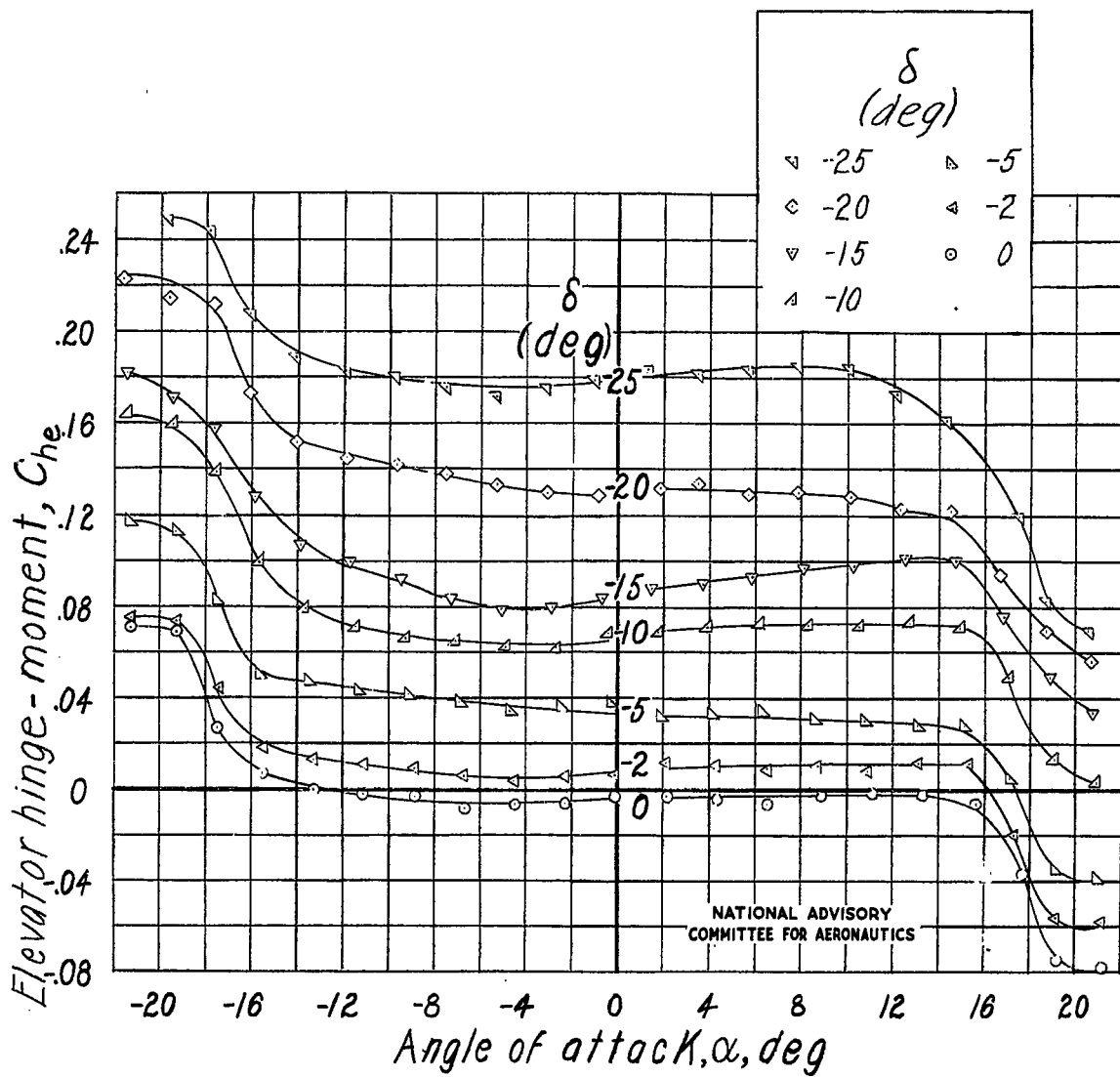
(c) Concluded.

Figure 25.- Continued. Tail 4.



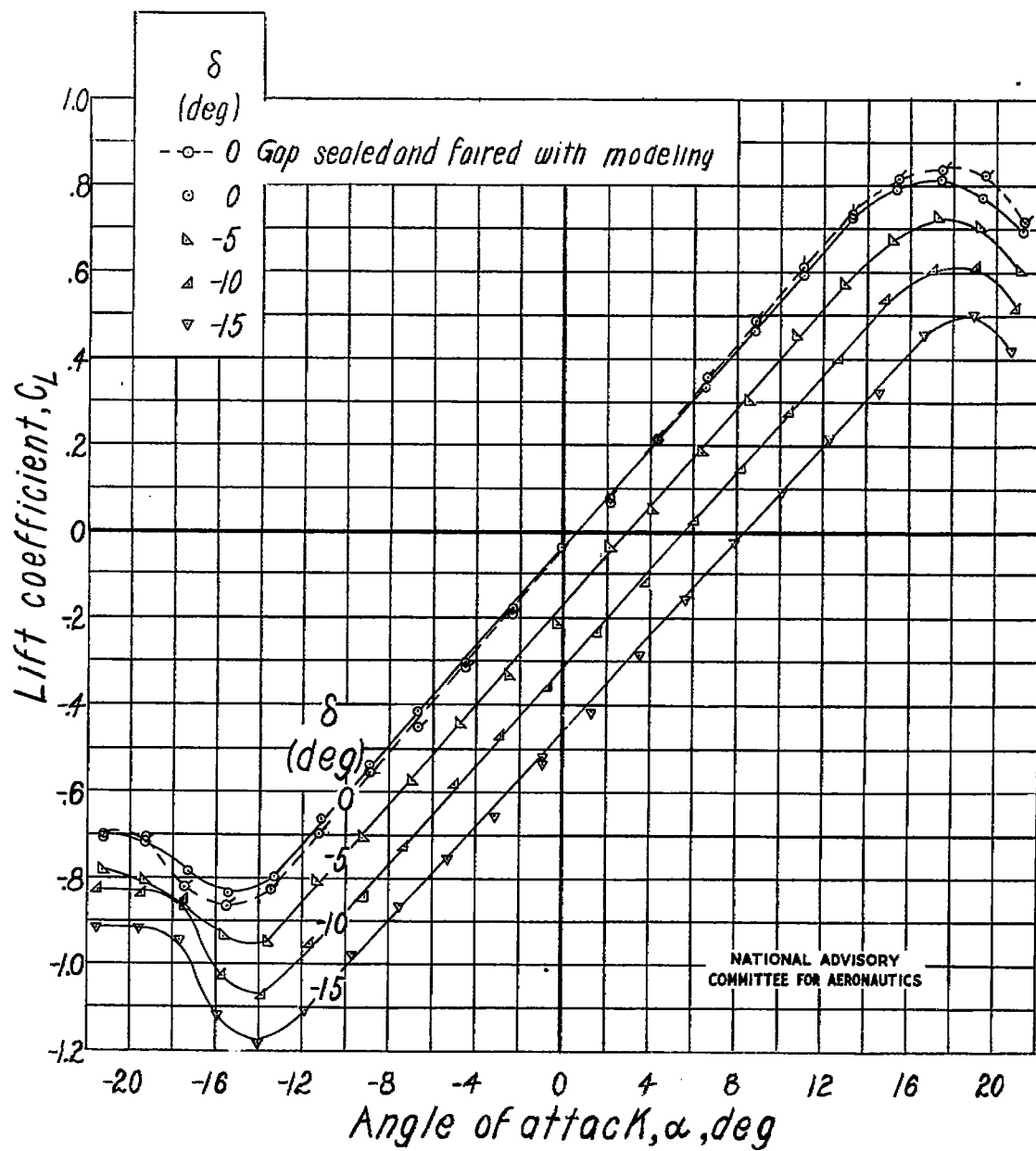
(d) Elevator cut-out filled and gap sealed with grease except where noted.

Figure 25.- Continued. Tail 4.



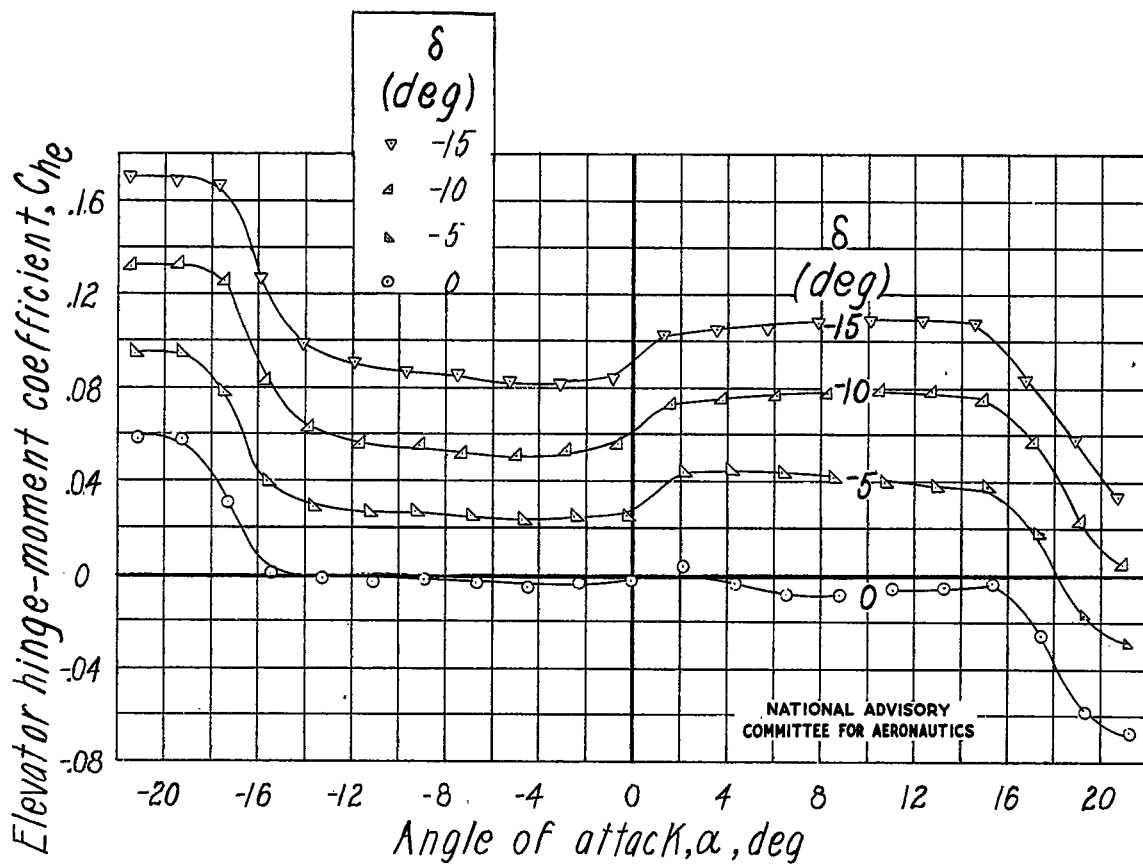
(c) Concluded.

Figure 25.- Continued. Tail 4.



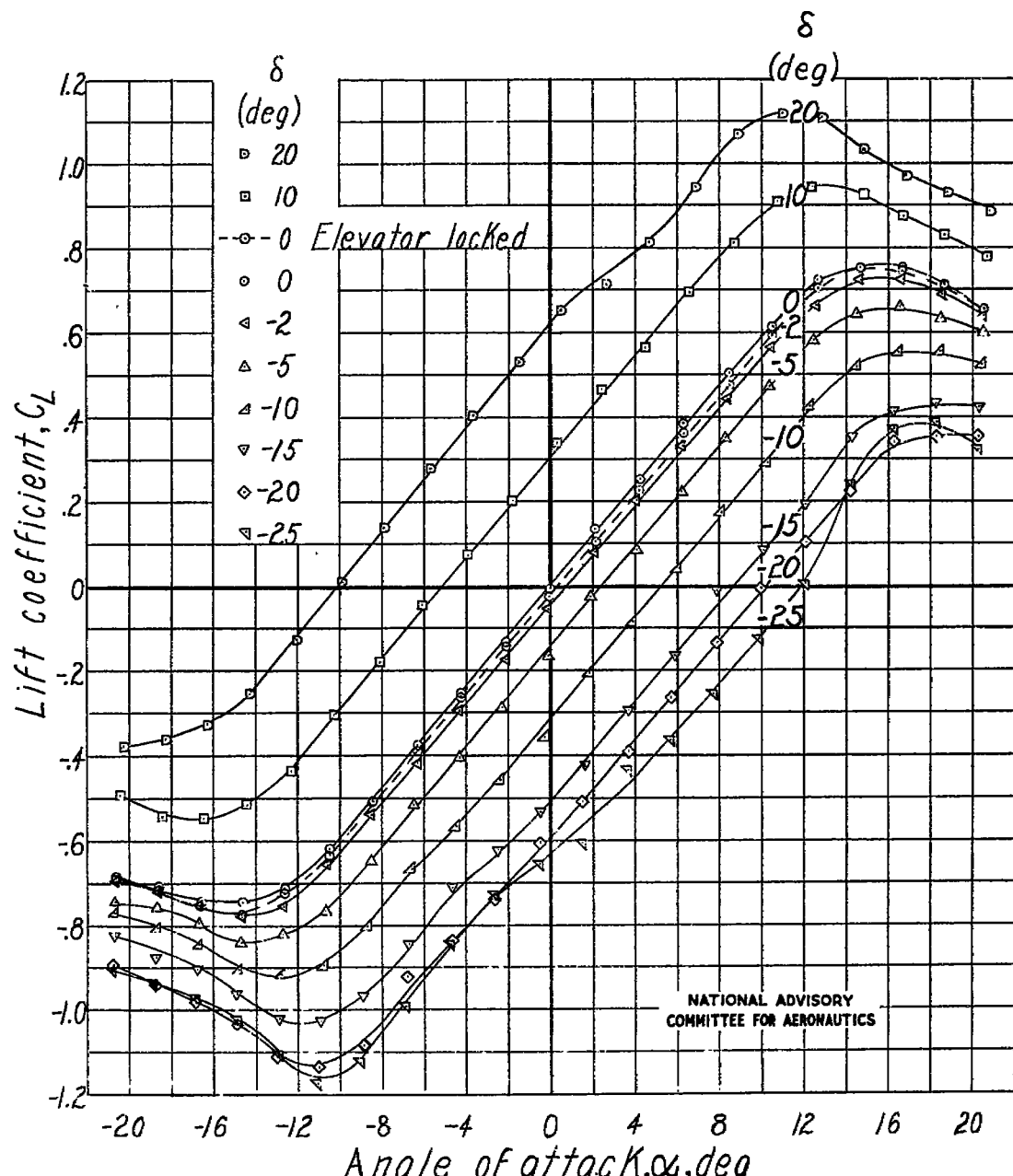
(d) Elevator cut-out filled and gap sealed with grease except where noted.

Figure 25.- Continued. Tail 4.



(d) Concluded.

Figure 25.- Concluded. Tail 4.



(a) Elevator gap open.

Figure 26.- Lift and hinge-moment characteristics of horizontal tail 5.

19

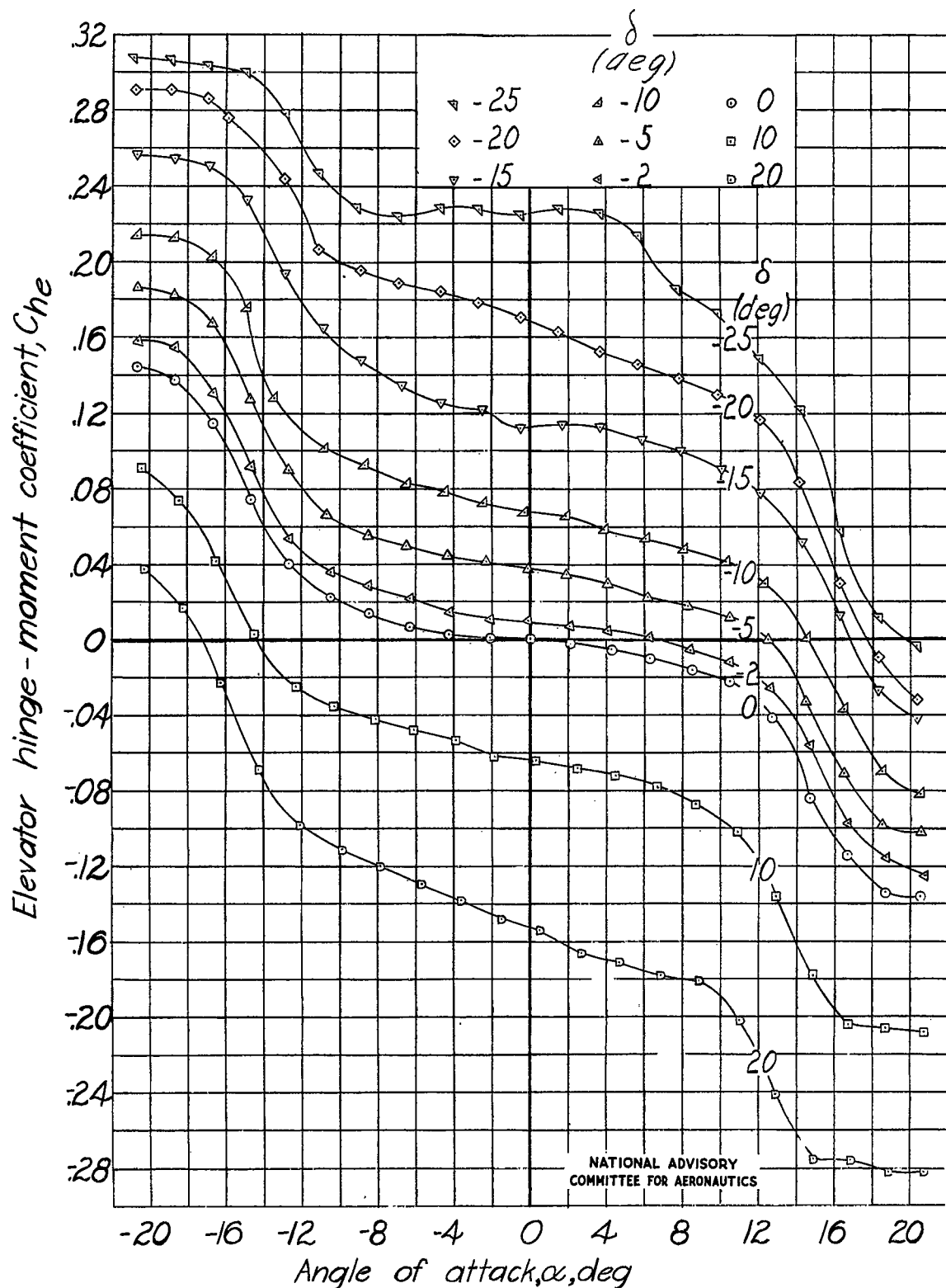
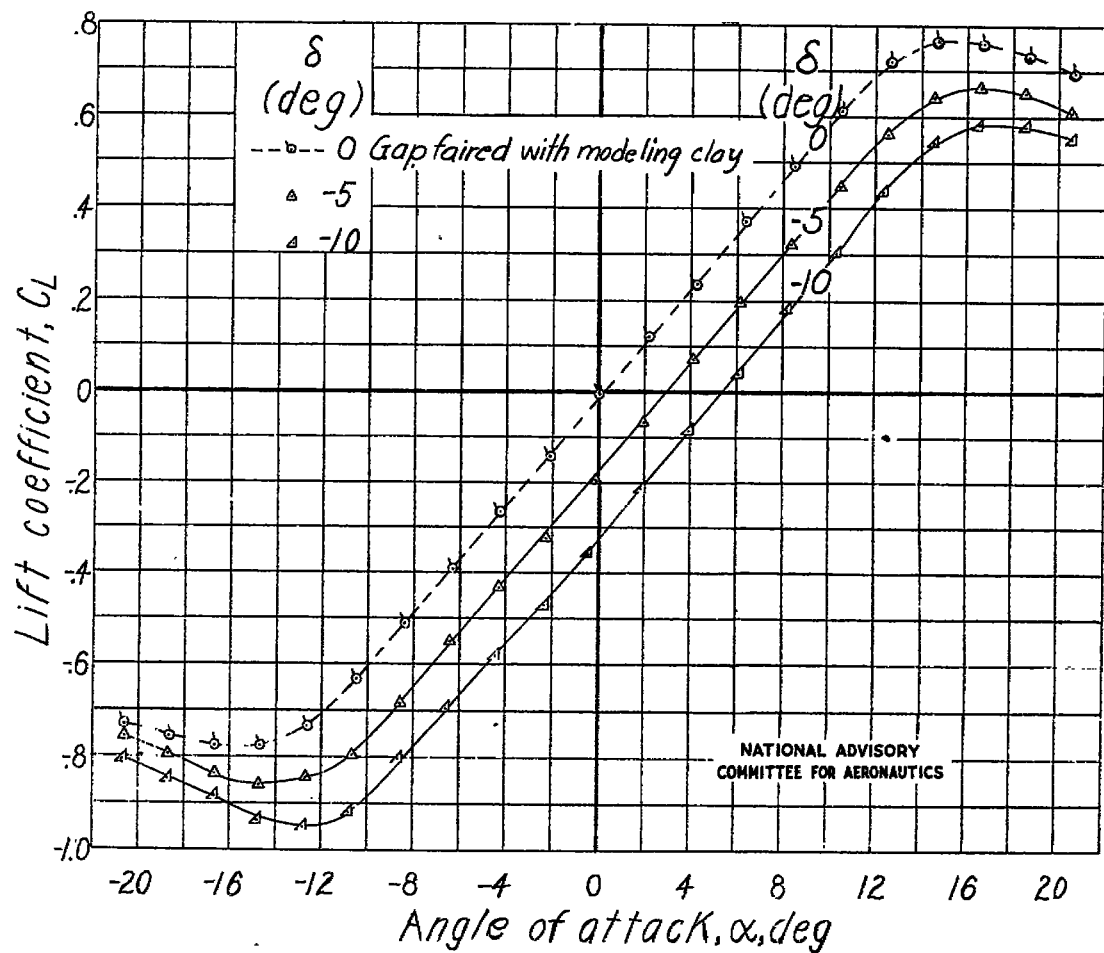
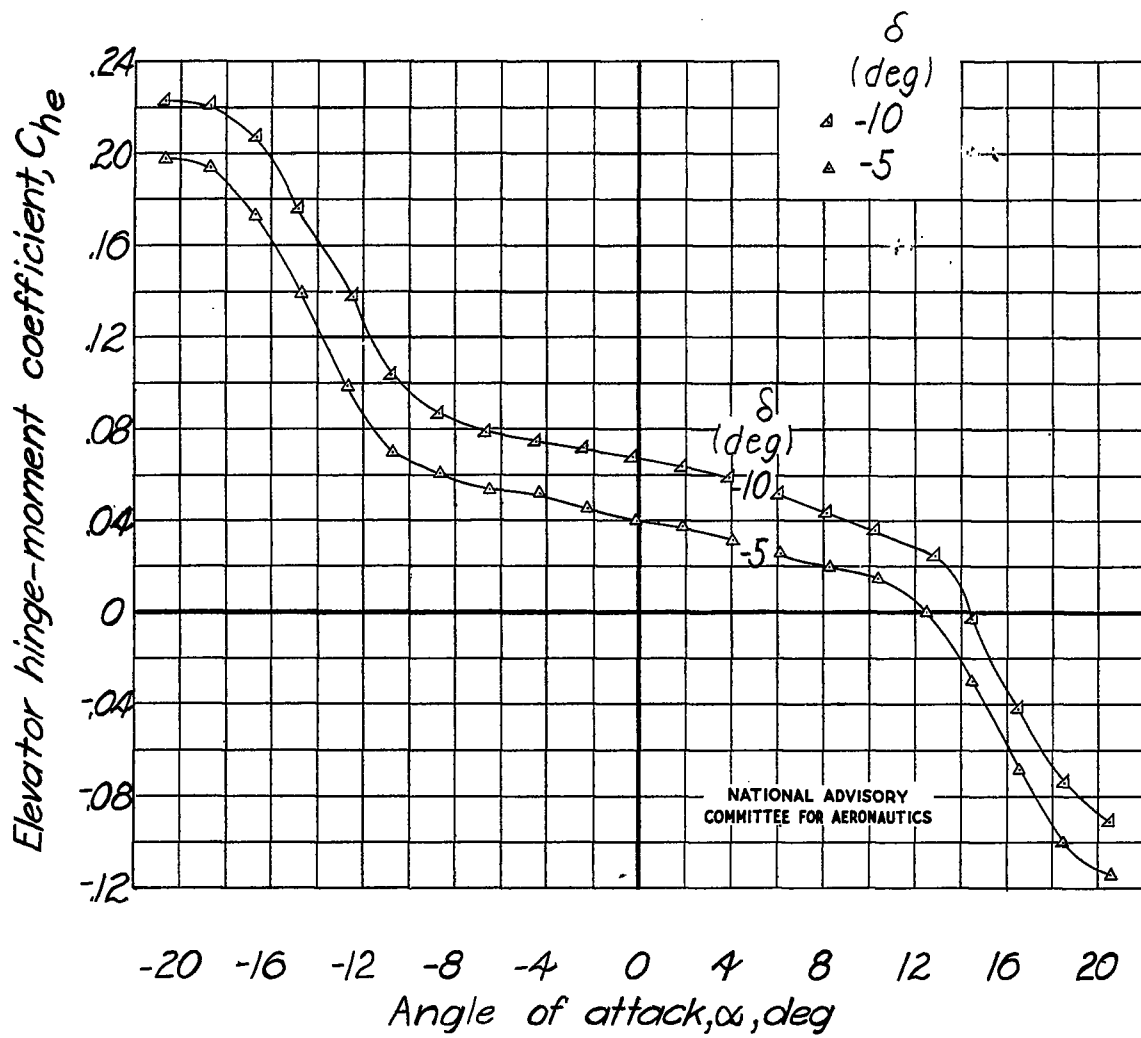


Figure 26.- Continued. Tail 5.



(b) Elevator gap sealed with grease except where noted.

Figure 26.- Continued. Tail 5.

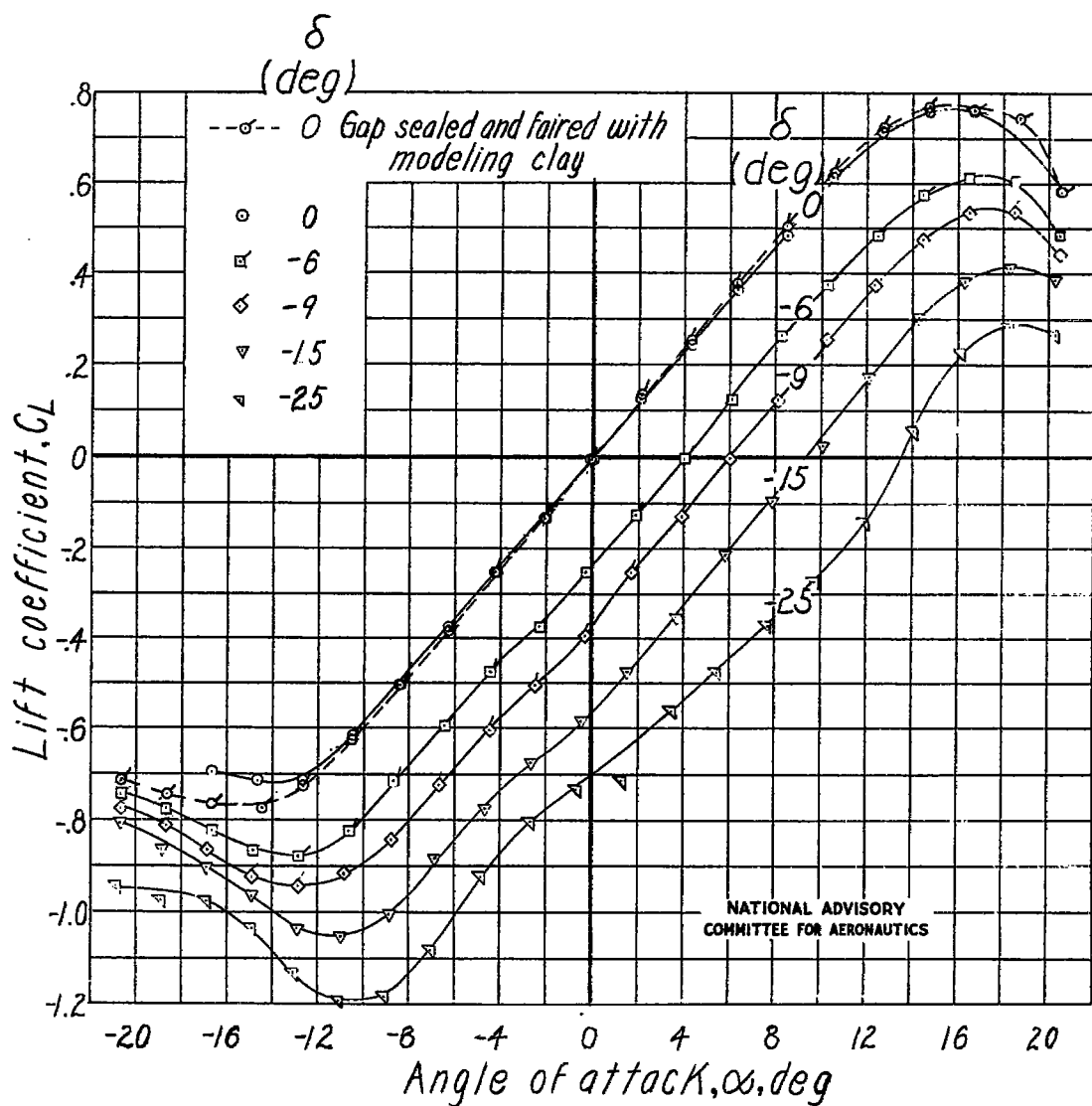


(b) Concluded.

Figure 26.- Continued. Tail 5.

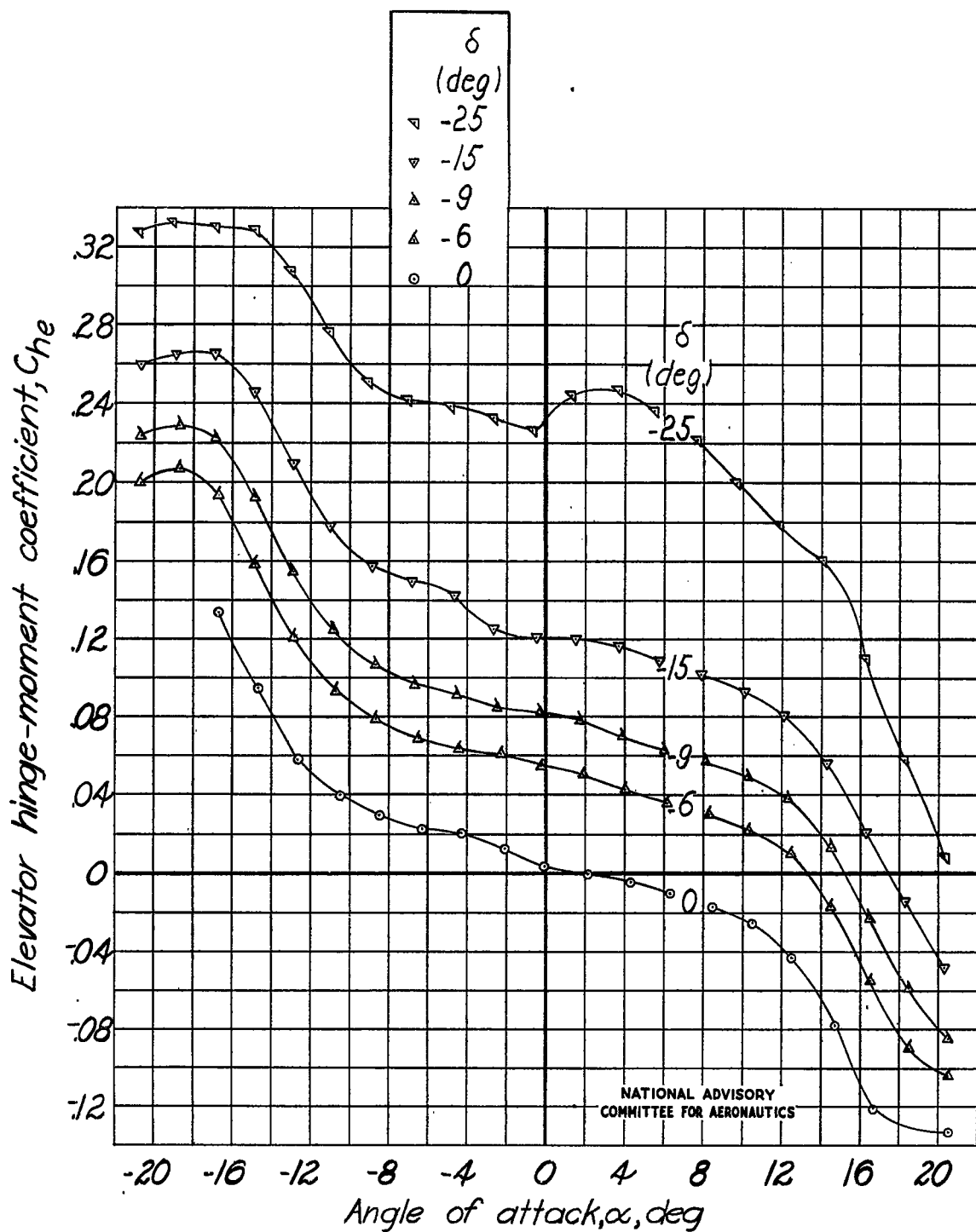
Fig. 26c

NACA TN No. 1291



(c) Elevator cut-out filled and gap open.

Figure 26.- Continued. Tail 5.

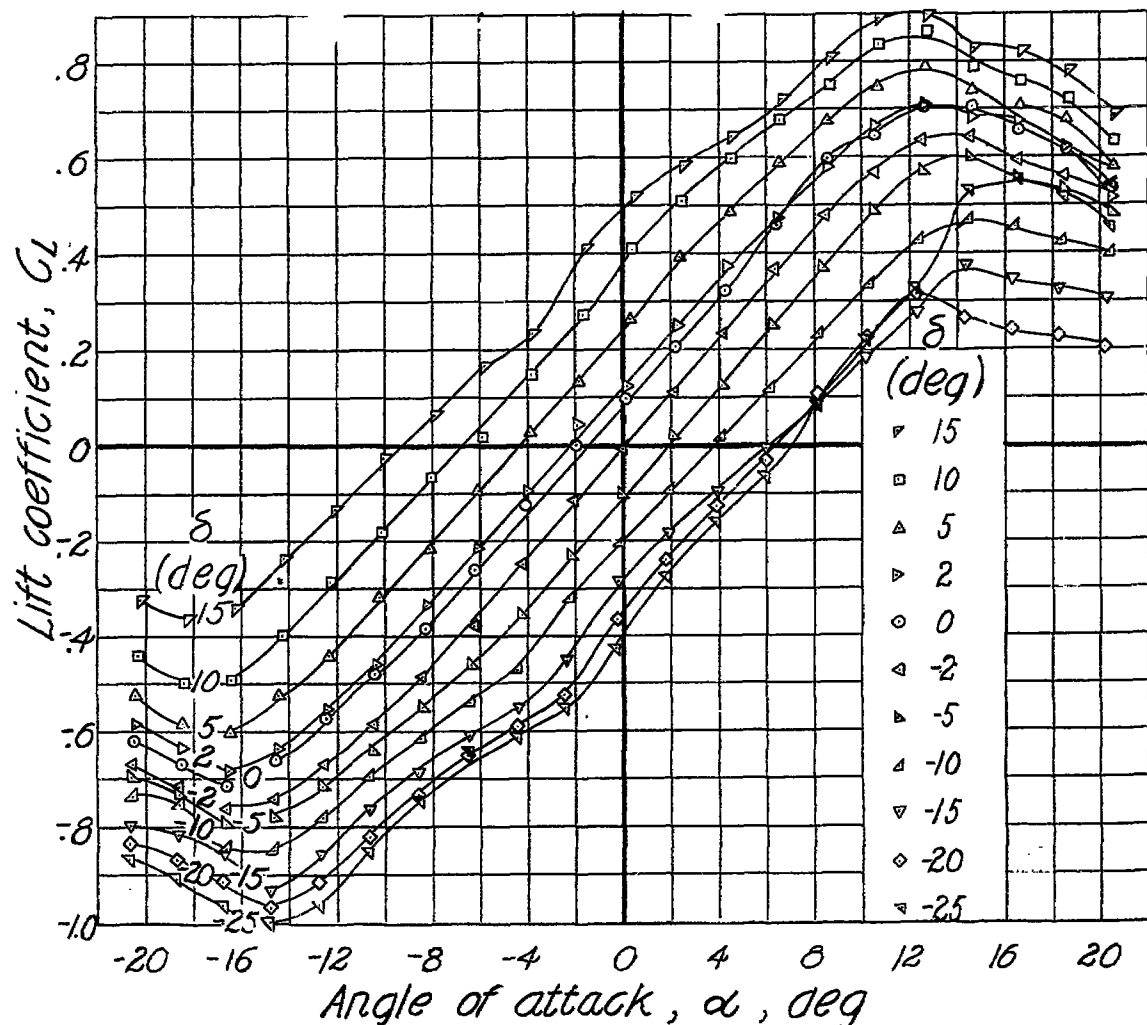


(c) Concluded.

Figure 26.- Concluded. Tail 5.

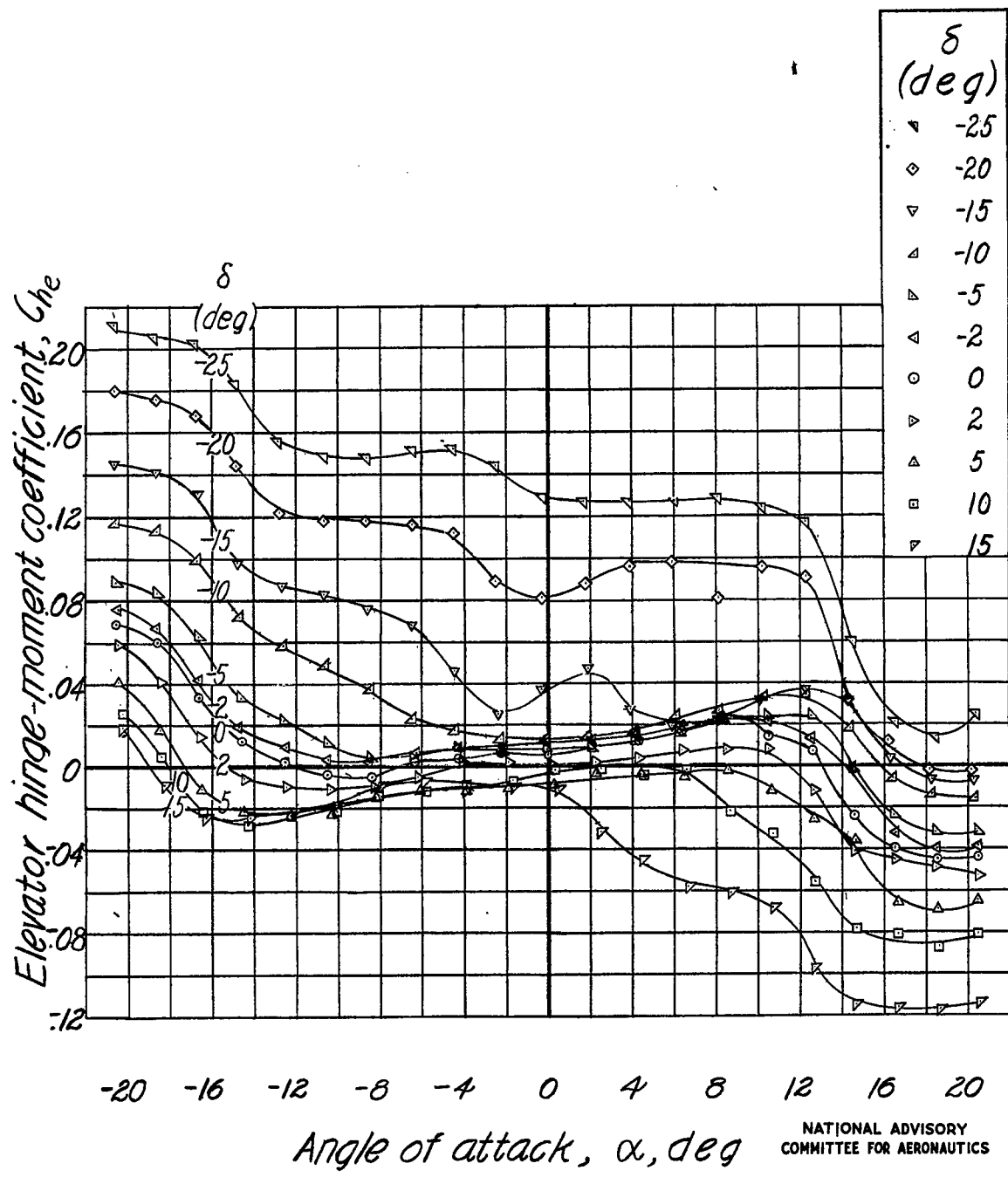
Fig. 27a

NACA TN No. 1291

NATIONAL ADVISORY
COMMITTEE FOR AERONAUTICS

(a) Elevator gap open.

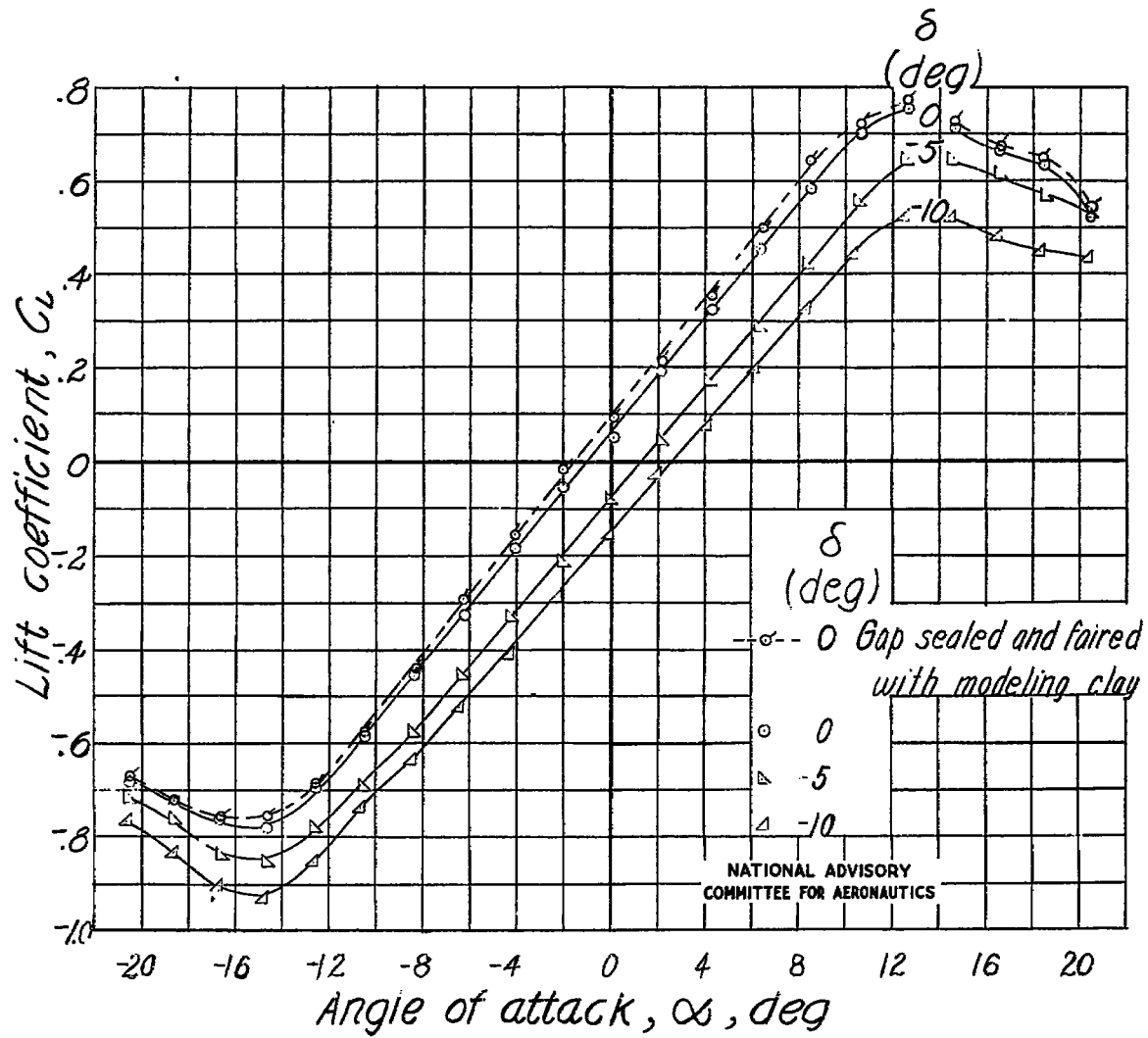
Figure 27.- Lift and hinge-moment characteristics of horizontal tail 6.



(a) Concluded.

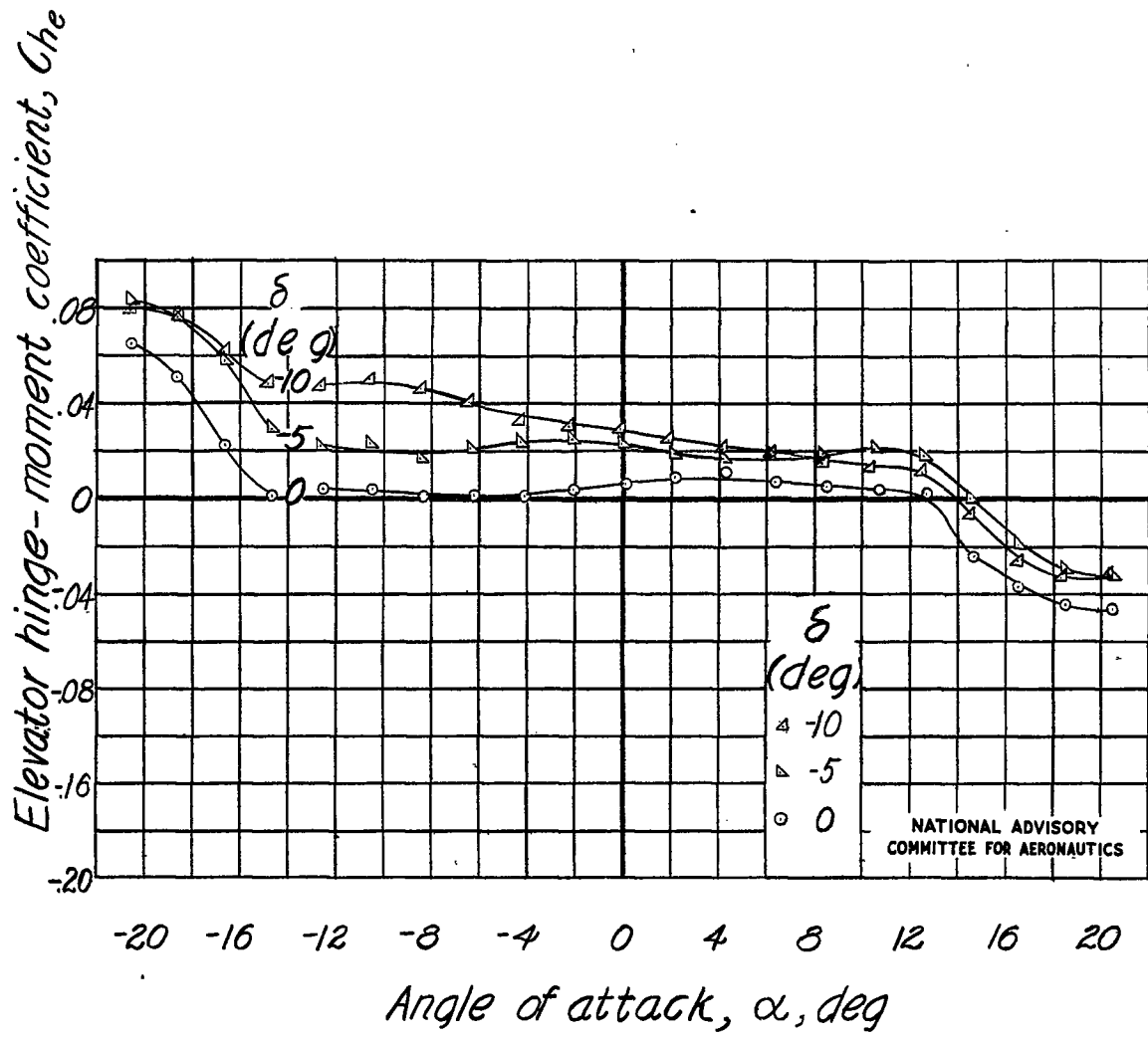
Figure 27.- Continued. Tail 6.

NATIONAL ADVISORY
COMMITTEE FOR AERONAUTICS



(b) Elevator gap sealed with grease except where noted.

Figure 27.- Continued. Tail 6.

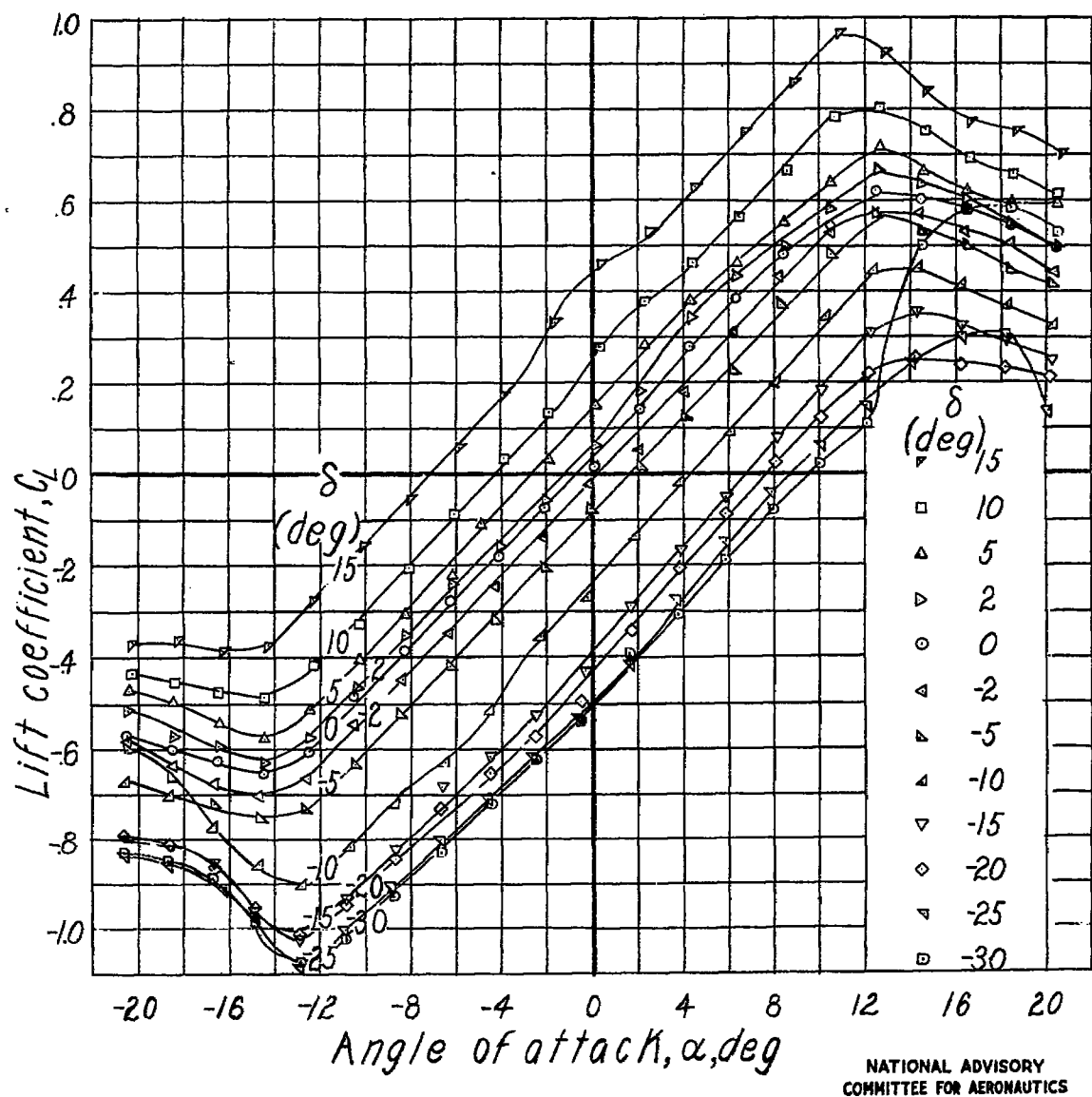


(b) Concluded.

Figure 27.- Concluded. Tail 6.

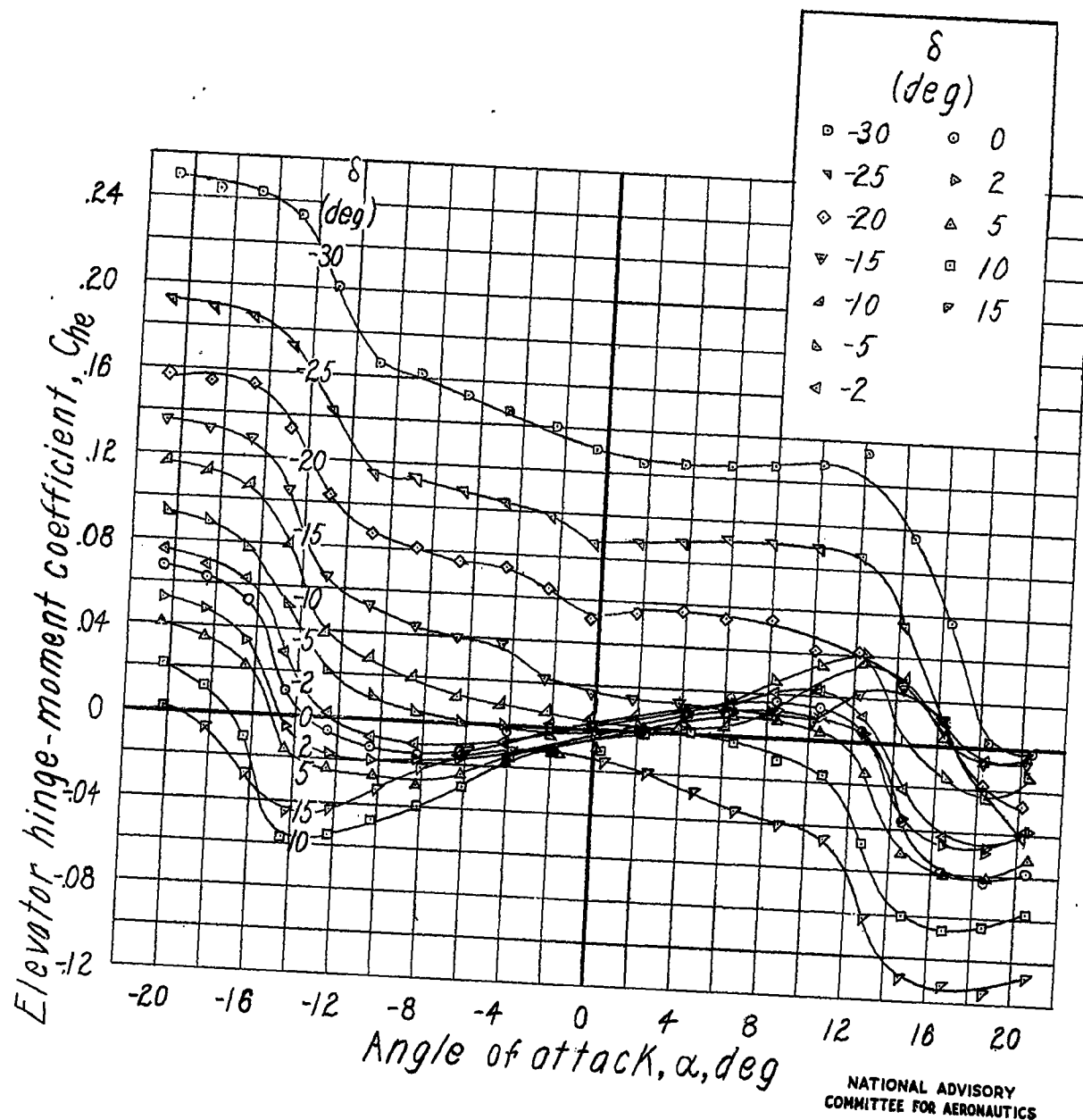
Fig. 28a

NACA TN No. 1291



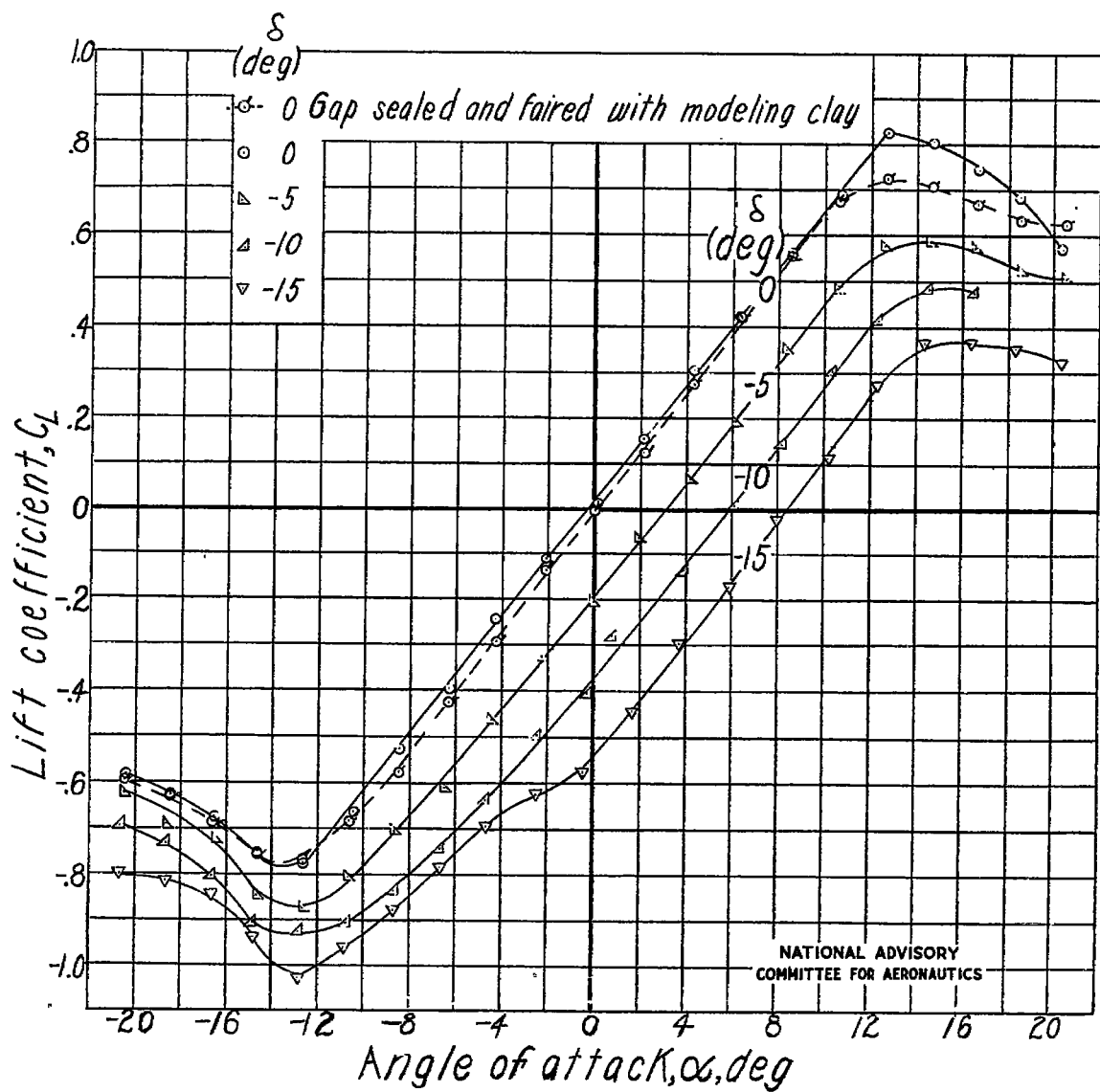
(a) Elevator gap open.

Figure 28.- Lift and hinge-moment characteristics of horizontal tail 7.



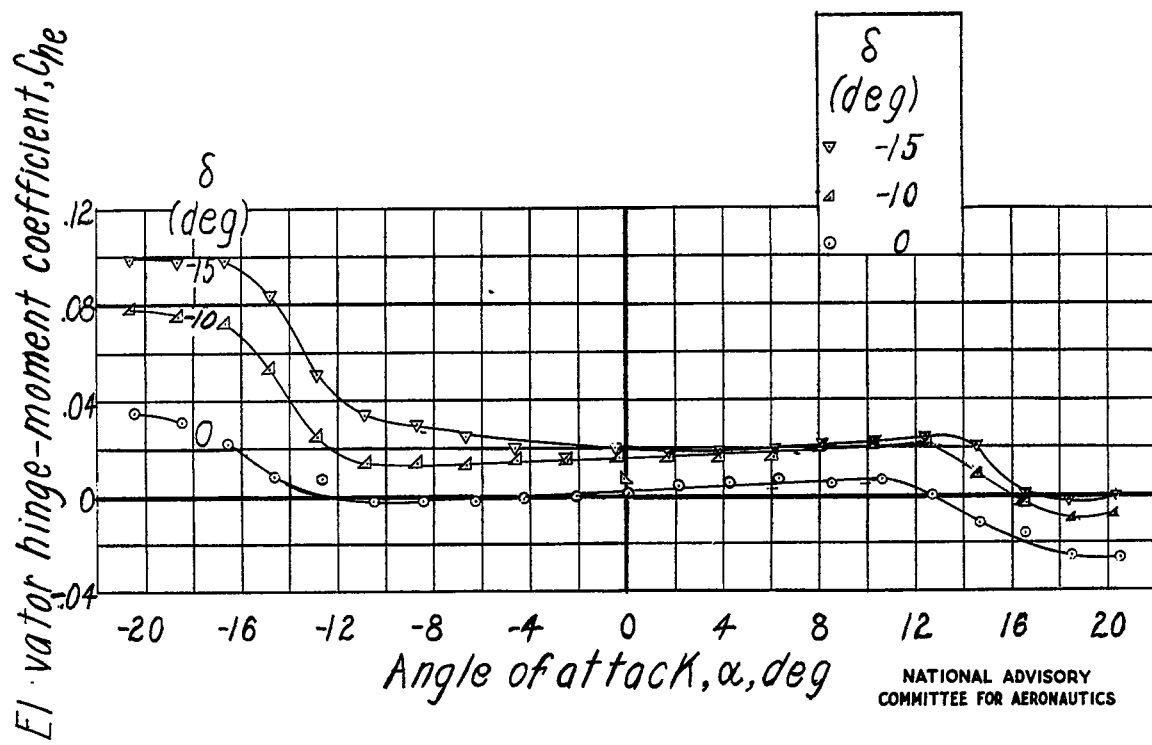
(a) Concluded.

Figure 28.- Continued. Tail 7.



(b) Elevator gap sealed with grease except where noted.

Figure 28.- Continued. Tail 7.



(b) Concluded.

Figure 28.- Concluded. Tail 7.

Fig. 29a

NACA TN No. 1291

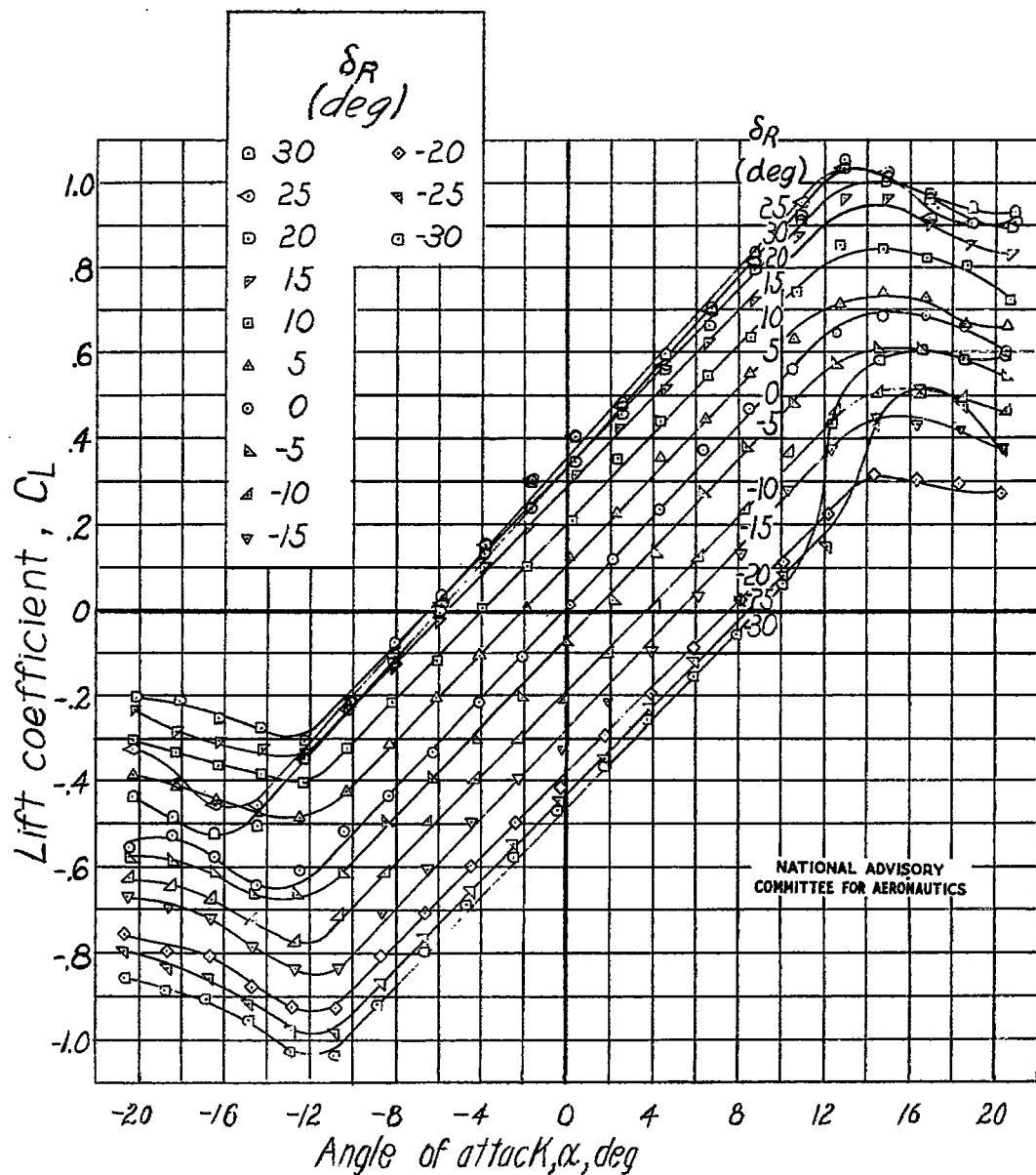
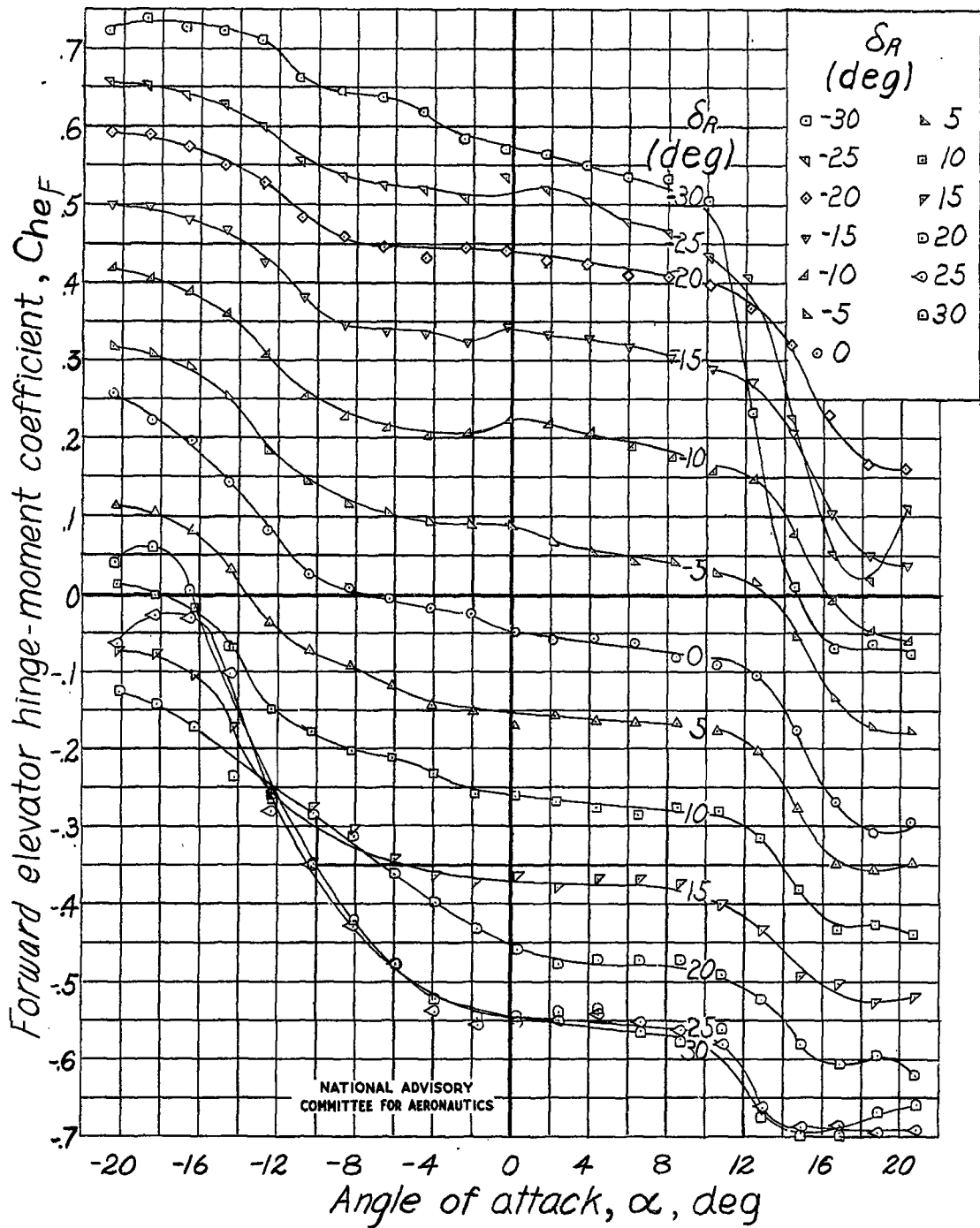
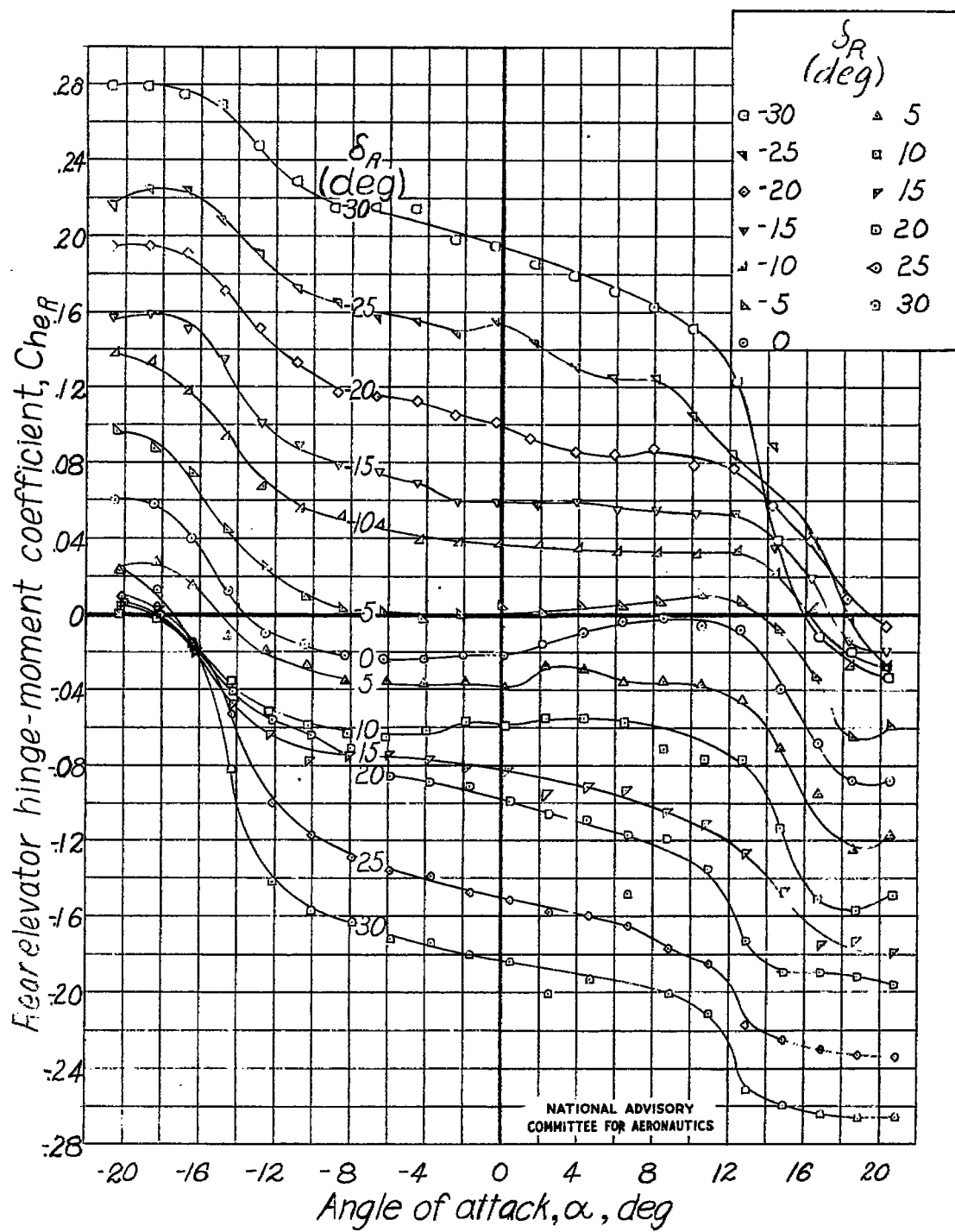
(a) Elevator gap open. $\delta_F = 0^\circ$.

Figure 29.- Lift and hinge-moment characteristics of horizontal tail 8.



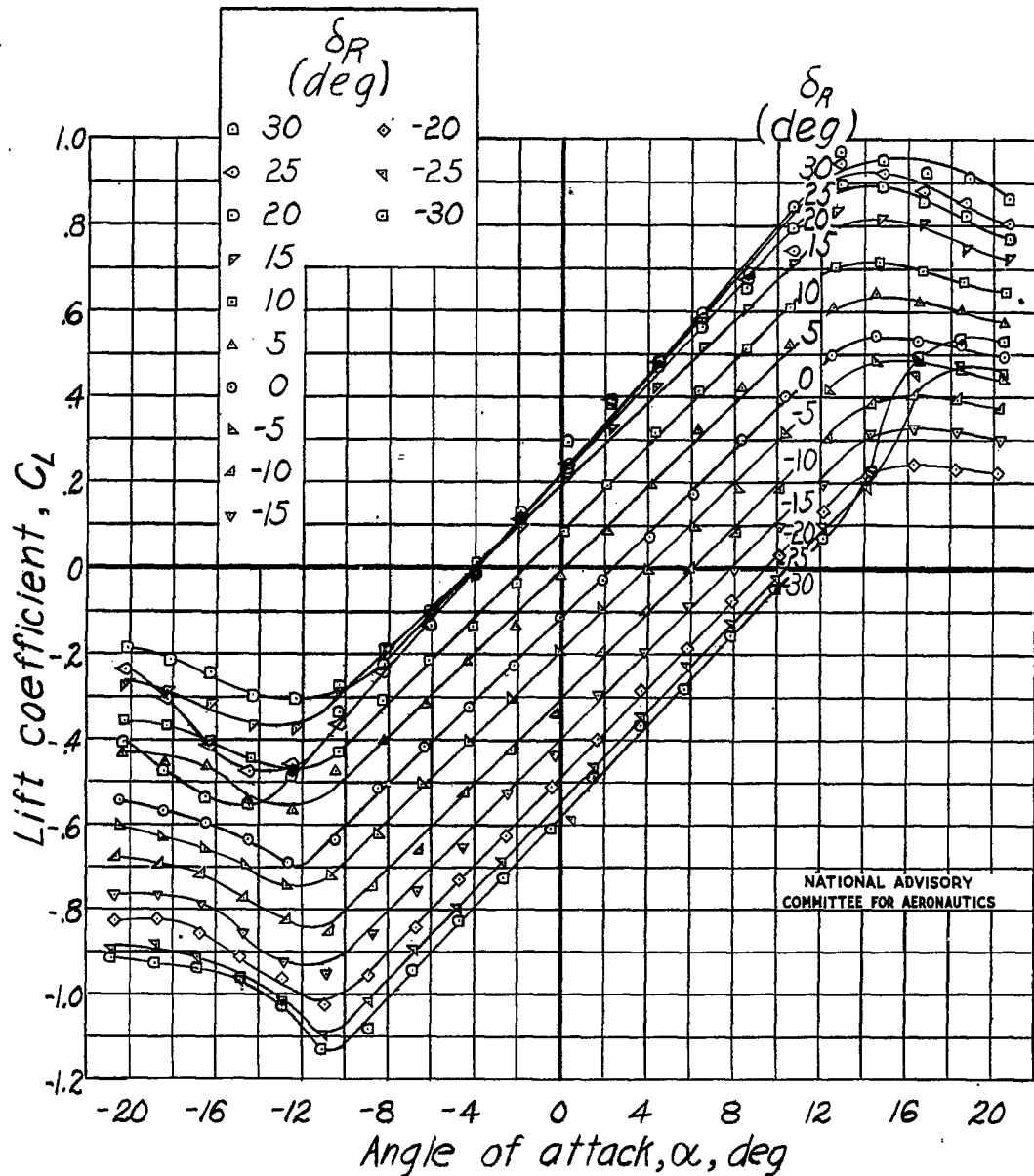
(a) Continued.

Figure 29.- Continued. Tail 8.



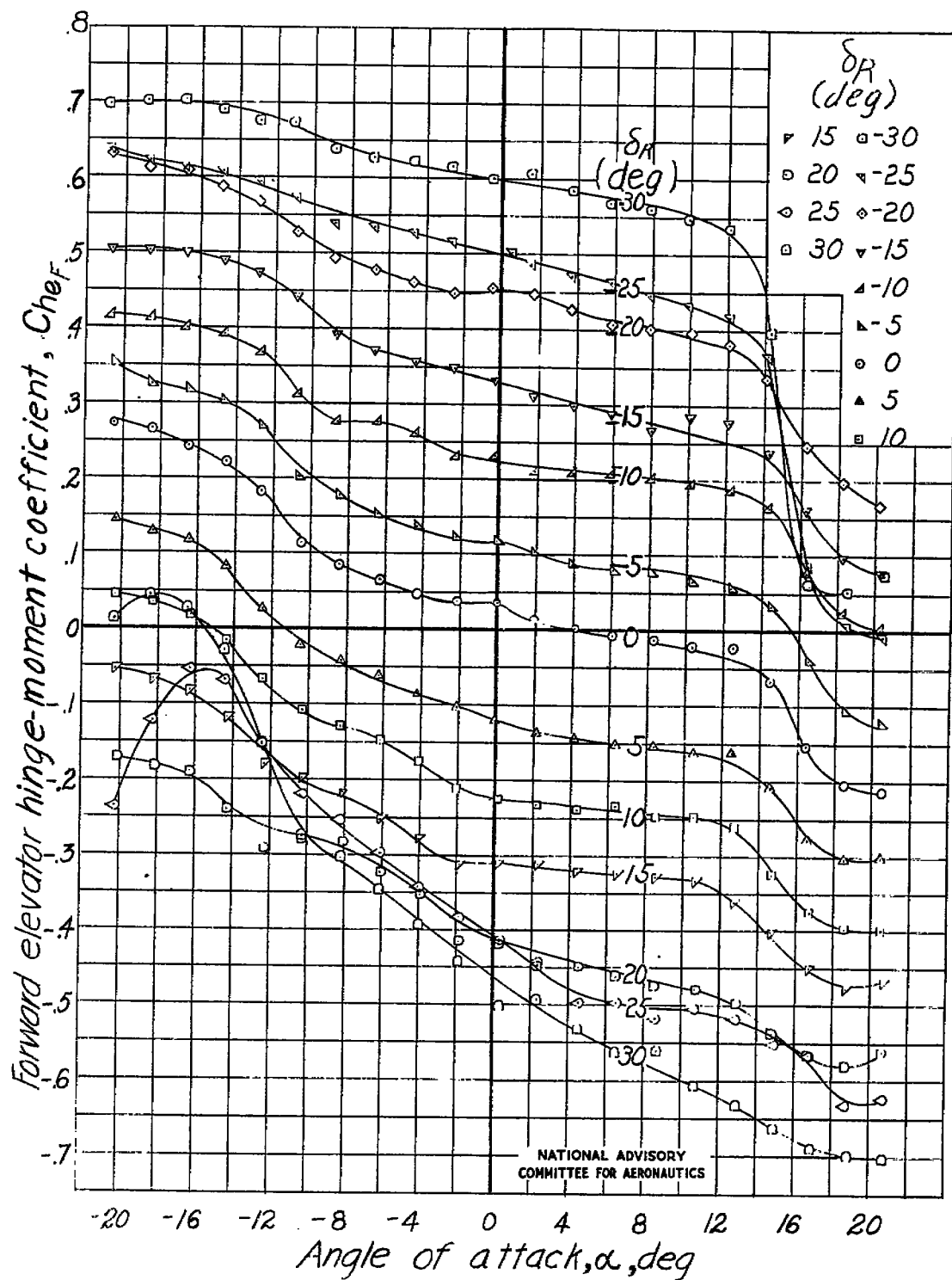
(a) Concluded.

Figure 29.- Continued. Tail 8.



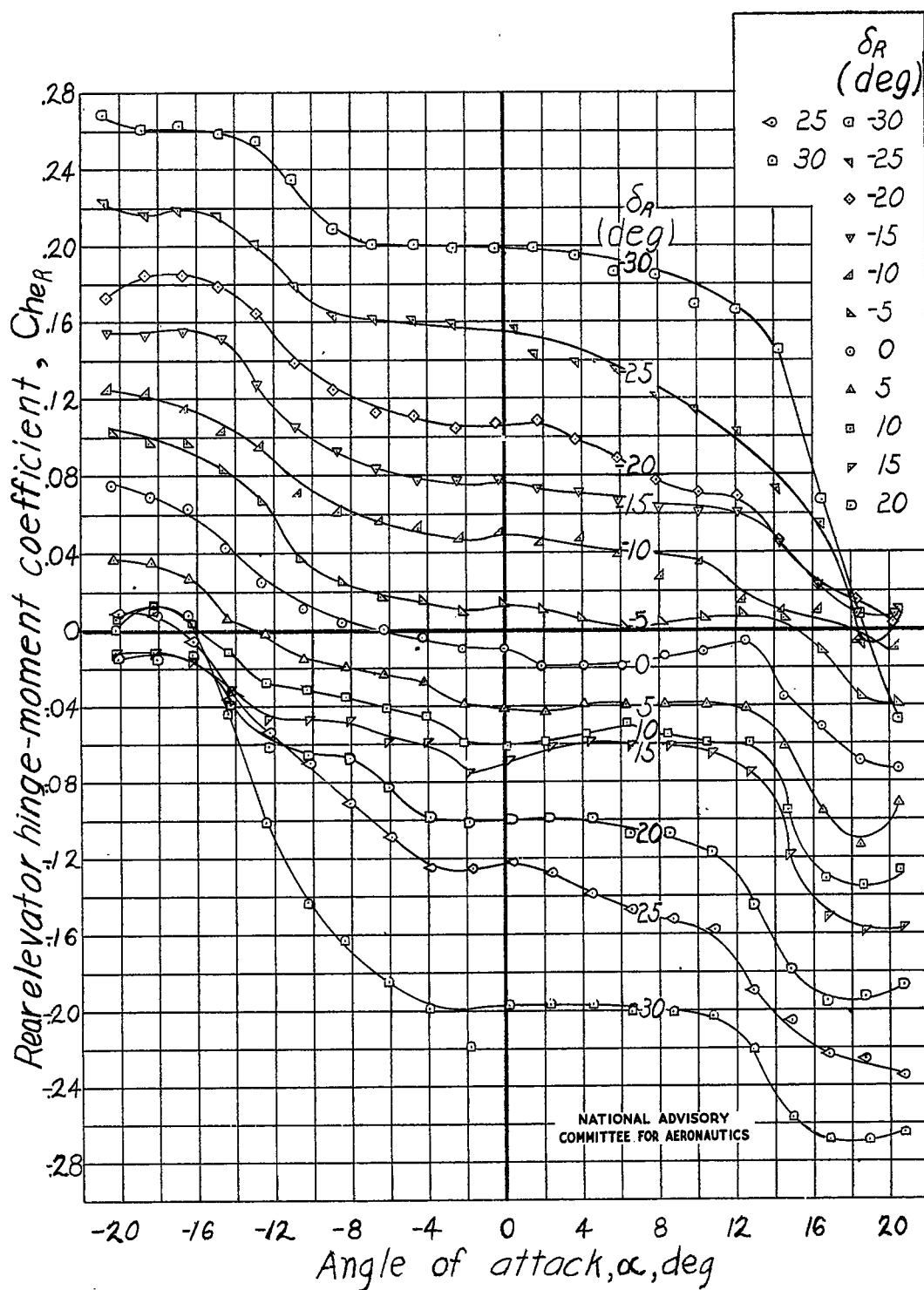
(b) Elevator gap open. $\delta_F = -5^\circ$.

Figure 29.- Continued. Tail 8.



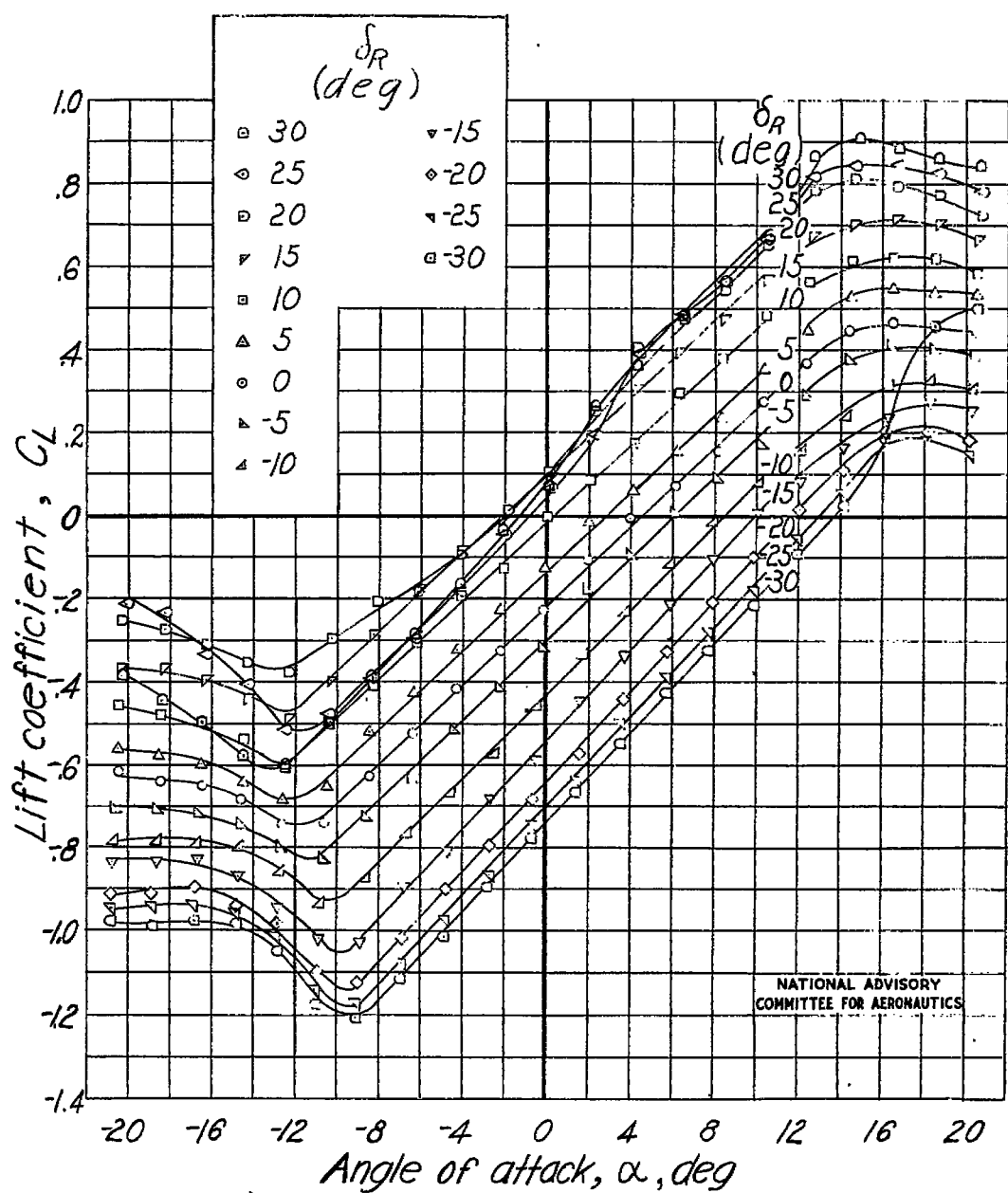
(b) Continued.

Figure 29.- Continued. Tail 8.



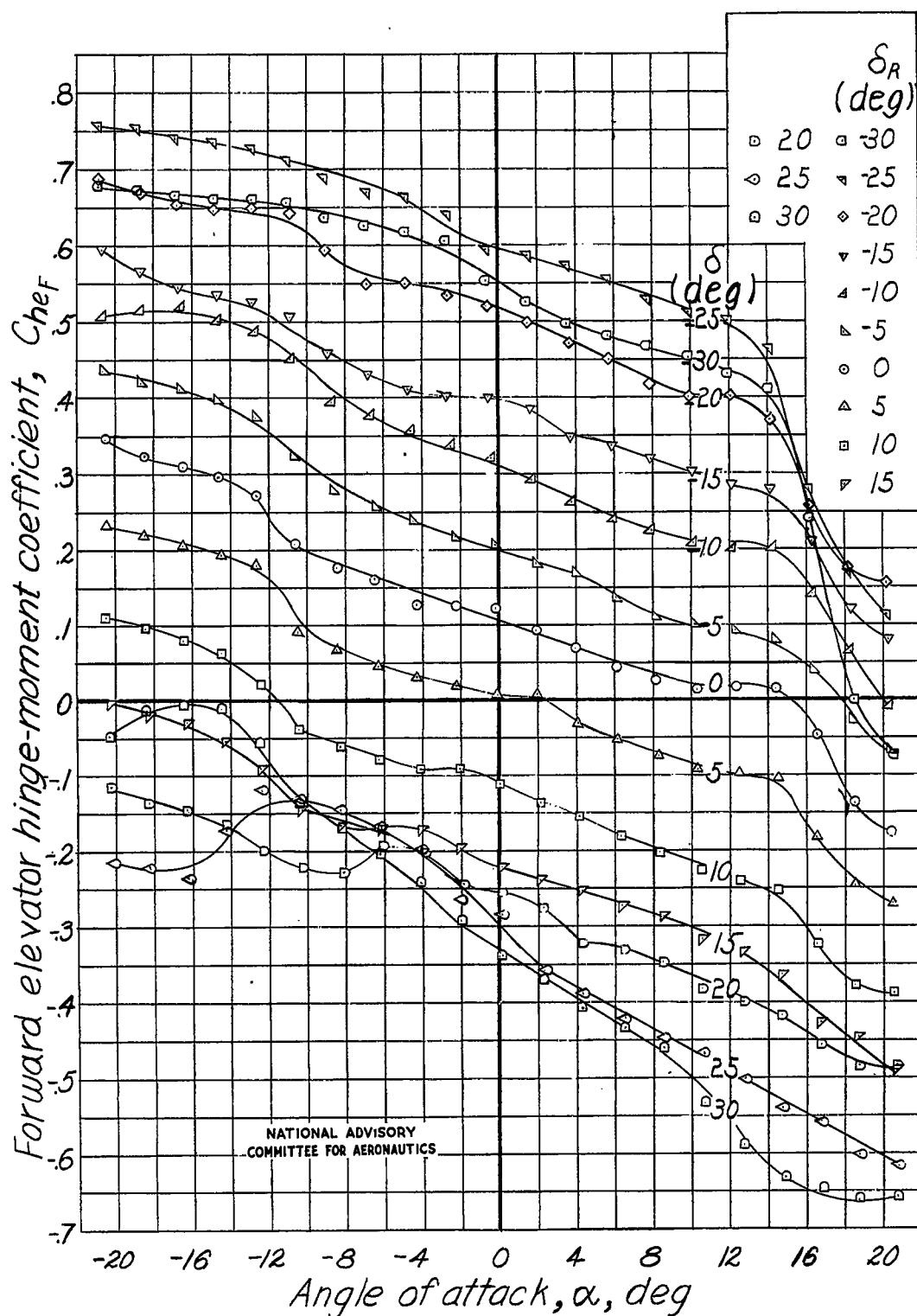
(b) Concluded.

Figure 29.- Continued. Tail 8.



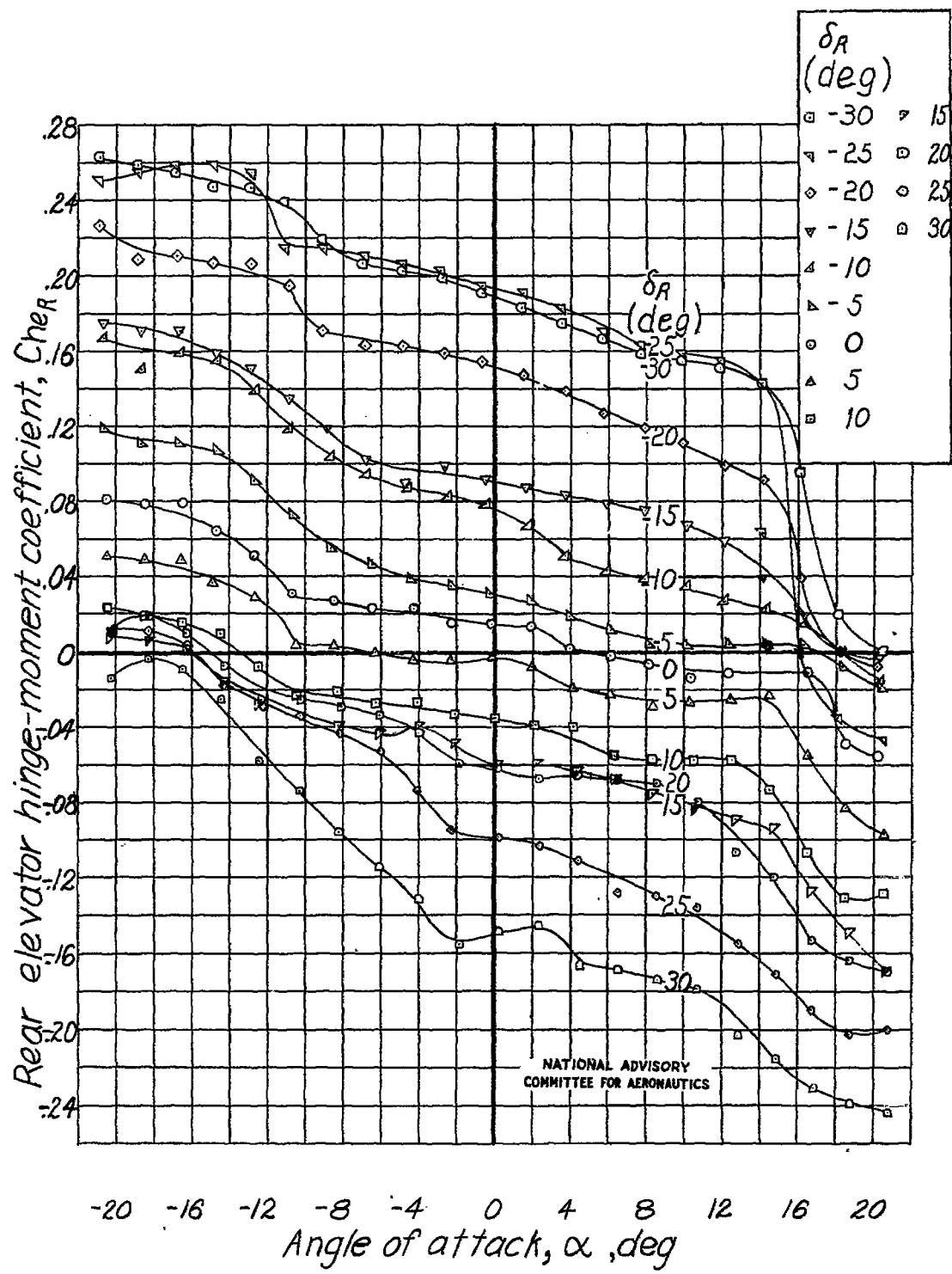
(c) Elevator gap open. $\delta_F = -10^\circ$.

Figure 29.- Continued. Tail 8.



(c) Continued.

Figure 29.- Continued. Tail 8.



(c) Concluded.

Figure 29.- Continued. Tail 8.

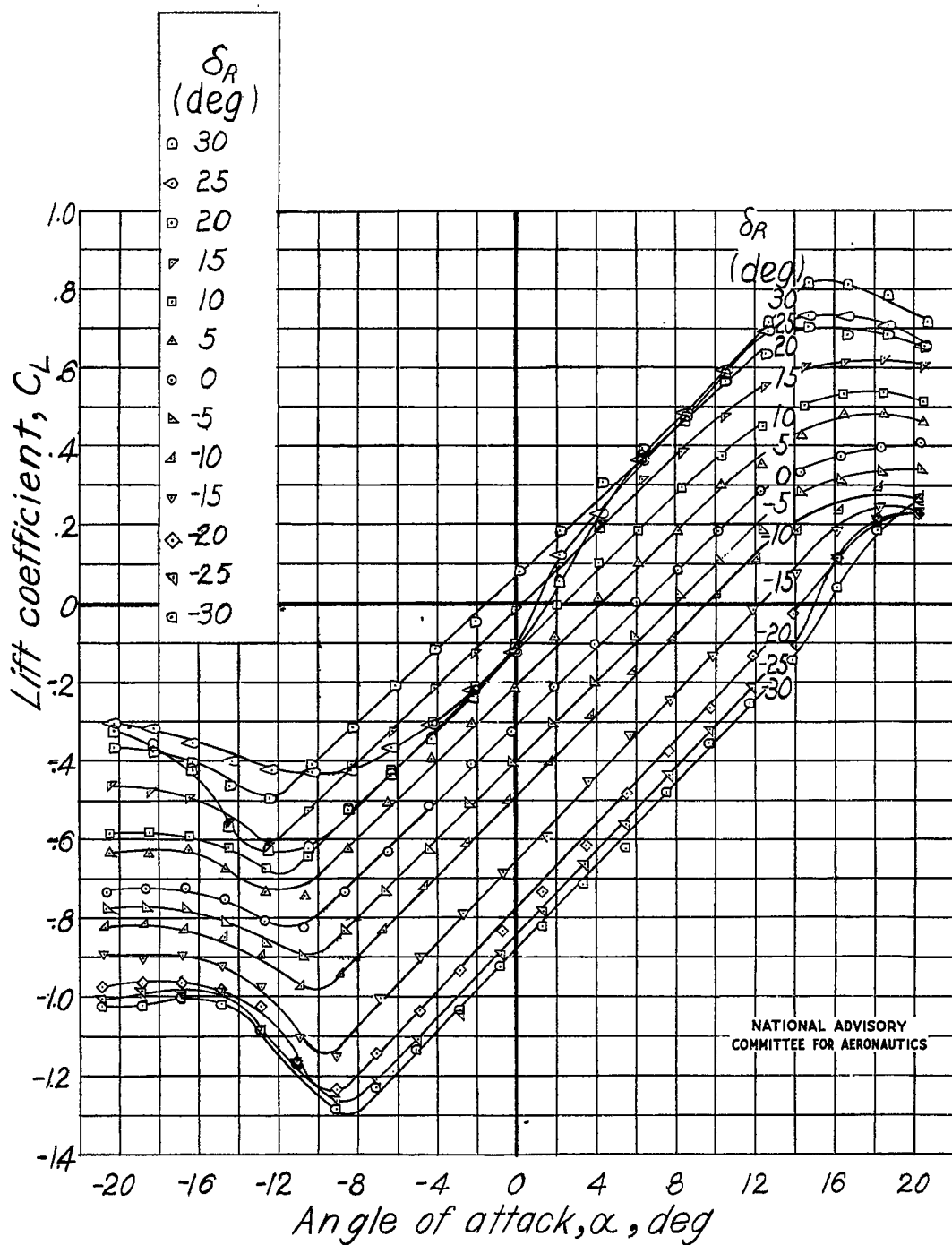
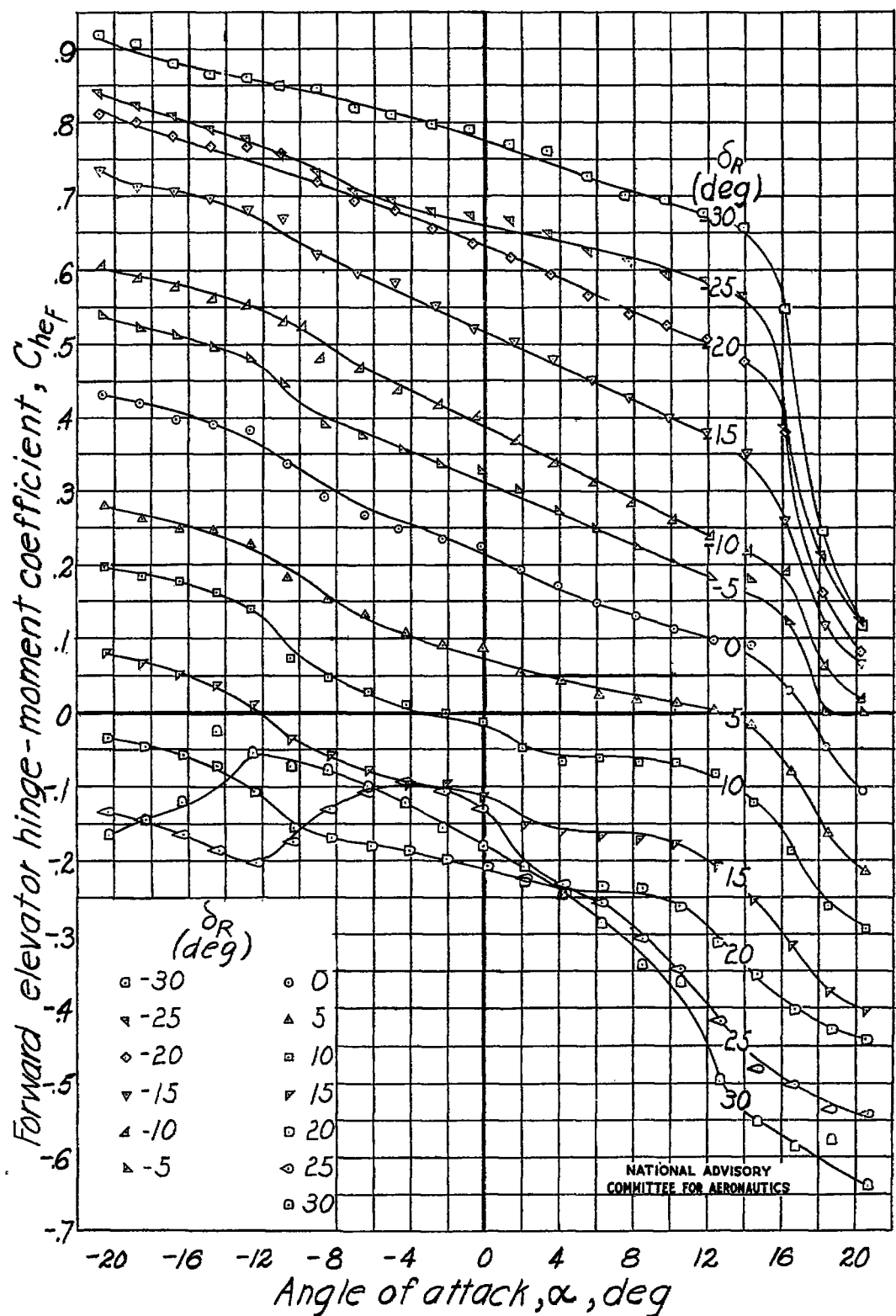
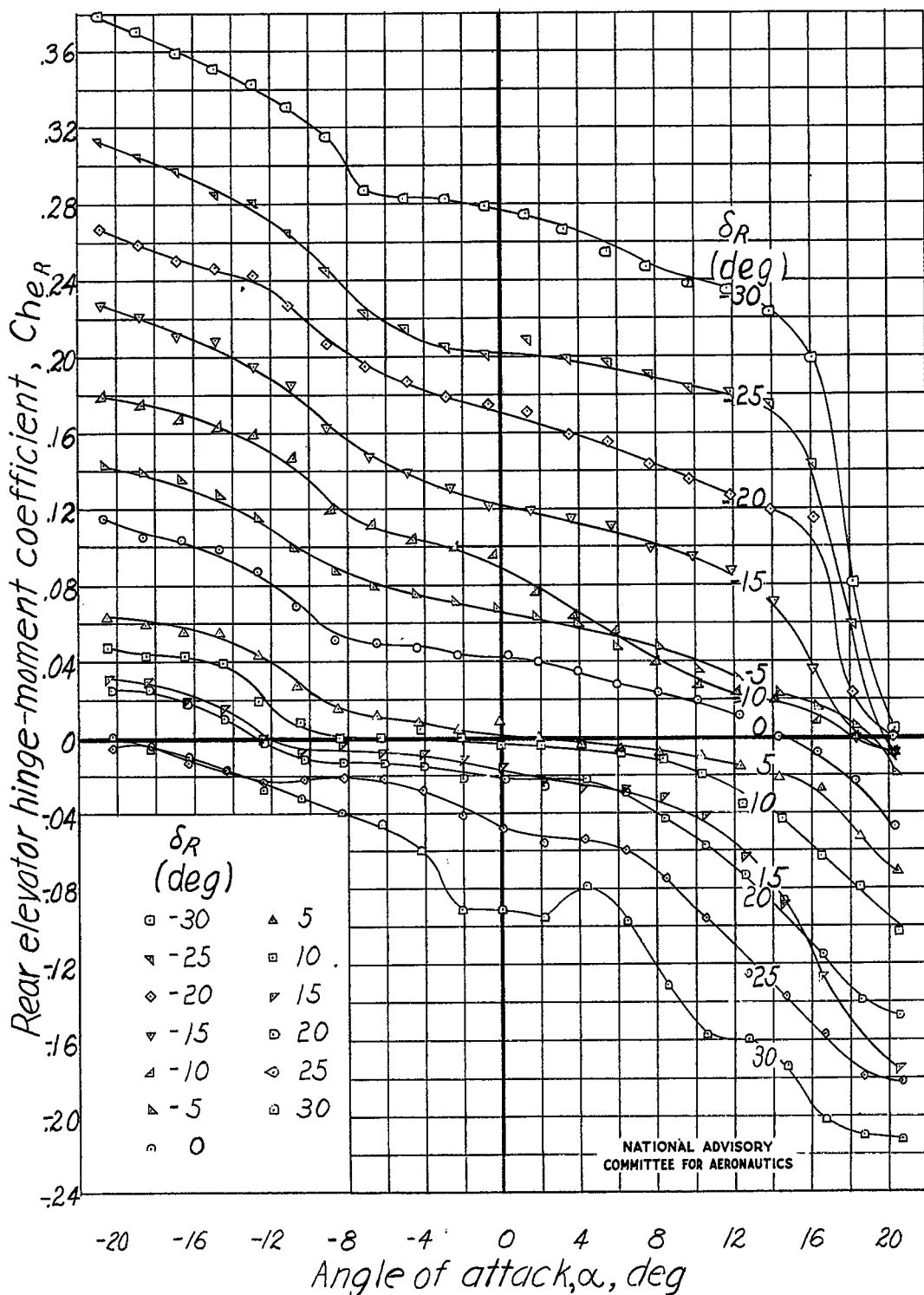
(d) Elevator gap open. $\delta_F = -15^\circ$.

Figure 29.- Continued. Tail 8.



(d) Continued.

Figure 29.- Continued. Tail 8.



(d) Concluded.

Figure 29.- Continued. Tail 8.

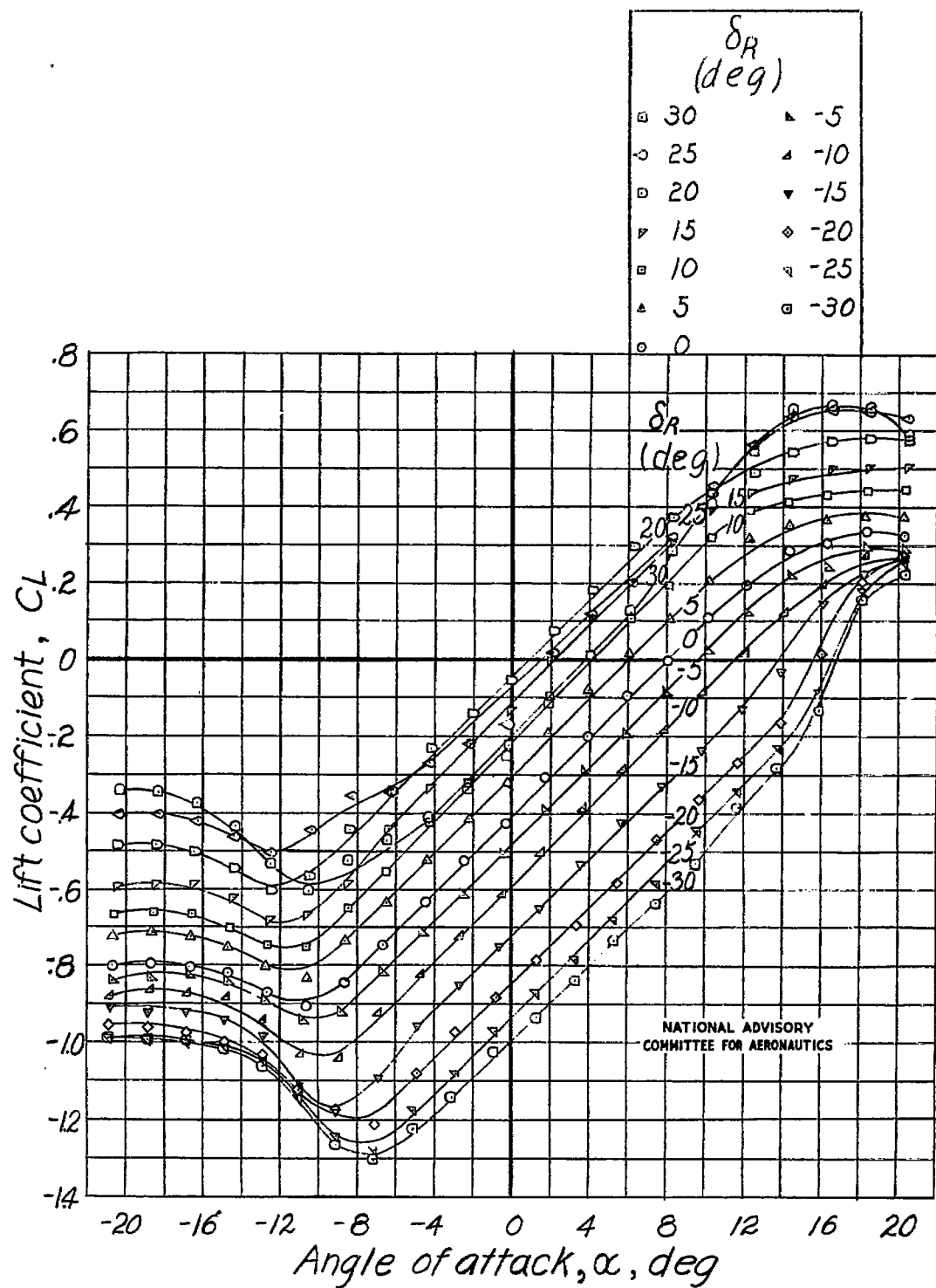
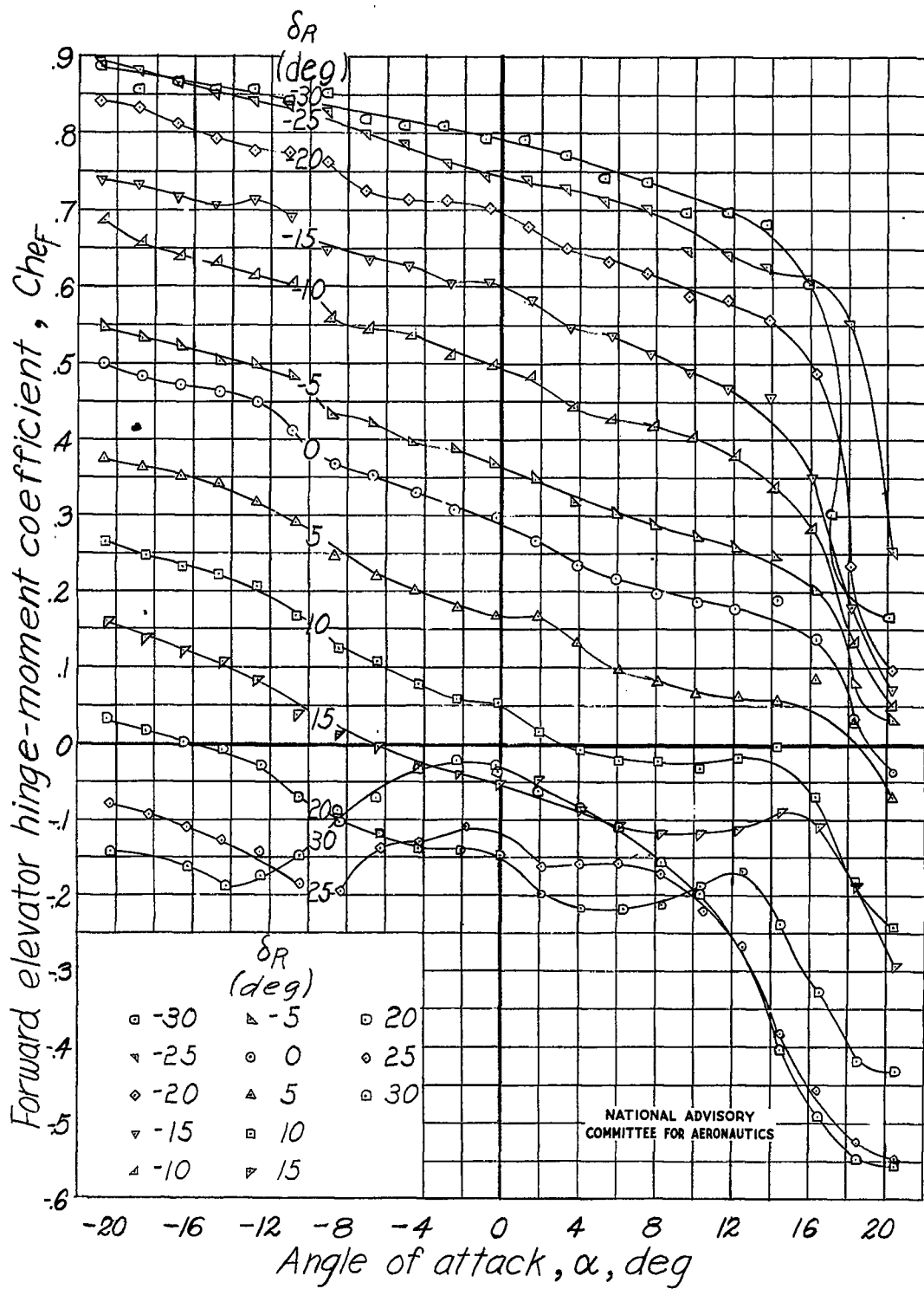
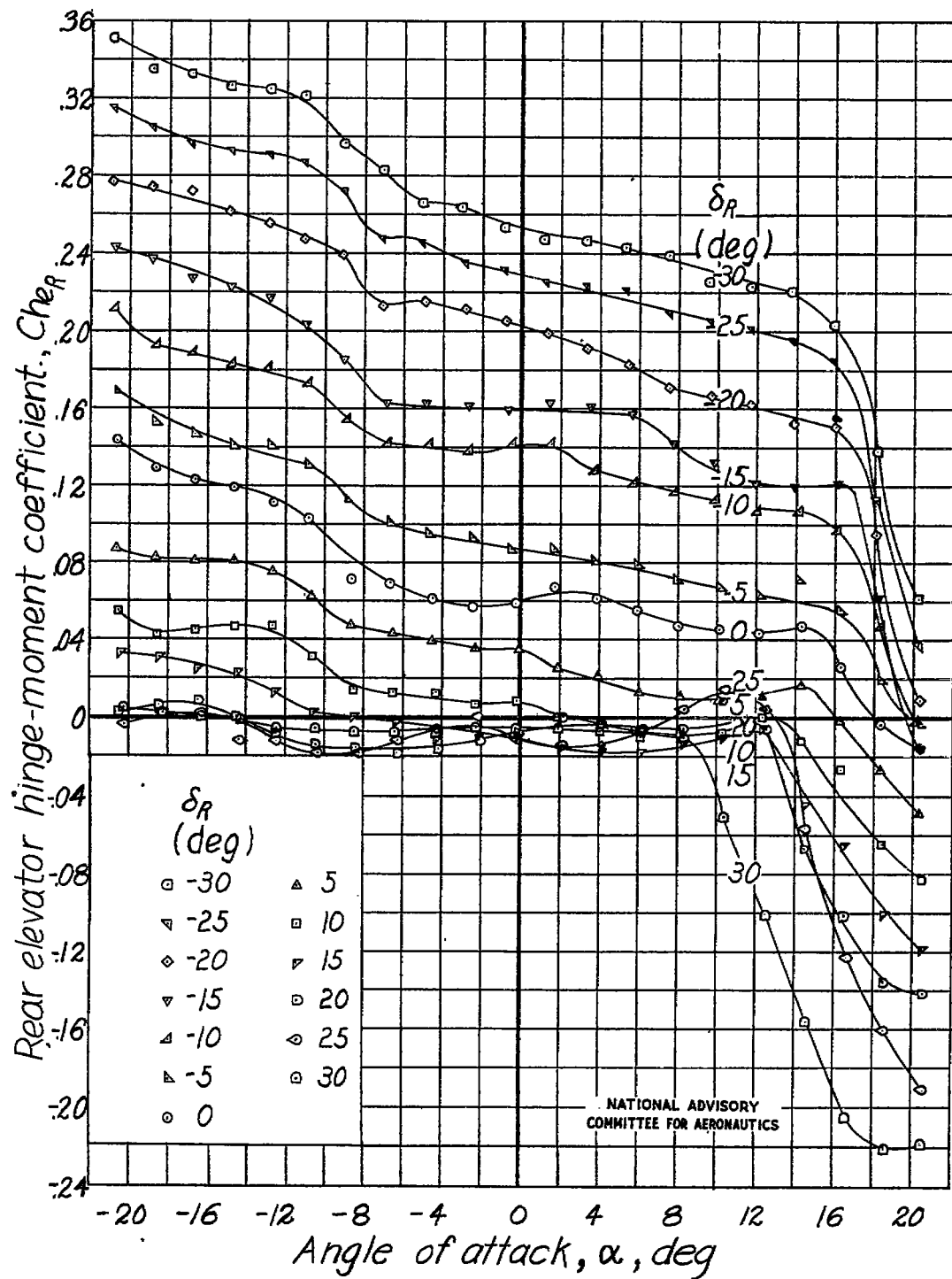
(e) Elevator gap open. $\delta_F = -20^\circ$.

Figure 29.- Continued. Tail 8.



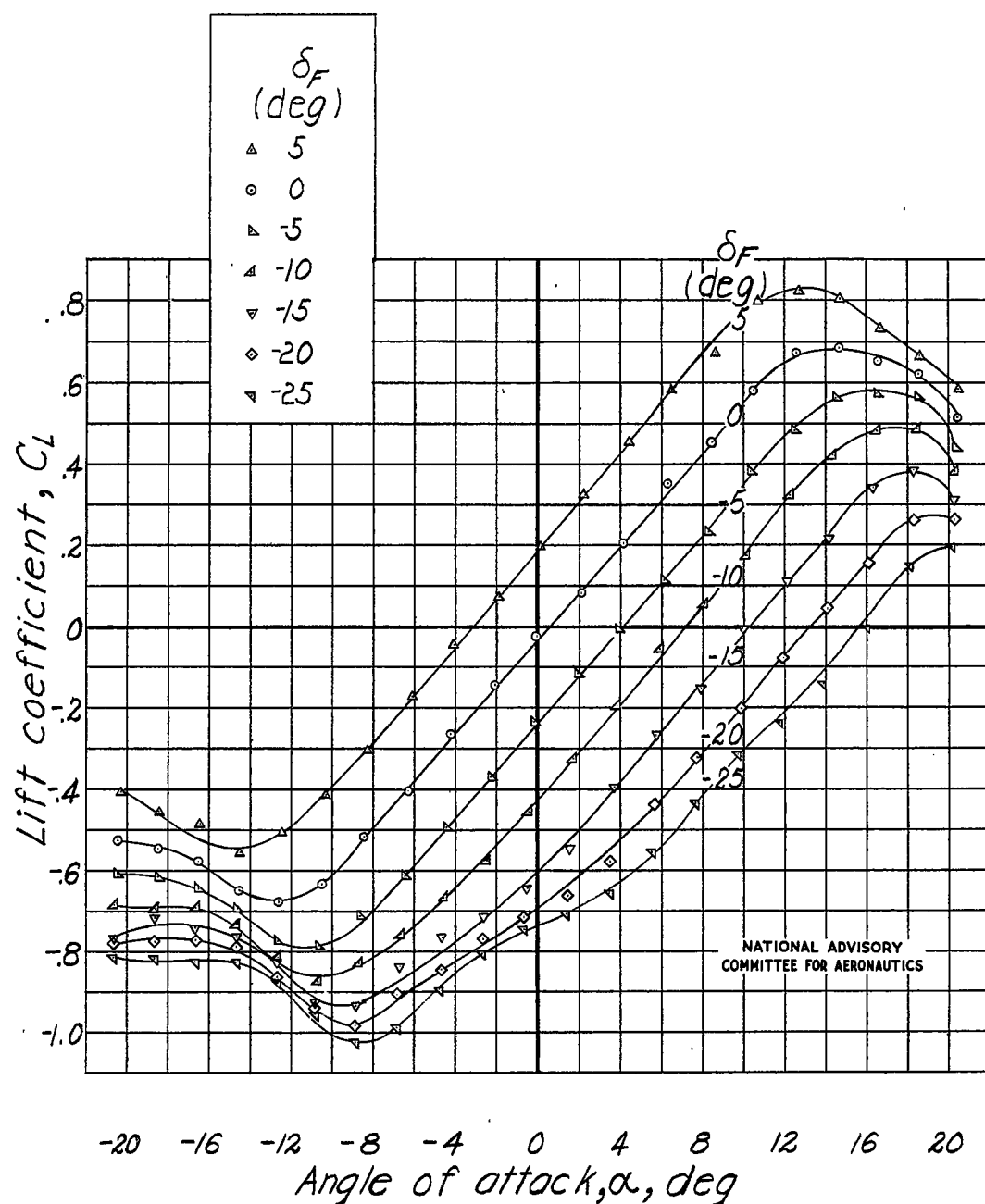
(e) Continued.

Figure 29.- Continued. Tail 8.



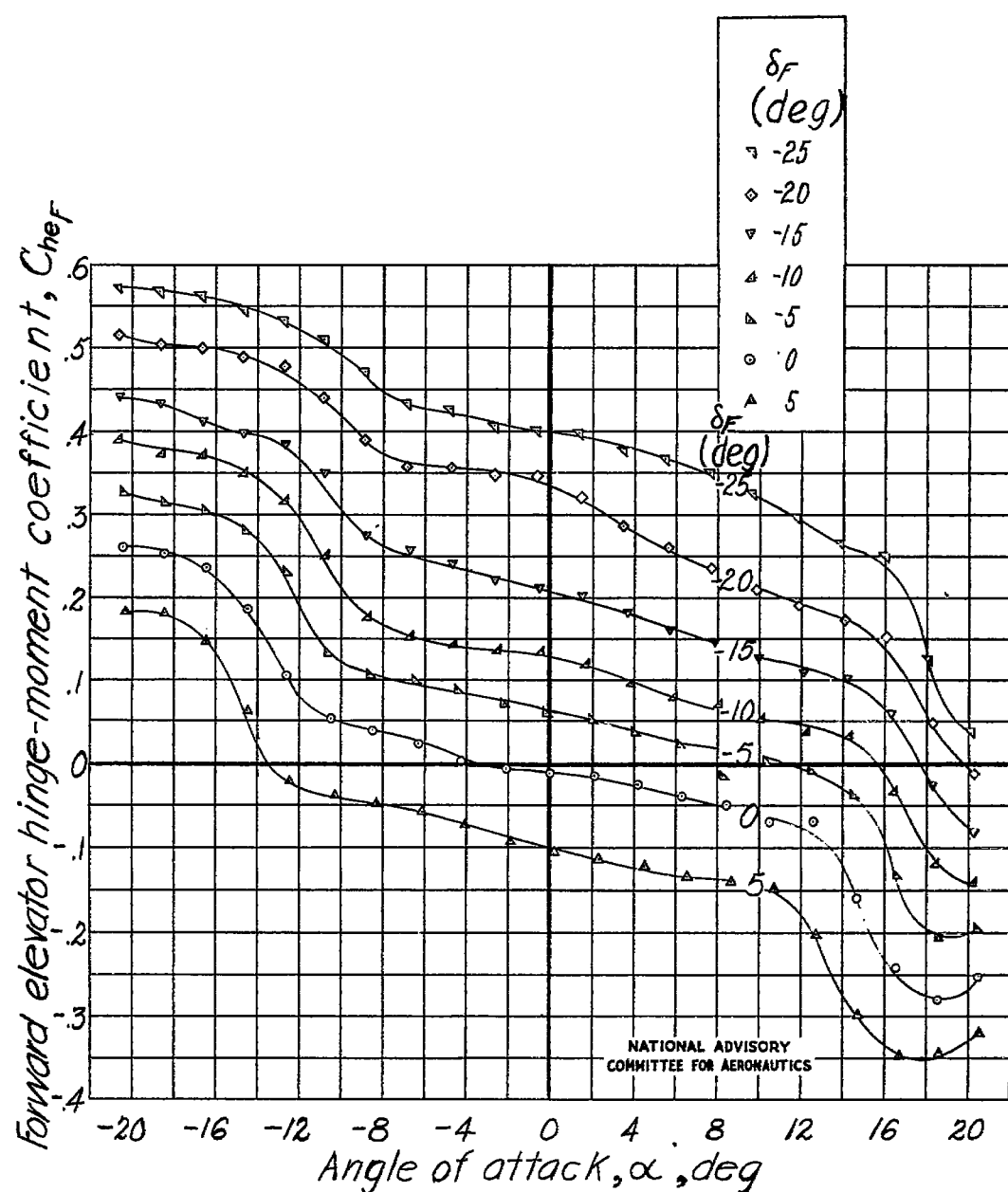
(e) Concluded.

Figure 29.- Continued. Tail 8.



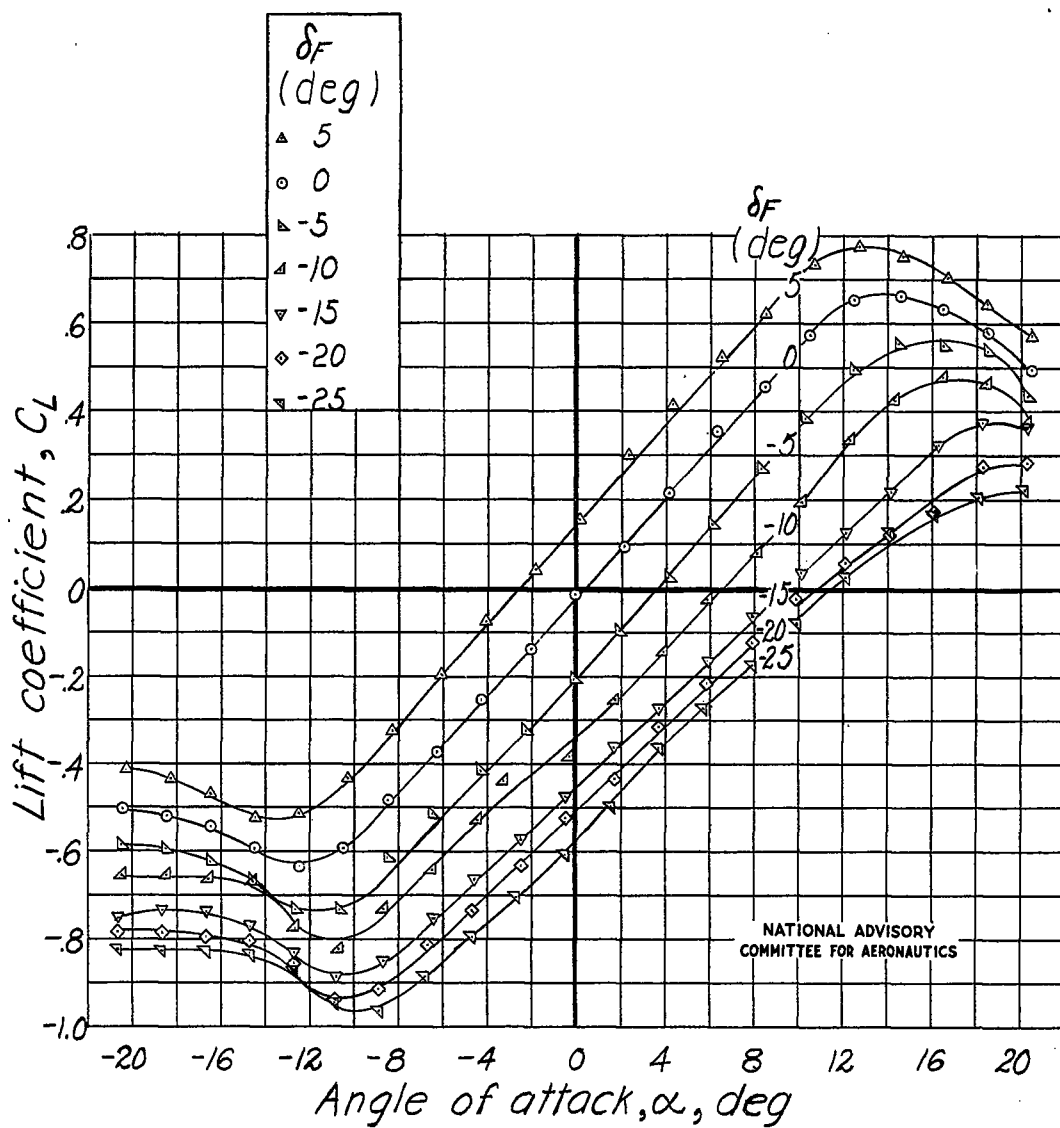
(f) Rear gap faired to airfoil contour; $\delta_R = 0^\circ$; forward gap sealed with grease.

Figure 29.- Continued. Tail 8.



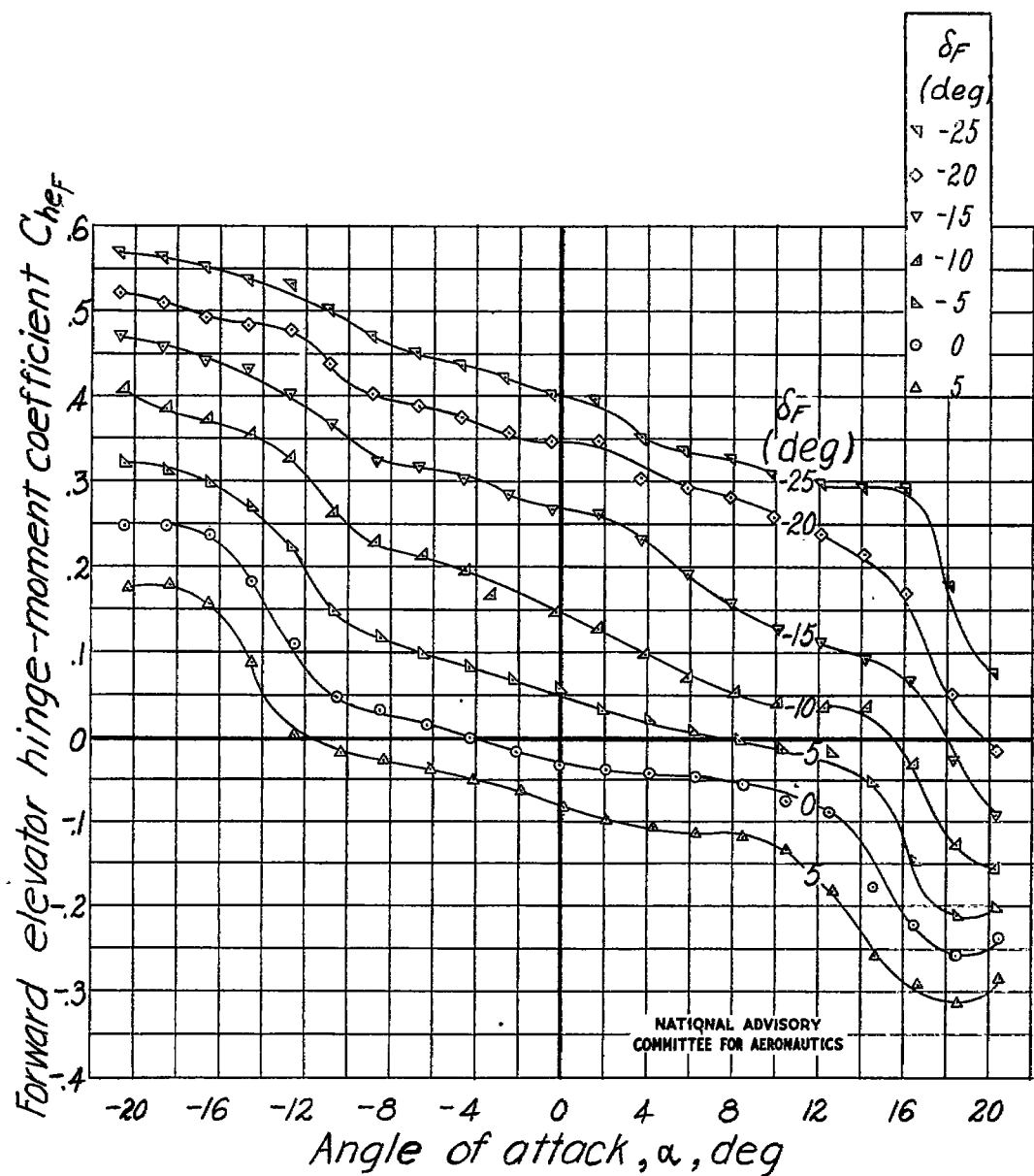
(f) Concluded.

Figure 29.- Continued. Tail 8.



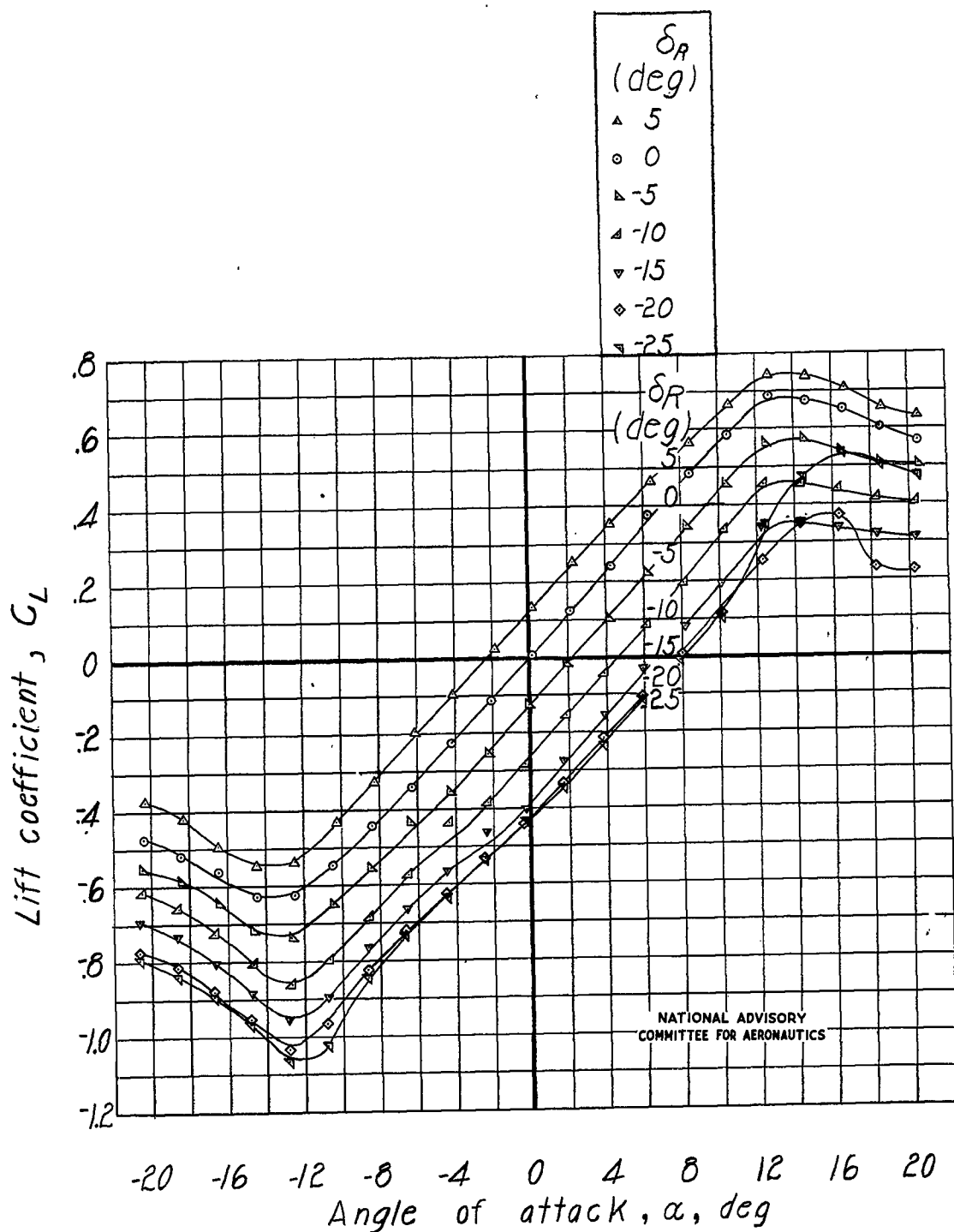
(g) Rear gap faired to airfoil contour; $\delta_R = 0^\circ$; forward gap open.

Figure 29.- Continued. Tail 8.



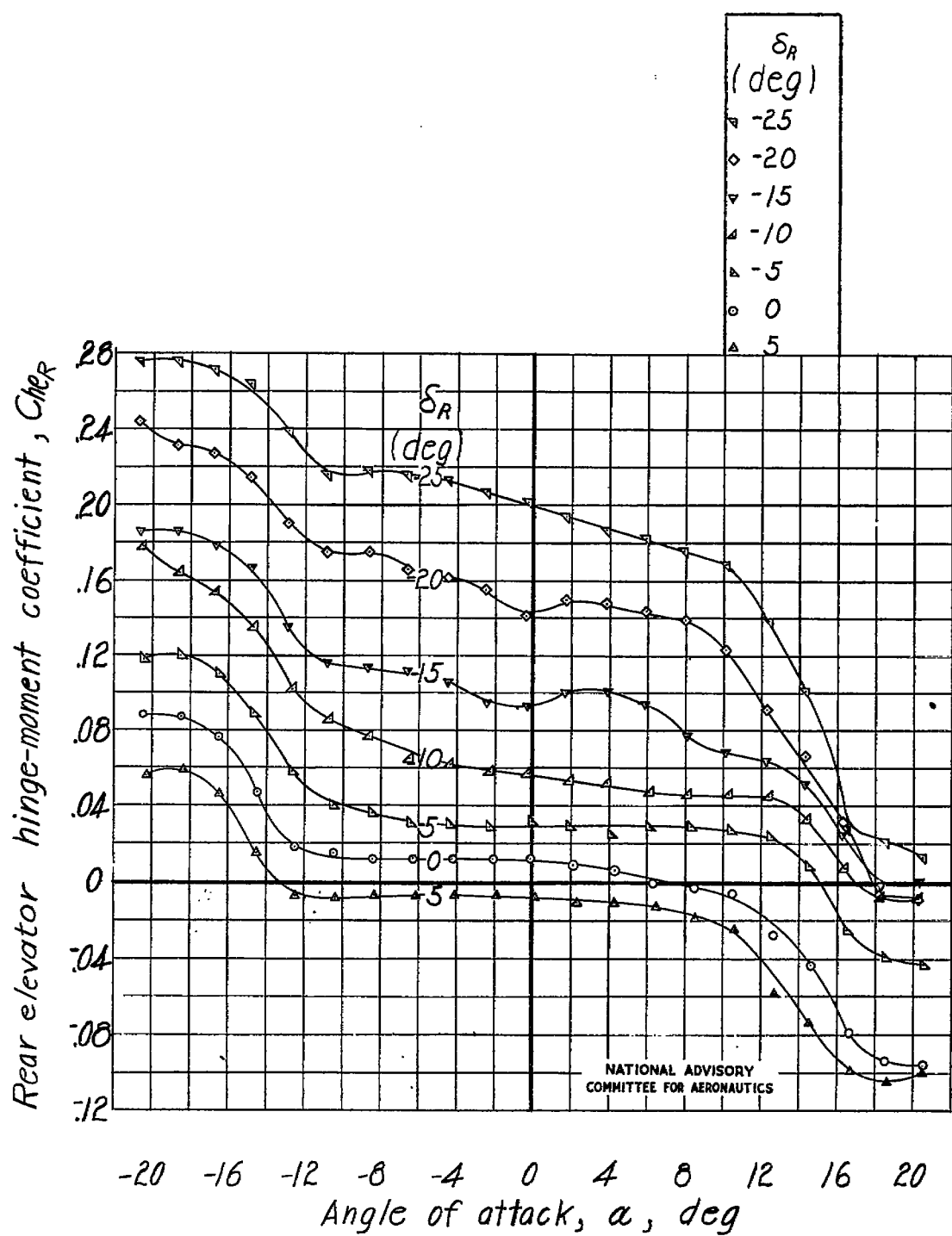
(g) Concluded.

Figure 29.- Continued. Tail 8.



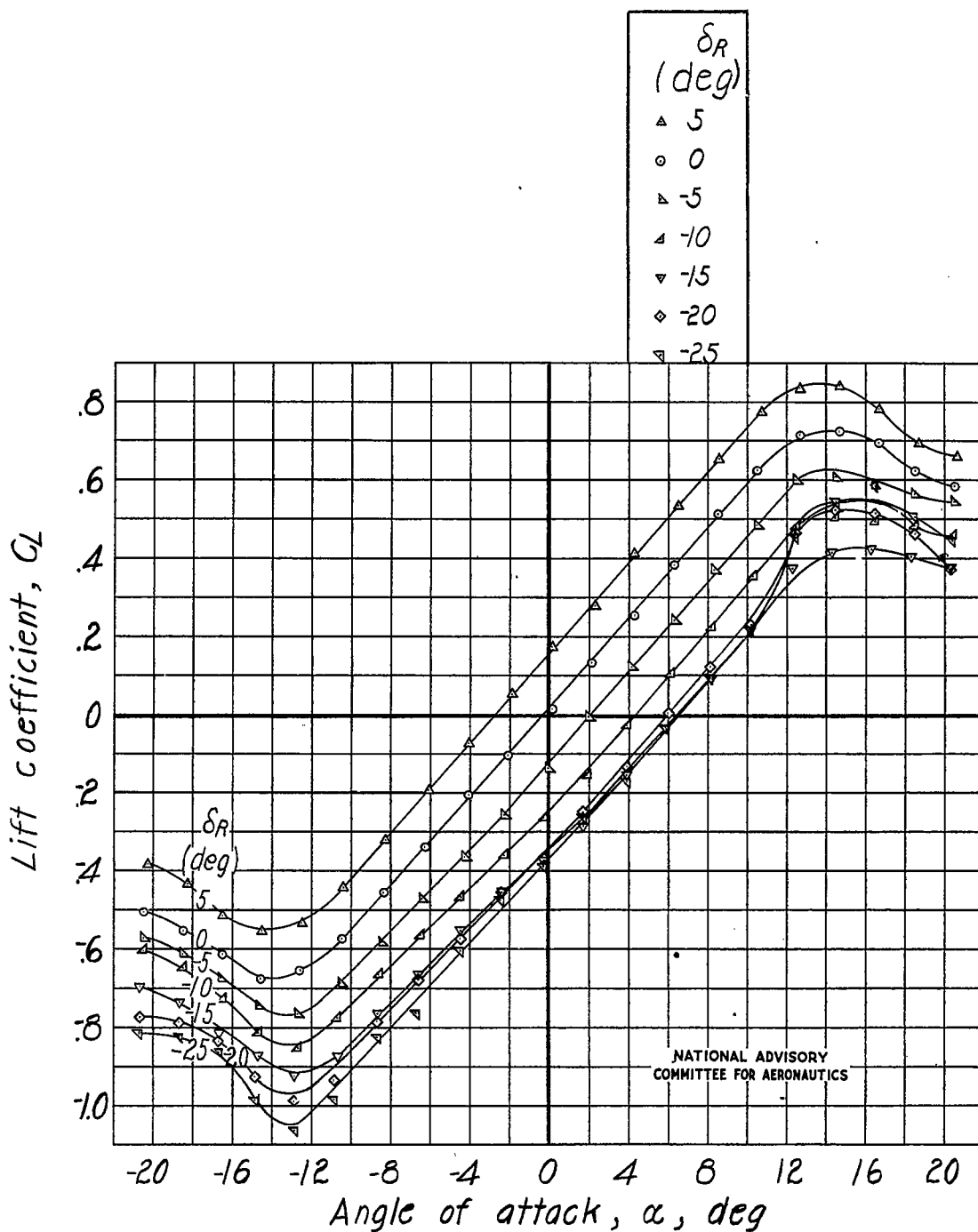
(h) Front gap faired to airfoil contour; $\delta_F = 0^\circ$; rear gap open.

Figure 29.- Continued. Tail 8.



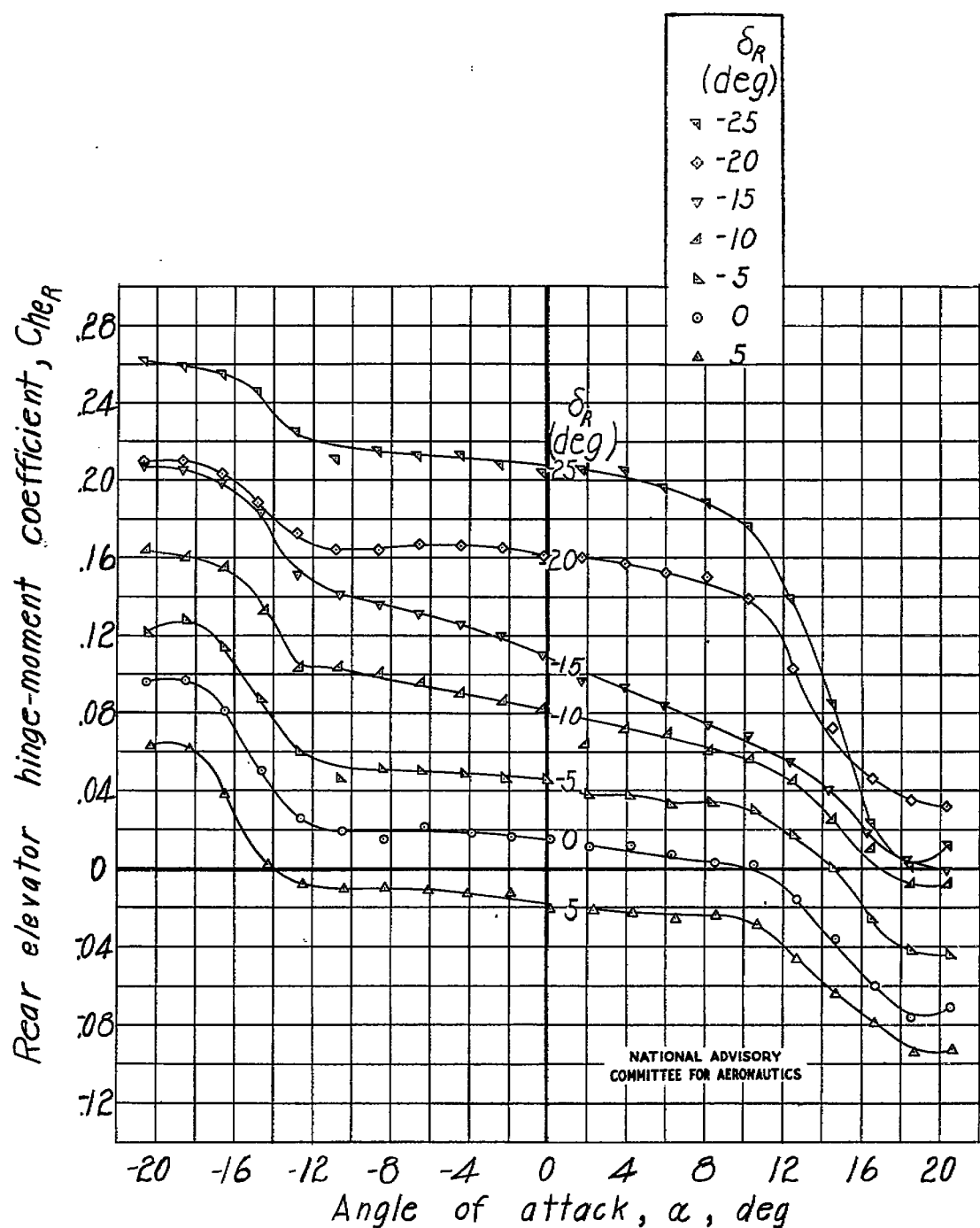
(h) Concluded.

Figure 29.- Continued. Tail 8.



- (i) Front gap faired to airfoil contour; $\delta_F = 0^\circ$; rear gap sealed with grease.

Figure 29.- Continued. Tail 8.

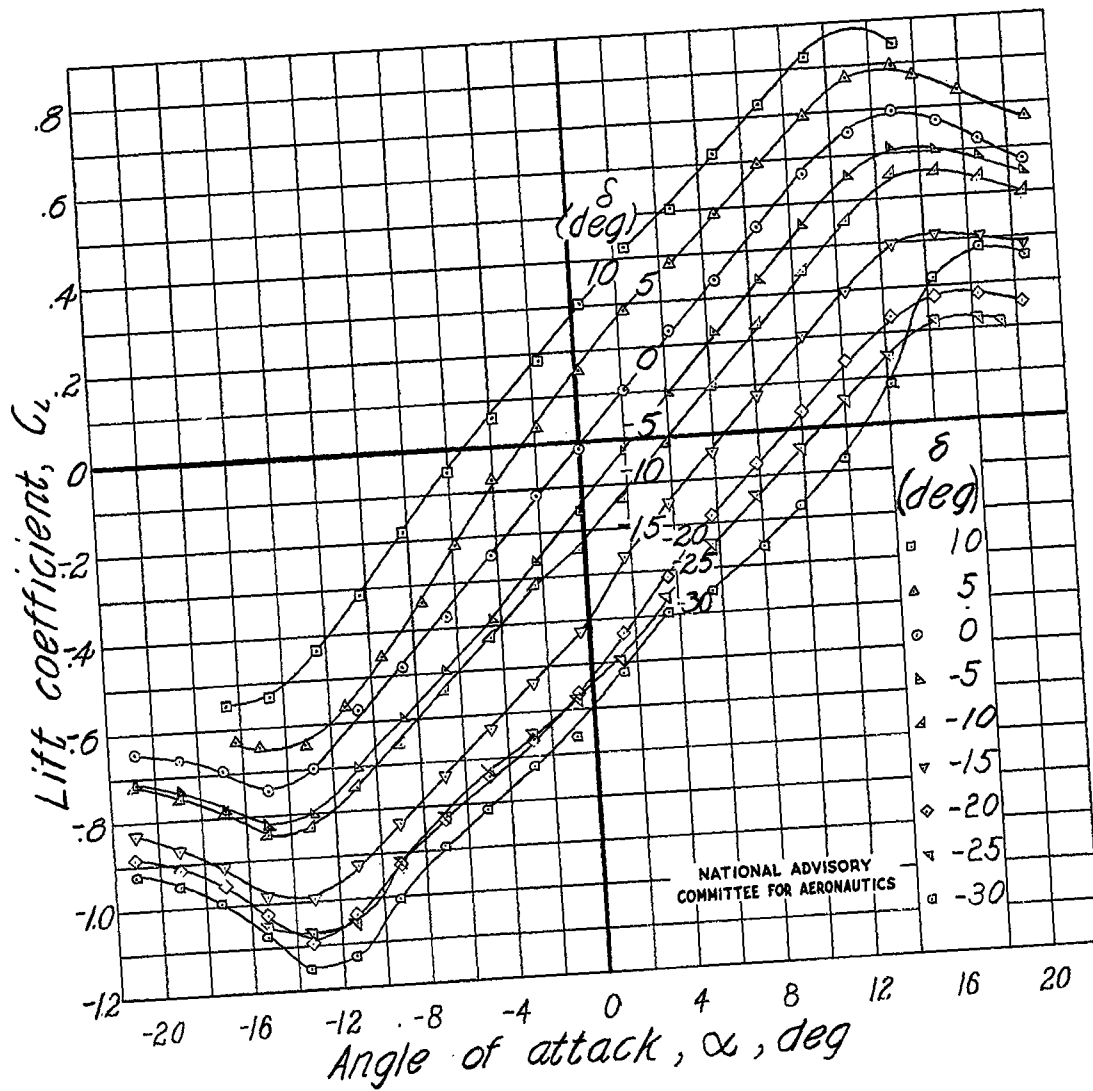


(i) Concluded.

Figure 29.- Concluded. Tail 8.

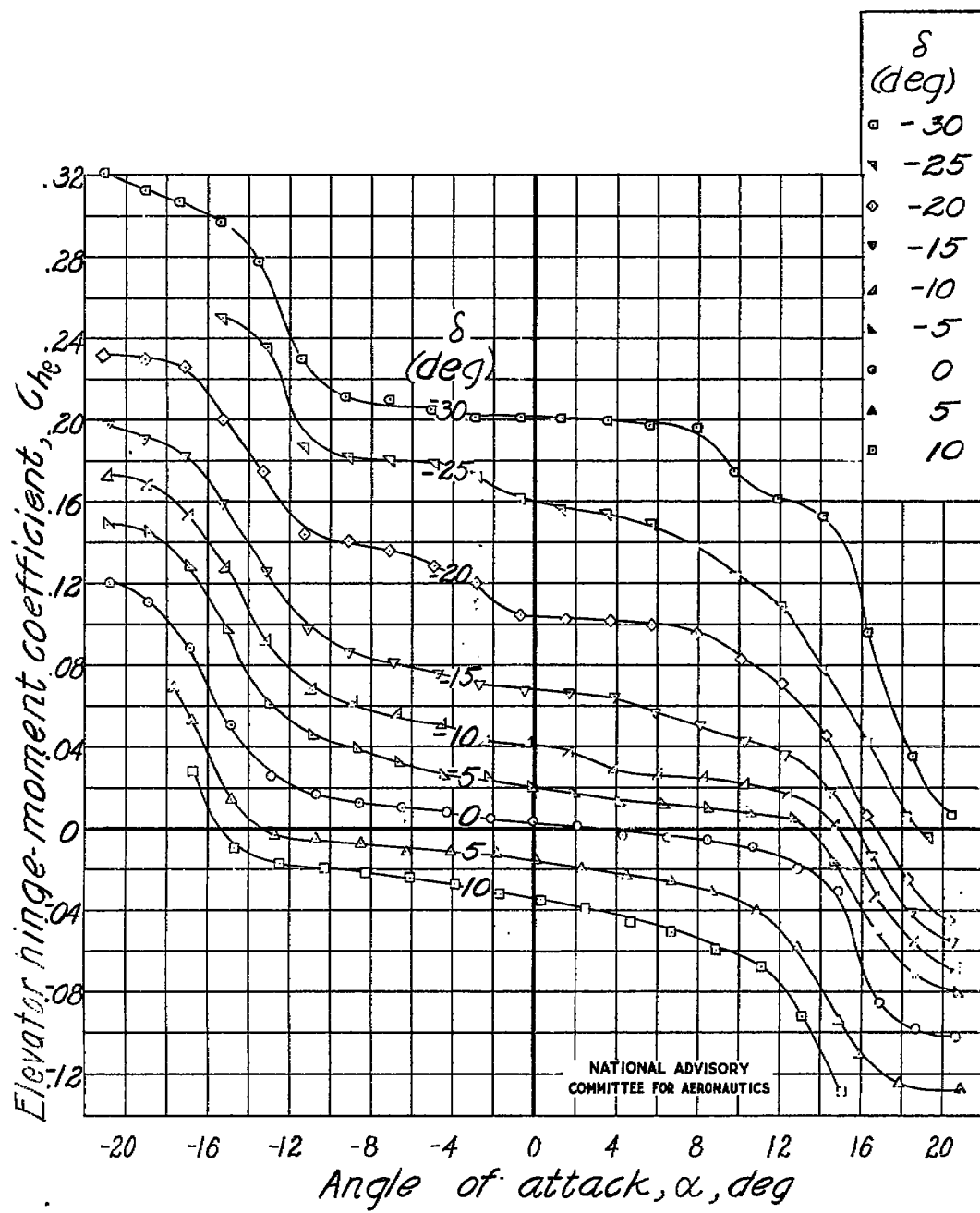
Fig. 30a

NACA TN No. 1291



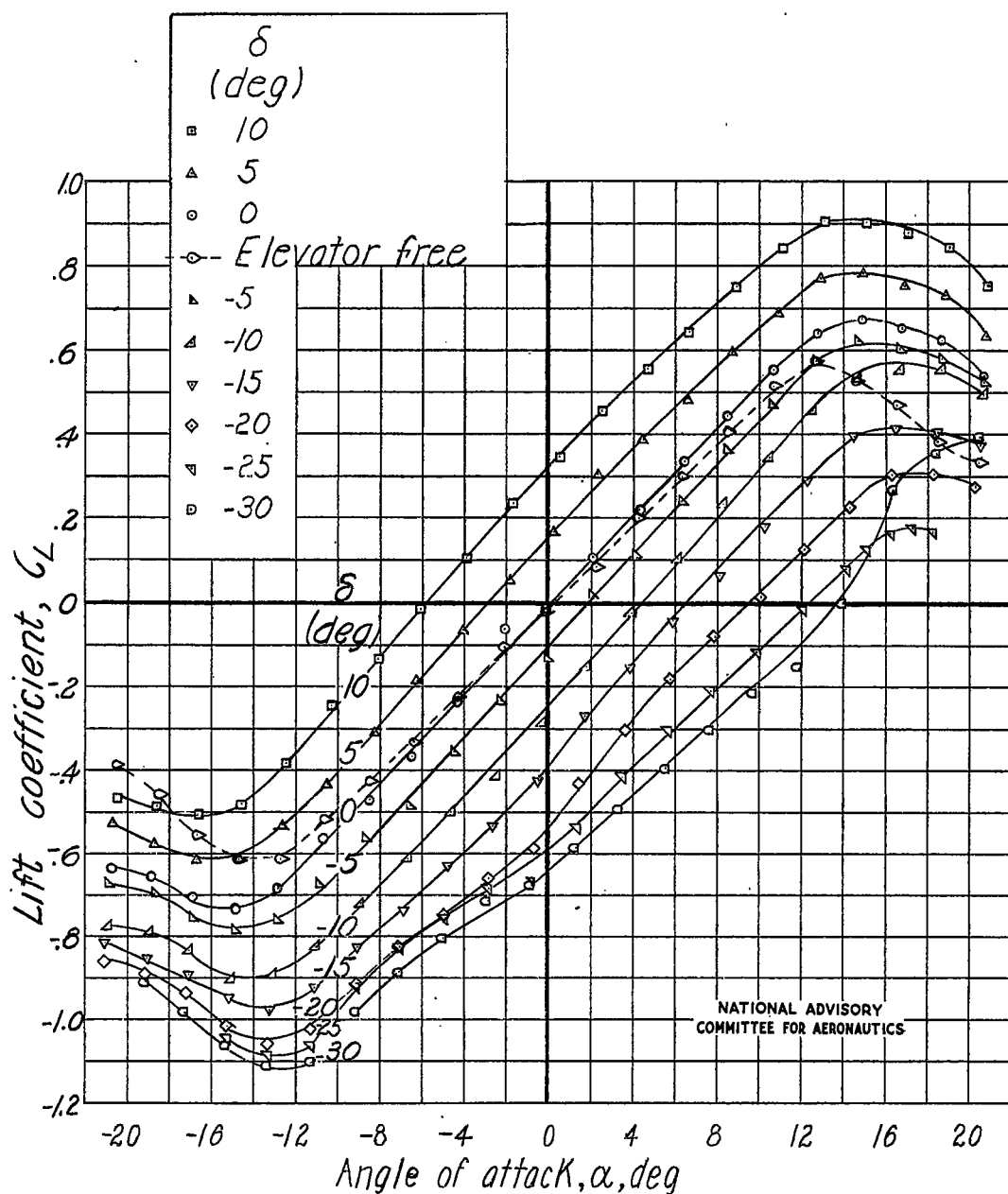
(a) Elevator gap open.

Figure 30.- Lift and hinge-moment characteristics of horizontal tail 9.



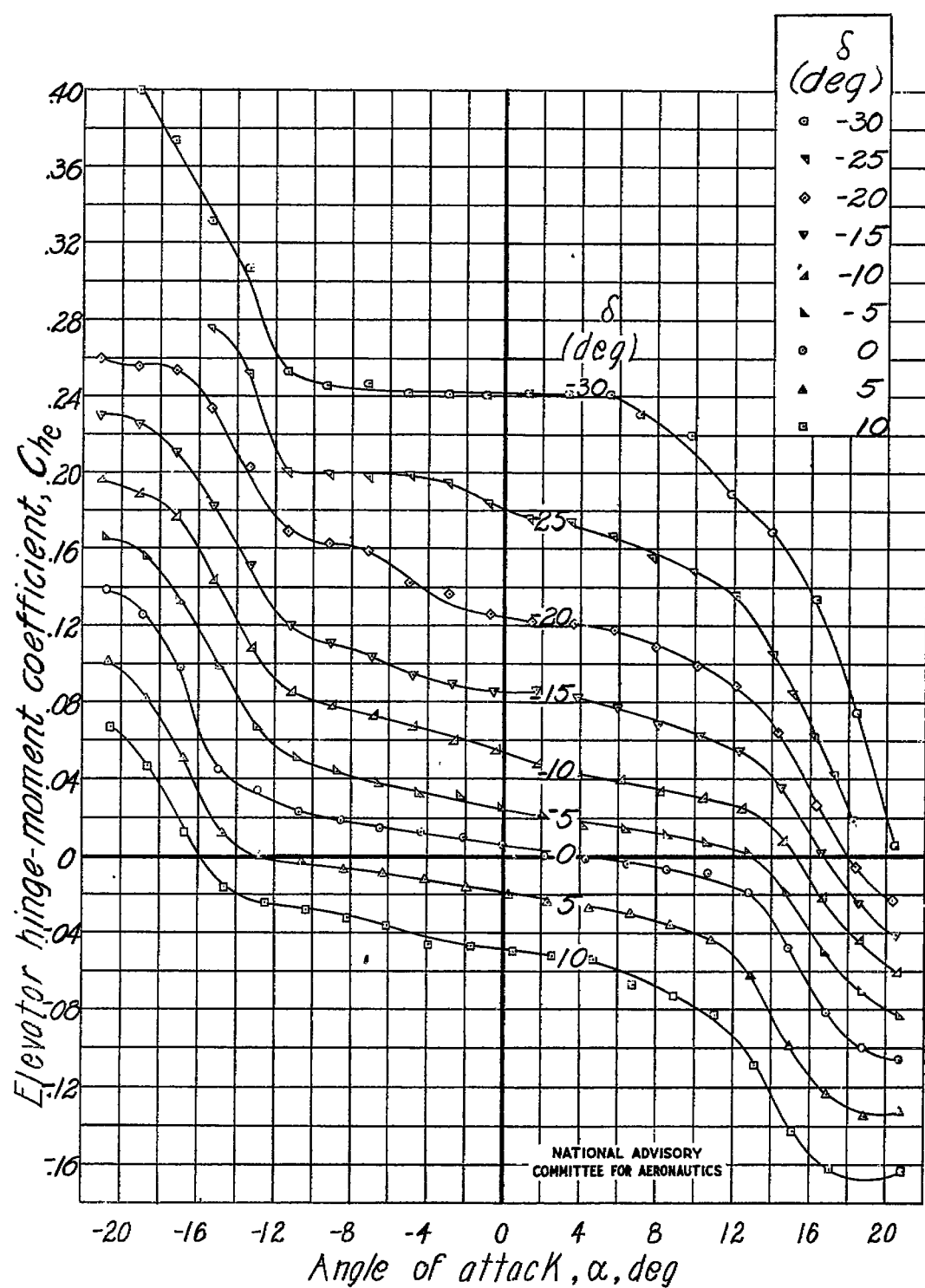
(a) Concluded.

Figure 30.- Continued. Tail 9.



(b) Elevator cut-out filled and elevator gap open.

Figure 30.- Continued. Tail 9.



(b) Concluded.

Figure 30.- Concluded. Tail 9.

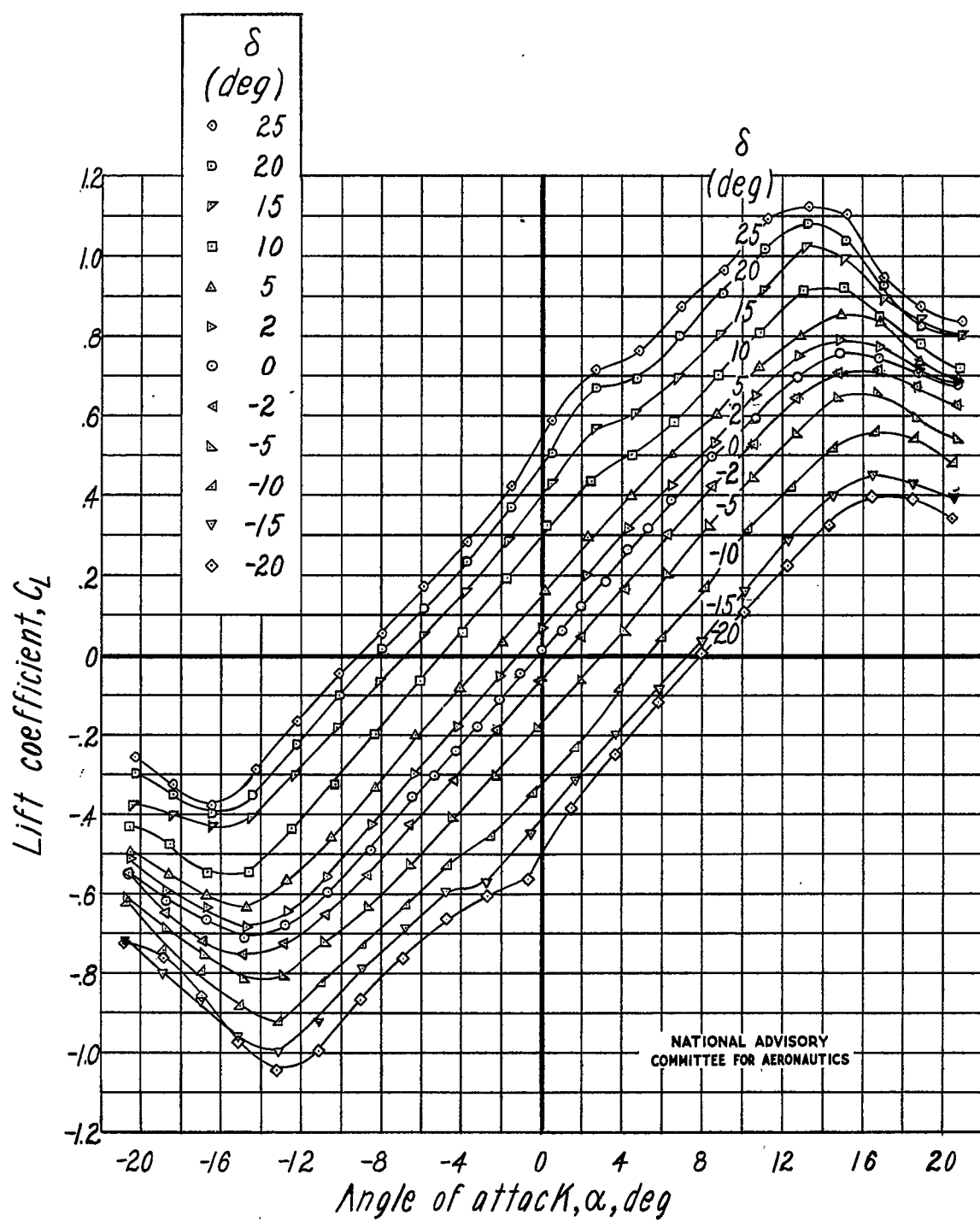


Figure 31.- Lift and hinge-moment characteristics of horizontal tail 10.
Elevator gap sealed with grease.

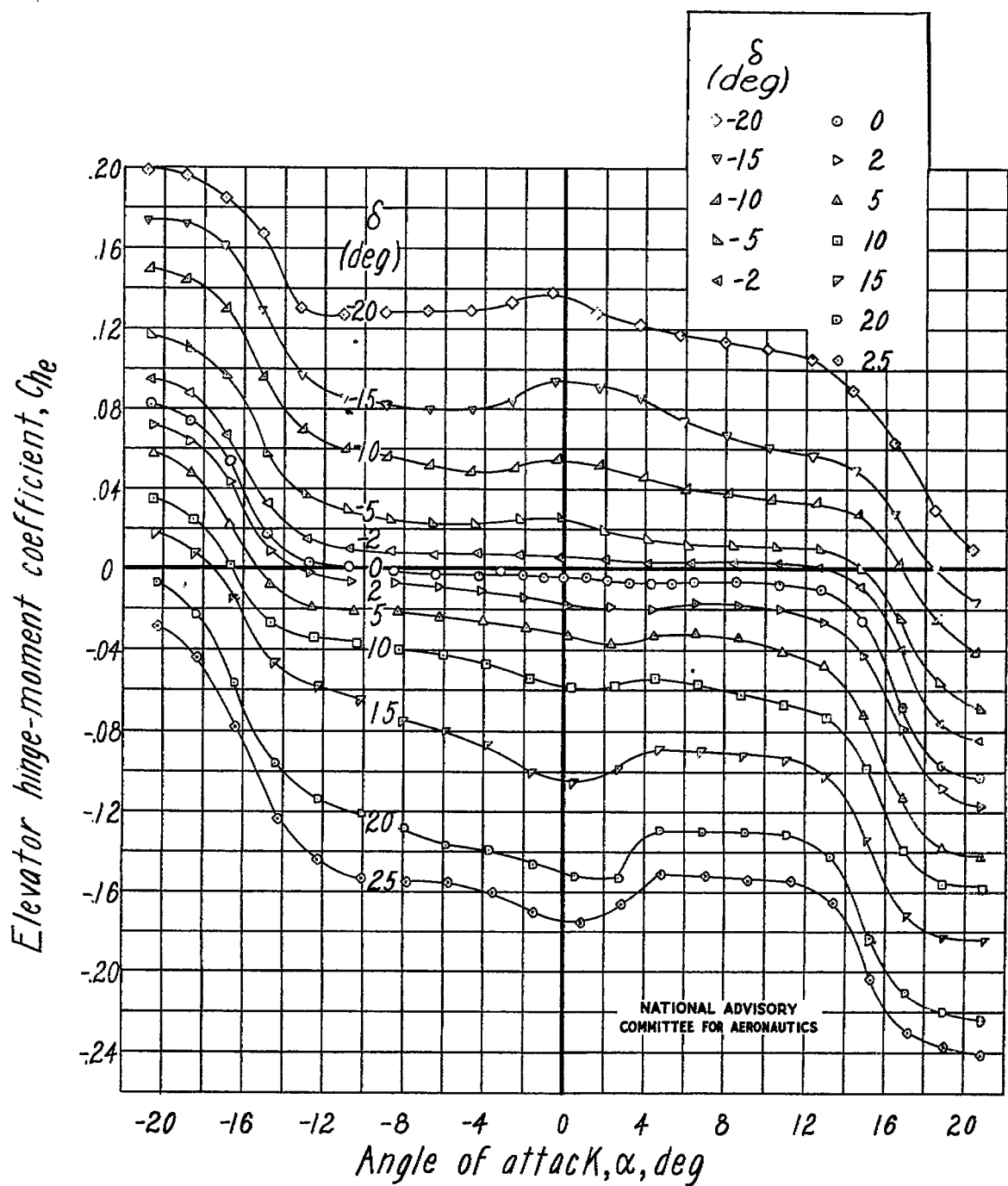


Figure 31.- Concluded. Tail 10.

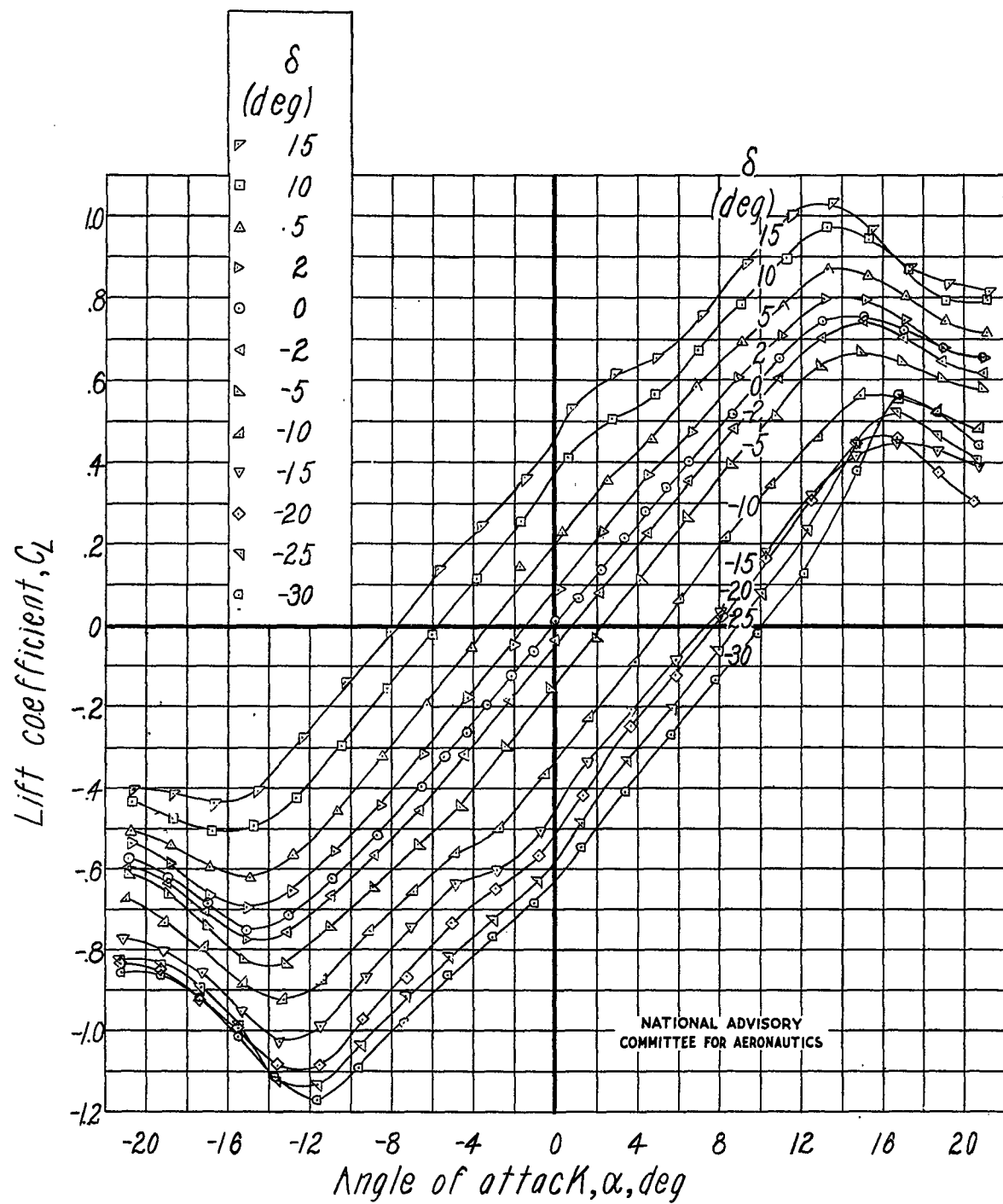


Figure 32.- Lift and hinge-moment characteristics of horizontal tail 11.
Elevator gap sealed with grease.

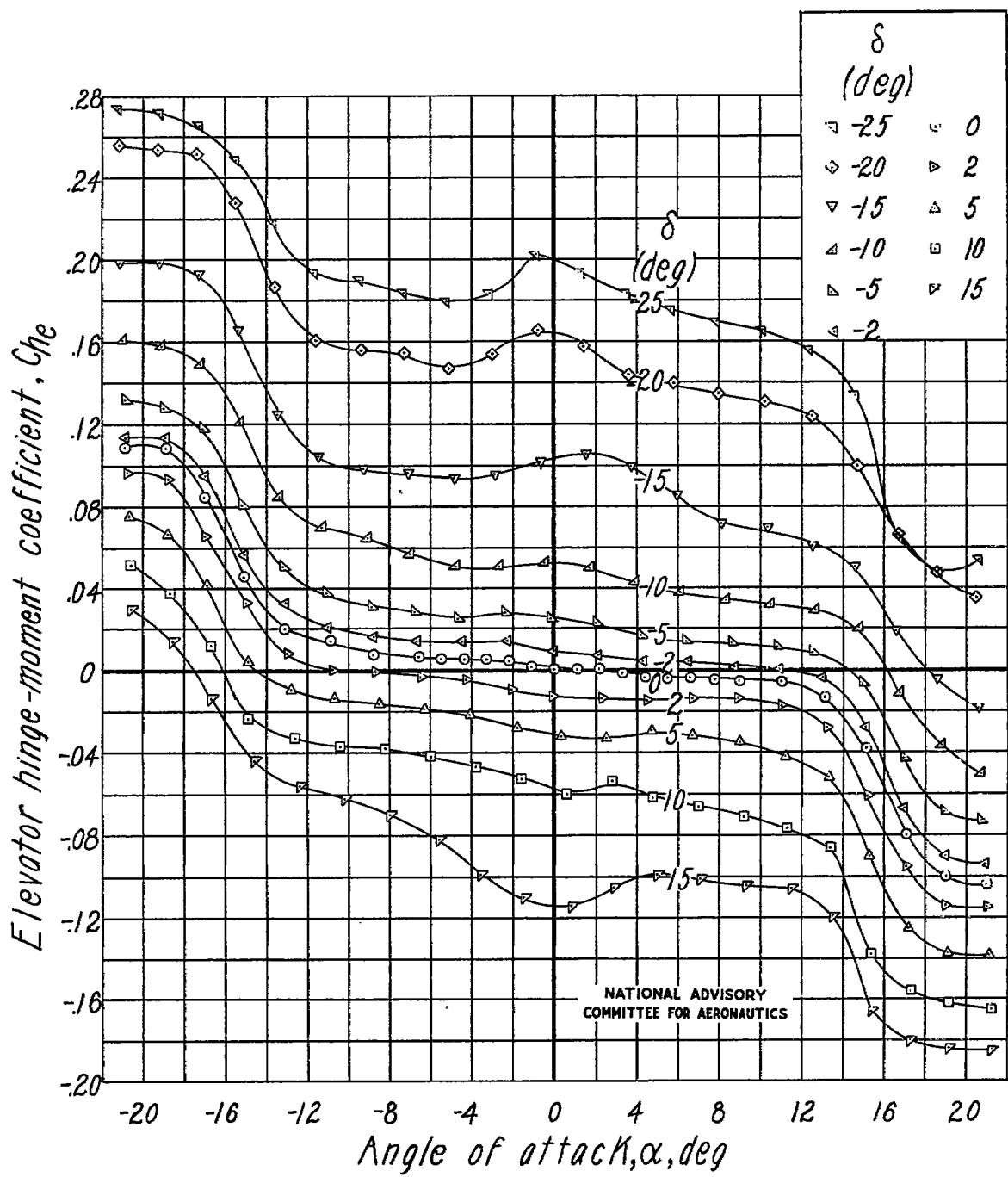
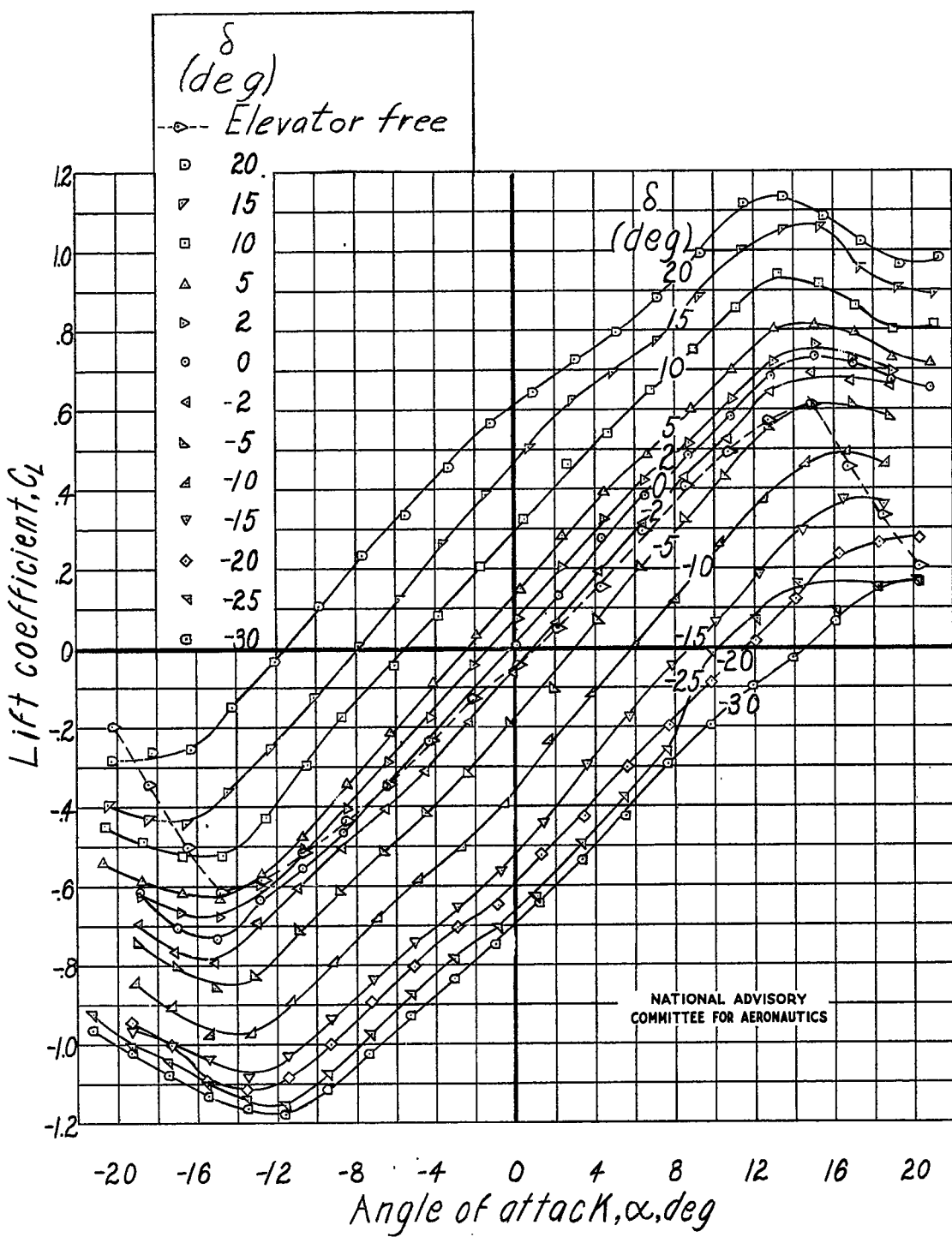
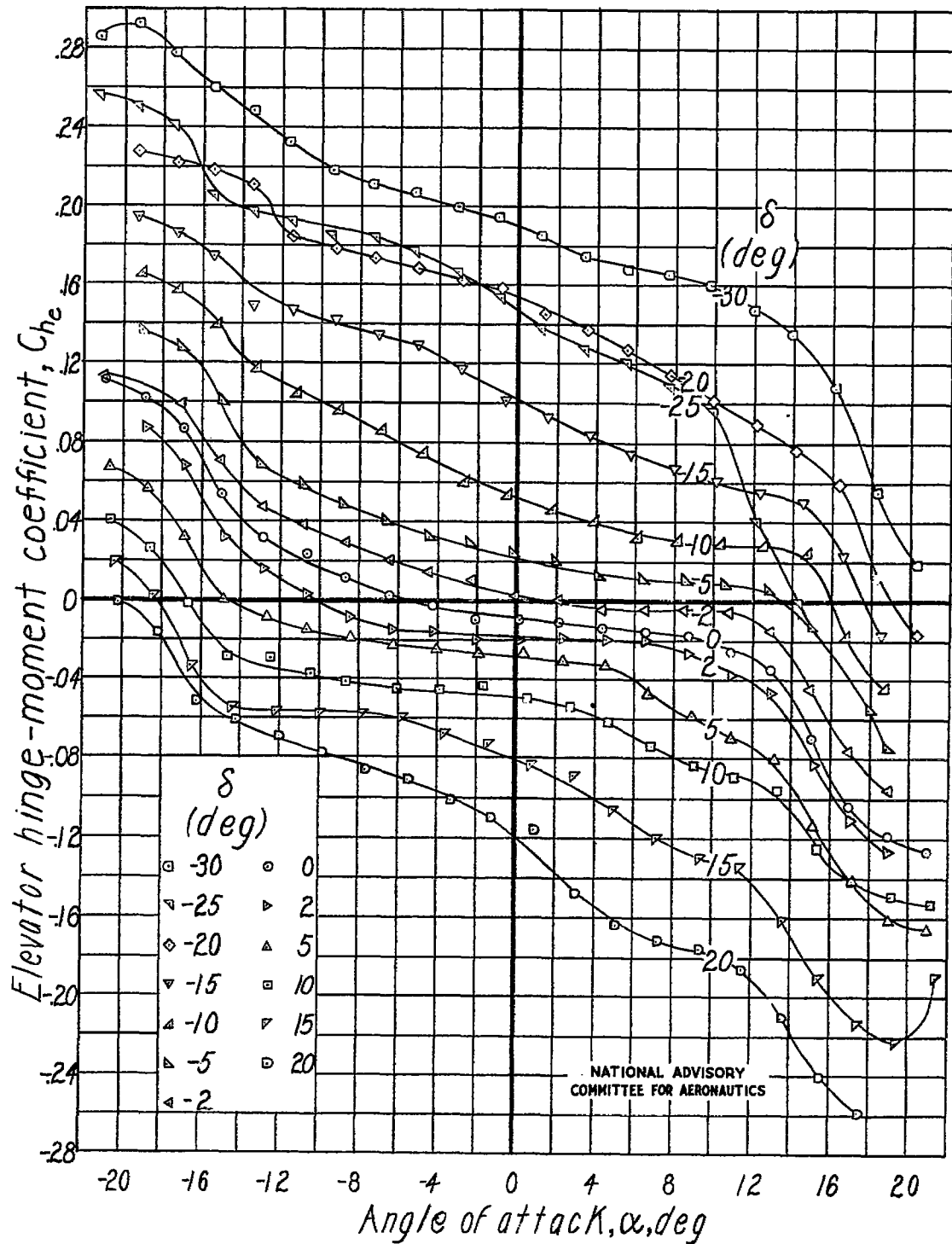


Figure 32.- Concluded. Tail 11.



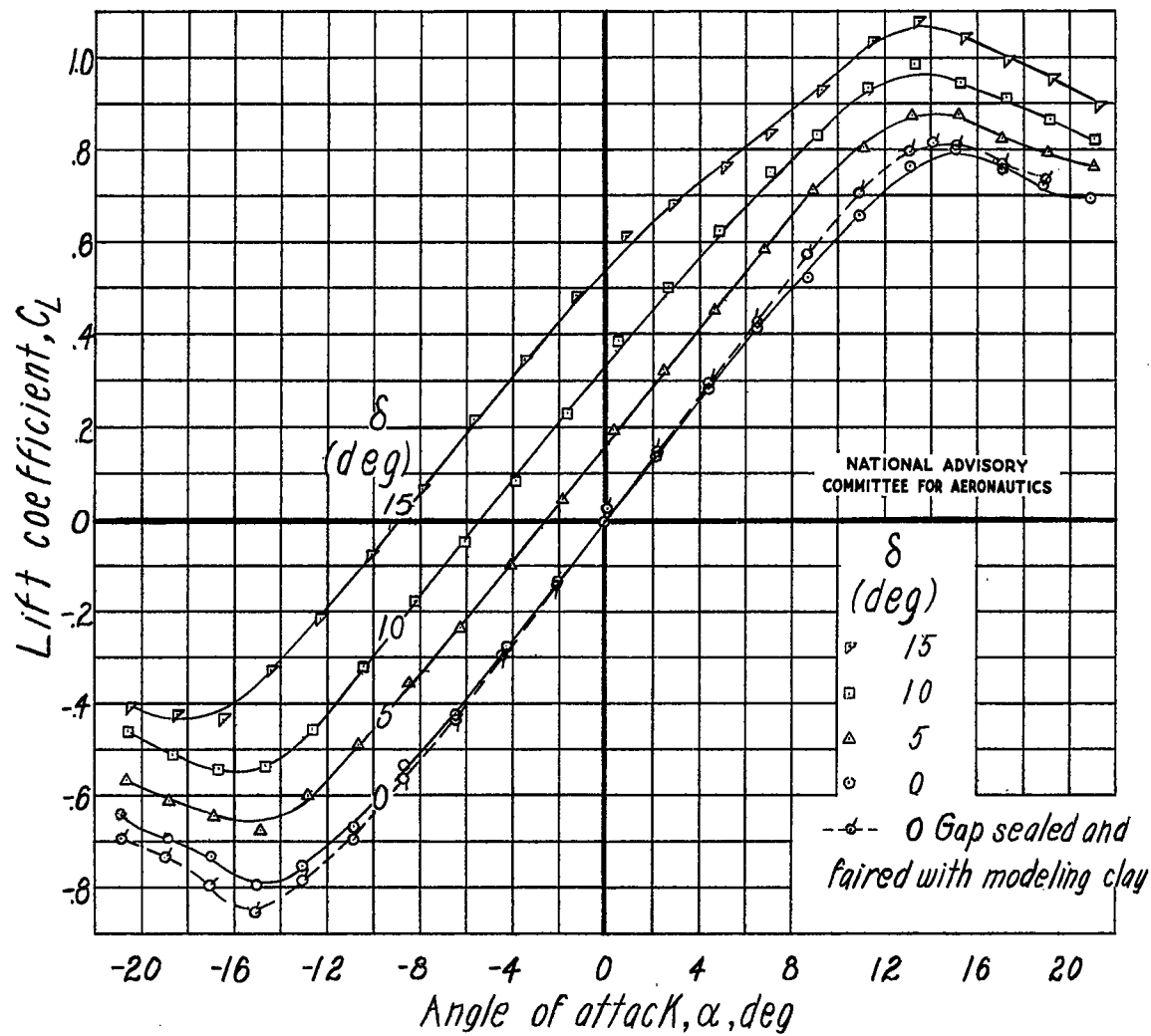
(a) Elevator gap open.

Figure 33.- Lift and hinge-moment characteristics of horizontal tail 12.



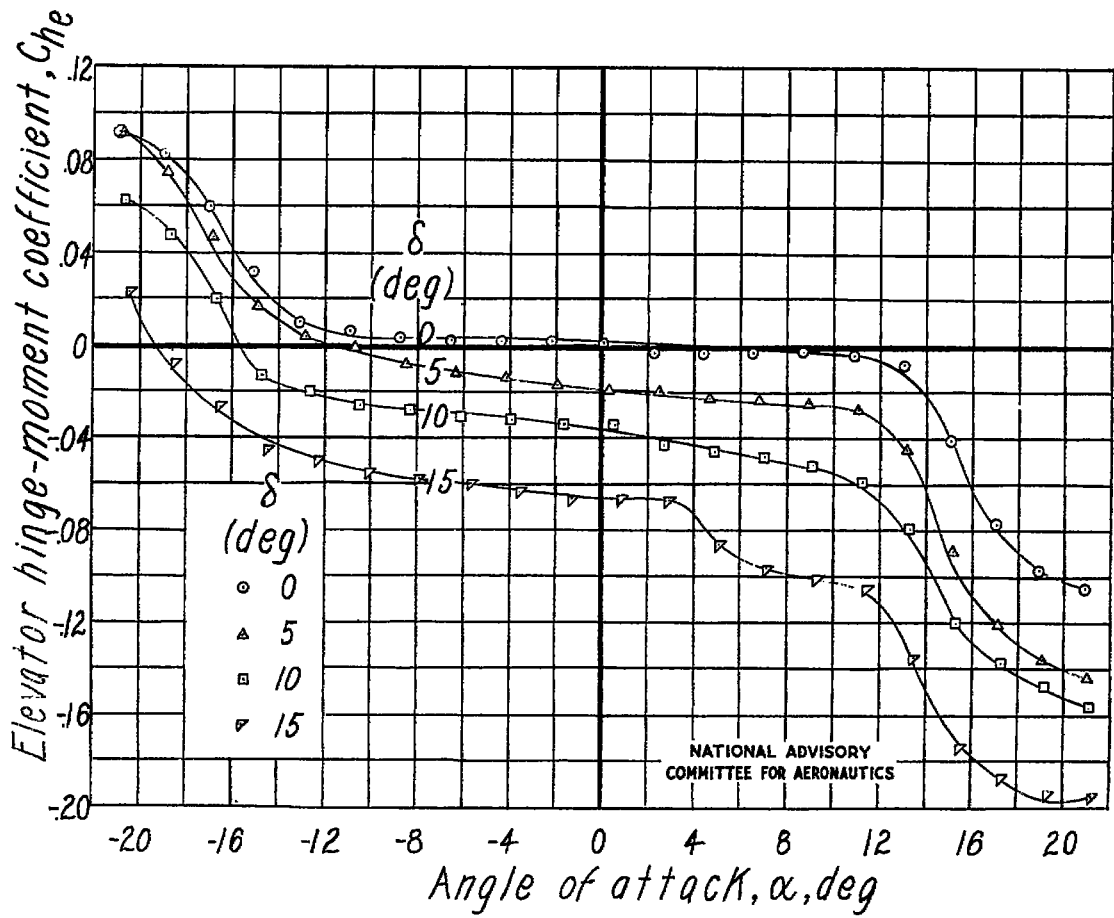
(a) Concluded.

Figure 33.- Continued. Tail 12.



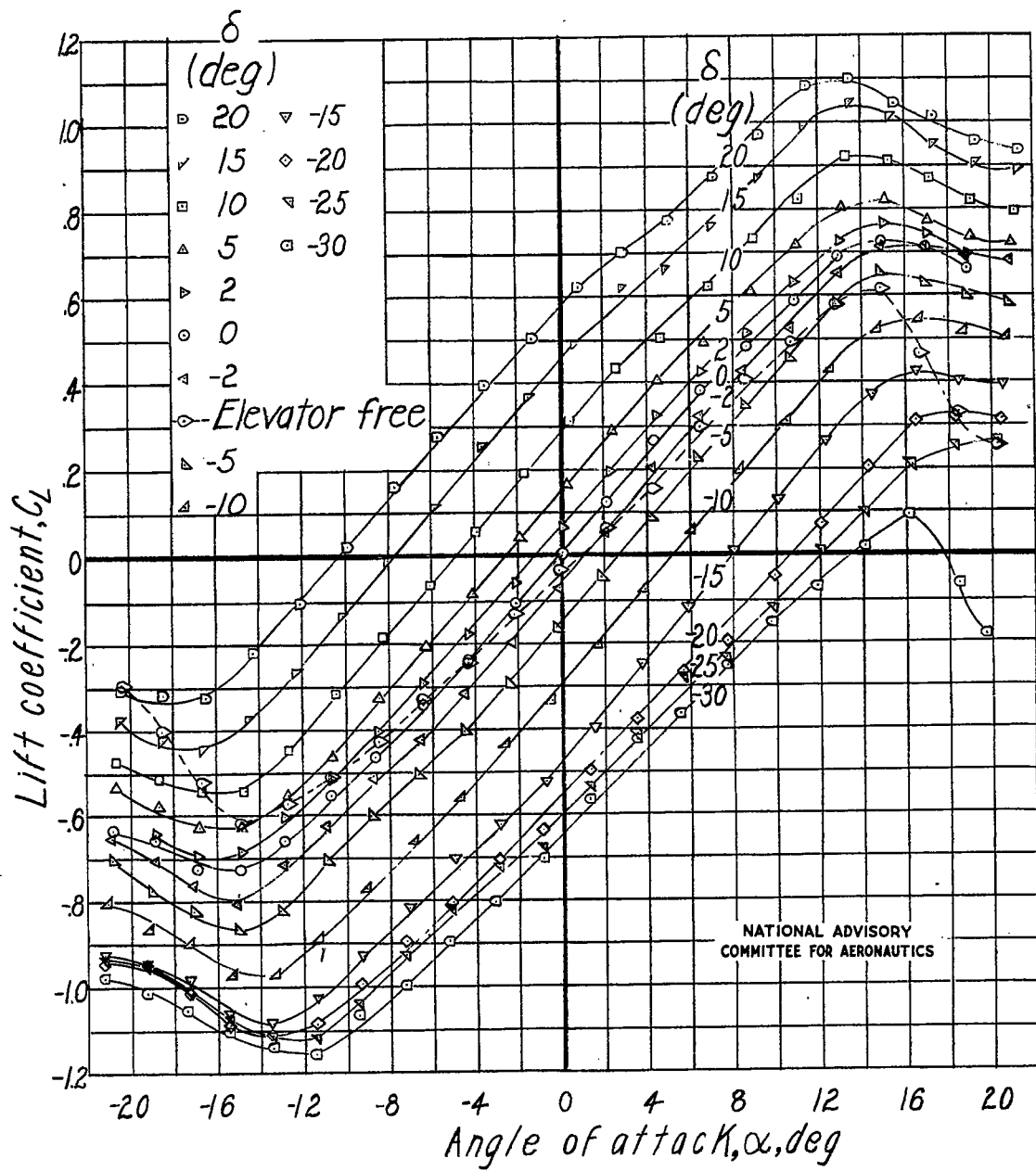
(b) Elevator gap sealed with grease except where noted.

Figure 33.- Continued. Tail 12.



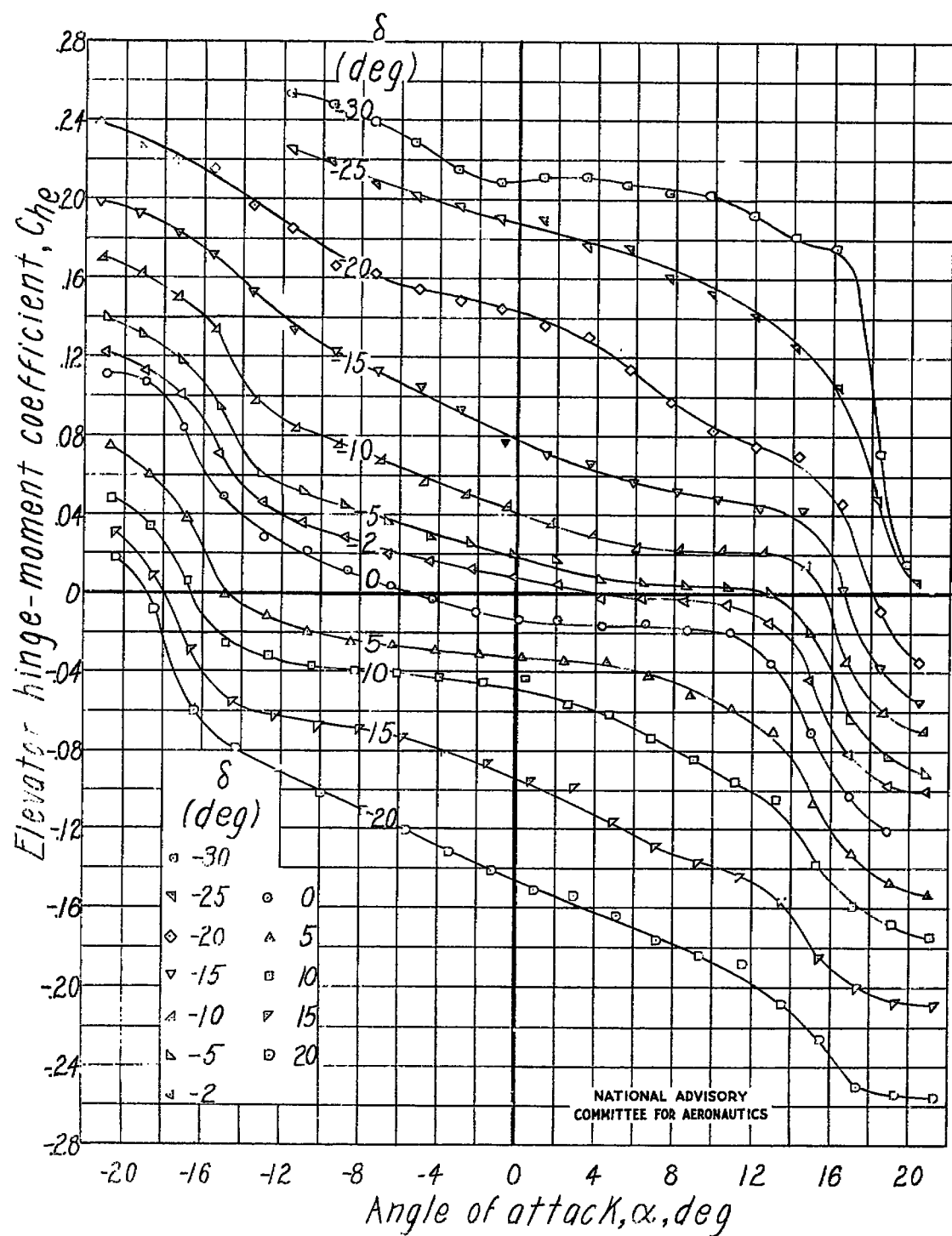
(b) Concluded.

Figure 33.- Continued. Tail 12.



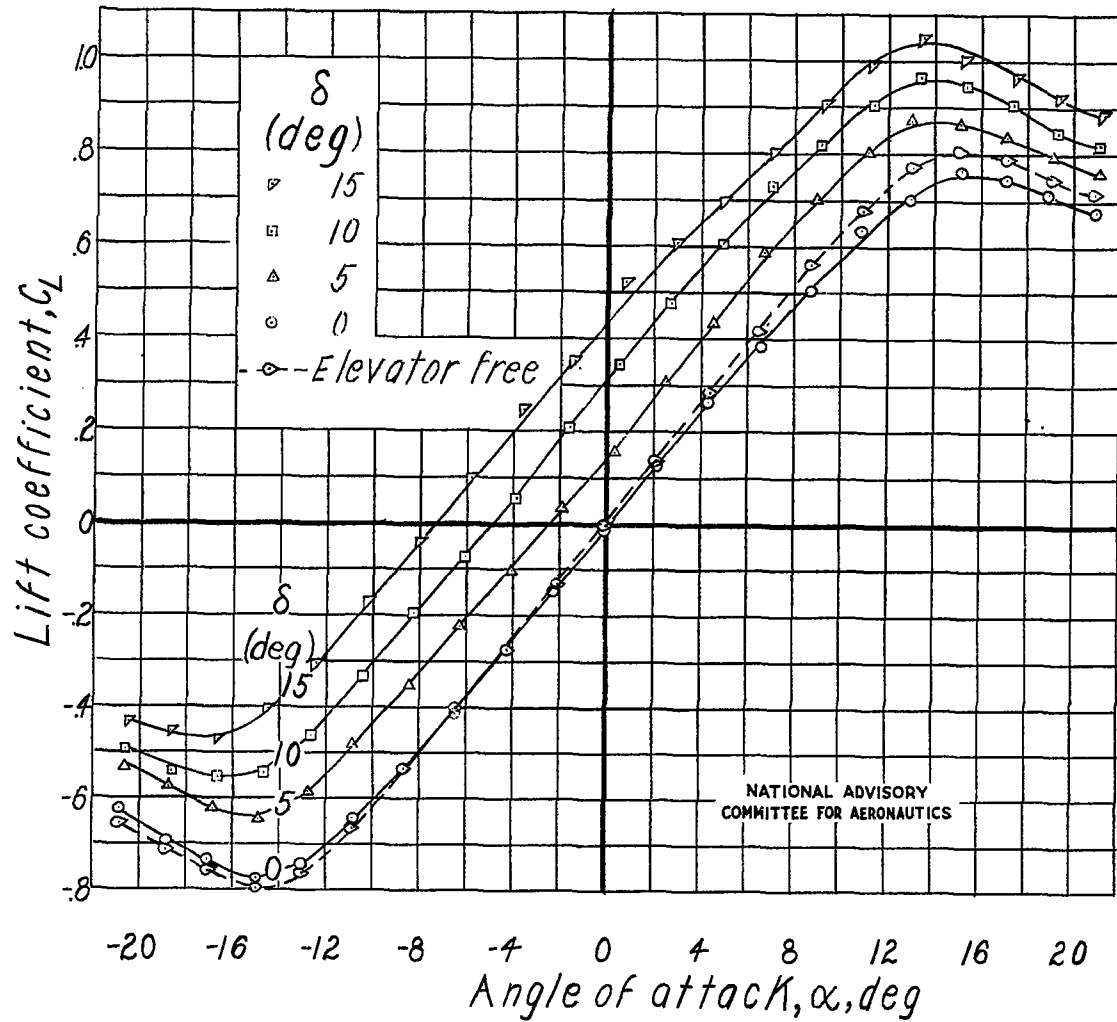
(c) Elevator cut-out filled and gap open.

Figure 33.- Continued. Tail 12.



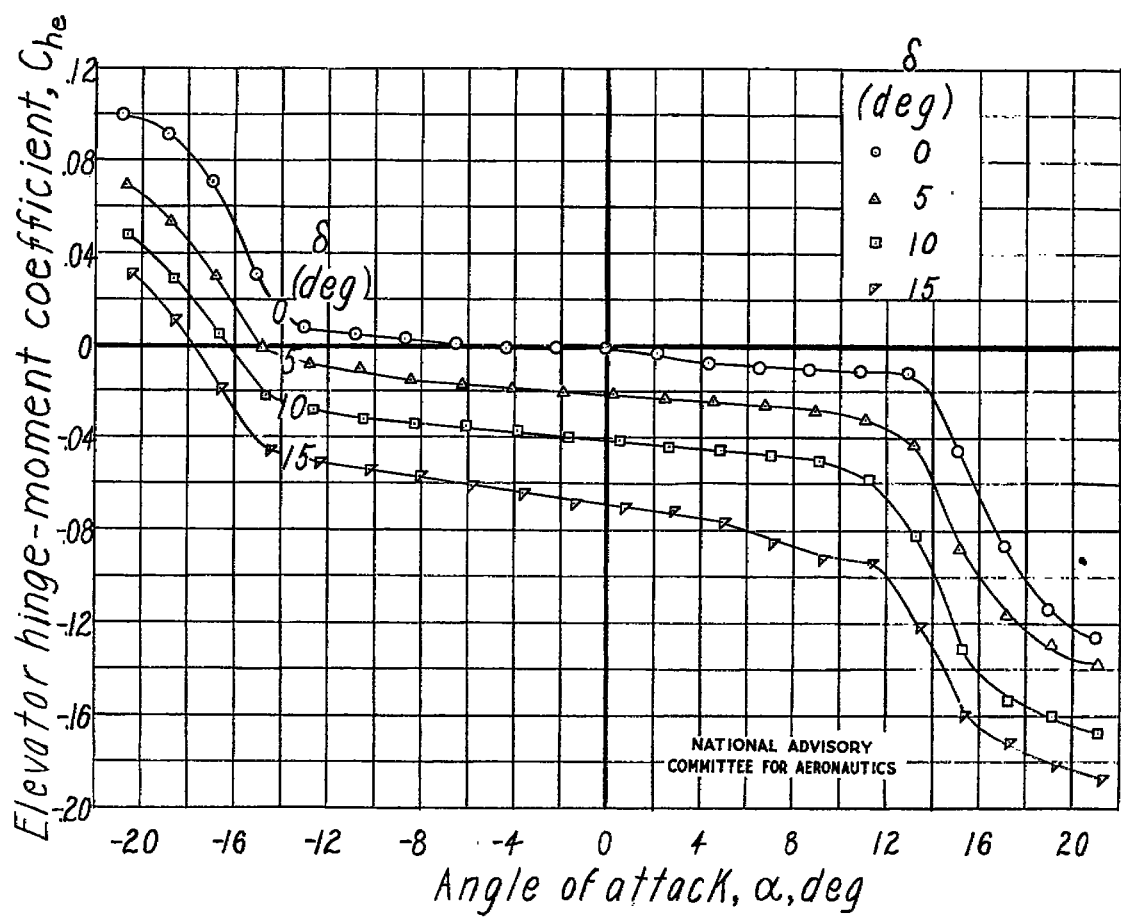
(c) Concluded.

Figure 33.- Continued. Tail 12.



(d) Elevator cut-out filled and elevator gap sealed with grease except where noted.

Figure 33.- Continued. Tail 12.



(d) Concluded.

Figure 33.- Concluded. Tail 12.

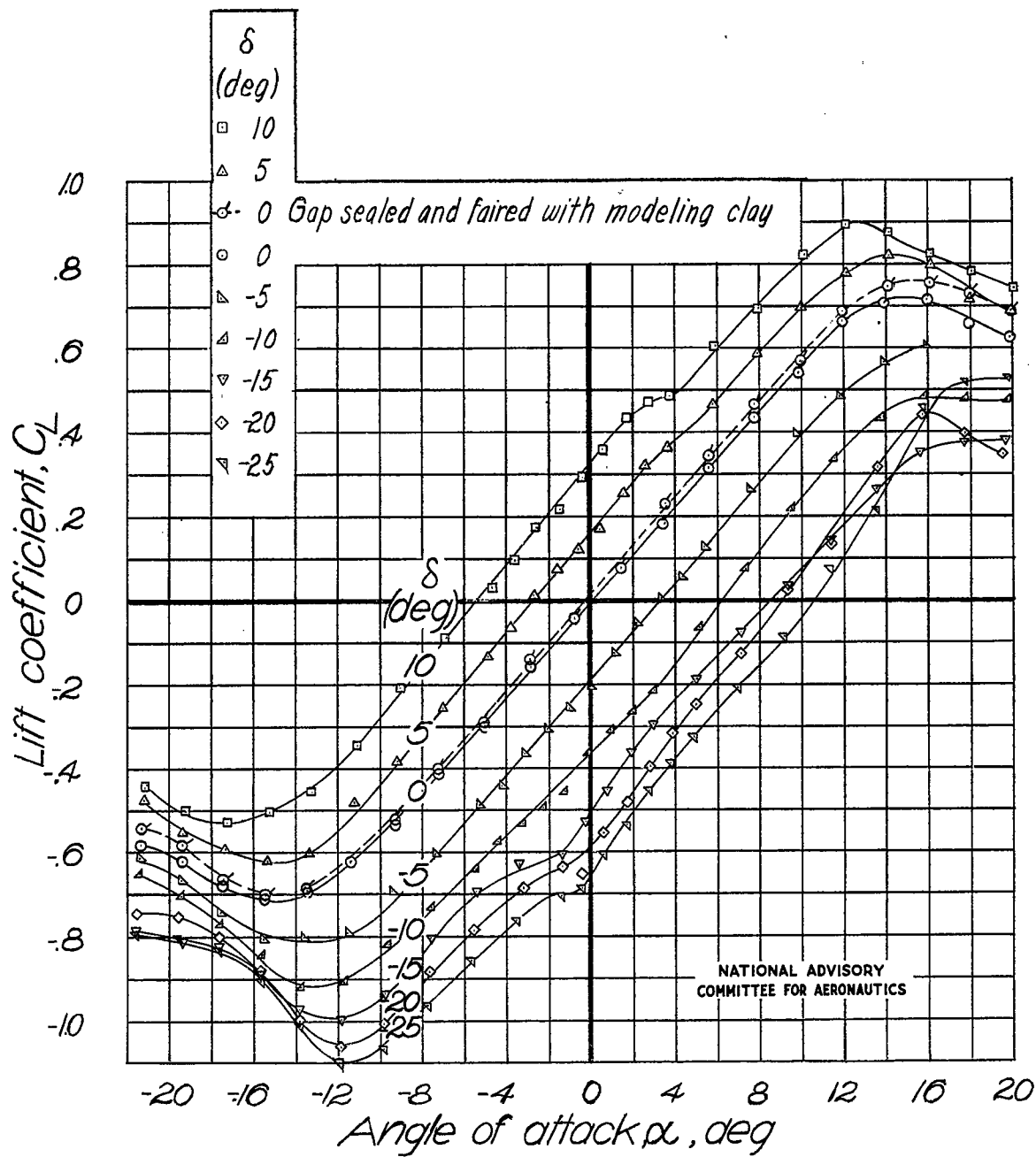


Figure 34.- Lift and hinge-moment characteristics of horizontal tail 13.
Elevator gap sealed with grease.

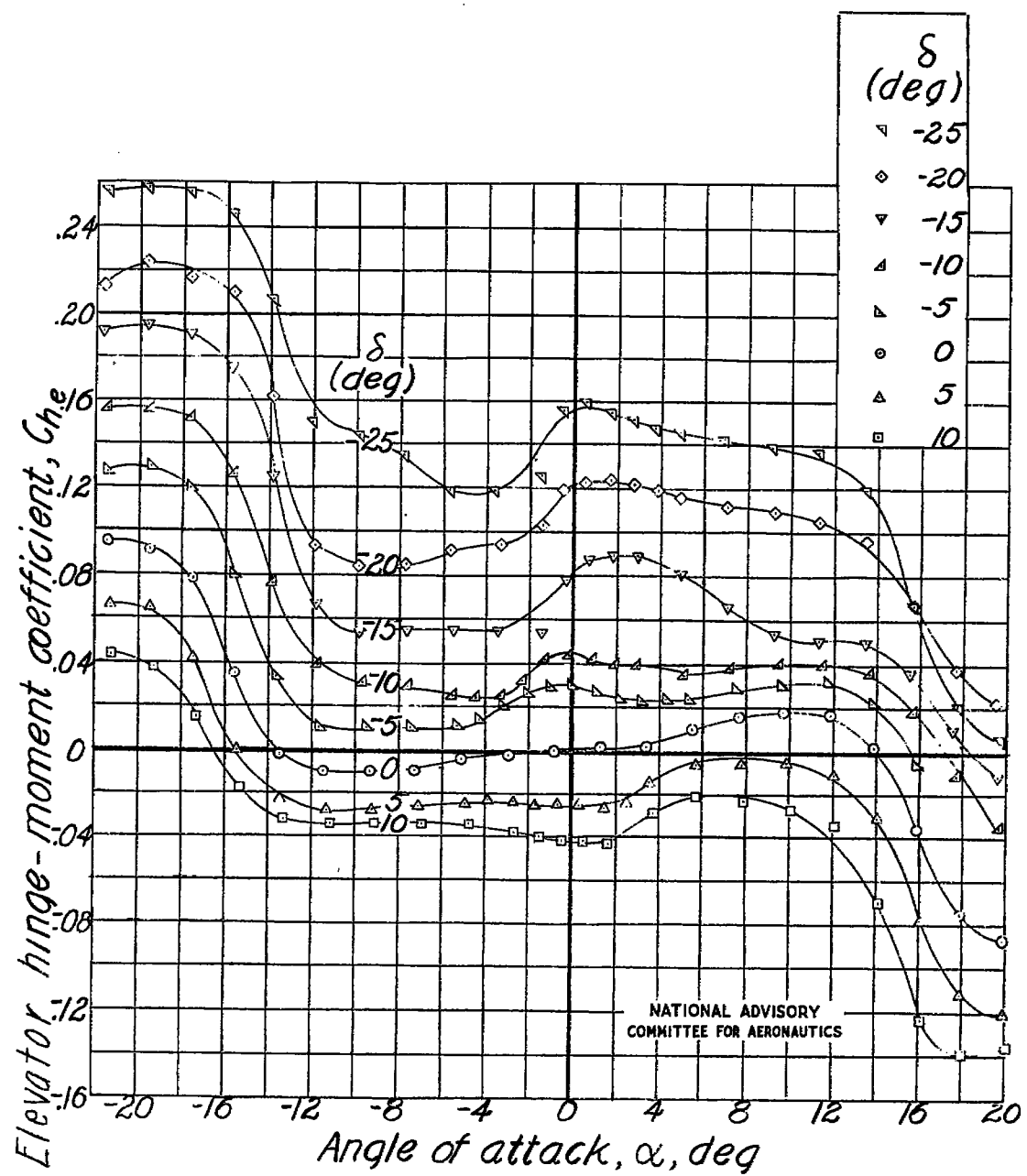
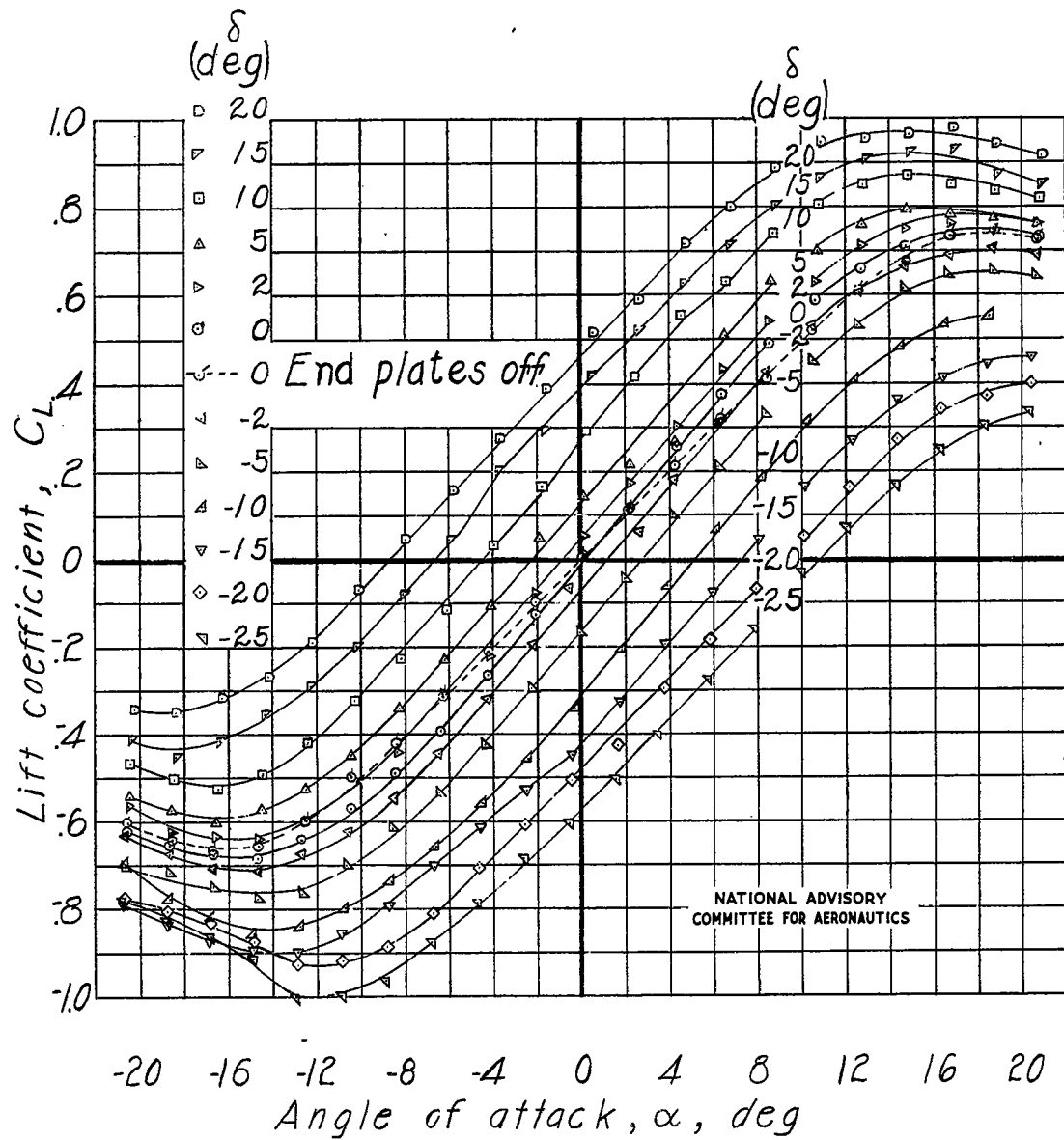
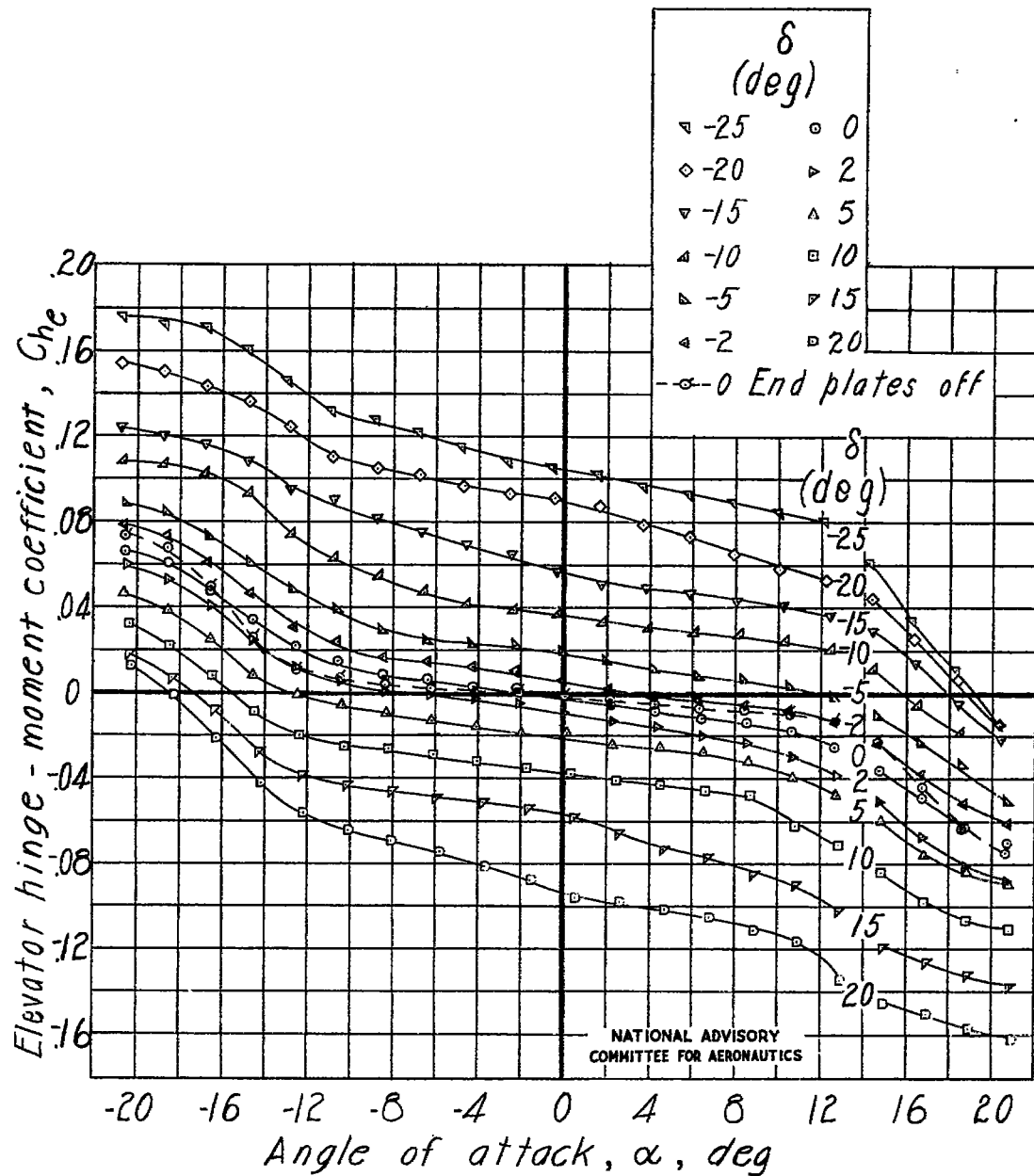


Figure 34.- Concluded. Tail 13.



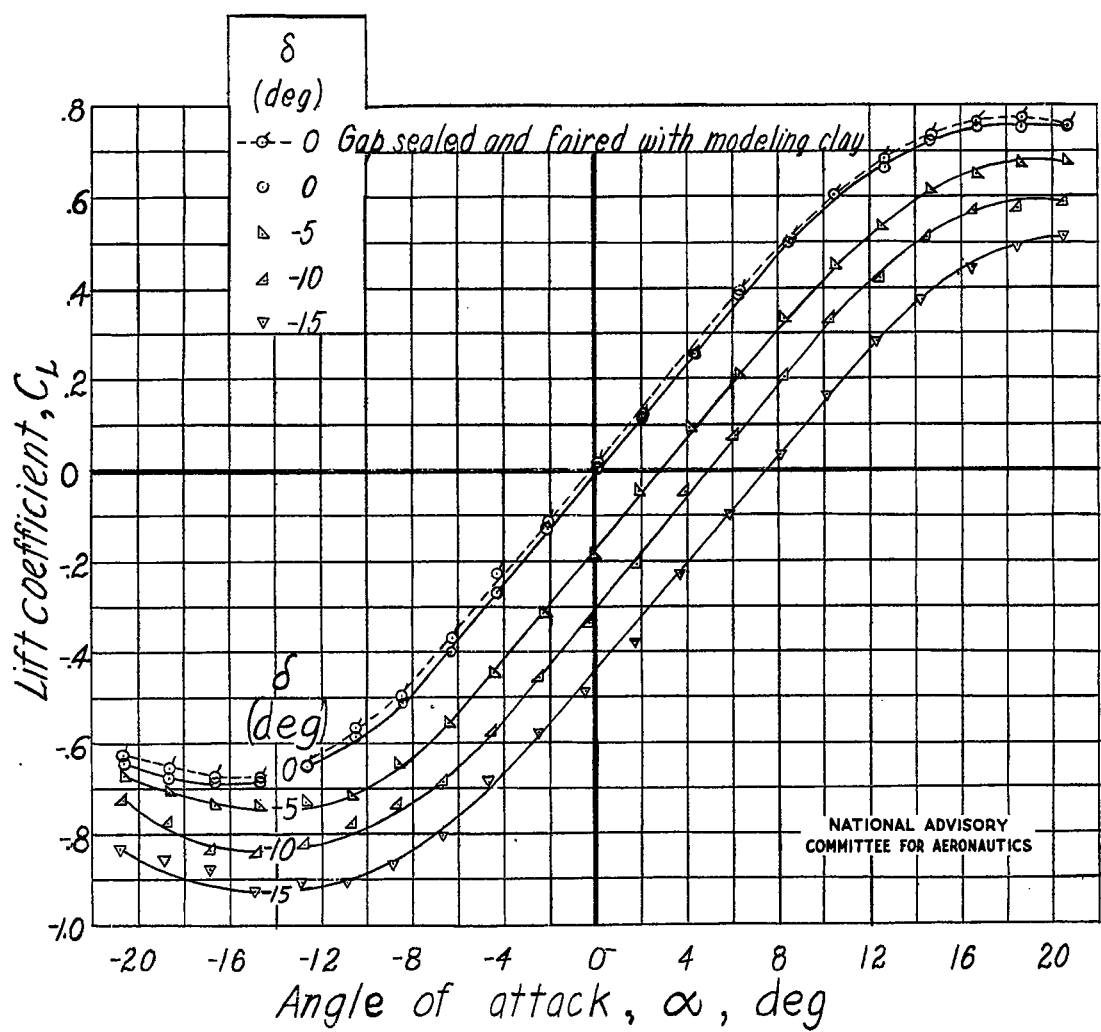
(a) Elevator gap open. End plates on except where noted.

Figure 35.- Lift and hinge-moment characteristics of horizontal tail 14.



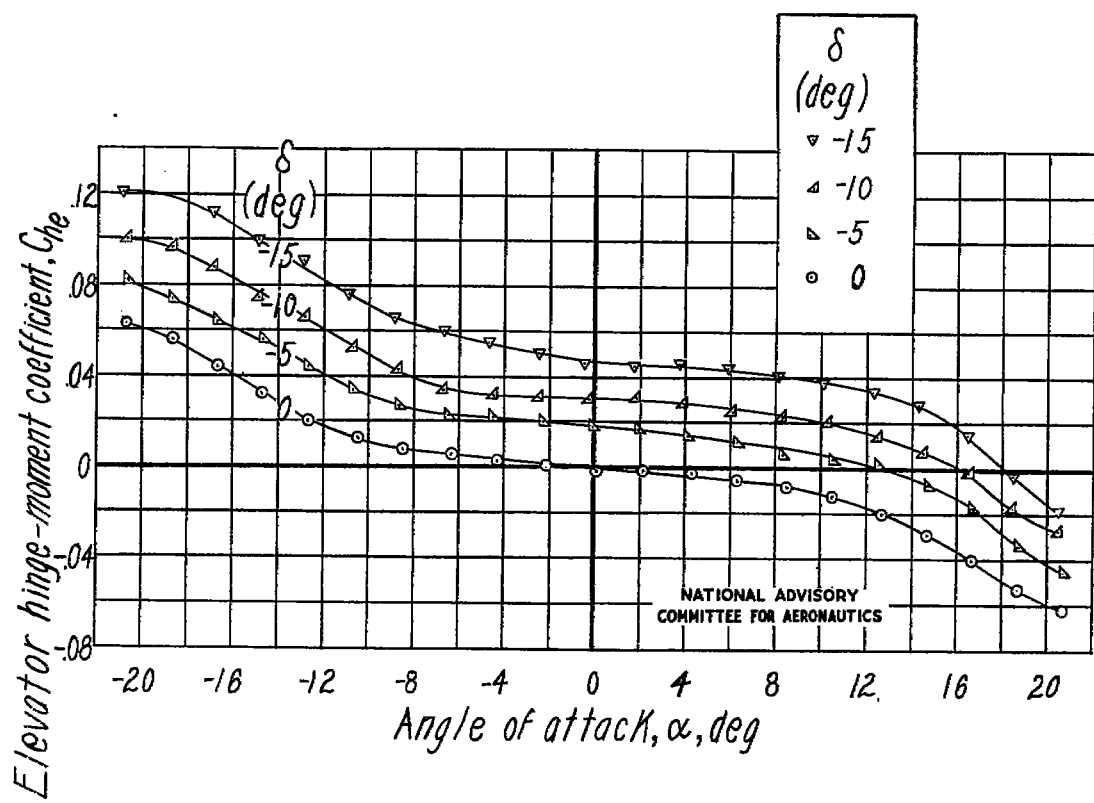
(a) Concluded.

Figure 35.- Continued. Tail 14.



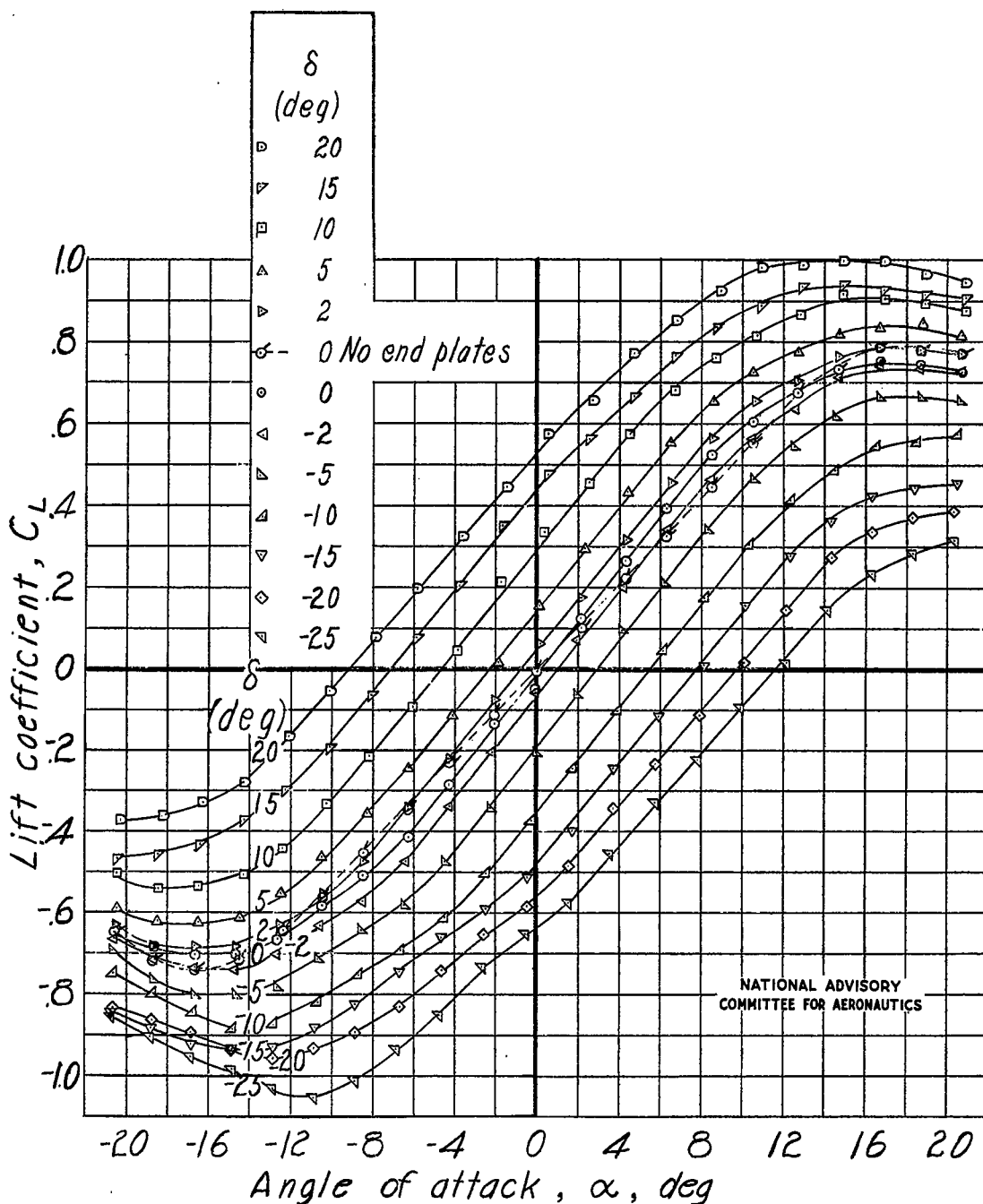
(b) Elevator gap sealed with grease except where noted. End plates on.

Figure 35.- Continued. Tail 14.



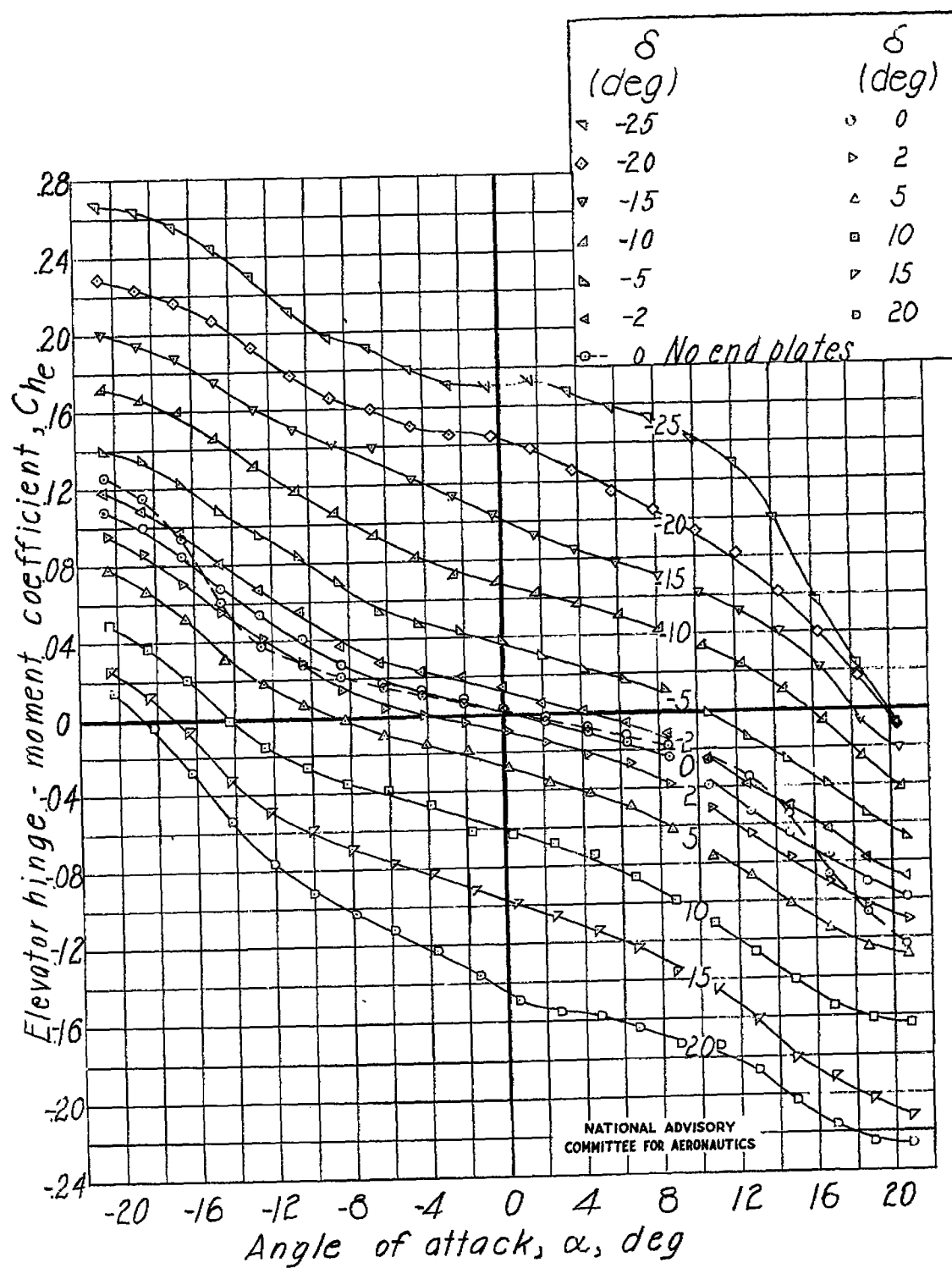
(b) Concluded.

Figure 35.- Continued. Tail 14.



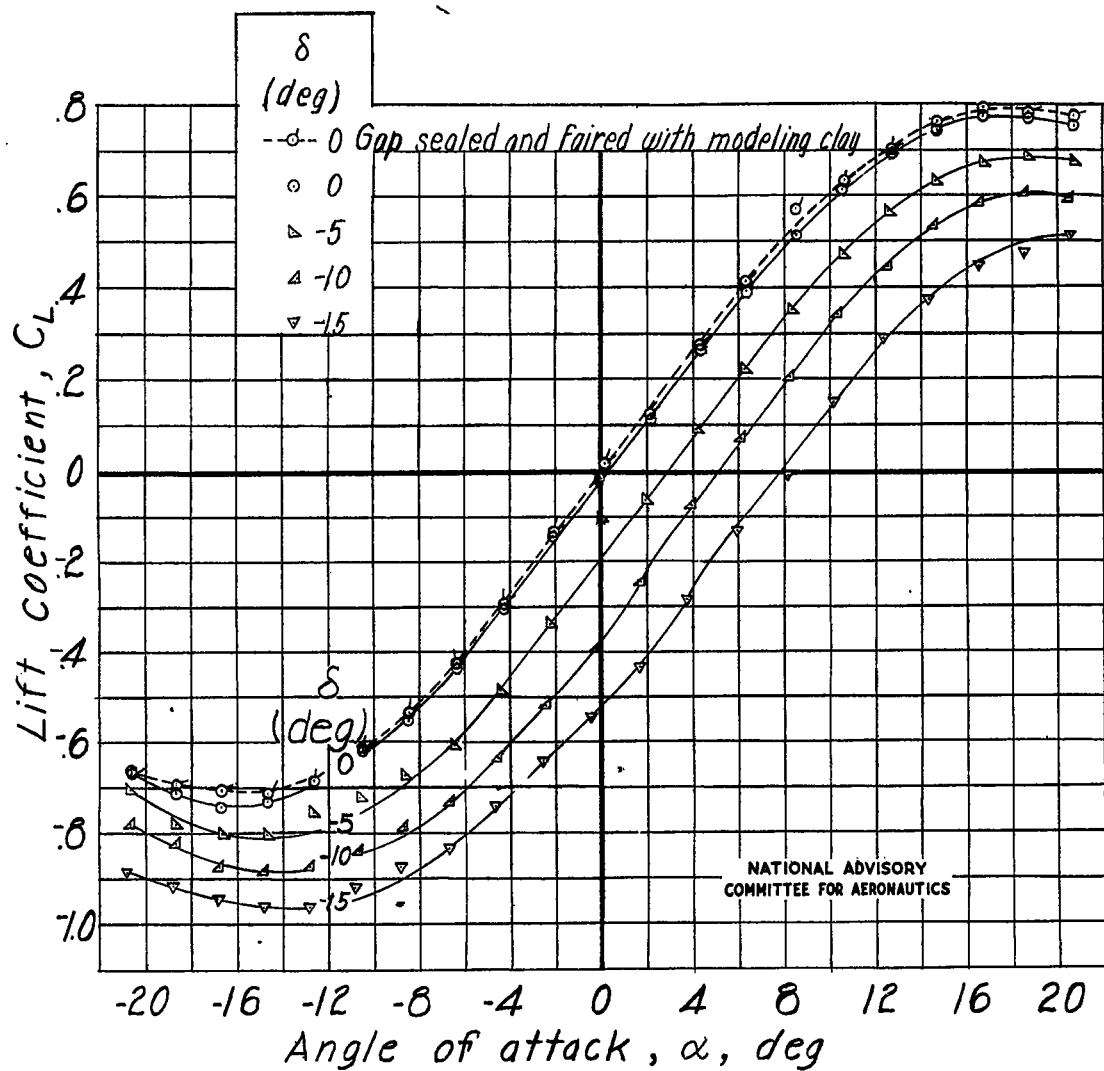
(c) Elevator cut-out filled and elevator gap open. End plates on except where noted.

Figure 35.- Continued. Tail 14.



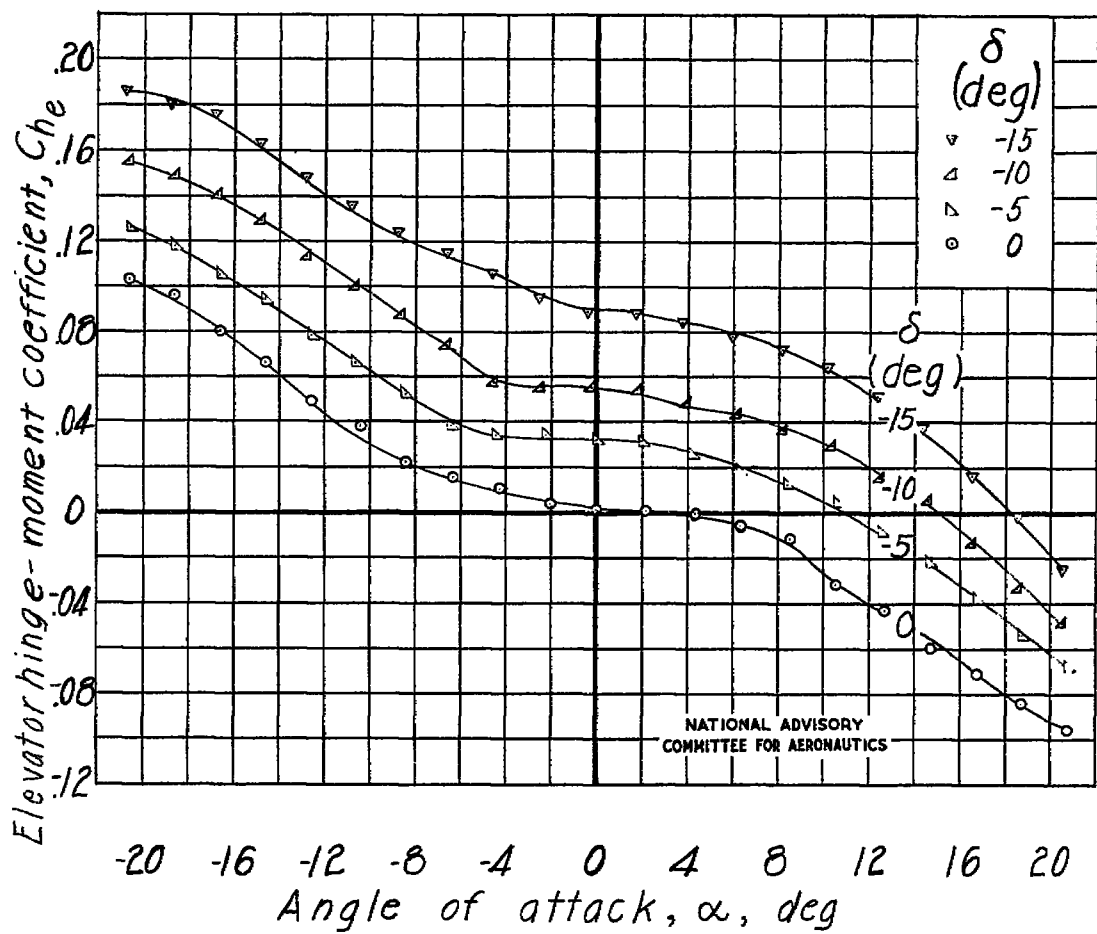
(c) Concluded.

Figure 35.- Continued. Tail 14.



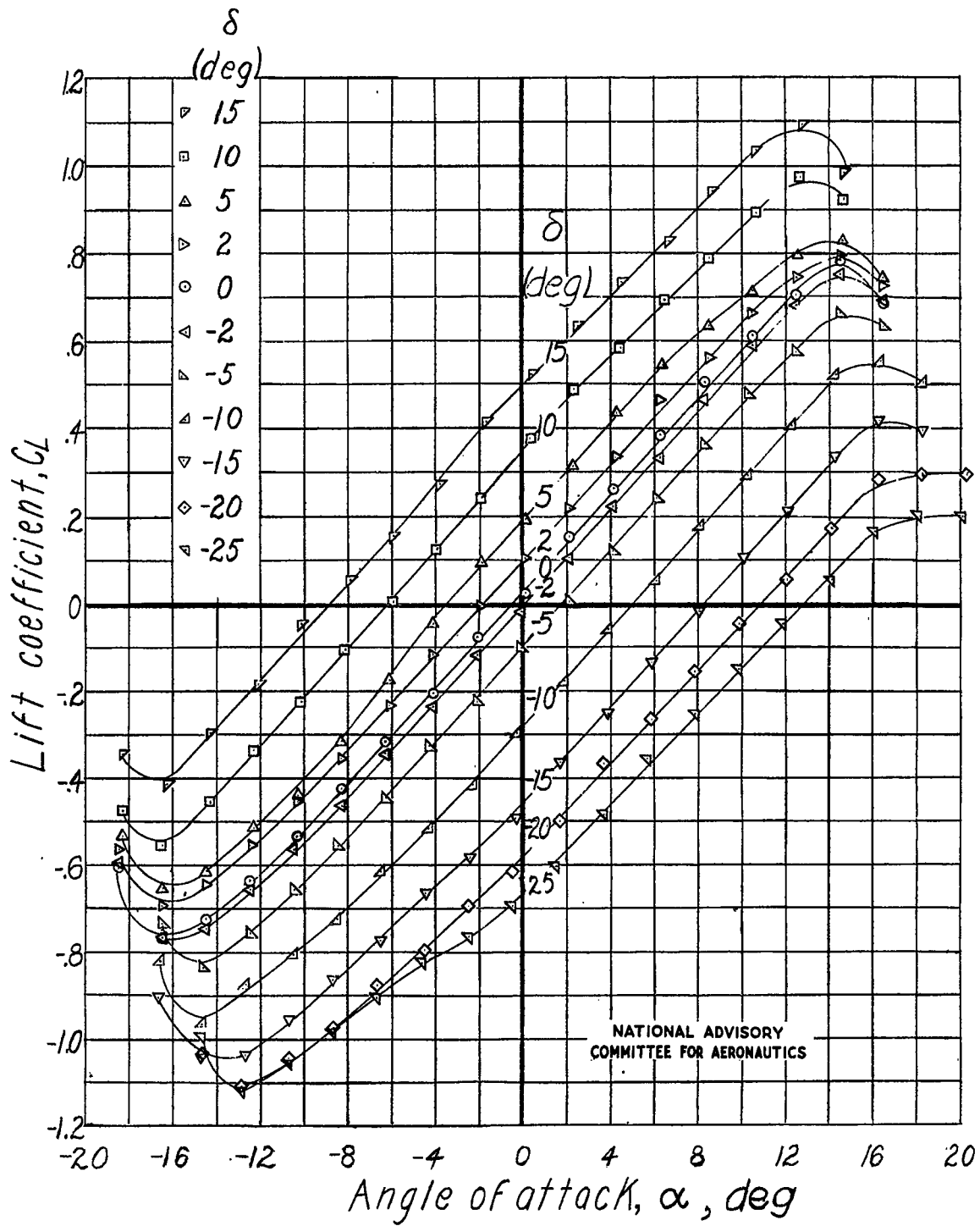
(d) Elevator cut-out filled and elevator gap sealed with grease except where noted. End plates on.

Figure 35.- Continued. Tail 14.



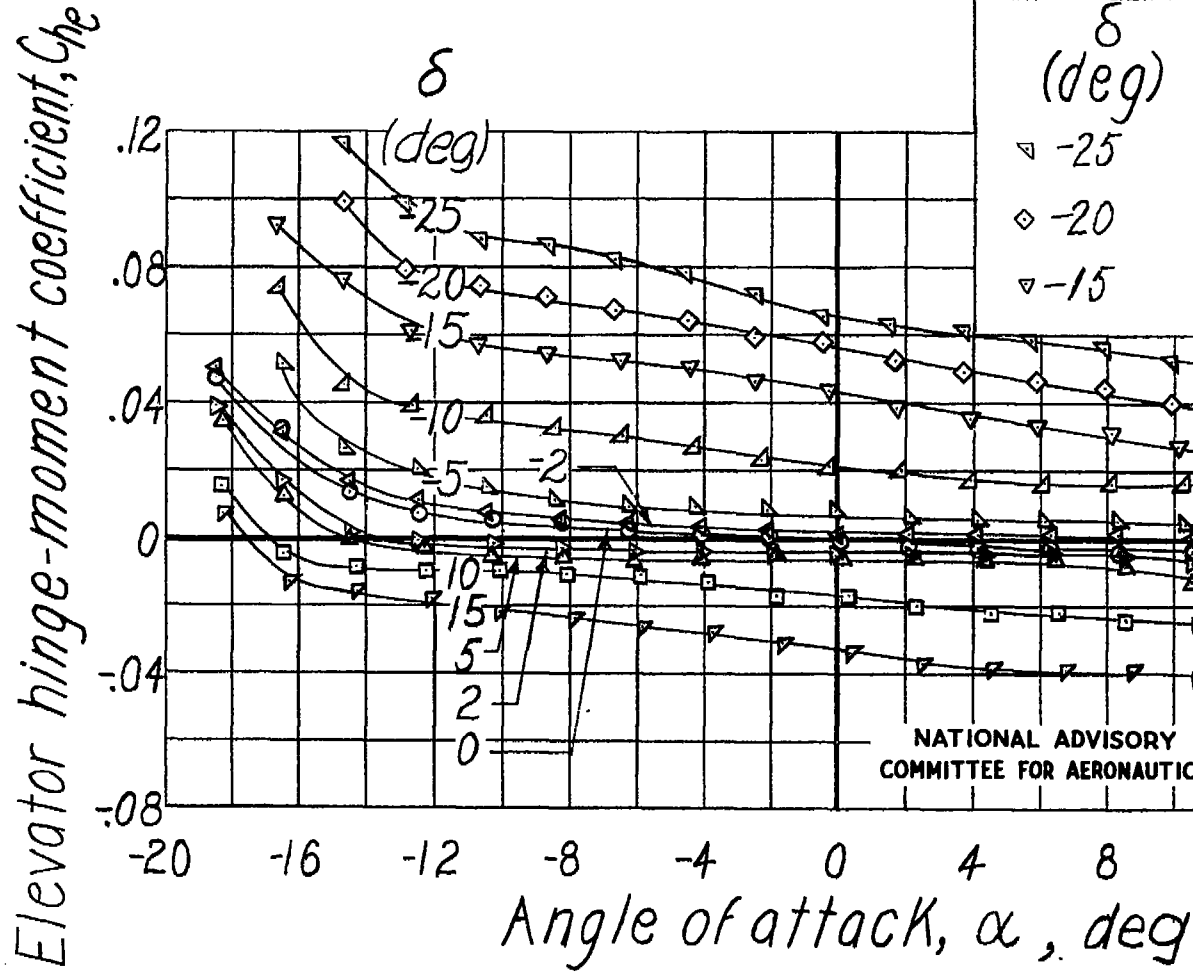
(d) Concluded.

Figure 35.- Concluded. Tail 14.



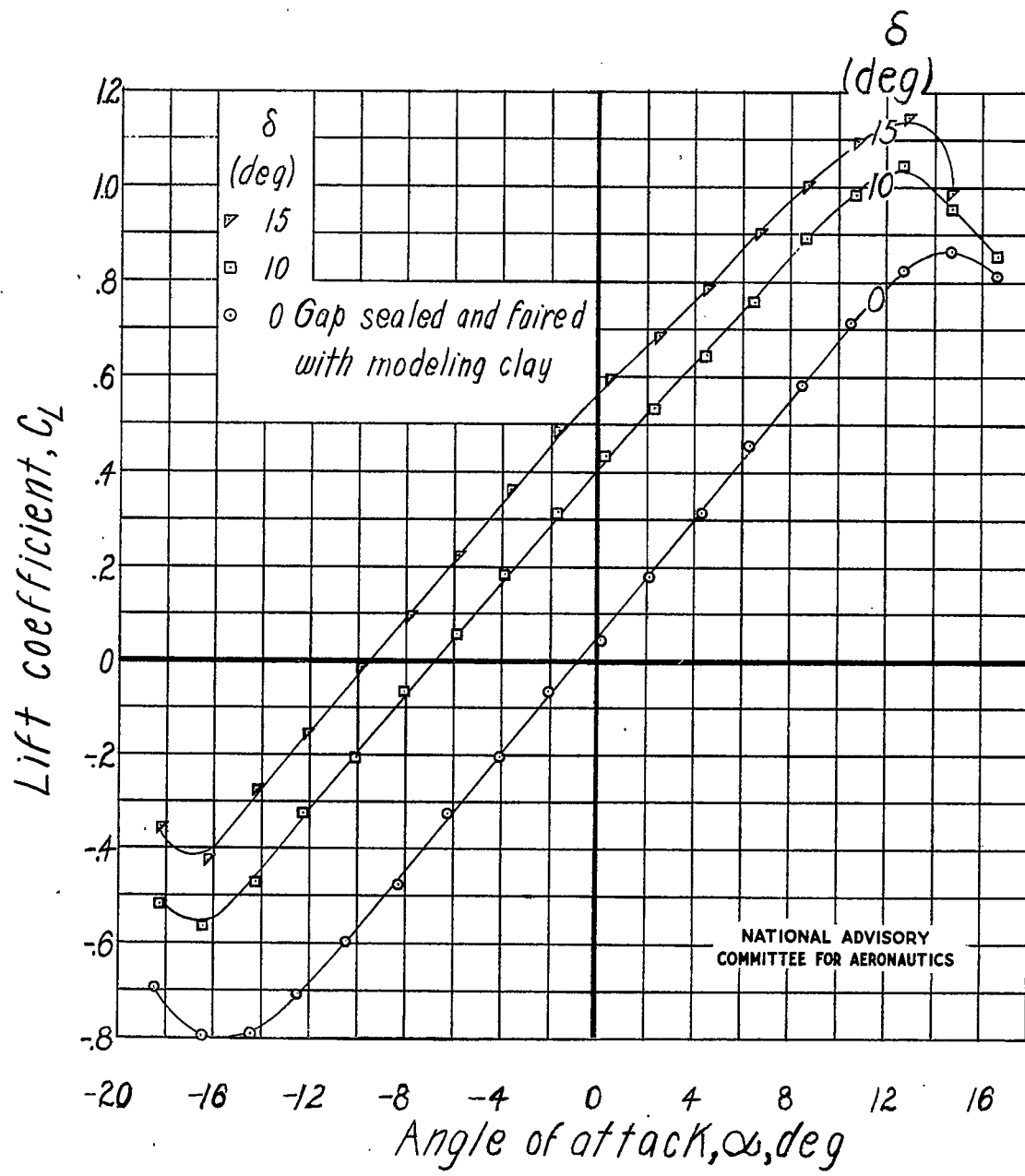
(a) Elevator gap open.

Figure 36.- Lift and hinge-moment characteristics of tail 15.



(a) Concluded.

Figure 36.- Continued. Tail 15.

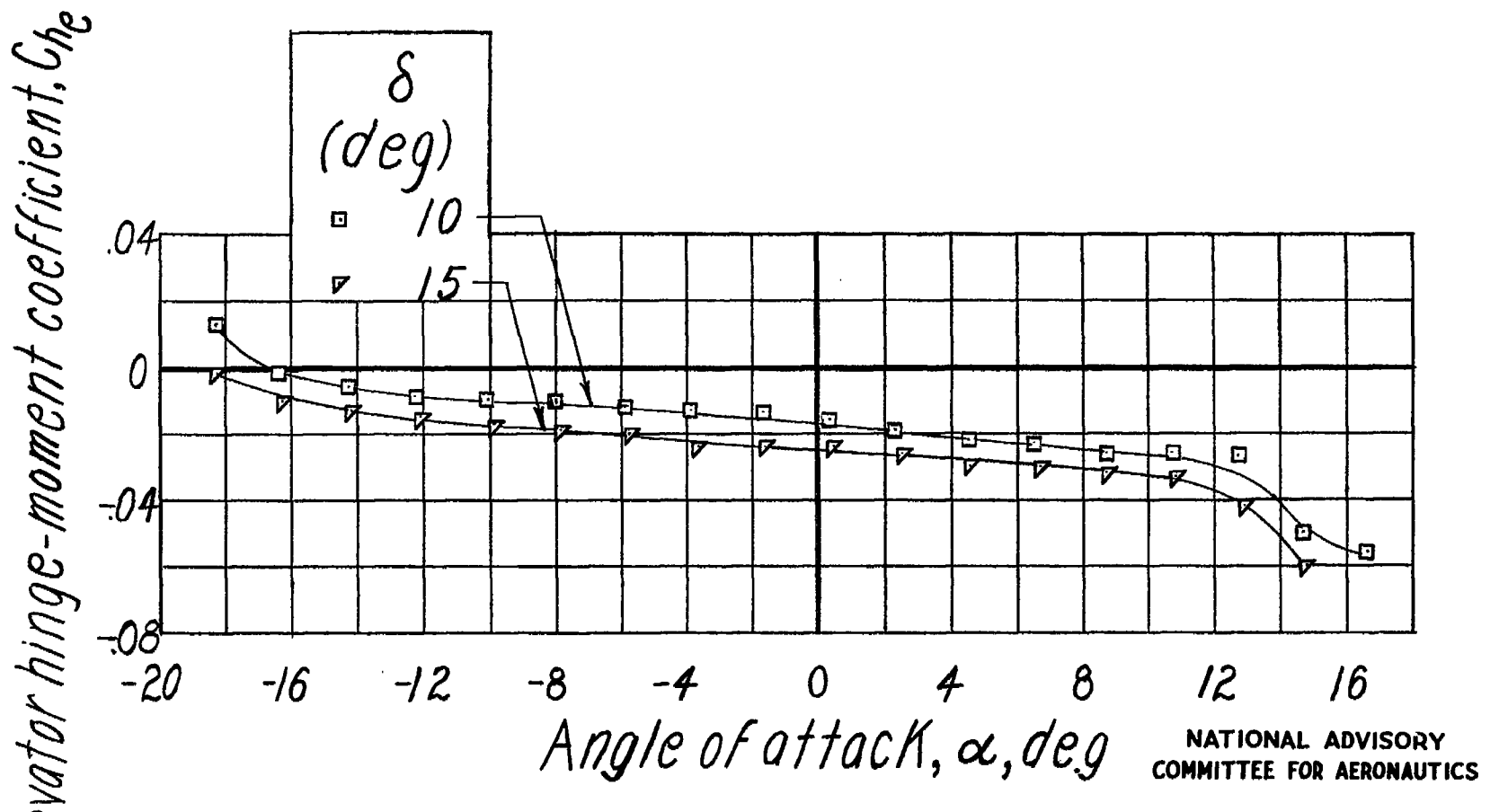


(b) Elevator gap sealed with grease except where noted.

Figure 36.- Continued. Tail 15.

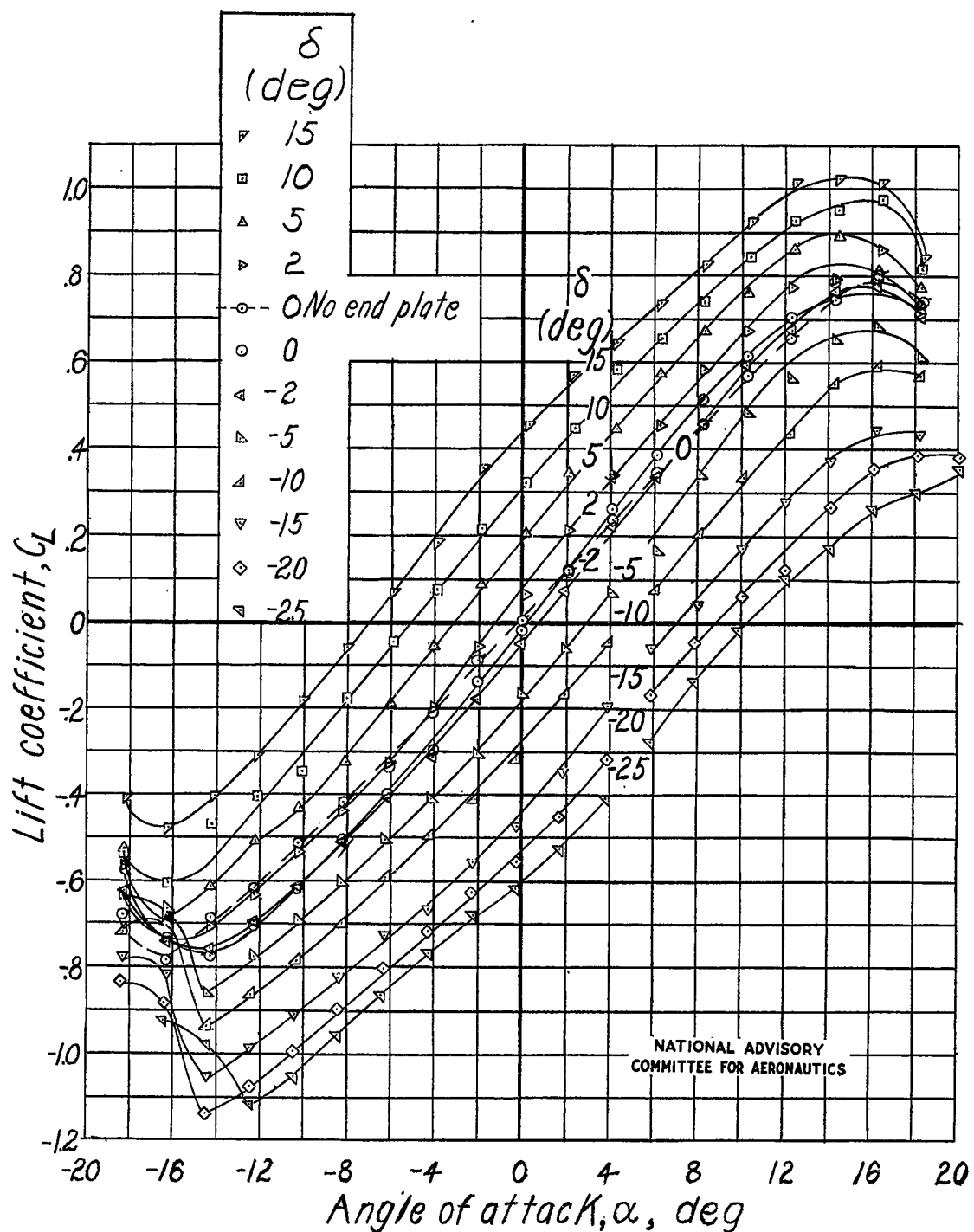
Fig. 36b conc.

NACA TN No. 1291



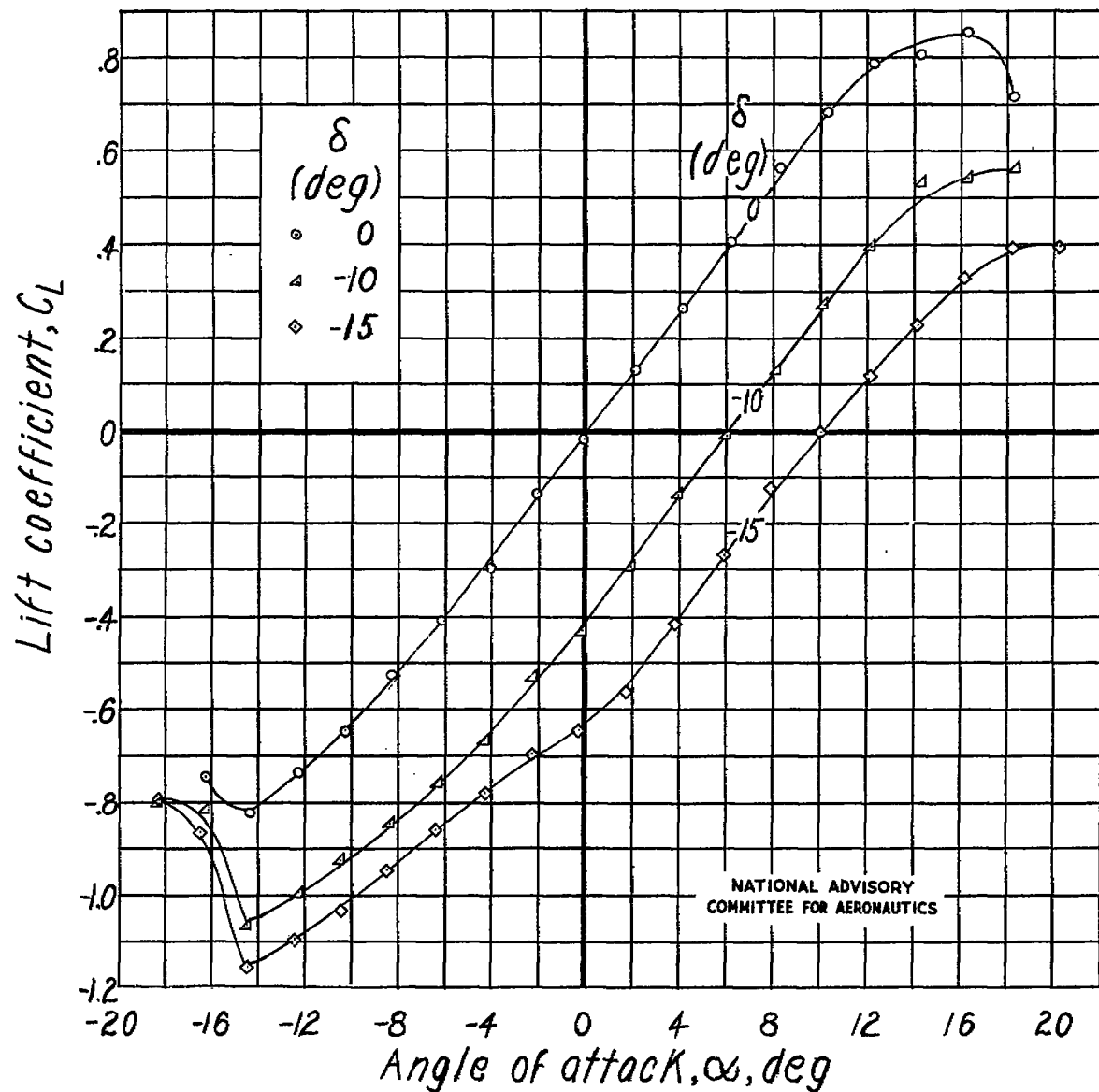
(b) Concluded.

Figure 36.- Concluded. Tail 15.



(a) Elevator gap open. End plates on except where noted.

Figure 37.- Lift and hinge-moment characteristics of horizontal tail 16.



(b) Elevator gap sealed with grease. End plate on.

Figure 37.- Concluded. Tail 16.

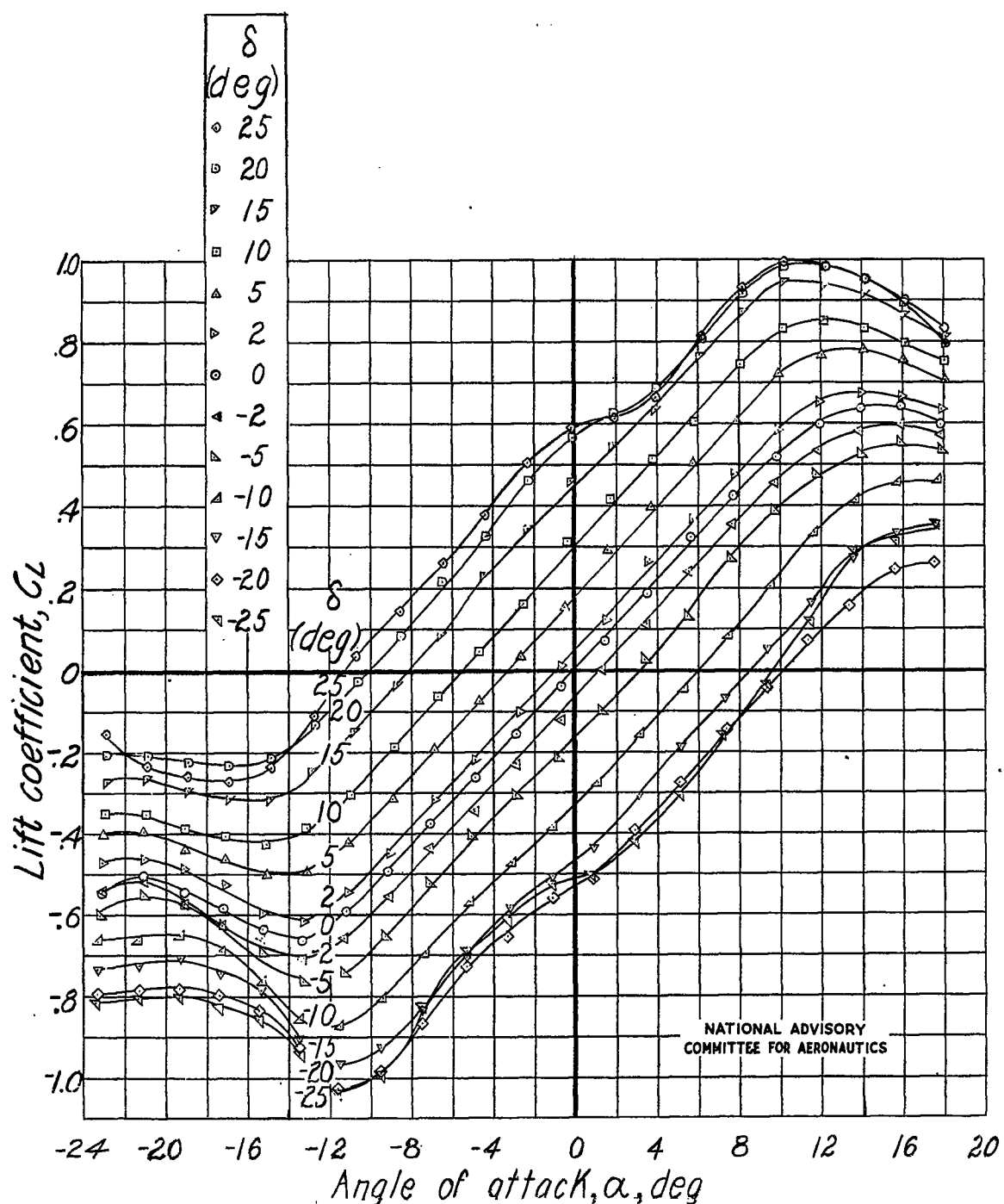


Figure 38.- Lift and hinge-moment characteristics of horizontal tail 17.
Elevator gap open.

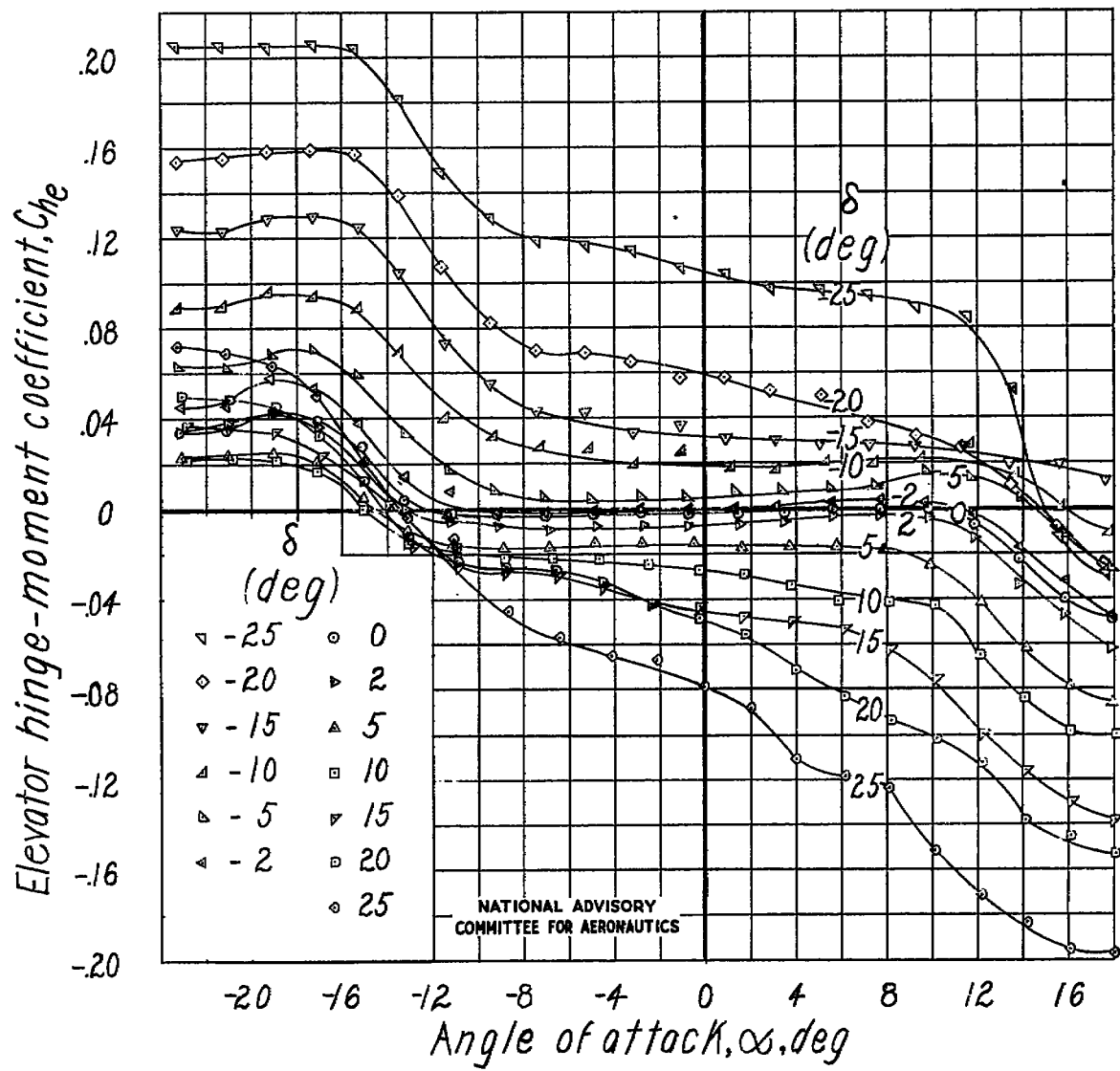


Figure 38.- Concluded. Tail 17.

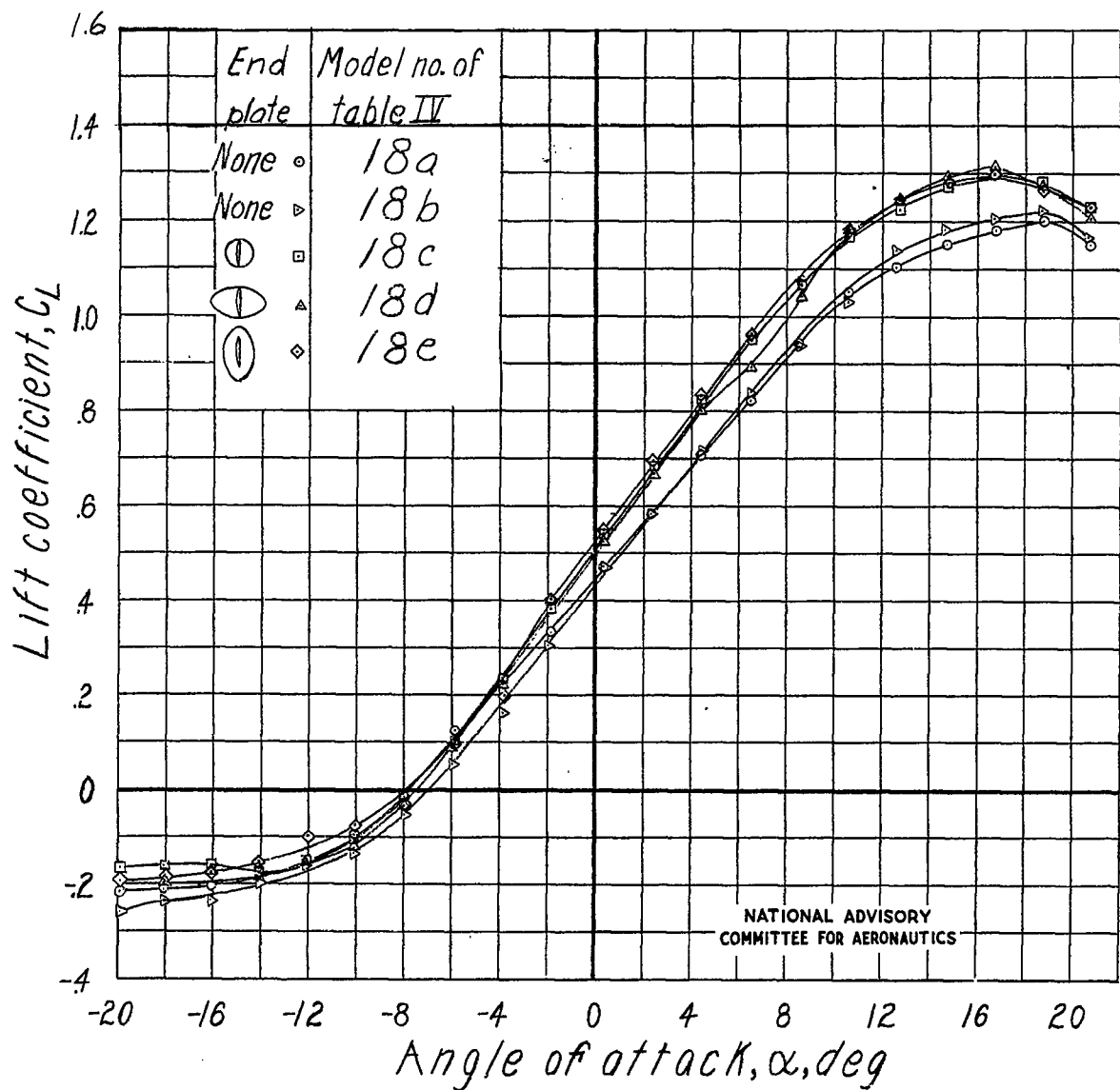


Figure 39.- Lift characteristics of airfoil 18.

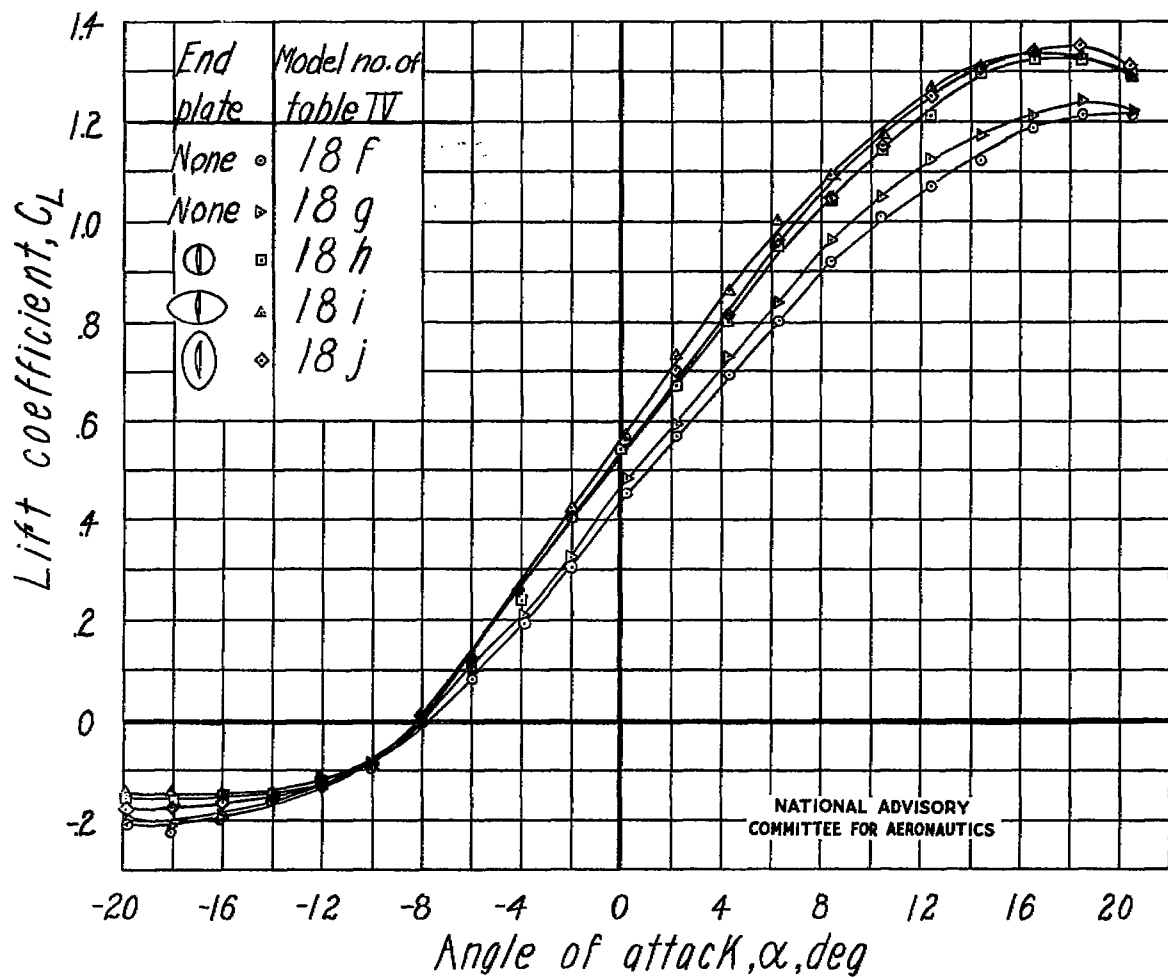


Figure 39.- Continued. Airfoil 18.

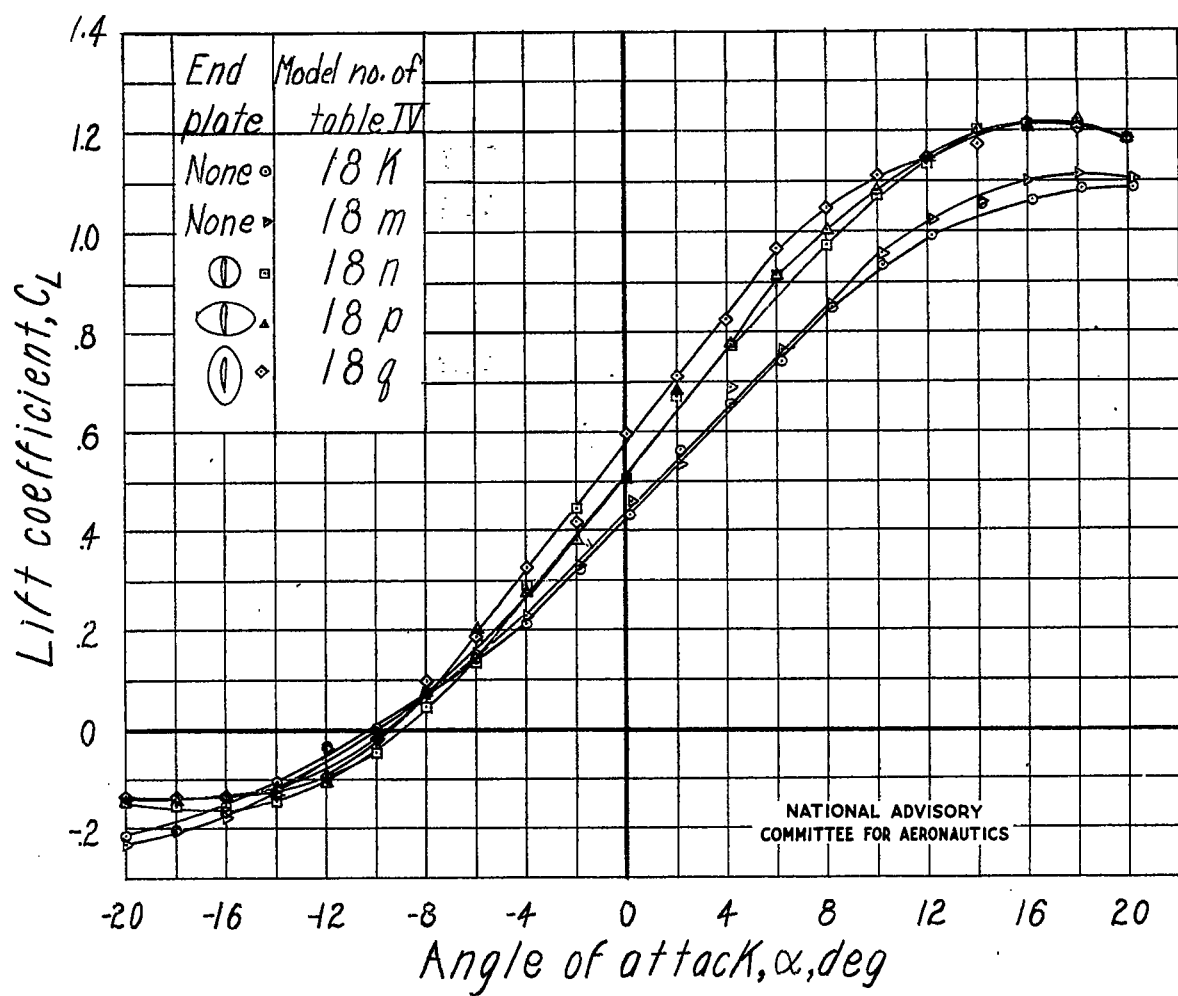


Figure 39.- Continued. Airfoil 18.

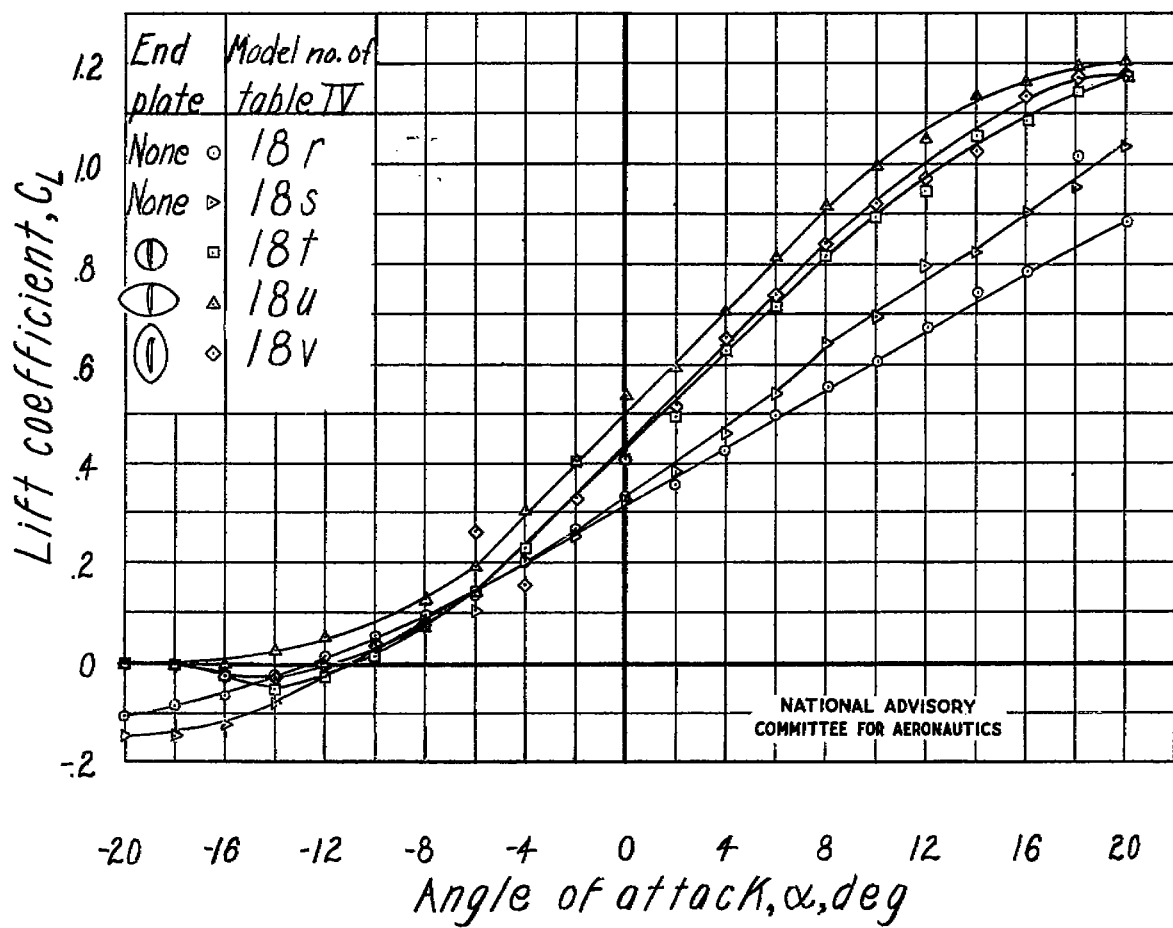


Figure 39.- Concluded. Airfoil 18.

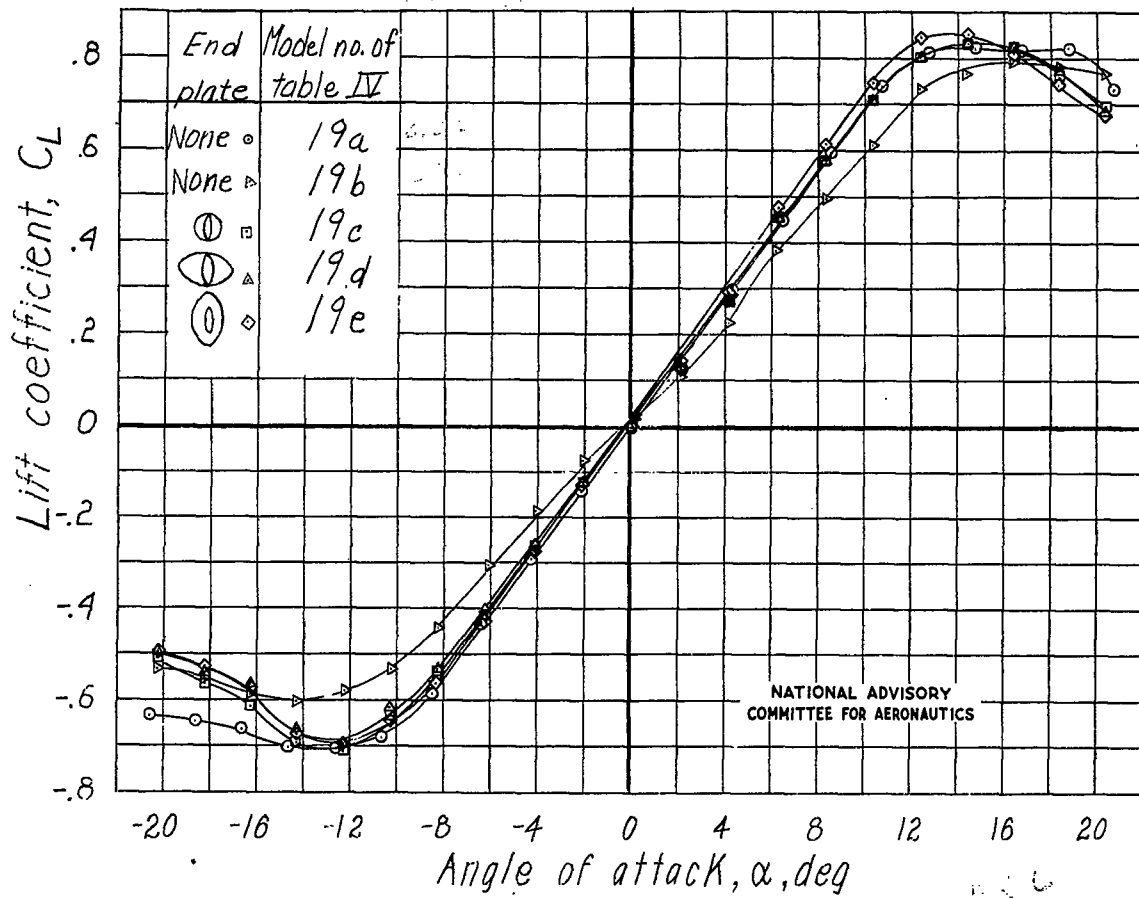


Figure 40.- Lift characteristics of airfoil 19.

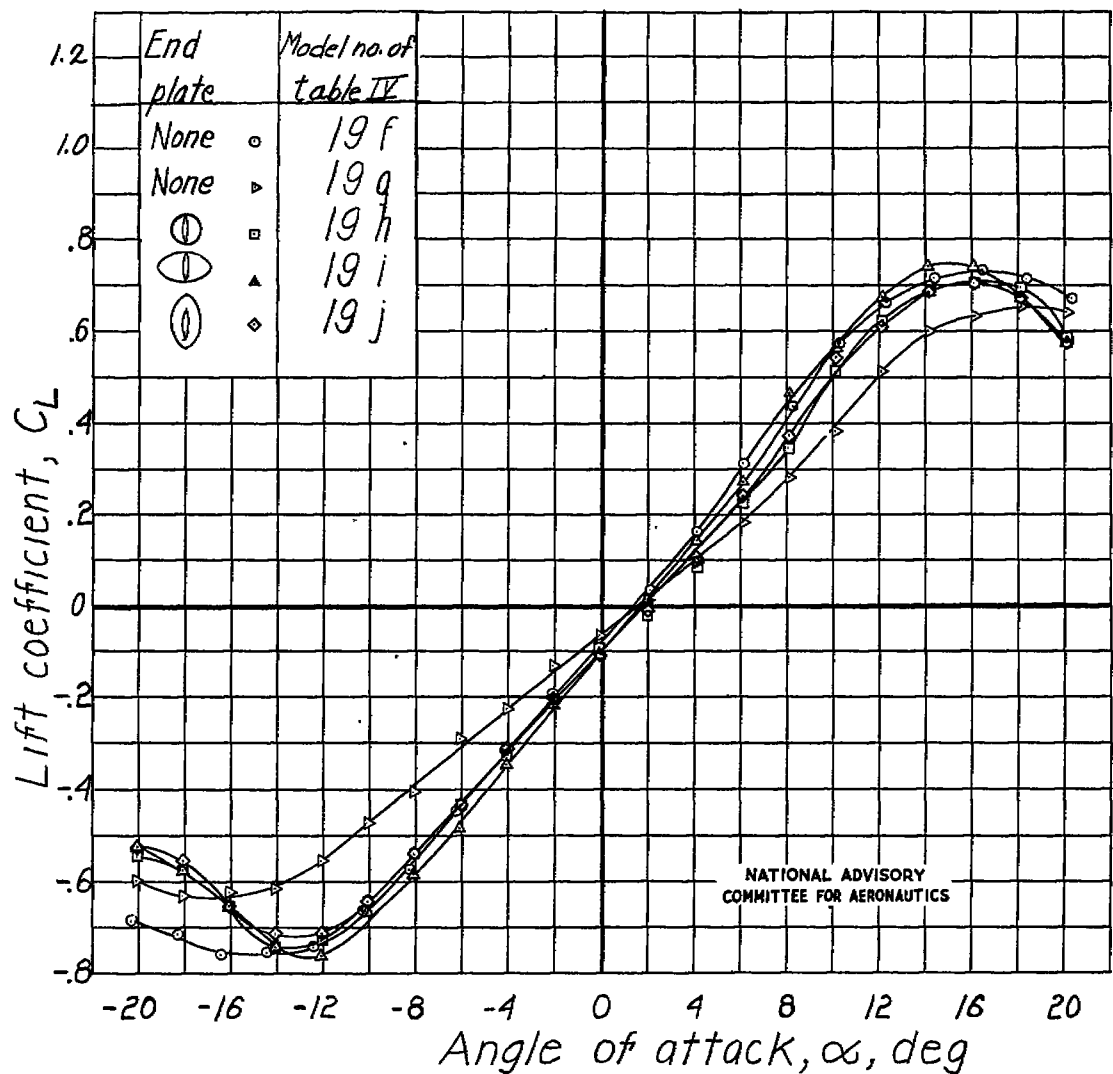


Figure 40.- Continued. Airfoil 19.

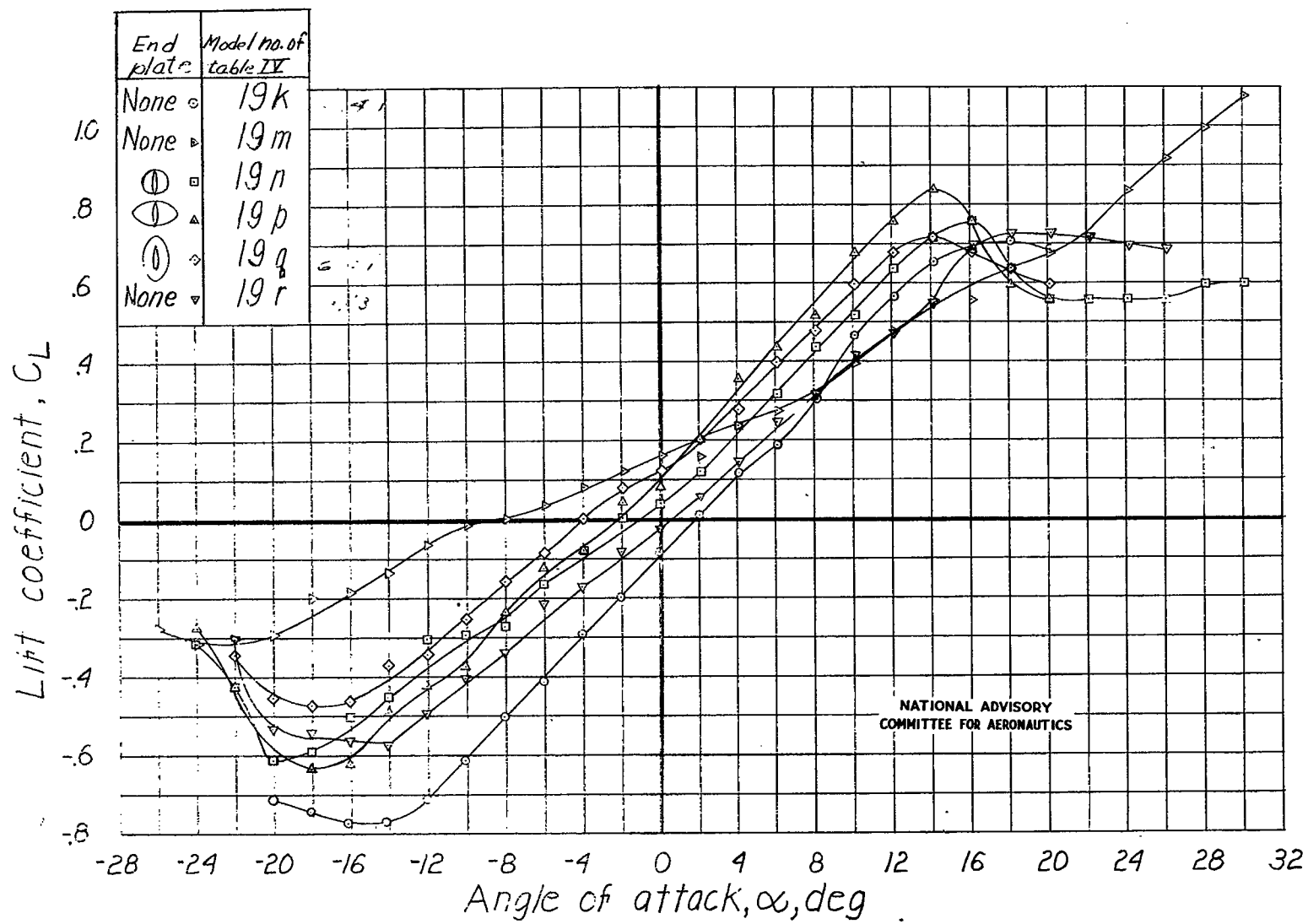


Figure 40.- Concluded. Airfoil 19.

Fig. 41

NACA TN No. 1291

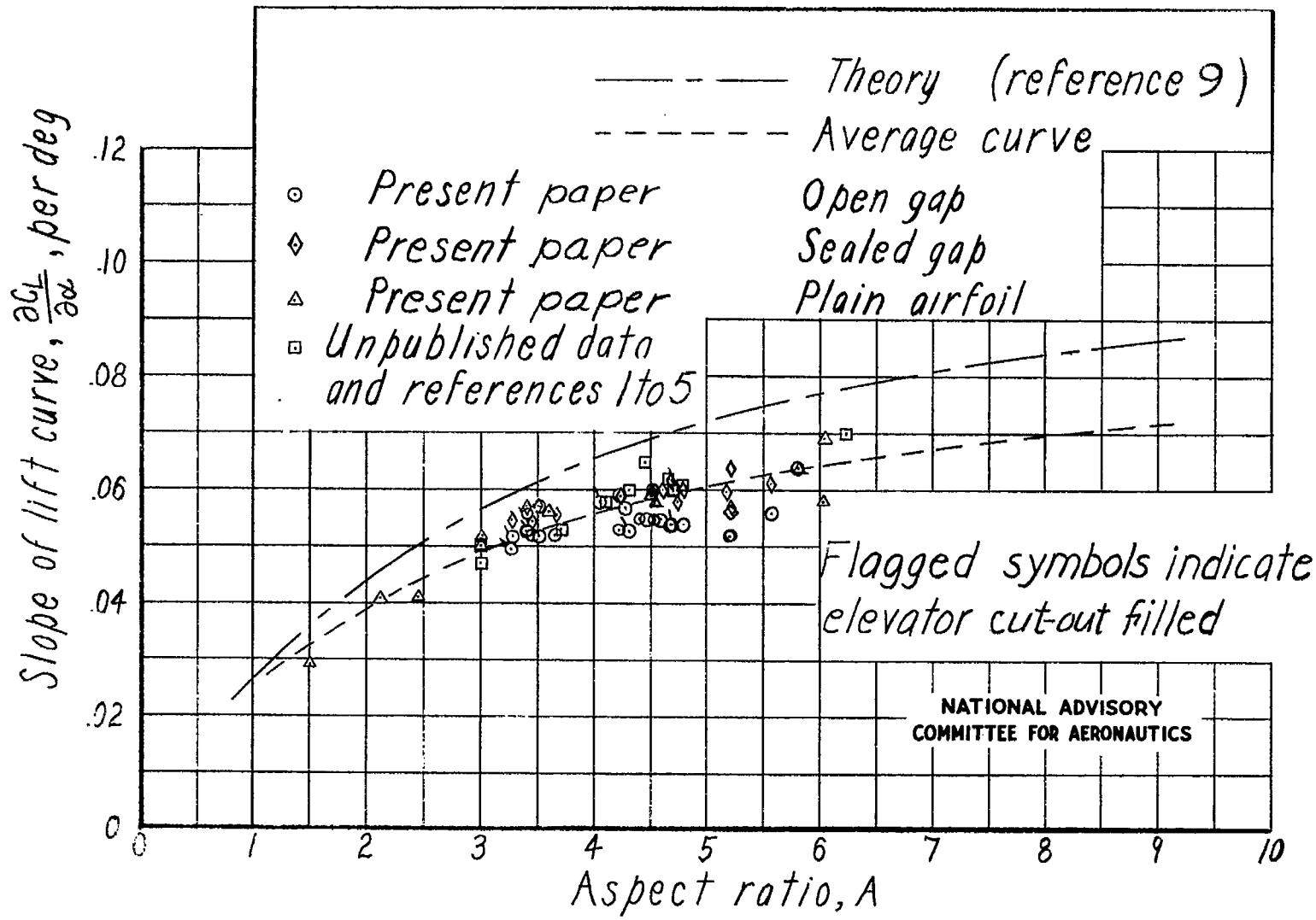


Figure 41.- Variation of lift-curve slope with aspect ratio, theoretical and experimental.

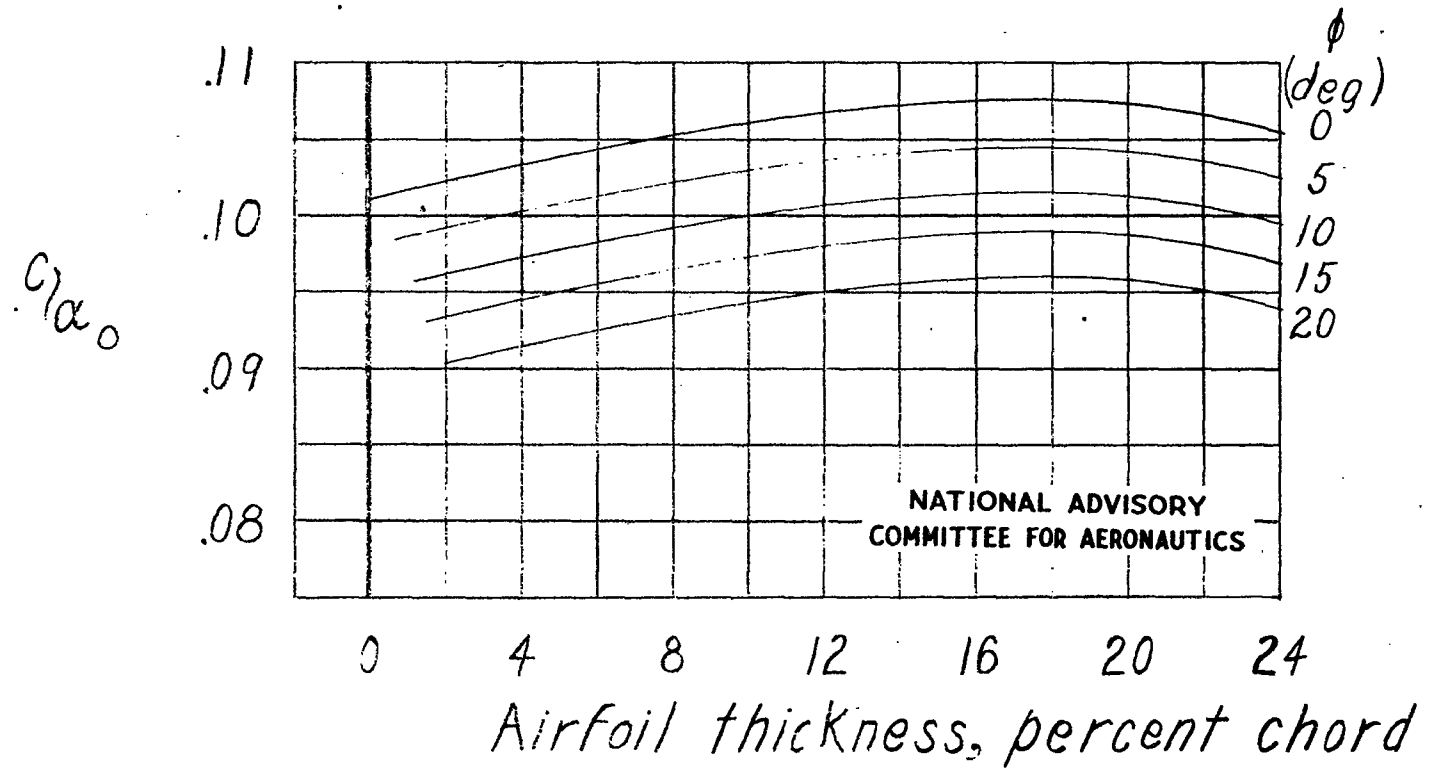


Figure 43.- Effect of airfoil thickness and trailing-edge angle on section lift-curve slope. Airfoils with maximum thickness at about 0.30 chord. Derived from data in references 10 to 14.

Fig. 43

NACA TN No. 1291

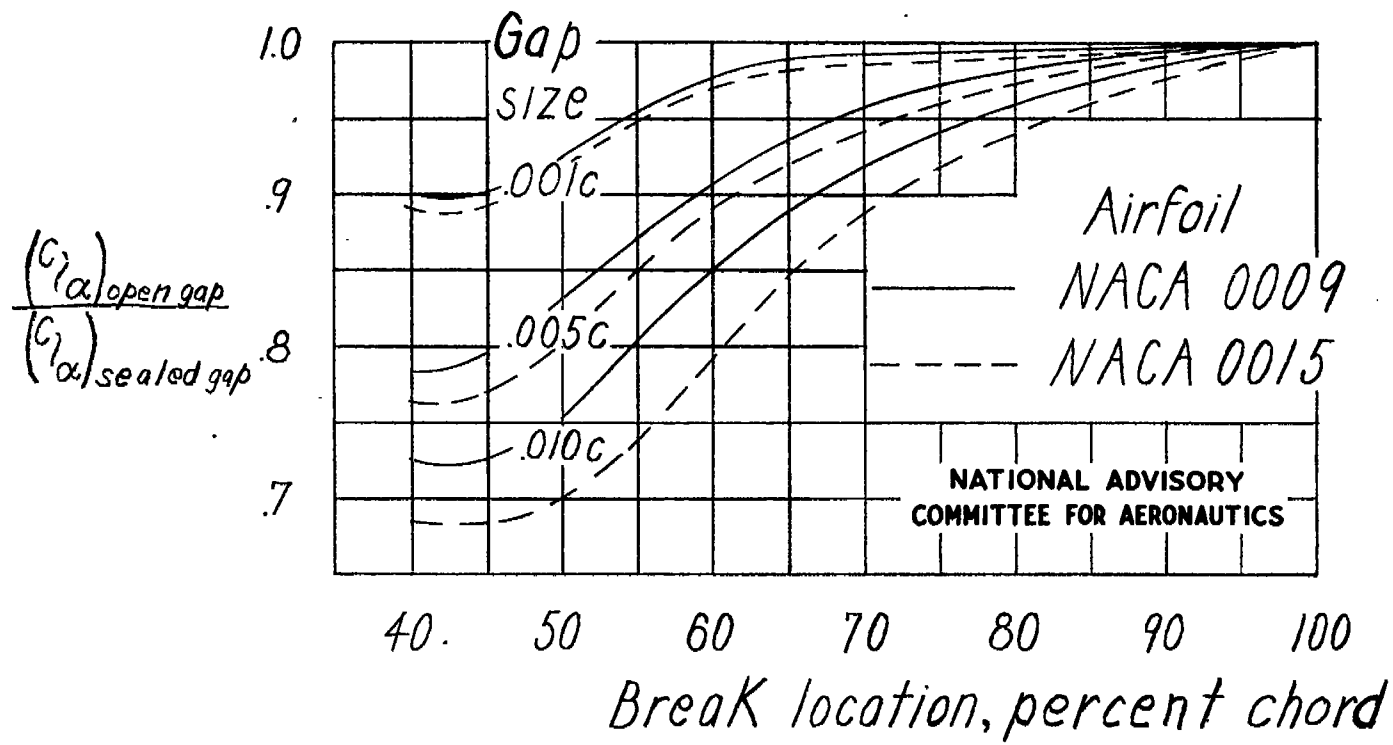


Figure 43.- Effect of gap on section lift-curve slope. NACA 0009 and 0015 airfoil sections. Plain flaps and blunt-nose balances. Derived from references 15 and 16.

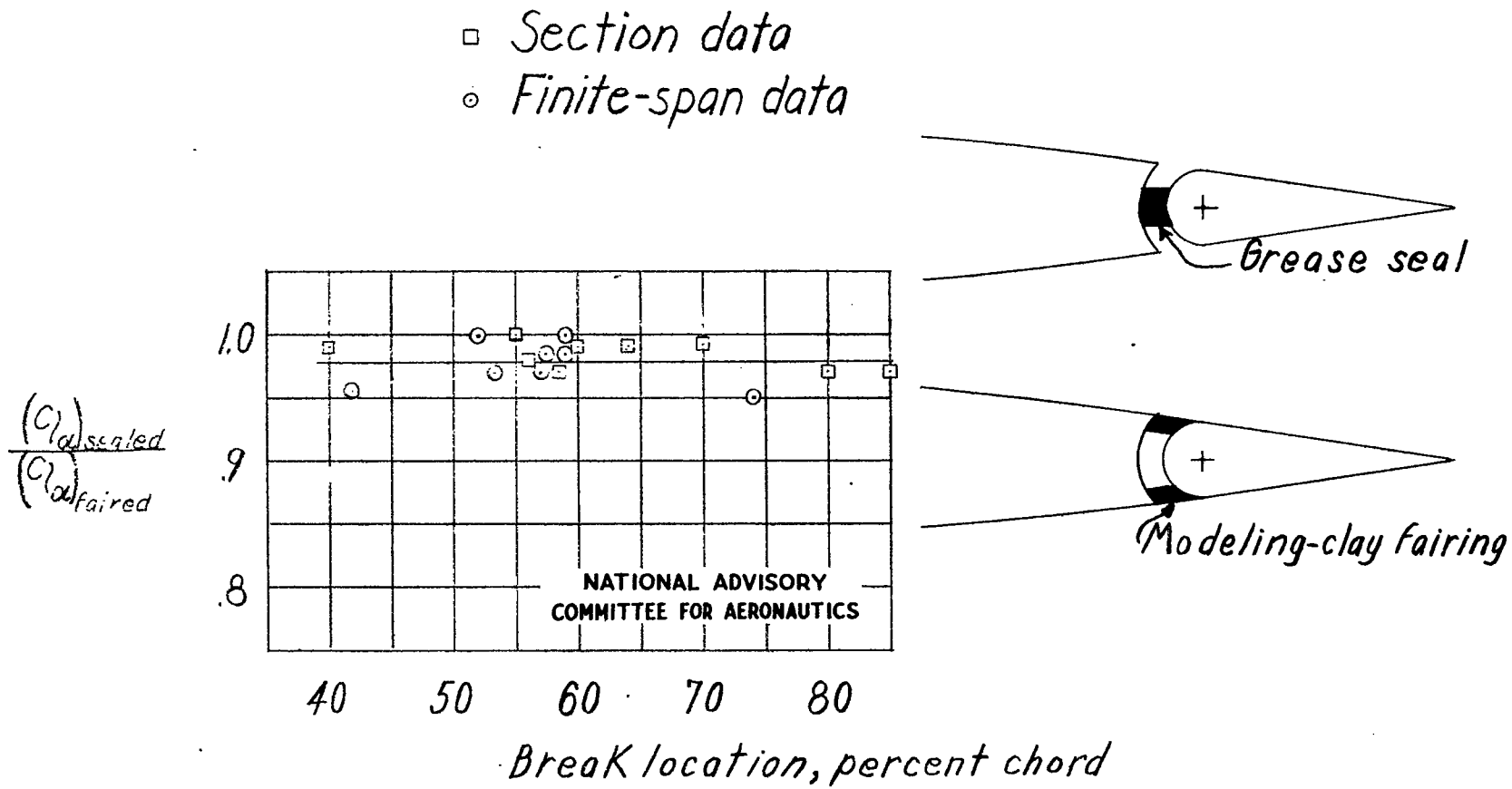


Figure 44.- Effect of break in airfoil contour on lift-curve slope.

Fig. 45

NACA TN No. 1291

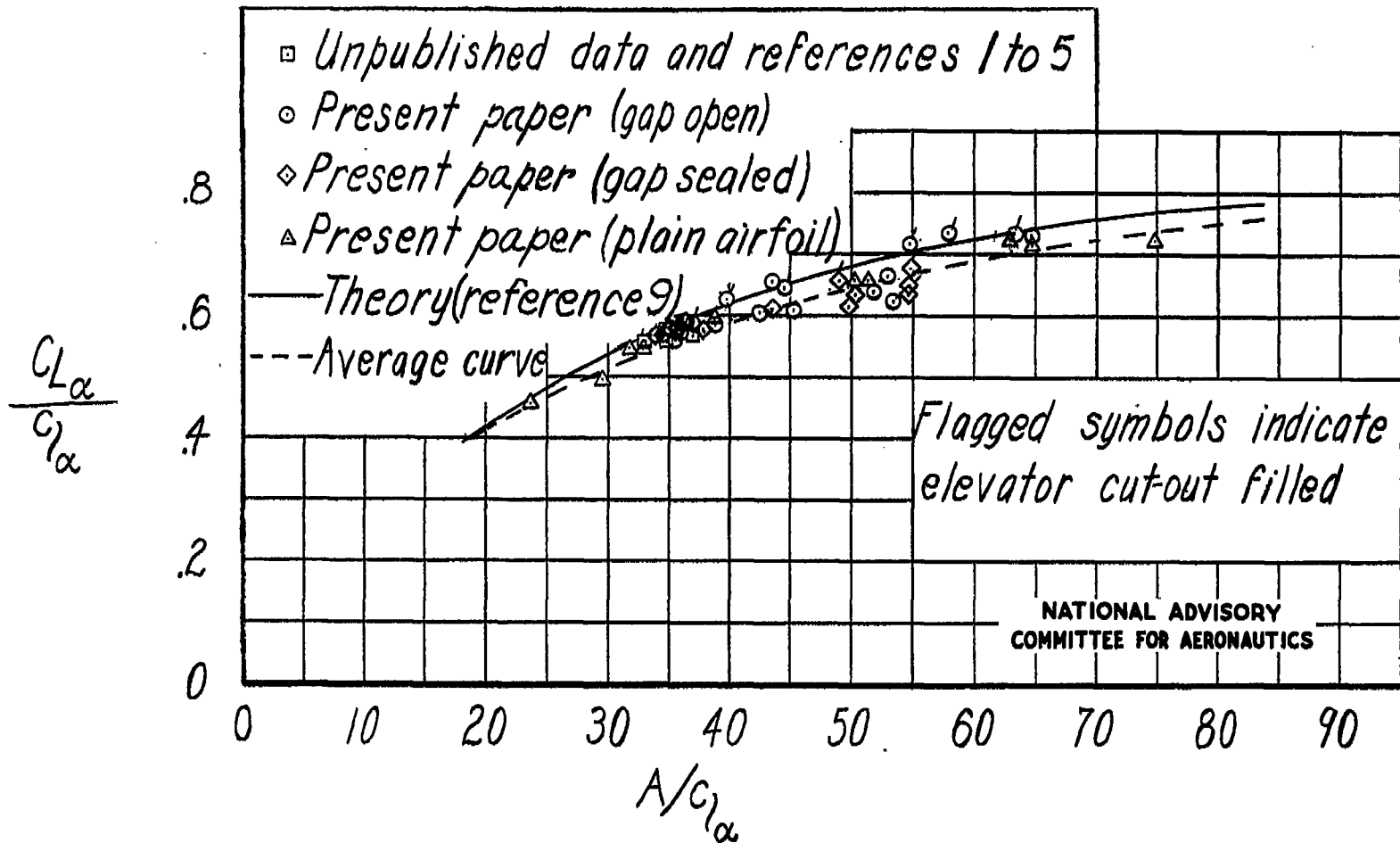


Figure 45.- Variation of ratio of lift-curve slope to section lift-curve slope with the ratio of aspect ratio to section lift-curve slope, theoretical and experimental.

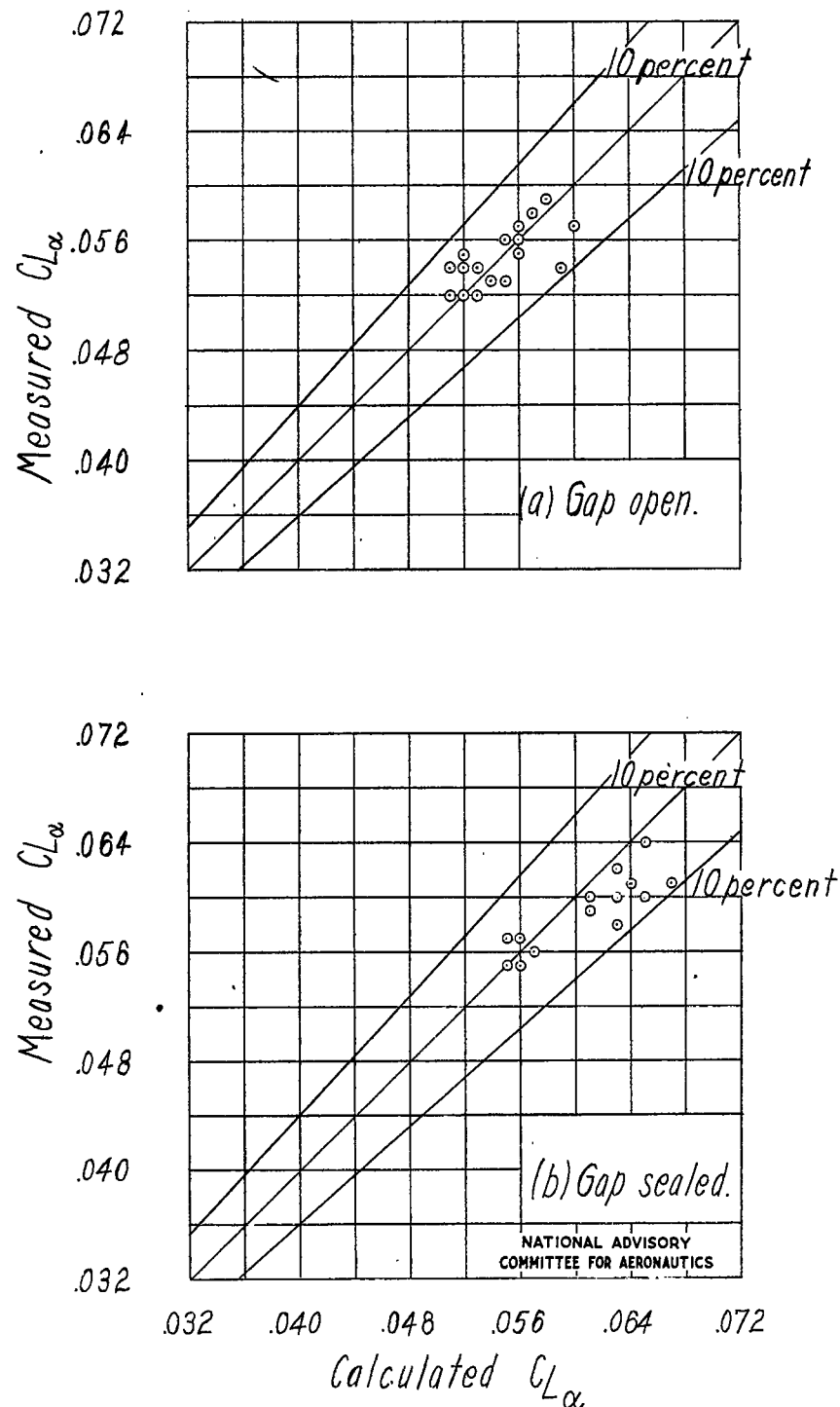


Figure 46.- Comparison of measured values of the lift-curve slope with values calculated from the equation

$$C_{L\alpha} = \left(\frac{\pi A}{\pi A E_e + 57.3 c_{l\alpha}} \right) c_{l\alpha} .$$

Fig. 47

NACA TN No. 1291

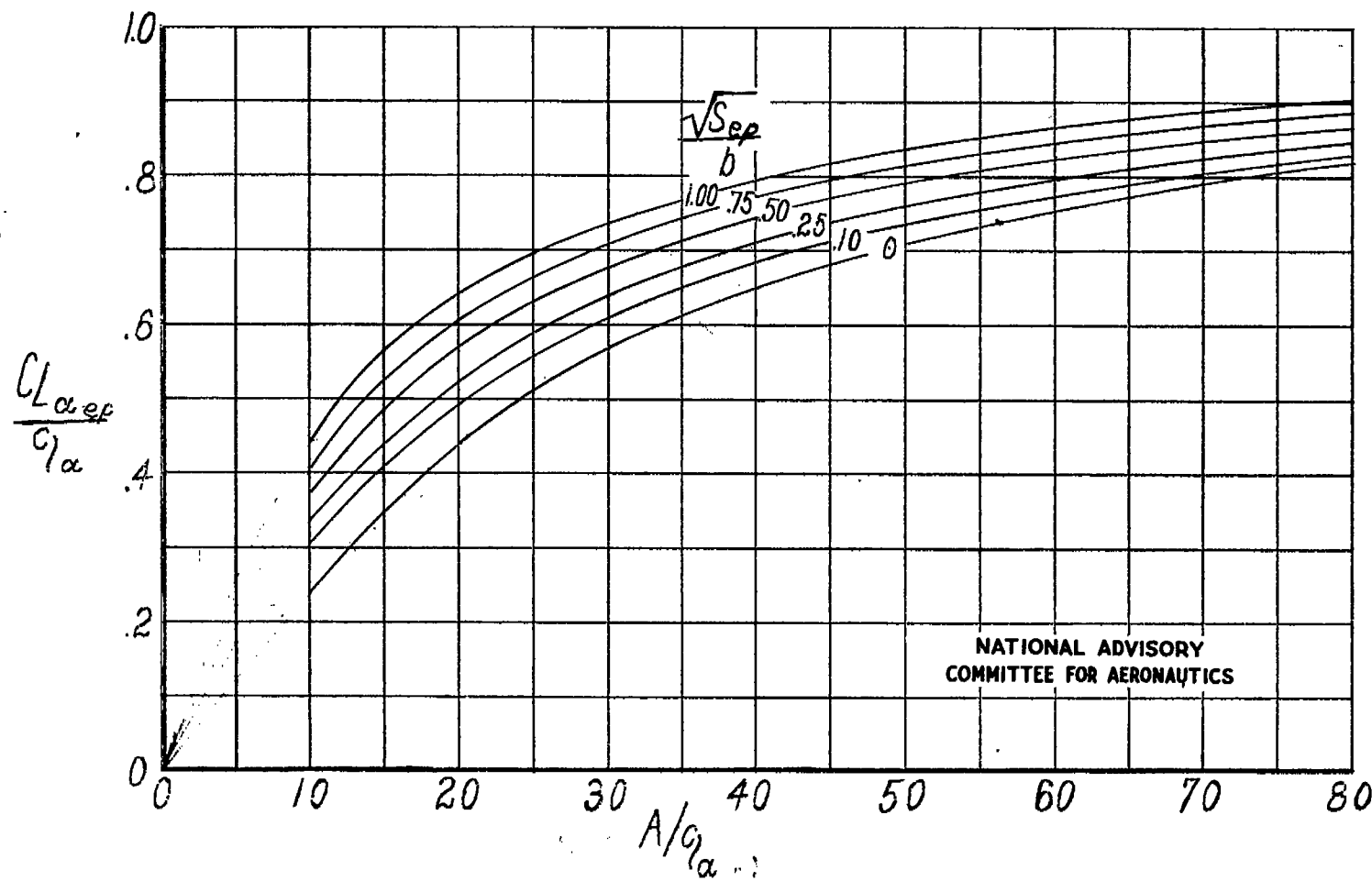


Figure 47.- Variation of ratio of lift-curve slope with double end plates to section lift-curve slope with the ratio of aspect ratio to section lift-curve slope for different ratios of effective end-plate height to airfoil span.

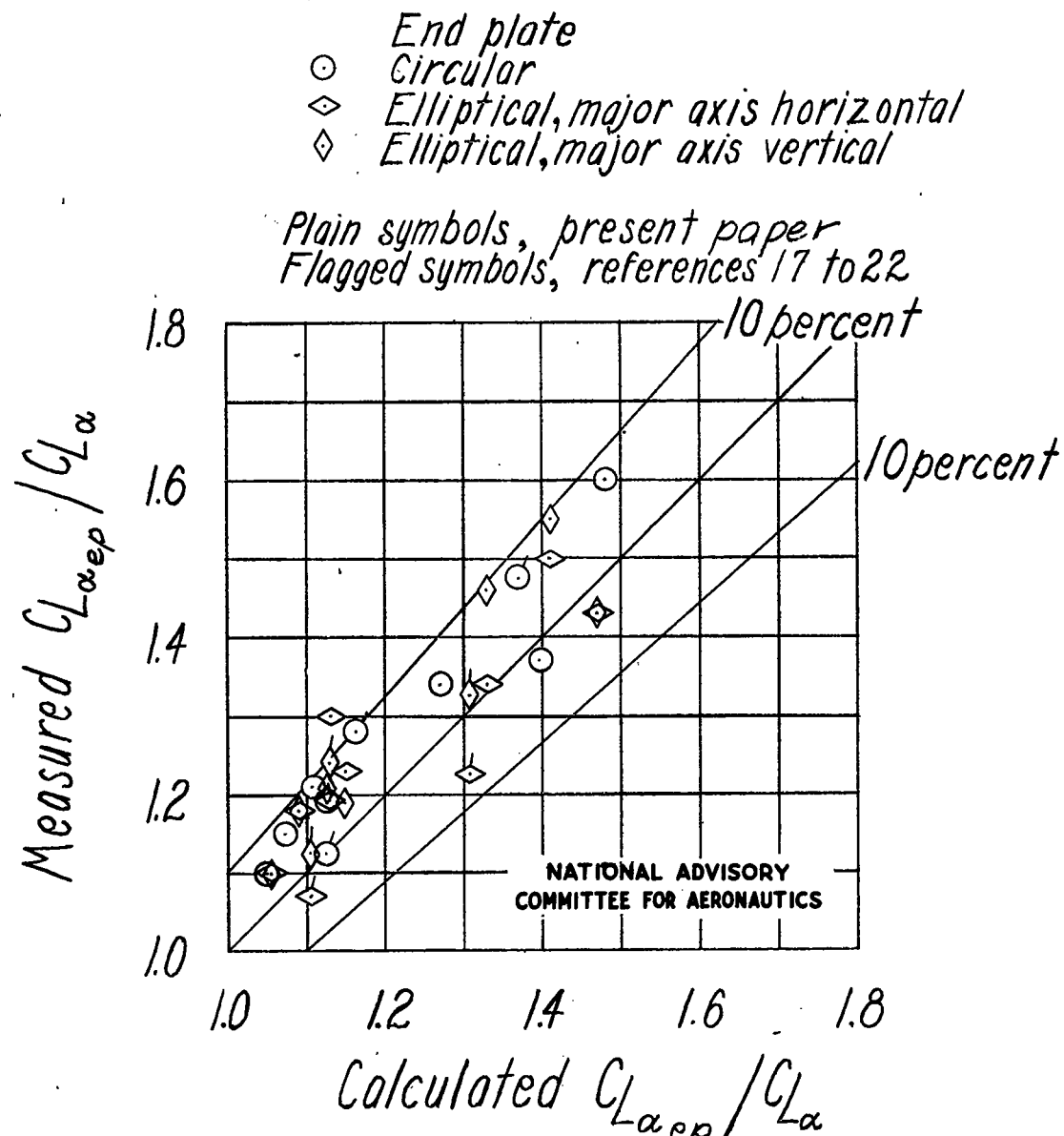


Figure 43.- Comparison of measured values and values obtained by use of figure 47 for $C_{L_{\alpha_{ep}}} / C_{L_{\alpha}}$

Fig. 49

NACA TN No. 1291

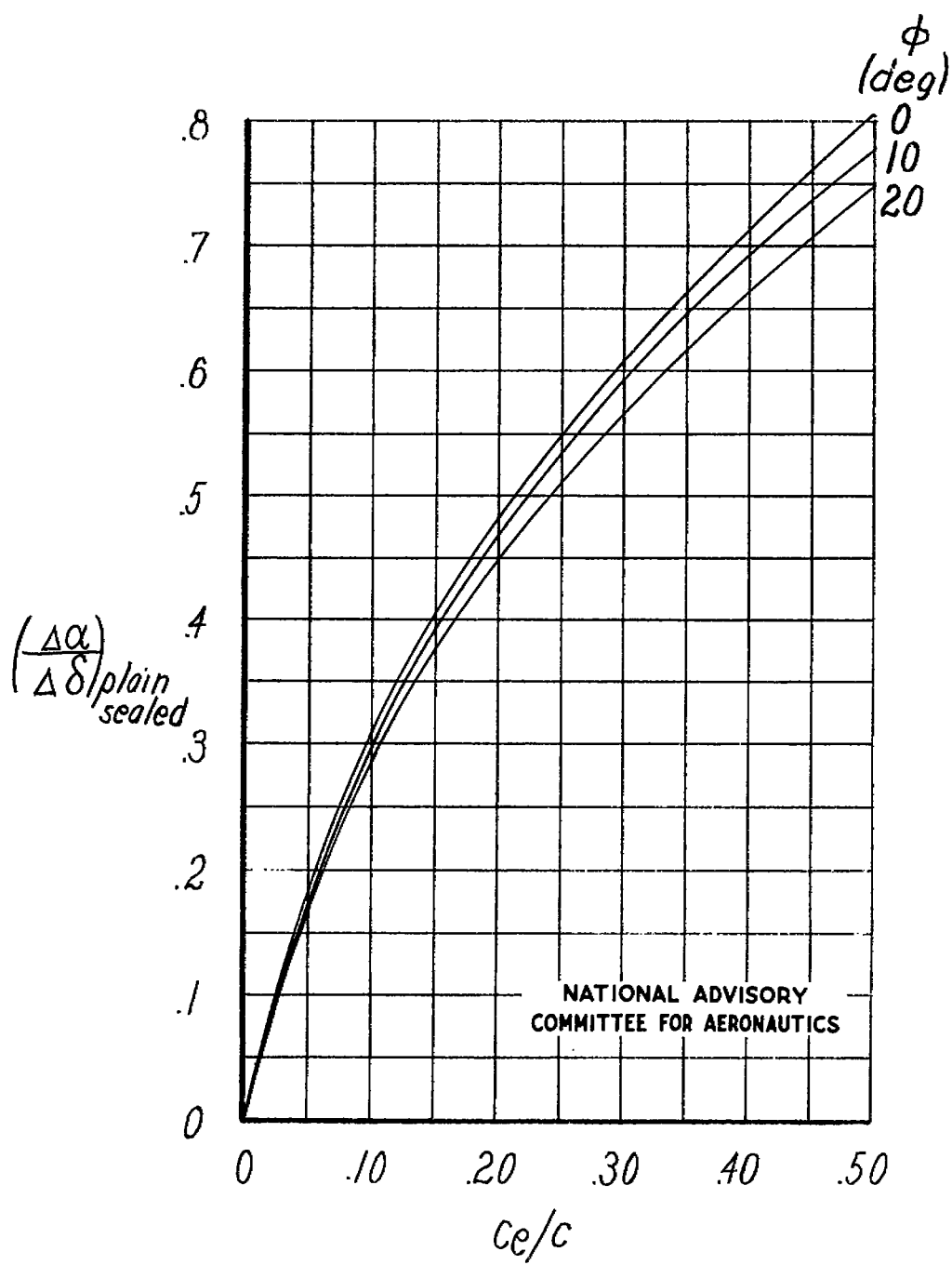


Figure 49.- Variation of lift-effectiveness parameter with elevator-chord ratio for various trailing-edge angles. Derived from figures 16 and 17 of reference 22.

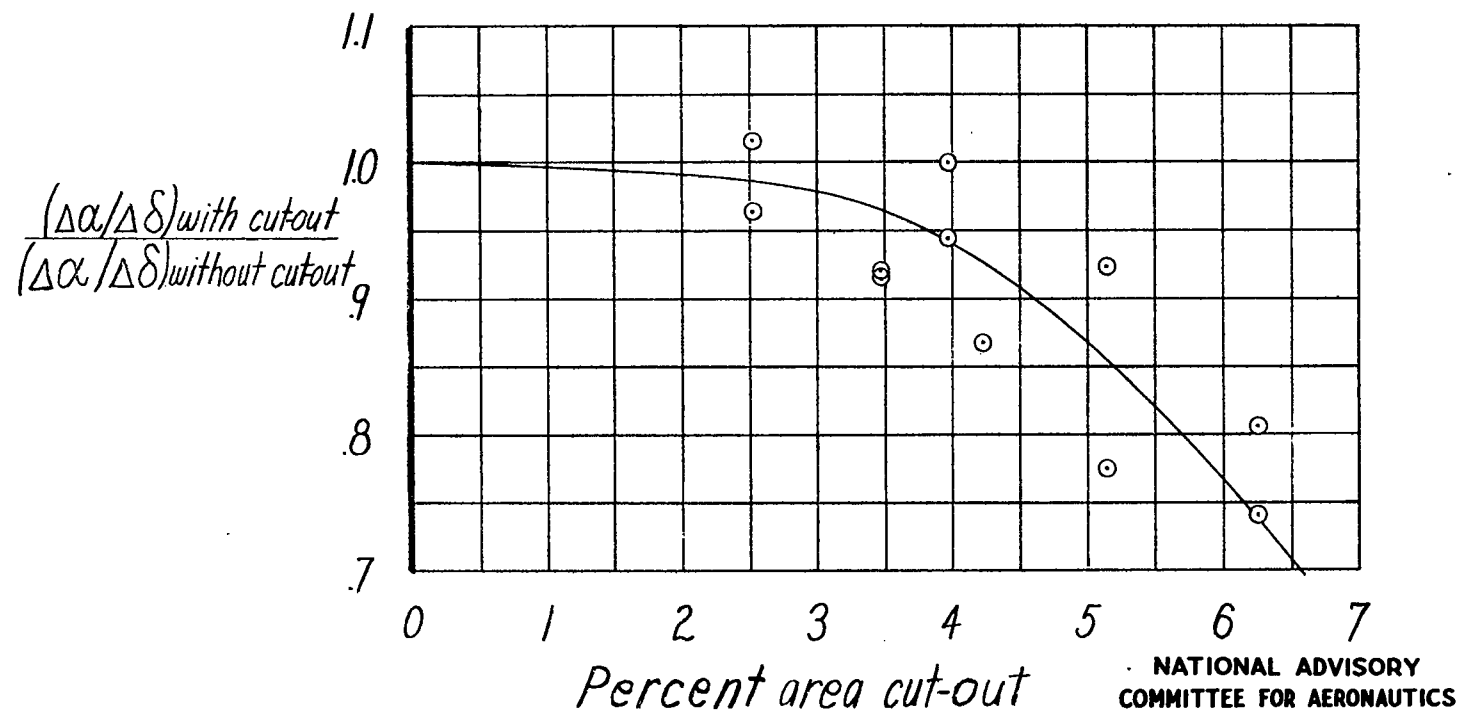


Figure 50.- Variation of lift-effectiveness parameter with elevator cut-out, relative to lift-effectiveness parameter without elevator cut-out, with percent area cut-out.

- Plain and gap sealed
- Plain and gap open
- Balanced and gap sealed
- Balanced and gap open

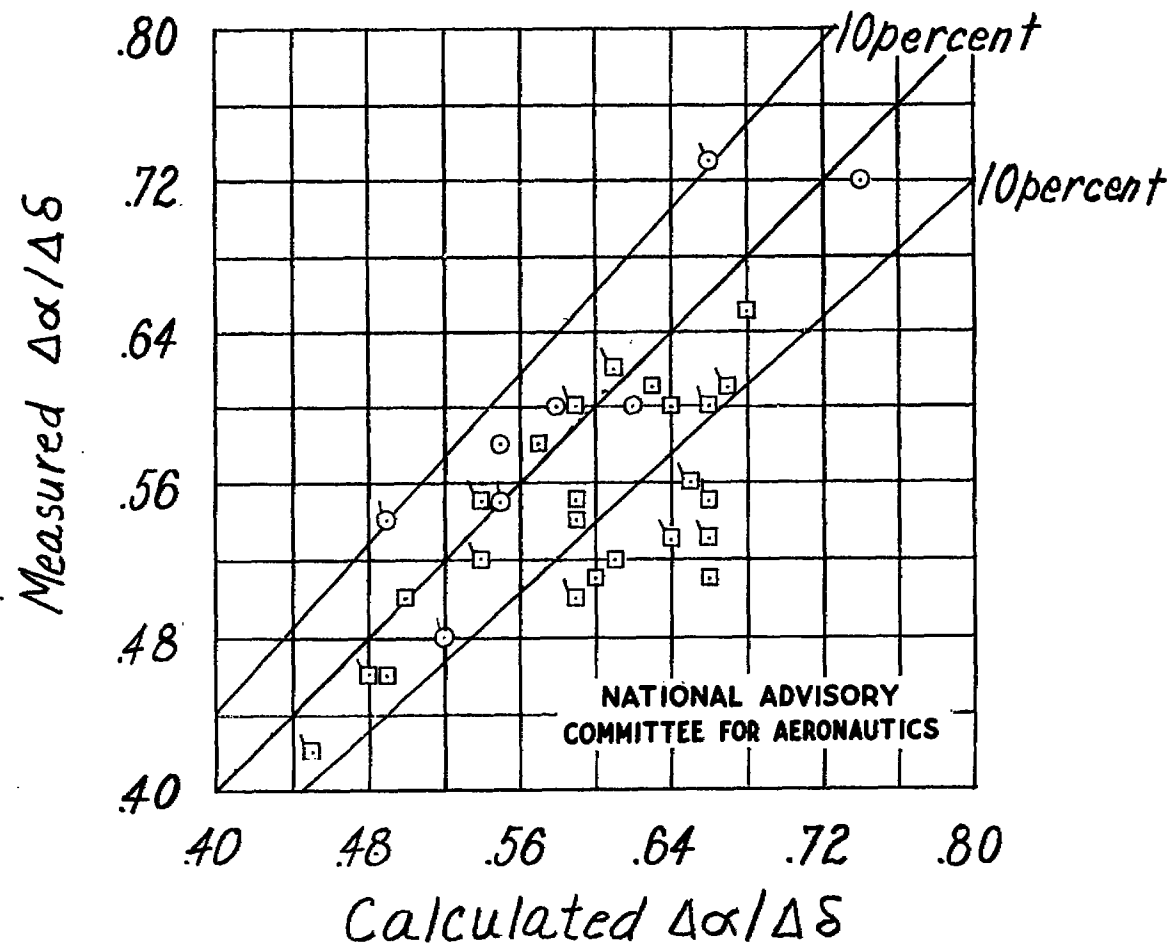
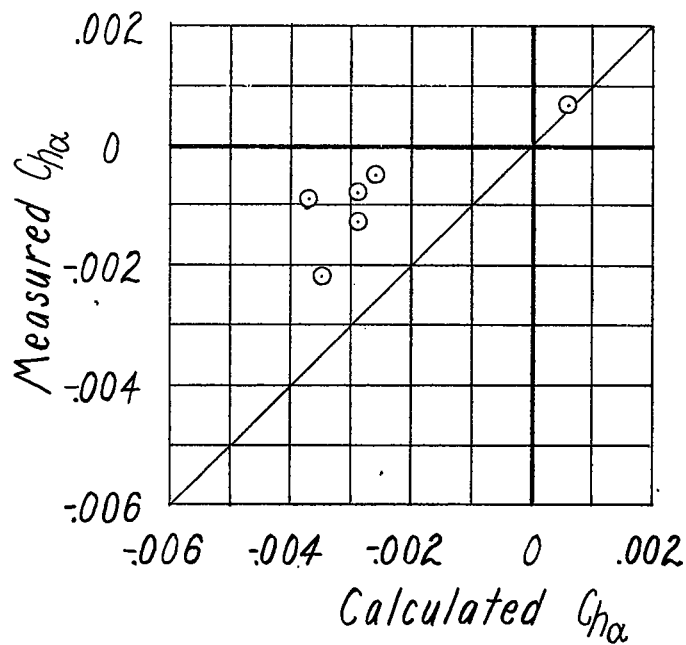
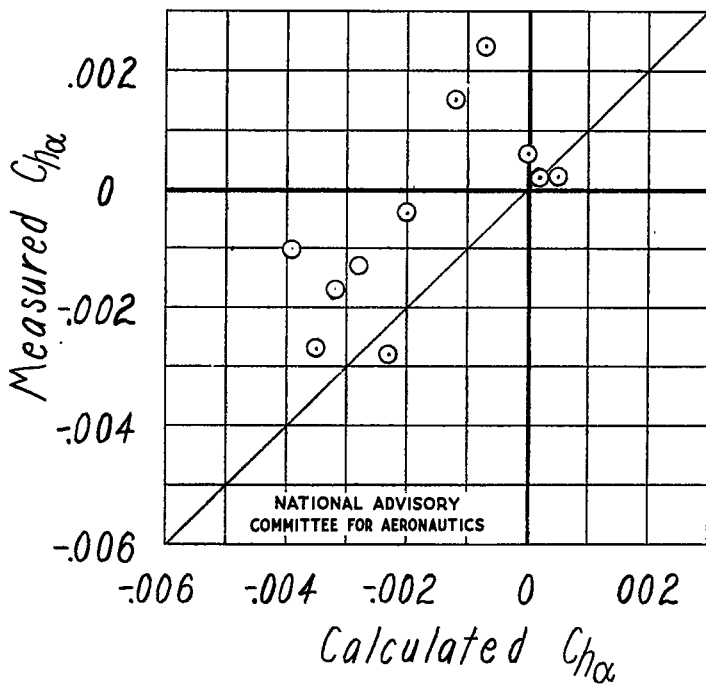


Figure 51.- Comparison of measured and calculated values of $\Delta\alpha/\Delta\delta$.

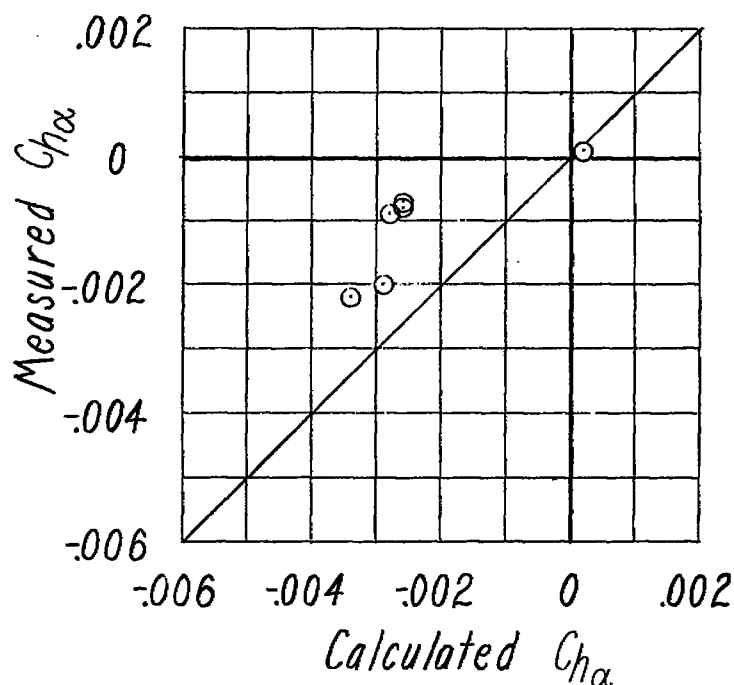


(a) Cut-out open.

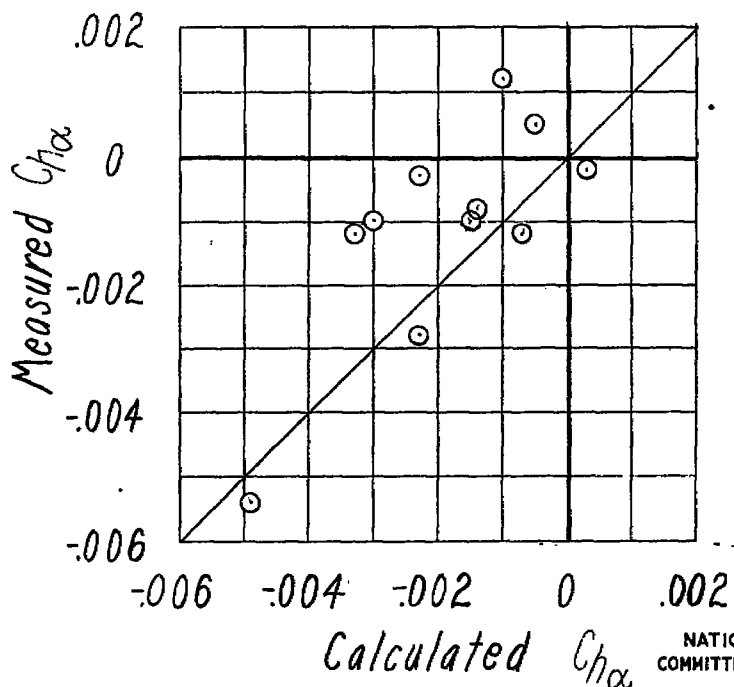


(b) Cut-out filled.

Figure 52.- Comparison of measured and calculated values of $C_{h\alpha}$. Elevator gap open.



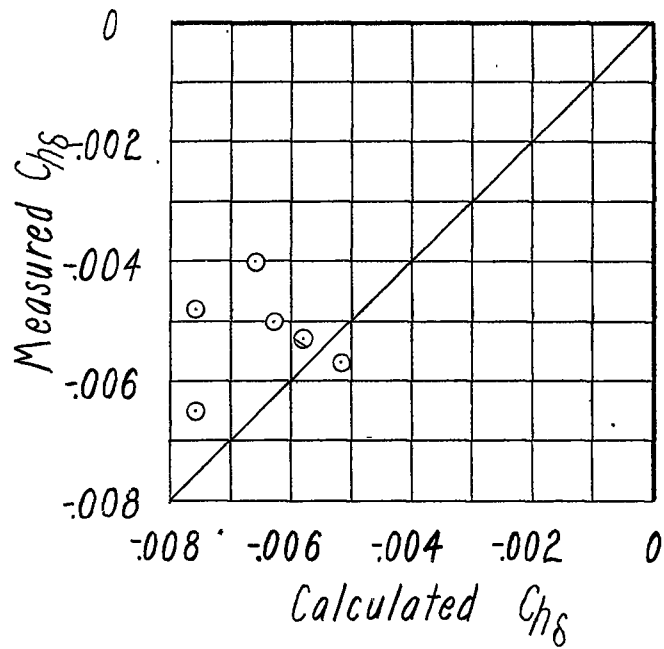
(a) Cut-out open.



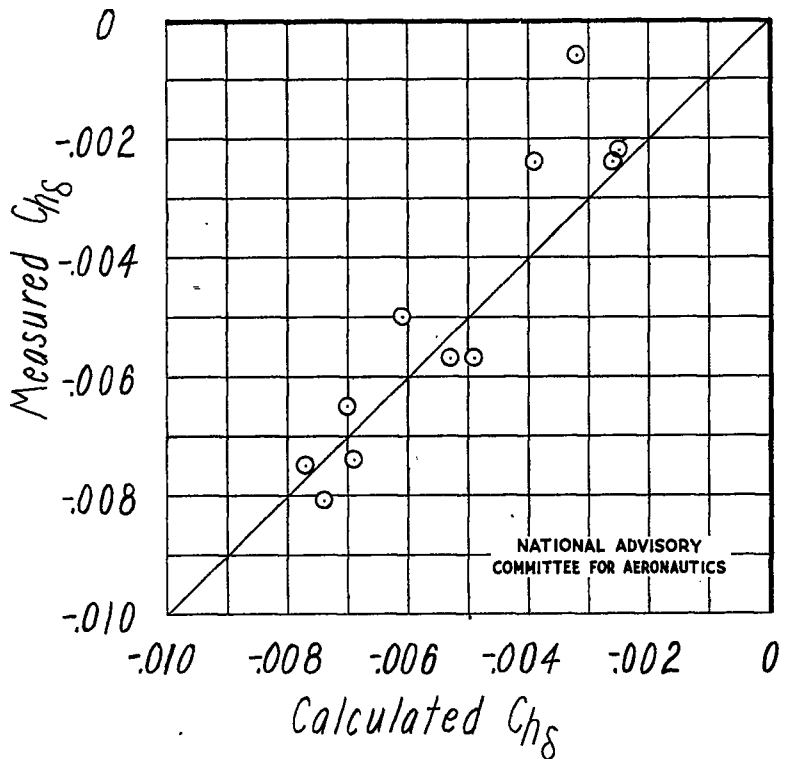
(b) Cut-out filled.

NATIONAL ADVISORY
COMMITTEE FOR AERONAUTICS

Figure 53.- Comparison of measured and calculated values of $C_{h\alpha}$. Elevator gap sealed.

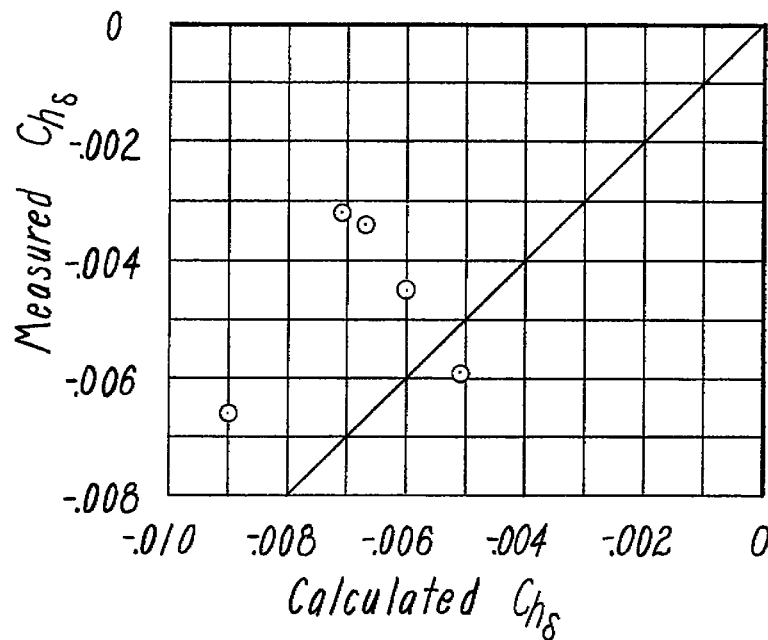


(a) Cut-out open.

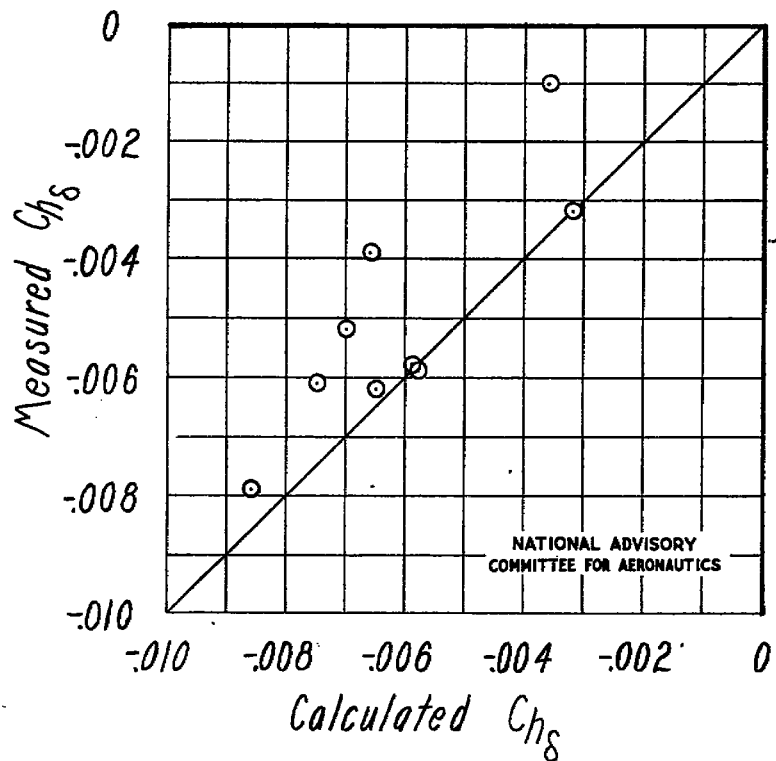


(b) Cut-out filled.

Figure 54.- Comparison of measured and calculated values of Ch_{δ} . Elevator gap open.



(a) Cut-out open.



(b) Cut-out filled.

Figure 55.- Comparison of measured and calculated values of $C_{h\delta}$. Elevator gap sealed.